Next-generation Outer Membrane Vesicle Vaccines

from concept to clinical trials

Bas van de Waterbeemd

Next-generation Outer Membrane Vesicle Vaccines

from Concept to Clinical Trials

Bas van de Waterbeemd

Thesis committee

Promotor
Prof. dr. R.H. Wijffels
Professor of Bioprocess Engineering
Wageningen University

Co-promotors
Dr. L.A. van der Pol
Head of Process Development department
Institute for Translational Vaccinology (Intravacc)

Dr. M.H.M. Eppink
Associate professor of Bioprocess Engineering
Wageningen University

Other members
Prof. dr. J. van der Oost, Wageningen University
Prof. dr. C.J.P. Boog, Institute for Translational Vaccinology (Intravacc), Bilthoven and Utrecht University
Dr. D.M. Granoff, Children's Hospital Oakland Research Institute (CHORI), USA
Dr. R. Segers, MSD Animal Health, Boxmeer

Next-generation Outer Membrane Vesicle Vaccines

from Concept to Clinical Trials

Bas van de Waterbeemd

Table of contents

Abbreviations and terminology

OMV	outer membrane vesicles
dOMV	detergent-extracted OMV (using deoxycholate)
nOMV	native OMV, detergent-free extraction with a chelating agent (EDTA)
sOMV	spontaneously released OMV, no extraction (detergent-free)
LPS	lipopolysaccharide (endotoxin)
DOC	deoxycholate
EDTA	ethylenediaminetetraacetic acid (chelates Ca^{2+} and Mg^{2+} ions)
lpxL1 mutation	prevents biosynthesis of acyl chain in lipid A (attenuates LPS toxicity)
rmpM mutation	disrupts membrane anchor protein (expected to improve OMV yield)
next-generation OMV	OMV from strain with *lpxL1*-LPS, produced with a detergent-free process
PorA	outer membrane porin A protein
fHbp	factor H binding protein
CPS	capsular polysaccharide
PL	phospholipid
PTAG	phospho-tag reagent (glyceraldehyde-3-phosphate)
TiO_2	titanium dioxide (captures PTAG)
SBA	serum bactericidal activity (measures functional immunogenicity)
MAT	IL-6 monocyte activation test (measures *in vitro* toxicity)
QbD	Quality by Design
DoE	Design of Experiments

Thesis abstract

Only vaccines containing outer membrane vesicles (OMV) have successfully stopped *Neisseria meningitidis* serogroup B epidemics. The OMV vaccines, however, provide limited coverage and are difficult to produce. This is caused by an obligatory detergent treatment, which removes lipopolysaccharide (LPS), a toxic OMV component. This thesis explored an alternative approach, based on OMV with attenuated *lpxL1*-LPS and a detergent-free process. The alternative approach is referred to as 'next-generation OMV' and provided vaccines with improved immunological and biochemical properties. In addition, quantitative proteomics demonstrated a preferred protein composition. This provided justification for further development towards clinical trials. After optimization of specific process steps, an improved pilot-scale production process was developed. The quality of OMV from this optimized process was stable and within pre-set specifications for nine consecutive batches. Studies in mice and rabbits suggested that next-generation OMV are immunogenic and safe for parenteral use in humans. Therefore these vaccines are now ready for clinical evaluation. Several groups are developing broadly protective OMV vaccines against *N. meningitidis* serogroup B, but also against other serogroups and other pathogens. OMV therefore have the potential to become a versatile technology platform for prophylactic and therapeutic vaccines. Such a platform requires a reliable production process to generate substantial quantities of high quality product. The process described in this thesis is well-suited for this purpose. The results encourage technology transfer to a commercial partner, with the goal to translate next-generation OMV technology into actual vaccines and improve global public health.

Chapter 1

General introduction

Background

The Health Council of the Netherlands recognized that the development of a serogroup B meningococcal disease vaccine is of major importance for national public health [1]. At present only vaccines containing outer membrane vesicles (OMV) have proven efficacy against specific serogroup B strains. These vaccines however do not provide broad coverage and are difficult to produce [2, 3]. To facilitate progress, the Institute for Translational Vaccinology (Intravacc, until recently part of the National Institute for Public Health and the Environment (RIVM)) received public funding to remove existing bottlenecks with a dedicated research program. Since the late 1990's this program has provided a vaccine concept with broad serogroup B coverage and a high-yield synthetic growth medium for meningococci. A gene mutation that attenuates toxic OMV components was also discovered and is expected to allow a more straightforward production process [4-7]. This thesis explores the benefits of such an alternative production strategy. New tools for product characterization and a novel pilot-scale production process for next-generation OMV vaccines were developed. The next-generation OMV vaccines are now ready for clinical evaluation. Relevance of this thesis for the broader field of vaccinology is discussed.

Meningococcal disease

Neisseria meningitidis is a gram-negative β-proteobacterium and member of the *Neisseriaceae* family [8]. It was identified as the causative agent of bacterial meningitis by Anton Weichselbaum in 1887 [9]. Meningococci reside in the nasopharyngeal mucosa of their human host. Approximately 8–20% of the adult population is colonized by meningococci, but most individuals will never develop symptoms of disease [10, 11]. Through a poorly understood mechanism, virulent *N. meningitidis* bacteria sometimes cross the mucosa to enter the bloodstream and cause invasive disease [12-14]. There are several different serogroups of *N. meningitidis* based on characteristics of its capsular polysaccharide. Six serogroups (A, B, C, W, X, and Y) are more virulent and cause the vast majority of life-threatening disease [14, 15]. The highest incidence occurs in young children under the age of four. Another incidence peak is observed among teenagers, most likely caused by increased exposure to risk factors like smoking or a high frequency of intimate contacts [16, 17]. Invasive meningococcal disease has devastating consequences caused by highly acute meningitis and septicemia. Fatality rates vary from 5–10% in industrialized countries up to 20% in developing countries. In addition about 10–20% of survivors have permanent health damage such as amputated of limbs, epilepsy, mental disabilities or deafness [18].

Epidemic outbreaks of meningococcal disease have been described in Europe since 1805 and for more than 100 years in sub-Saharan Africa, known as the 'African meningitis belt' (Figure 1) [18, 19]. Incidence rates of invasive meningococcal disease vary from very rare to 100–1000 cases per 100,000 inhabitants per year in specific regions during an epidemic outbreak. *N. meningitidis* serogroup A causes the highest disease incidence, as illustrated by repeated outbreaks in the African meningitis belt every 5–10 years and to a lesser extent in Russia and China over the past few decades [19, 20]. Serogroup B is predominant in industrialized countries, where it

accounts for 30–40% of all cases in North America and up to 80% in European countries [21, 22]. Even though serogroup B is associated with lower incidence rates than serogroup A, prolonged outbreaks have caused a substantial number of cases [23, 24]. The other virulent serogroups also have a high incidence and a distinct geographical distribution (Figure 1) [14]. The severity and global character of meningococcal disease emphasizes the need for an effective vaccine prevention strategy [24].

A worldwide distribution of meningococcal disease outbreaks by serogroup

Norway, 1969

Oregon, 1994

B, C

A, C

B, C, Y

Spain, 1974

Japan, 1979

Cuba, 1980

A, C, X, W

African meningitis belt 1996, 2009

Chile, 1985

B, C

Brazil, 1985

B, C

South Africa, 1980

Australia, 1982

New Zealand, 1992

B WHO reported cases in the African meningitis belt

1996

1978

1989

2009
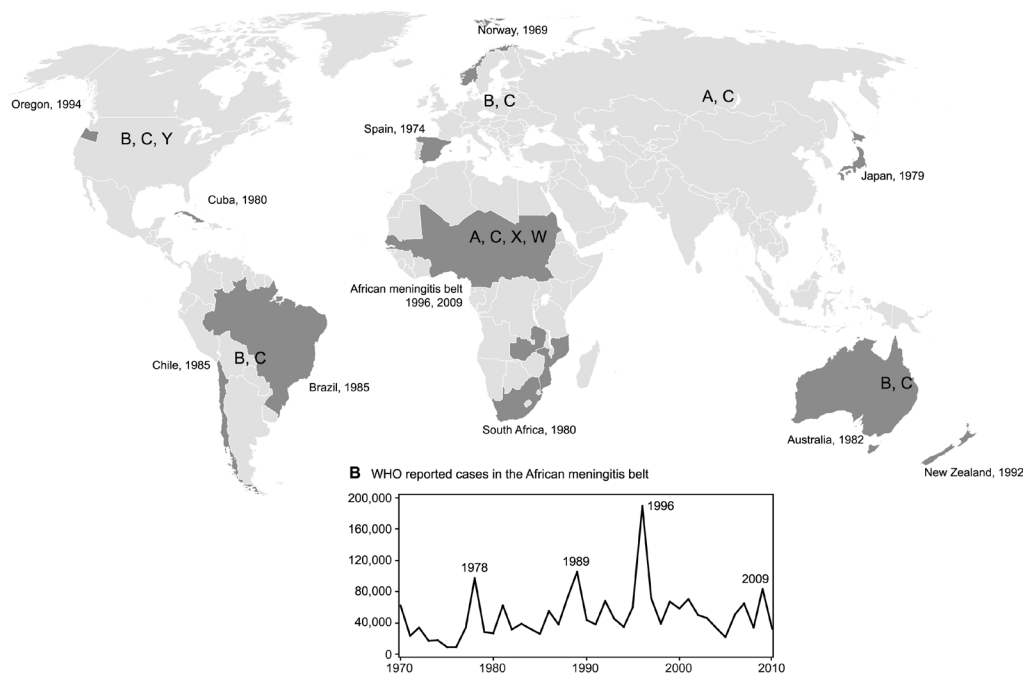
Figure 1. Epidemiology of meningococcal disease.
(A) Worldwide distribution of meningococcal disease by serogroup. Countries with epidemic outbreaks are depicted in dark grey. The predominant serogroups are shown for each continent (adapted from [24]). (B) The number of WHO reported cases of meningococcal disease in the African meningitis belt countries from 1970 to 2010. Devastating epidemic outbreaks occur approximately every ten years with local incidences of 100–1000 reported cases per 100,000 inhabitants, with a mortality rate of approximately 20% (source: www.who.int).

The first vaccines against *N. meningitidis* contained purified capsular polysaccharide (CPS) of serogroups A and C. They were safe and moderately effective in preventing serogroup C disease in the U.S. military and in controlling serogroup A epidemics in the African meningitis belt [25, 26]. After the emergence of serogroup W, a quadravalent vaccine was developed, containing CPS from serogroups A, C, W and Y [25, 27]. Unfortunately, purified CPS vaccines proved to be poorly immunogenic in young infants and failed to induce long-term immunological memory [18, 28]. Based on experience with conjugate vaccines against *Haemophilus influenzae*, meningococcal CPS was chemically conjugated to toxoid carrier protein. These CPS–protein conjugate vaccines were safe, had a greatly improved immunogenicity in young infants and were able to induce

immunological memory in toddlers and adolescents [29-31]. Conjugated vaccines have now been used in routine vaccination programs for several years, which decreased the number of deaths and clinical cases with more than 90%. Disease incidence in non-vaccinated individuals also decreased due to herd immunity [32-35]. Despite the major successes with other serogroups, conjugate vaccines containing serogroup B capsular polysaccharide had a poor immunogenicity [36]. The suspected cause was a structural similarity with sialic acid in glycoproteins from human neural tissue [37]. An attempt to solve this problem by replacing the N-acetyl groups of sialic acid residues yielded a conjugate vaccine that was safe in phase I clinical trials, but unable to induce functional immunogenicity [38, 39].

Outer membrane vesicle vaccines

Disappointing results with the conjugate approach shifted serogroup B research towards surface-exposed subcapsular antigens of the outer membrane. Like *Escherichia coli* or *Vibrio cholerae*, meningococci released outer membrane vesicles (OMV) containing proteins, CPS, lipopolysaccharide (LPS), phospholipids (PL) and periplasmic constituents [40-42]. The OMV were immunologically similar to the *N. meningitidis* outer membrane, since they contained all major membrane proteins in their native conformation (Figure 2) [43]. OMV induced good functional immunogenicity in humans, but detergent-extraction was necessary to ensure safety [44-46]. The detergent removed most of the LPS from the vesicles, which would otherwise have a highly endotoxic effect [47, 48]. After development of a production process by the Norwegian Institute for Public Health (NIPH), detergent-extracted OMV vaccines were used to control epidemic outbreaks in several different countries [49]. To date, these are the only interventions with proven efficacy against serogroup B meningococcal disease [3]. Efficacy was demonstrated in Chile, Cuba, Norway, Brazil and New-Zealand, where one specific strain had caused epidemic outbreaks for several decades [50-54]. The excellent safety record and high efficacy were a major milestone for the application of OMV in vaccinology.

Detergent-extracted OMV vaccines are well-suited for the control of epidemic outbreaks due to a high strain specificity [3]. A significant limitation however is that the immune response is almost exclusively directed against the immuno-dominant porin A antigen (PorA), especially in young infants and children [55-57]. PorA is variable between circulating serogroup B strains, which complicates development of a broadly protective vaccine [58]. To increase coverage, Intravacc developed recombinant strains with multiple PorA subtypes. The *cps* locus was also deleted to improve biosafety and remove the undesired CPS antigen of serogroup B [7, 37, 59]. This multivalent OMV concept initially consisted of two trivalent vaccine strains (HexaMen) and provided broad functional immunogenicity in phase II clinical trials [60, 61]. Potential European coverage was further increased to 80% of circulating strains by adding a third trivalent strain (NonaMen) [5, 62]. Other groups have improved vaccine coverage by complementing multiple PorA's with other immunogenic antigens, like factor H binding protein (fHbp) or iron-regulated proteins (e.g. FetA) [63, 64]. In addition OMV were used in a vaccine containing purified recombinant proteins (Novartis, Bexsero). The recombinant proteins were discovered by 'reverse vaccinology' [65], but the presence of detergent-extracted OMV was required for sufficient immunogenicity [66-68].
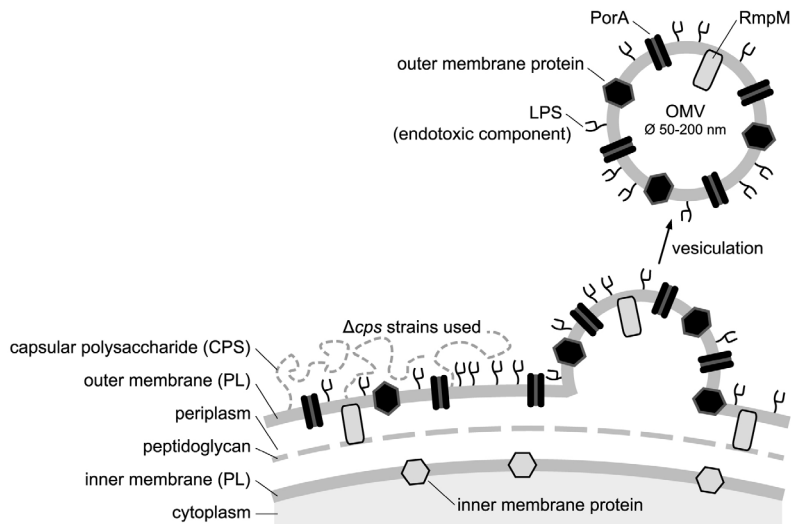
Figure 2. Vesiculation from the cell envelope of *Neisseria meningitidis*.
N. meningitidis can release outer membrane vesicles (OMV) through vesiculation [76]. OMV are spherical particles with a diameter of 50-200 nm, containing outer membrane proteins in their natural conformation, capsular polysaccharide (CPS), lipopolysaccharide (LPS), phospholipid (PL) and periplasmic constituents. OMV can be used as a vaccine since they are immunologically similar to the pathogen. PorA was identified as the immuno-dominant antigen of OMV vaccines that successfully stopped serogroup B epidemics in Norway, New Zealand, Cuba, Brazil and Chile [50-54]. Wild-type LPS of *N. meningitidis* however is endotoxic and must be removed with detergent-extraction to obtain a safe vaccine. Alternatively, it can be attenuated with the Δ*lpxL1* mutation (see Figure 3). RmpM is an anchor protein, which connects the outer membrane to a rigid peptidoglycan layer. Therefore Δ*rmpM* strains have a higher OMV yield. For *N. meningitidis* serogroup B vaccines, Δ*cps* capsule deletion mutants are used to prevent suspected cross-reactivity with human neural tissue [37].

In addition to a limited coverage, LPS removal with detergents caused production problems like aggregation. OMV aggregates interfere with sterile filtration, leaving the use of potentially toxic preservatives (i.e. thiomersalate) as the only remaining option to ensure sterility. Residual detergent in the OMV vaccine can stabilize aggregates, but deoxycholate is a component of animal origin [2, 61]. These challenges complicate compliance to current regulatory requirements, which has delayed the late-phase development and registration of detergent-extracted OMV vaccines [69]. Intravacc succeeded to attenuate LPS by introducing the *lpxL1* mutation, rather than physically remove it with deoxycholate (Figure 3) [6]. The attenuated LPS had a highly reduced endotoxic activity, which enabled the development of next-generation OMV vaccines for human use [70, 71]. Next-generation OMV are produced completely detergent-free, which preserves the native (attenuated) LPS content and retains protective lipoproteins like fHbp. This is expected to improve immunogenicity and cross-protection [72-74]. Therefore the development of next-generation OMV vaccines may resolve the disadvantages associated with detergent-extraction.
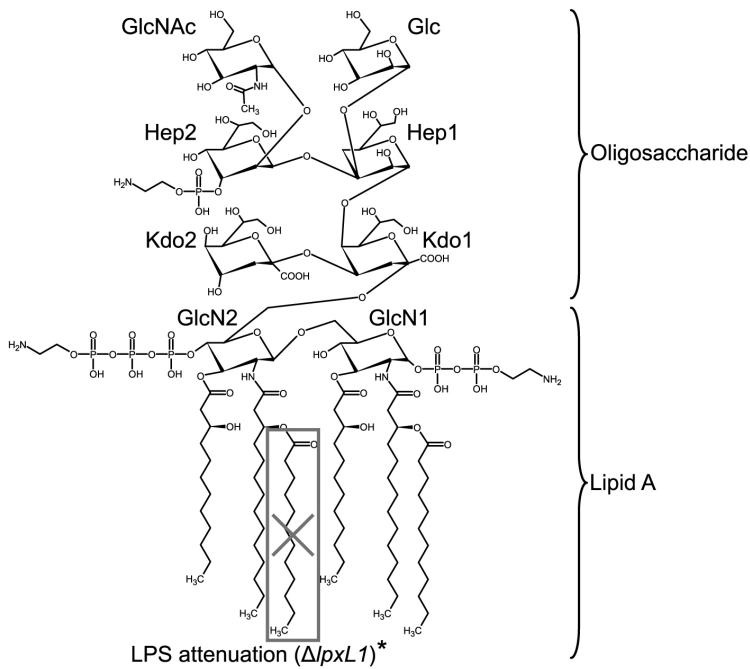
Figure 3. Lipopolysaccharide of *N. meningitidis*.
Wild-type lipopolysaccharide (LPS) of *N. meningitidis* has a strong endotoxic effect in humans. Therefore the production of OMV vaccines requires LPS removal with detergents, which complicates processing [2, 61]. Alternatively, LPS toxicity can be attenuated by introducing the *lpxL1* mutation which may enable a detergent-free production process [6]. The strains that were used in this thesis had an additional *galE* truncation in the oligosaccharide part of the LPS, resulting from deletion of the *cps* capsule locus [59]. *Biosynthesis of the outlined secondary acyl chain of lipid A is prevented by *lpxL1* gene deletion.

Objectives and thesis outline

After many years of extensive fundamental and applied research, broadly protective OMV vaccines against serogroup B meningococcal disease are now on the horizon [71]. Production and quality issues related to LPS removal with detergent have prevented successful introduction of promising vaccine concepts for humans use, like HexaMen [7, 61]. This thesis explores the use of next-generation OMV vaccines as an improved alternative for detergent-extracted vaccines. The designation 'next-generation OMV' refers to the combination of vaccine strains with attenuated *lpxL1*-LPS and a detergent-free process. These changes may have a profound impact on process and vaccine characteristics. Therefore, the central question of this thesis is:

Do next-generation OMV vaccines provide improved quality and process robustness?

With the central research question in mind, five hypotheses were formulated and tested in this thesis:

1) Next-generation OMV vaccines provide improved quality compared to detergent-extracted OMV.
2) Biomass extraction during processing changes the immunogenic protein content of OMV vaccines.
3) Biological stimuli can trigger OMV release by *N. meningitidis* and can be applied to improve vaccine production.
4) Next-generation OMV vaccines allow a more consistent and efficient large-scale production process.
5) Despite a high LPS content, next-generation OMV vaccines are safe for parenteral use in humans.

The hypotheses were tested in different chapters of this thesis, as outlined in Figure 4. Chapter 2 compared the properties of detergent-extracted reference OMV with detergent-free alternatives. This was done at small-scale, in the context of vaccine strains with systematic combinations of two different gene deletions. The Δ*lpxL1* mutation was used to attenuate LPS [6] and the Δ*rmpM* mutation was expected to improve yield [75]. Biochemical composition, yield and functional properties of the resulting OMV vaccines were analyzed with the goal to identify the best combination of strain and process for further scale-up (hypothesis 1).

In chapter 3 and 4, the effect of different production processes on the protein content of OMV vaccines was assessed with proteomics. Chapter 3 is a qualitative study, which demonstrated that a newly developed affinity tag (PTAG) can be used to reduce sample complexity while preserving the original proteome fingerprint. The relevance of such an approach for the analysis of complex protein products like OMV vaccines, is substantiated. Chapter 4 added a robust quantification method to the PTAG protocol, based on stable isotope labeling of free amino groups. This method was used to quantify the protein content of OMV vaccines from different production processes, followed by functional annotation of differentially expressed proteins (hypothesis 2).

Based on the results of chapters 2, 3 and 4, a Δ*lpxL1*-Δ*rmpM* mutant strain was selected and combined with a detergent-free process for further process development. A central step in this new process was biomass extraction with a chelating agent (detergent-free). Chapter 5 systematically optimized this step by measuring the impact of five potentially critical process parameters on OMV quality with Design of Experiments (DoE) [77, 78]. Two critical process parameters were identified, which were tuned to optimize the detergent-free extraction step.

In *E. coli*, different biological stimuli for the spontaneous release of OMV have been identified, including nutrient starvation [41, 79-81]. It was hypothesized that such stimuli can trigger OMV release in *N. meningitidis* as well and improve the yield of an OMV production process. The results of chapter 5 already pointed in this direction since one of the critical process parameters was related to both nutrient starvation and increased OMV yield, but this observation required additional experimental validation. This was done in chapter 6, which identified cysteine as the limiting medium component for growth. Next, the impact of cysteine depletion on spontaneous OMV release was measured and an underlying mechanism was proposed. The added value of such an approach for production of next-generation OMV vaccine was also assessed (hypothesis 3).

In parallel with chapters 5 and 6, a pilot-scale GMP production process was developed based on three different Δ*lpxL1*-Δ*rmpM* strains expressing multiple recombinant PorA antigens (next-generation NonaMen vaccine [5, 70]). Chapter 7 evaluated process robustness and consistency of replicate cultivations at 40 L scale. GMP quality control was performed to assess if OMV product quality was within preset preliminary specifications. In addition, yield and reproducibility of the new detergent-free process was compared with published reference processes (hypothesis 4).
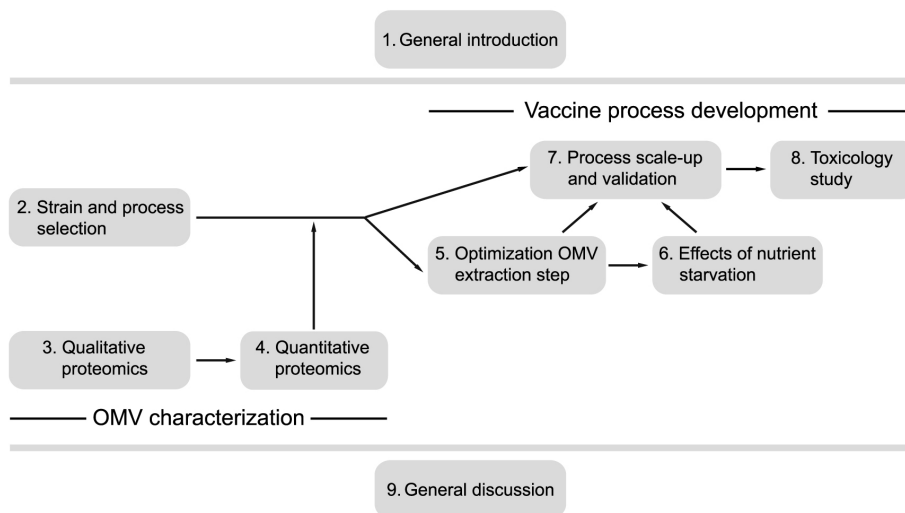
Figure 4. Thesis outline.
The central research question and hypotheses were tested in different chapters of this thesis. Chapter 3 and 4 describe the development of a novel quantitative proteomics method for characterization of OMV protein content. The other research chapters describe the process development of next-generation OMV vaccine.

Chapter 7 demonstrated that next-generation NonaMen vaccine met all preset specifications, therefore the vaccine was tested for preclinical immunogenicity and toxicology (mice and rabbits; chapter 8). Since next-generation NonaMen has a high attenuated LPS content compared to detergent-extracted vaccines, safety and toxicity testing is of special importance. Chapter 8 verified whether *in vitro* observed LPS attenuation after *lpxL1* deletion translates to low toxicity in rabbits (hypothesis 5).

This thesis covers all major aspects of preclinical vaccine development, from concept evaluation to pilot-scale GMP production. Preclinical toxicology and immunogenicity testing in chapter 8 provides justification for future clinical trials. Therefore this thesis represents an important step towards the introduction of next-generation OMV vaccine for human use. The scope of these results is discussed, since the new production process is not necessarily restricted to NonaMen and may be applicable for other meningococcal serogroups or other gram-negative pathogens like *Vibrio cholerae* or *Bordetella pertussis* [82-84]. Such a technology platform facilitates the development and clinical evaluation of new OMV concepts and supports the ongoing global effort to fight infectious diseases through vaccination.

Chapter 2

●●

Improved OMV vaccine against *Neisseria meningitidis* using genetically engineered strains and a detergent-free purification process

Bas van de Waterbeemd[1]
Mathieu Streefland[1,2]
Peter van der Ley[1]
Gijsbert Zomer[1]
Harry van Dijken[3]
Dirk Martens[2]
René H. Wijffels[2]
Leo A. van der Pol[1]

[1]   Institute for Translational Vaccinology (Intravacc), Bilthoven, The Netherlands
[2]   Wageningen University, Department of Bioprocess Engineering, Wageningen, The Netherlands
3   National Institute for Public Health and the Environment, Centre for Immunology of Infectious
     Diseases and Vaccines, Bilthoven, The Netherlands

Abstract

The use of detergent-extracted outer membrane vesicles (OMV) is an established approach for development of a multivalent PorA vaccine against *N. meningitidis* serogroup B. Selective removal of lipopolysaccharide (LPS) decreases toxicity, but promotes aggregation and narrows the immune response. Detergent-free OMV vaccines retain all LPS, which preserves the native vesicle structure, but results in high toxicity and lower yield. The present study assesses the effects of gene mutations that attenuate LPS toxicity (*lpxL1*) or improve OMV yield (*rmpM*) in combination with the available OMV purification processes. The results substantiate that OMV from a strain with both mutations, produced with a detergent-free process provide better vaccine characteristics than the traditional detergent-based approach. With comparable toxicity and yield, no aggregation and cross-protection against other PorA subtypes, these OMV vaccines are potentially safe and effective for parenteral use in humans.

Introduction

Neisseria meningitidis is a human pathogen that can cause acute meningitis and septicemia, with fatality rates around 15% [18]. Serogroup B meningitis accounts for 30-40% of meningitis cases in North America [21, 85] and up to 80% in some European countries [22, 86], yet a broadly protective vaccine is not available. Effective vaccines against other serogroups have been developed based on capsular polysaccharide conjugated to a carrier protein [31]. This approach was not feasible for serogroup B, due to poor immunogenicity [87] and concerns for vaccination-induced autoimmunity [37]. To date, vaccines based on outer membrane vesicles (OMV) are the only vaccines that successfully controlled serogroup B epidemics with examples in Norway, Cuba, and New Zealand [49-51, 53, 88].

OMV are released from the outer membrane of gram negative bacteria and consist of a phospholipid (PL) bilayer that contains outer membrane proteins, lipopolysaccharide (LPS) and periplasmic constituents [89]. PorA protein was identified as the major protective antigen in OMV, but is highly variable between the circulating serogroup B strains which complicates vaccine development [57, 90]. For this reason, the Netherlands Vaccine Institute (Bilthoven, The Netherlands) developed an OMV vaccine based on genetically modified *N. meningitidis* strains that express multiple PorA subtypes. This multivalent OMV vaccine was initially made with 2 trivalent PorA strains, expressing a total of 6 PorA subtypes [7, 61] and provided functional immunogenicity in phase II clinical trials [60]. To ensure sufficient coverage for serogroup B strains circulating globally, a third trivalent strain was added [5].

OMV vaccines are traditionally prepared with detergent extraction (dOMV purification process) to remove LPS and increase vesicle release. The LPS of *N. meningitidis* is highly toxic, but residual amounts (approx. 1%) are needed to maintain vesicle structure and adjuvate the immune response against PorA [91-93]. With balanced detergent concentrations the dOMV purification process provides these requirements, however there are major disadvantages. Along with LPS, detergent removes PL and also lipoproteins that contribute to immunogenicity, such as factor H binding protein [73, 94]. The resulting immune response is directed against a specific PorA subtype, without eliciting cross-protection [87, 95]. In addition, selective removal of LPS and PL changes the native vesicle structure and promotes aggregation [3, 96]. Detergent treatment is necessary to decrease LPS toxicity, but has detrimental side effects that complicate vaccine development.

Detergent-free OMV purification processes retain all LPS, resulting in a preserved native vesicle structure, but also in vaccines that are inherently toxic when used for parenteral immunization [3]. Two detergent-free purification processes have been described. The native OMV (nOMV) process [44] is similar to dOMV except for a detergent-free extraction step and the spontaneous OMV (sOMV) process [97-99] utilizes ultrafiltration or ultracentrifugation to purify spontaneously released OMV's from the culture supernatant, without extraction. nOMV vaccines produced encouraging results in animals and humans, but high LPS content limited applicability of the vaccine to intranasal administration [100-103]. Preclinical data on sOMV vaccines includes a study in mice, reporting cross-protection against a panel of serogroup B strains that was not found

with dOMV, but potential differences in toxicity were not addressed [104]. Other studies with sOMV vaccines in mice and rhesus monkeys also reported a broad immunogenicity [73, 94, 190]. The sOMV process however imposes an additional challenge, since it produces OMV yields that are too low for feasible process development [97, 98, 104]. To date, a direct and comprehensive comparison of the available OMV purification processes has not been made.

Discovery of *lpxL1* mutant strains provided a solution for the LPS toxicity issue [6]. Deletion of *lpxL1* attenuated LPS toxicity, while preserving the adjuvant activity needed for the immune response [6, 72, 94]. It was established that the immunogenicity of OMV from LPS deficient strains could be restored by adding external *lpxL1* LPS [105, 106]. In addition, *rmpM* deletion mutants were found to have a loosely attached outer membrane which could increase OMV release [107]. Absence of RmpM did not affect immunogenicity or bacterial growth characteristics [108], but to date the effect on OMV yield has not been scrutinized. In theory, a combination of *lpxL1* and *rmpM* mutations could solve the toxicity and yield problems associated with detergent-free OMV vaccines. The present study provides the first comprehensive analysis of *N. meningitidis* serogroup B vaccine performance, using OMV from the available purification processes (dOMV, nOMV and sOMV) in combination with *lpxL1* and *rmpM* genetic modifications (Figure 1). The OMV vaccines were analyzed for yield, toxicity, functional immunogenicity and aggregation with the objective to select the best approach for vaccine development. Beneficial effects were found for both gene mutations, enabling the use of detergent-free methods as the better alternative to traditional, detergent-based OMV purification processes.
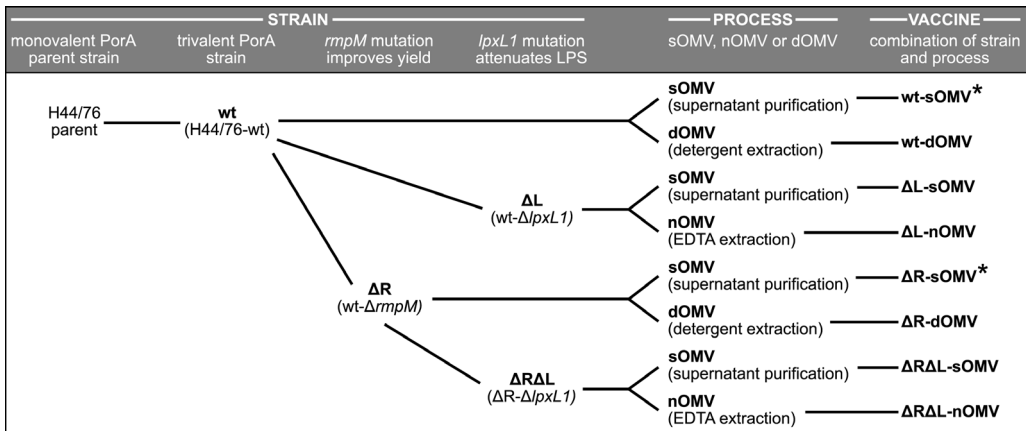
Figure 1. Experimental outline.
From a shared genetic background (H44/76), four bacterial strains were constructed expressing three PorA subtypes and combinations of *lpxL1* and *rmpM* gene mutations (wt, ΔR, ΔL and ΔRΔL strains). The strains were processed with three different purification processes (dOMV, nOMV and sOMV) producing eight OMV vaccines with distinct characteristics. The detergent-based dOMV process was used to reduce toxicity of strains with normal LPS (detergent extraction of wt and ΔR), while the detergent-free nOMV process was exclusively used for strains with attenuated LPS toxicity (EDTA extraction of ΔL and ΔRΔL). The detergent-free sOMV process was used on all four strains, providing two inherently toxic control vaccines (marked with asterikses) and two sOMV vaccines with attenuated LPS toxicity.

Materials and methods

Bacterial strains and growth conditions

All *N. meningitidis* strains that were used are recombinant non-encapsulated variants of the group B isolate H44/76 [109], combining one wild type and two recombinant PorA subtypes (trivalent PorA: subtypes P1.7,16, P1.5-1,2-2 and P1.19,15) with a non-functional *porB* gene [7] and truncated *galE* LPS [110]. Additional mutations in *lpxL1* and/or *rmpM* genes are strain-specific and summarized in Figure 1, resulting in 4 different strains (wt, ΔR, ΔL and ΔRΔL). Inactivation of *lpxL1* resulted in loss of the secondary acyl chain of lipid A, which was verified by mass spectrometry [6]. All bacterial cultures were grown in chemically defined medium. Disposable, baffled 500 mL erlenmeyer shake flasks with vented closure (Nalgene, Rochester, New York, U.S.A.) containing 150 mL medium, were inoculated with 10 mL working seedlot (cells at OD_{590} = 1.00 ± 0.05; stored at -135°C with 17.4% (v/v) glycerol) and incubated at 35°C, 200 rpm. Glucose concentration of the medium was monitored at-line with a YSI-2700 analyzer (Yellow Springs Instruments, Yellow Springs, Ohio, U.S.A.). Cells were harvested for OMV purification during late-exponential growth phase, at a residual glucose concentration of 5 mM.

OMV purification processes

The dOMV purification process utilizes deoxycholate (DOC) extraction of the bacterial outer membrane in the presence of EDTA, as described previously [61]. The nOMV process was based on the method described by Zollinger *et. al.* [44]. In this study, the consecutive steps of the nOMV process were identical to dOMV, however without DOC. OMV release is stimulated using EDTA alone, which is a chelating agent that destabilizes the bacterial outer membrane [111]. Supernatants from the initial harvesting step of the dOMV and nOMV processes were used as starting material for the sOMV purification process. After 0.2 μm filtration (Millipore, Billerica, Massachusetts, U.S.A.), OMV were concentrated and diafiltrated in Tris-sucrose buffer (10 mM Tris-HCl, pH 7.4; 3% sucrose (w/v)), using 100 kD ultrafiltration units (Millipore) driven by centrifugal force (3000 xg; 4°C). Additional purification and concentration of OMV in the retentate was done by ultracentrifugation (60 minutes at 125000 xg; 4°C). The final OMV pellets were homogenized in Tris-sucrose buffer and diluted to a total protein concentration of 0.5 mg/mL. All OMV purification processes were performed at small-scale (<0.5 L).

OMV vaccines

Bacterial strains with *lpxL1* and *rmpM* genetic modifications were systematically combined with OMV purification processes to obtain 8 OMV vaccines with distinct characteristics (Figure 1). The dOMV process was used to decrease toxicity of OMV vaccines with normal LPS (wt and ΔR strains), while the detergent-free nOMV process was exclusively used for strains with attenuated, non-toxic LPS (ΔL and ΔRΔL). These restrictions were used, because there should be no need for detergents when an OMV vaccine contains non-toxic LPS. To obtain inherently toxic OMV vaccines that were needed as controls for the toxicity analysis, the detergent-free sOMV process was used for all 4 bacterial strains, including those with toxic LPS.

Biochemical composition and OMV yield

Total protein concentration of OMV vaccines was measured using the Peterson's method [112]. PorA and 'other protein' content was measured with quantitative SDS gel electrophoresis under denaturing conditions [112, 113]. Per lane, 4 μg total protein from OMV vaccines was loaded. Gels were stained with Novex Colloidal Blue (Invitrogen, Carlsbad, California, U.S.A.) and PorA and 'other protein' was quantified as a percentage of total protein using TL100 1D gel analysis software (Totallab, Newcastle upon Tyne, U.K.). Residual DNA in the OMV vaccines was quantified with fluorescence spectroscopy using ethidium bromide (MP Biochemicals, Illkirch, France) as described before [4, 114]. Fatty acid composition was analyzed to quantify LPS and PL content, using a modified gas chromatography method [115, 116]. LPS was isolated by hot phenol-water extraction as described before [117] and quantified using the peak height of C14:0-3OH with C12:0-2OH as the internal standard (two C14:0-3OH residues per LPS), while PL was quantified using the peak heights sum of C16:0, C16:1, C18:0 and C18:1 with C15:0 as the internal standard. Specific protein yields (μg total protein and μg trivalent PorA per 10^{10} bacteria) were used to estimate OMV yield. Optical density was measured to calculate the number of harvested bacteria (1 OD unit at 590 nm corresponds to 4.4 x 10^9 cfu/mL).

Immunizations and functional immunogenicity

Immunizations were performed with 4 groups consisting of 15 female BALB/c mice per group, which were 6 to 8 weeks old. Group 1 mice received ΔR-dOMV vaccine, group 2 mice were immunized with ΔRΔL-nOMV vaccine and group 3 mice received ΔRΔL-sOMV vaccine. Group 4 received mock immunizations. All OMV vaccines were administered in a 0.3 mL dose, containing AlPO$_4$ as an adjuvant. Vaccines were prepared less than 24 hours before immunization by mixing OMV containing 1.5 μg PorA per subtype per dose (4.5 μg trivalent PorA per dose) with 0.45 mg AlPO$_4$ overnight at 4°C. Immunizations were given twice, subcutaneously on days 0 and 28, and serum was collected on day 42. Functional immunogenicity was determined by measuring serum bactericidal activity (SBA) as described before [118]. Statistical analysis of the obtained non-parametric data was done using the Kruskal-Wallis test to compare titers for each PorA subtype between the experimental groups (unpaired observations). P-values below 0.05 were considered to be significant.

Toxicity

The toxicity of the OMV vaccines was measured as described before for *B. pertussis* [119]. Stimulation of IL-6 production was tested with the human macrophage cell line MM6 [120]. Macrophages were seeded in 24-wells plates (2.5 x 10^5 cells/well) in 400 μl of IMDM medium (Invitrogen, Breda, The Netherlands) supplemented with penicillin, streptomycin, L-glutamine and fetal calf serum. The cells were stimulated with 100 μl of OMV in fivefold dilution series. The stimulation lasted 16 to 18 h at 37°C in a humid atmosphere with 5% CO_2. Following stimulation, IL-6 concentrations in the culture supernatants were quantified using an ELISA against human IL-6 according to the manufacturers' instructions (PeliKine Compact, Amsterdam, The Netherlands). One-way ANOVA statistical analysis with post-testing was used to detect significant p-values between any of the OMV vaccines.

OMV size and aggregation

Vesicle size distribution of OMV vaccines was measured by dynamic light scattering (DLS) at 25°C with a Malvern 4700 system equipped with a 488 nm Argon ion laser (Uniphase, San José, California, U.S.A.) and PCS software version 1.35 (Malvern Ltd., Malvern, UK). For refractive index and viscosity the values of pure water were used. The vesicle size distribution was reflected in the polydispersity index (PdI), which ranges between 0.0 (mono-dispersed) and 1.0 (entirely hetero-dispersed). OMV aggregation was quantified by comparing the total protein content of OMV starting material with the total protein content of the OMV pellet after centrifugation at low RCF. Starting material (1 mL) was centrifuged at 5000 xg for 10 minutes, 4°C and the pellet was resuspended in 1 mL buffer (10mM Tris-HCl, pH 7.4, 3% sucrose (w/v)) and analyzed for total protein content. Aggregation was calculated by expressing the total protein content of the pellet as a percentage of total protein in the starting material. Measurements were performed one month after purification of the OMV, before formulation with adjuvant.

Results

Biochemical composition and OMV yield

The effect of purification process type on the biochemical composition of OMV vaccines was quantified by measuring PorA, other protein, PL, LPS and DNA content. The results are shown in Table 1. The major biochemical components of dOMV vaccines was PorA protein (63.0 ± 2.0% (weight %)) and other protein (29.4 ± 2.2%). Protein content of detergent-free nOMV and sOMV vaccines was lower, due to increased amounts of LPS and PL. In sOMV vaccines LPS and PL content was highest (24.3 ± 6.6% and 33.7 ± 8.1%, respectively) and detergent-treatment in dOMV vaccines selectively removed both molecules, resulting in 2.8 ± 0.4% LPS and 2.5 ± 0.3% PL (p < 0.001). Residual DNA was low for all three purification processes due to efficient removal during ultracentrifugation. Protein composition analysis of OMV vaccines (Figure 2B) designated PorA as the most abundant protein (66.6 ± 0.4% of total protein) and confirmed absence of RmpM in deletion mutant strains (ΔR and ΔRΔL). Specific protein yields of total protein and PorA were used to estimate OMV yield (Figure 2A). *RmpM* mutant strains had higher OMV yields than strains with functional RmpM. Strain ΔRΔL had 4.2 ± 0.4 fold higher yield than ΔL and strain ΔR had a 2.1 ± 0.4 fold higher yield than wt (combined averages of OMV from different purification processes). In addition, a purification process effect was found. For all bacterial strains, sOMV vaccines had significantly lower yields than the corresponding nOMV or dOMV vaccines (p < 0.05). The *lpxL1* mutation had a negative effect on yield (2.6 ± 1.0 fold reduction).

Table 1.
Biochemical composition (weight %) of OMV vaccines from three purification processes. OMV's were extracted from concentrated bacterial cells using detergent extraction (dOMV) or EDTA extraction (nOMV), or harvested directly from the culture supernatant (sOMV). The content of five major biochemical compounds of OMV vaccines was analyzed: trivalent PorA, other protein, phospholipid (PL), lipopolysaccharide (LPS) and residual DNA. Detergent in the dOMV process selectively removed PL and LPS from the OMV's. Similar observations were made for the nOMV process, however to a lesser extent than for dOMV. Error margins represent standard deviations.

	dOMV (detergent-extraction)	nOMV (EDTA extraction)	sOMV (spontaneous OMV)
trivalent PorA	63.0 ± 2.0%	31.9 ± 6.9%	21.9 ± 11.9%
other protein	29.4 ± 2.2%	25.2 ± 7.6%	15.7 ± 4.8%
PL	2.5 ± 0.3%	27.5 ± 0.7%	33.7 ± 8.1%
LPS	2.8 ± 0.4%	13.3 ± 0.7%	24.3 ± 6.6%
residual DNA	2.4 ± 0.4%	2.2 ± 0.3%	4.4 ± 1.5%

Toxicity and functional immunogenicity

To predict toxicity in humans, high yield OMV vaccines were tested for their ability to stimulate IL-6 production in a human macrophage cell line. In OMV with normal LPS there is a known correlation between IL-6 production and toxicity [119, 120]. This was confirmed by ΔR-dOMV and ΔR-sOMV vaccines with low and high toxicity, respectively. In OMV vaccines with attenuated LPS (ΔRΔL strain) such correlation was not found. Despite high LPS content (comparable to ΔR-

A

B
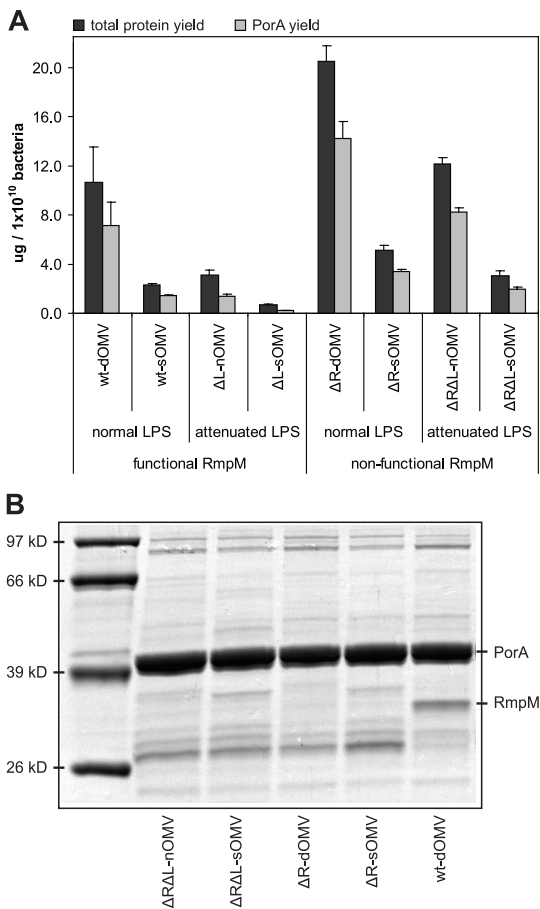
Figure 2.
(A) OMV yields of eight vaccines, estimated with the specific total protein yield (black bars) and the specific, trivalent PorA yield (grey bars). Increased yield was found for strains with non-functional RmpM (ΔR and ΔRΔL). Error bars represent standard deviations from triplicate experiments. (B) Absence of RmpM was confirmed with SDS gel electrophoresis. Molecular weight standard (left) indicates protein weight and protein names are indicated on the right. wt-dOMV was included as a control for presence of RmpM. All OMV vaccines were trivalent PorA (subtypes P1.7,16; P1.5-1,2-2 and P1.19,15-1).

sOMV), IL-6 levels were comparable to ΔR-dOMV (Figure 3A). Functional immunogenicity was determined by measuring SBA titers in mice sera. All OMV vaccines combined the same 3 PorA subtypes (P1.7,16; P1.5-1,2-2 and P1.19,15-1) and were tested against a panel of 8 monovalent H44/76-derived bacterial strains each expressing a single PorA subtype, or no PorA at all (ΔPorA strain). Table 2 shows the SBA titers of three high yield OMV vaccines with low toxicity. The fourth high yield vaccine (ΔR-sOMV) was not tested in mice, due to inherent toxicity (see Figure 3A). Two PorA subtypes that were included in the vaccines (P1.7,16 and P1.5-1,2-2) confirmed high bactericidal titers against their monovalent target strains, with 94.4% of the mice responding to immunization. Titers against P1.5-1,2-2 were higher for ΔRΔL-sOMV than for the other vaccines ($p < 0.05$). Only 15.6% of the mice responded to the third subtype (P1.19,15-1), with no responders

at all for the ΔR-dOMV vaccine and low titers with few responders for ΔRΔL-nOMV and ΔRΔL-sOMV (detergent-free). Analysis of bactericidal titers against PorA subtypes that were not included in the vaccines confirmed that ΔR-dOMV (detergent-treatment) did not induce cross-protection. Remarkably, ΔRΔL-sOMV (detergent-free) did elicit broad cross-protection against all monovalent PorA strains, including three responders against the ΔPorA strain. Improved cross-protection was also observed for ΔRΔL-nOMV (detergent-free), however less pronounced with a few responders against 2 out of 6 non-included PorA subtypes (P12-1,13 and P1.7,1-1; not significantly higher than ΔR-dOMV).

OMV size and aggregation

Vesicle size analysis of OMV vaccines from high yield strains (ΔR and ΔRΔL) revealed that vesicle size was dependent on purification process type (Figure 3B). Both sOMV vaccines had identical vesicle sizes (80.2 ± 2.2 nm) and formed a near-homogeneous population with low polydispersity index (PdI) of 0.143 ± 0.017. The nOMV vaccine was also near-homogeneous, but with a larger average size of 106.5 ± 1.7 nm ($p < 0.001$ when compared to sOMV). In contrast, the dOMV vaccine formed a heterogeneous population, with high PdI (0.460 ± 0.112). Within this population, vesicle size varied between 550 and 5500 nm. In concordance with these observations, OMV aggregation percentage was low for all detergent-free vaccines, with averages of 6.9 ± 3.0% and significantly higher for dOMV vaccines (95.5 ± 1.0%; $p < 0.001$).

Table 2.
Bactericidal titers (SBA) against a panel of monovalent PorA strains after immunization with trivalent PorA vaccines that combined high yield with low toxicity. Three groups of 15 mice were immunized with either ΔR-dOMV, ΔRΔL-nOMV or ΔRΔL-sOMV vaccine. PorA subtypes that were not included in the vaccines were used to assess cross-protection, which was restricted to detergent-free OMV vaccines (especially ΔRΔL-sOMV). Total number of responders is listed for each group (max. 15). Mean SBA titers (>90% killing) of responders are summarized on a ^{2}log scale and error margins represent standard deviation. Statistically significant results ($p < 0.05$) are marked with asterisrkses for the comparison with ΔR-dOMV (*) or ΔRΔL-nOMV (‡).

monovalent PorA strain	PorA included in vaccine	mean SBA titer responders			number of responders		
		ΔR-dOMV	ΔRΔL-nOMV	ΔRΔL-sOMV	ΔR-dOMV	ΔRΔL-nOMV	ΔRΔL-sOMV
P1.7,16	yes	10.8 ± 1.5	11.0 ± 1.1	11.2 ± 1.2	14	14	15
P1.5-1,2-2	yes	12.2 ± 2.3	12.5 ± 1.8	15.0 ± 1.7*‡	13	14	15
P1.19,15-1	yes	0.0	5.3 ± 2.8	8.3 ± 2.1*	0	2	5
P1.5-2,10	no	0.0	0.0	12.2 ± 3.9*‡	0	0	14
P12-1,13	no	0.0	7.7 ± 1.2	12.4 ± 2.3*‡	0	3	15
P1.7-2,4	no	0.0	0.0	9.5 ± 1.4*‡	0	0	12
P1.22,14	no	0.0	0.0	9.7 ± 1.0*‡	0	0	12
P1.7-1,1	no	0.0	6.3 ± 0.0	9.3 ± 2.1*‡	0	2	14
ΔporA	no	0.0	0.0	10.3 ± 0.0	0	0	3
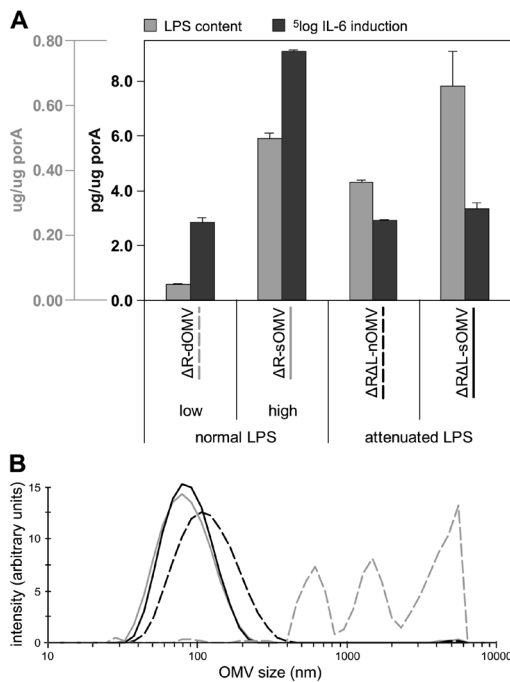
Figure 3.
(A) Toxicity and LPS content of OMV vaccines from high yield strains (ΔR and ΔRΔL). OMV's with attenuated LPS (ΔRΔL strain) had low toxicity despite high LPS content. Black bars represent the average IL-6 induction from ^{5}log dilution series, normalized per μg PorA (predictor of toxicity) and grey bars indicate LPS content as weight percentage of the PorA content. Error bars represent standard deviations from triplicate experiments. (B) The vesicle size distribution was measured. ΔRΔL-sOMV (black line), ΔR-sOMV (grey line), ΔRΔL-nOMV (black intersected line) and ΔR-dOMV (grey intersected line) are depicted, corresponding to the OMV vaccines in Figure 3A. Detergent-free OMV's (nOMV and sOMV) had defined size distributions around 90 nm, while the dOMV vaccine had an undefined distribution, caused by detergent-induced vesicle aggregation.

Discussion

The use of *N. meningitidis* outer membrane vesicles (OMV) as a delivery vehicle for immuno-dominant PorA protein is a well-established approach for the development of a vaccine against *N. meningitidis* serogroup B [7, 60, 61]. In the present study, three different OMV purification processes are systematically combined with bacterial strains containing *lpxL1* and *rmpM* genetic modifications, with the objective to select the best approach for vaccine development (Figure 1). The resulting OMV vaccines have distinct characteristics regarding yield, toxicity, immunogenicity and aggregation.

RmpM-related yield improvement has been found for all three small-scale OMV purification processes in this study. This is especially important for feasibility of the sOMV process, since it does not involve extraction to increase OMV release. RmpM is proposed to act as an anchor protein containing domains that interact with outer membrane proteins and the peptidoglycan layer, providing stability to the bacterial cell wall [121-123]. *RmpM* deletion mutants have been associated with a loosely attached outer membrane and an effect on OMV yield was hypothesized [107]. The data in this study (Figure 2A) now provide clear evidence for the link between non-functional RmpM protein and increased OMV yield.

To predict toxicity in humans, OMV vaccines from high yield, *rmpM* mutant strains have been used to stimulate IL-6 production in macrophage cells (Figure 3A). Vaccines with normal LPS confirm the relation between LPS content and toxicity. This relation has not been found in detergent-free vaccines with attenuated LPS, which produce IL-6 levels comparable to ΔR-dOMV (low toxicity), despite high LPS content. This beneficial effect of the *lpxL1* mutation is supported by the results of other studies [72, 94]. The remaining IL-6 induction of OMV vaccines with attenuated LPS can be caused by non-LPS components, such as lipoproteins, which are known TLR-2 activators [124]. IL-6 induction by human macrophage cells is increasingly used as predictor of clinical toxicity [125], therefore OMV vaccines with attenuated LPS are potentially safe for parenteral use in humans.

Functional immunogenicity of high yield, trivalent PorA vaccines with low toxicity has been measured (Table 2). One PorA subtype that was included in the immunizations (P1.19,15-1) is known to produce low bactericidal titers in mice [5, 61, 118, 126], but induces sufficient titers in rabbits [5] and humans [60]. Functional immunogenicity against P1.5-1,2-2 is higher for detergent-free sOMV vaccine (ΔRΔL-sOMV) than for the other two vaccines. In addition, this vaccine elicits cross-protection against the complete panel of monovalent PorA strains. Similar results have been found before [104], but toxicity was not addressed despite presence of toxic LPS. The sOMV vaccine in this study combines broad cross-protection with confirmed low toxicity. The low cross-protection observed for ΔRΔL-nOMV and ΔR-dOMV can be caused by decreased amounts of bactericidal lipoproteins with low antigenic variability, like factor H binding protein or GNA2132 [73, 94, 127, 128]. Detergent treatment of ΔR-dOMV removes all lipoproteins from the vaccine, while EDTA extraction (ΔRΔL-nOMV) destabilizes the outer membrane [111]. This destabilization causes loss of LPS (as confirmed in table 1) [129], but may also decrease lipoprotein content. It is

established that ΔRΔL-sOMV has improved overall functional immunogenicity, however with a lower OMV yield than ΔRΔL-nOMV.

In addition to yield, toxicity and immunogenicity, OMV aggregation is an important criterion for selection of a preferred vaccine development strategy. To obtain regulatory approval it is required to ensure consistent product quality throughout the manufacturing lifetime [130]. Due to lack of homogeneity, aggregated OMV vaccines are likely to impose difficulties. One month after purification, aggregation percentages were low for vaccines from detergent-free processes (nOMV and sOMV) resulting in well-defined vesicle size, while detergent extraction (dOMV process) resulted in outer membrane aggregates with significant size heterogeneity (Figure 3B). Such aggregation has not been reported for dOMV vaccines that were used to control epidemics in Norway, Cuba and New Zealand [50, 51, 53], however these vaccines were produced with large-scale, optimized processes. dOMV aggregates can be separated from intact vesicles with a filtration step, but this results in major yield loss. The observed aggregation can be explained with the data in Table 1, where detergent treatment selectively removes negatively charged LPS and PL molecules. This is likely to promote aggregation, since neutralization of OMV surface charge eliminates electrostatic repulsion [96, 131, 132]. The aggregation effect is not fully understood nor controlled, resulting in a dOMV vaccine that is less attractive for process development than nOMV or sOMV vaccines. Another argument to avoid using DOC in the dOMV process is its animal origin.

OMV vaccines from a detergent-based purification process (dOMV vaccines) give adequate protection in humans [50, 51, 53, 88] however the present work indicates that detergent-free alternatives provide highly reduced OMV aggregation and comparable yield and toxicity. In addition, improved cross-protection is observed. The use of detergent-free OMV purification processes is enabled by the *lpxL1* mutation, which genetically attenuates LPS toxicity [6]. OMV yield of all purification processes improves significantly by introducing the *rmpM* deletion, which increases feasibility of the sOMV process for further process development. The presented results substantiate that OMV from a bacterial strain with both genetic modifications (*lpxL1* and *rmpM*), made with a detergent-free purification process (either nOMV or sOMV) are the best available approachs for vaccine development. It may provide vaccines that are broadly protective against *N. meningitidis* serogroup B and potentially safe for parenteral use in humans.

Acknowledgments

Chapter 3

●●

Unbiased selective isolation of protein N-terminal peptides from complex proteome samples using phospho tagging (PTAG) and TiO$_2$-based depletion

Bas van de Waterbeemd[‡,1]
Geert P.M. Mommen[‡,1,2,3]
Hugo D. Meiring[1]
Gideon Kersten[1]
Albert J. R. Heck[2,3]
Ad P.J.M. de Jong[1]

[‡] Both authors contributed equally
[1] Institute for Translational Vaccinology (Intravacc), Bilthoven, The Netherlands
[2] Biomolecular Mass Spectrometry and Proteomics, Bijvoet Center for Biomolecular Research and Utrecht Institute for Pharmaceutical Sciences, Utrecht, The Netherlands
[3] Netherlands Proteomics Centre, Utrecht, The Netherlands

Abstract

A positional proteomics strategy for global N-proteome analysis is presented based on phospho tagging (PTAG) of internal peptides followed by depletion by titanium dioxide (TiO_2) affinity chromatography. N-terminal and lysine amino groups are initially completely dimethylated with formaldehyde at the protein level, after which the proteins are digested and the newly formed internal peptides modified with the PTAG reagent glyceraldhyde-3-phosphate in nearly perfect yields (> 99%). The resulting phospho-peptides are depleted through binding onto TiO_2, keeping exclusively a set of N-acetylated and/or N-dimethylated terminal peptides for analysis by LC-MS/MS. Analysis of peptides derivatized with differentially labeled isotopic analogues of the PTAG reagent reveals a high depletion efficiency (> 95%). The method enables identification of 753 unique N-terminal peptides (428 proteins) in *N. meningitidis* and 928 unique N-terminal peptides (572 proteins) in *S. cerevisiae*. These include verified neo-N-termini from subcellular-relocalized membrane and mitochondrial proteins. The presented PTAG approach is therefore a novel versatile and robust method for mass spectrometry-based N-proteome analysis and identification of protease-generated cleavage products.

Introduction

In shotgun proteomics, proteins are digested into peptides, typically using trypsin as protease, separated by liquid chromatography and analyzed by online-coupled tandem mass spectrometry (LC-MS/MS). Identifying significant portions of all proteins present in complex samples by LC-MS remains a major challenge, even for advanced proteomics workflows [133]. To address the challenges, new concepts in sample preparation have been proposed, aiming at reduction of sample complexity while preserving the proteome fingerprint [134-136]. The most useful methods for this purpose yield a single, positional-defined peptide for each individual protein. McDonald and Beynon argued that the two most obvious positional locations within every protein are the extreme ends, thus the N-terminal and the C-terminal peptides (positional proteomics) [134]. As a result of drastic sample simplification, positional proteomics analysis provides insights in a variety of post translational modification (PTM) processes and proteolytic processing which proteins may undergo at their N-terminal and C-terminal ends [137, 138].

Positional proteomics strategies rely on the ability to differentiate between the N- or C-terminal parts of a protein and the internal counterparts [139, 140]. Protocols for targeted enrichment of C-terminal peptides have only recently been introduced [141, 142], mainly due to lower chemical reactivity of C-terminal carboxyl groups compared to N-terminal amino groups. Gevaert *et al.* [136, 143] introduced the well-established combined fractional diagonal chromatography (COFRADIC) technology. In their method, N-terminal sequences are distinguished and separated from the internal peptides by differential labeling of protein N-terminal amino groups on the one hand and the α-amino groups of internal proteolytic peptides on the other hand such that the latter obtain a shift in retention on reversed phase chromatography. To prevent the discriminative retention shift for N-terminal amino acid sequences, free amino groups of protein N-termini (α-amino) and lysine side chains (α-amino group) are protected by acetylation prior to digestion. Another negative selection approach, proposed by McDonald *et al.* [134, 135] involves the protective blocking of amino groups at the protein level followed by digestion and subsequent depletion of internal peptides by reaction with an amine reactive scavenger resin. Kleifeld *et al.* [144, 145] have developed terminal amine isotope labeling of substrates (TAILS) for the negative selection of N-terminal peptides and identification and quantification of proteolytic events. They used a novel water-soluble aldehyde polymer for the selective binding of α-amine containing internal peptides [146].

Positive selection methods employ a reversed approach [147]. These protocols are based on the incorporation of an affinity group (e.g. biotin) to the protein N-terminal amino groups, followed by digestion and enrichment of the modified N-terminal peptides [148, 149]. Unwanted cross-reaction with the side chain amino group of lysines is prevented by guanidination (lysine to homo-arginine conversion) at the protein level. Selective and complete lysine labeling on the protein level can be problematic, hence the group of Wells introduced an enzymatic approach to selectively label the protein N-terminal amino group in a single step [150]. A severe drawback of positive selection approaches is the loss of N-terminal peptides for proteins having naturally acetylated or otherwise modified N-termini, because these termini do not react with the affinity labeling agents.

Selective enrichment of N-terminal peptides constitutes a major challenge due to the consecutive sample preparation steps (i.e. protective labeling, purification and enrichment), each prone to side reactivity and sample losses. Moreover, tryptic protein digests contain many more internal peptides than N-terminal peptides, therefore posing high demands on the efficiency of depletion to prevent significant contamination of the final sample fraction with internal peptides [147]. For example, Timmer *et al.* [148] used NHS-activated biotin for the positive selection of protein N-termini, however it was stated that a substantial portion of positive identifications were observed as a result of nonspecific biotinylation [137]. In case of amine-reactive scavenger beads, multiple incubation steps were needed for effective coupling of internal peptides [135, 151]. Zhang *et al.* reported specific loss of histidine-containing N-terminal peptides when using NHS-activated sepharose [151]. In addition, histidine- and arginine-containing N-terminal peptides are generally underrepresented in N-terminomics when SCX is used for pre-enrichment prior to depletion of internal peptide [152]. N-acetylated N-termini, widely present in higher eukaryotes, can be enriched more easily using SCX fractionation (without derivatization chemistry), but unfortunately such approaches are blind for unmodified protein N-termini [153-155]. TAILS, however, used water-soluble aldehyde polymer for effective coupling and depletion of internal peptides in a single-step, thereby minimizing possible sample losses [144].

In view of the challenges associated with the enrichment of N-terminal peptides, a novel positional proteomics strategy was developed. The strategy utilizes a highly selective PTAG-labeling reagent for the modification of internal peptides, after initial protection of protein N-termini and lysine side chains. PTAG-derivatized peptides have similar properties as naturally phosphorylated peptides in terms of binding to titanium dioxide (TiO_2). Hence, the flow-through fraction of TiO_2 affinity chromatography is highly enriched in N-terminal peptides and could be directly analyzed by LC-MS/MS. It is demonstrated that PTAG is a straightforward and efficient N-proteome enrichment strategy due to the use of highly selective derivatization chemistry, both at the protein and peptide level, in combination with robust and easy-to-implement TiO_2 technology.

Materials and Methods

Cell culture

Neisseria meningitidis strain used in this study is a recombinant non-encapsulated variant of the group B isolate H44/76, with a nonfunctional *porB* gene and truncated *galE*-LPS [156]. Bacterial cultures were grown at 35 °C in a chemically defined medium (150 mL) in disposable, baffled 500-mL erlenmeyer shake flasks with vented closure (Nalgene, Rochester, NY, U.S.A.) by shaking at 200 rpm [156]. Cells were harvested by centrifugation at 13,000xg for 2 min at 4 °C and resuspended in TE buffer (0.1 M EDTA, 1 M Tris-HCl pH 8.0, Sigma Aldrich, Zwijndrecht, The Netherlands) containing 0.5 mg/ml lysozyme (Sigma Aldrich, Zwijndrecht, The Netherlands) and incubated at 4 °C for 3 minutes in this medium. Next, proteins were extracted with Trizol (Invitrogen, Blijswijk, The Netherlands) according to the manufacturer's protocol and stored at -80 °C prior to use. Outer membrane vesicles (OMV) from *N. meningitidis* (grown as described above) were released by adding EDTA extraction buffer (0.01M EDTA, 0.1M Tris-HCl pH 8.6) and further purified by consecutive centrifugation and ultracentrifugation steps, as described by van de Waterbeemd *et al.* (NOMV protocol) [156]. Concentrated OMV (approximately 100 μl sample, containing 1 mg total protein) were mixed with 1 mL Trizol reagent and proteins were extracted and stored as described above. *Saccharomyces cerevisiae* strain BJ5460 (LGC Standards, Almere, The Netherlands) was cultured in 150 mL YPD medium in baffled 500-mL erlenmeyer shake flasks with vented closure (Nalgene, Rochester, NY, U.S.A.) at 30 °C, by shaking at 200 rpm. Cells were harvested from 300 mL culture (OD_{590}=1.7) by centrifugation at 2,000xg for 5 min. Cells were washed three times with PBS and resuspended in 200 μL lysis buffer (2 M guanidine hydrochloride, 12 mM EDTA, 50 mM Tris-HCl, pH 7.5 (Sigma Aldrich, Zwijndrecht, The Netherlands) to which 5 μL protease inhibitor cocktail (Sigma Aldrich, Zwijndrecht, The Netherlands) was added. The cell suspension was subjected to three rounds of freeze-thaw cycles. Next, cleaned glass beads were added and cells were further disrupted by 6 vortex cycles with intermediate cooling steps (at 4 °C). Supernatants after each cycle were pooled and centrifuged at 2,000xg at 4 °C for 10 min. The resulting supernatant was incubated overnight with a 4-fold excess of acetone (v/v) at -20 °C and proteins were subsequently pelleted at 13,000xg at 4 °C for 10 min. The protein pellet was washed twice with acetone/water 4/1 (v/v), pelleted after each wash step as described before and dried for 5 min by vacuum centrifugation at room temperature.

Dimethylation of primary amines

The protocol for dimethylation of primary amines was adopted from Boersema *et al.* [157]. An aliquot corresponding to 100 μg of protein was dissolved in 100 mM KH_2PO_4 (the pH adjusted to 7.5) containing 4 M guanidine hydrochloride. Disulfide bridges were reduced by adding dithiotreitol (Sigma Aldrich, Zwijndrecht, The Netherlands) to a final concentration of 20 mM and incubated 37 °C for 30 min. Free thiol groups were alkylated by adding iodoacetamide (Sigma Aldrich, Zwijndrecht, The Netherlands) to a final concentration of 100 mM and incubation at room temperature for 30 min in the dark. Excess reagent was exhausted by the addition of dithiotreitol at a final concentration of 100 mM (incubated at 37 °C for 30 min). The free N-terminal and lysine amino groups were dimethylated by formaldehyde at a final concentration of 180 mM (CH_2O, Sigma Aldrich, Zwijndrecht, The Netherlands) in the presence of 30 mM freshly prepared sodium cyanoborohydride (NaCNBH$_3$, Sigma Aldrich, Zwijndrecht, The Netherlands)

at room temperature. Freshly prepared sodium cyanoborohydride at a final concentration of 30 mM was added after 1-h and 2-h time intervals and the sample was further incubated overnight. Subsequently, the mixture was diluted 4 times with water to decrease the guanidine hydrochloride concentration to less than 1 M and proteins were extracted by acetone precipitation as described above. Precipitated proteins were reconstituted in 15 μL of 100 mM KH_2PO_4 (pH 7.5) containing 4 M guanidine hydrochloride. Excess formaldehyde was exhausted by the addition 50 μL of 1 M ammonia hydroxide (Zwijndrecht, The Netherlands) and incubation at room temperature for 1 h. Ammonium hydroxide was removed by vacuum centrifugation at room temperature till dryness.

Protein digestion

Dimethylated proteins were (parallel) digested in 50μl 100 mM KH_2PO_4 (pH 7.5) and guanidine hydrochloride with a concentration of less than 1 M with either chymotrypsin (Roche, Woerden, The Netherlands) in 4 mM calcium chloride (Sigma Aldrich, Zwijndrecht, The Netherlands) at 37 °C, trypsin (Promega, Leiden, The Netherlands) at 37 °C or endoprotease GluC (Roche, Woerden, The Netherlands) at room temperature, all with an enzyme/protein ratio of 1/20 (w/w). After 1 h, digest mixtures were diluted twice with 100 mM KH_2PO_4 (pH 7.5) to reduce to guanidine concentration to less than 0.5 M. Fresh enzyme was added at a enzyme/protein ratio of 1/20 w/w and the mixture was further incubated overnight at similar temperature conditions as described above.

Removal of pyroglutamate

N-terminal glutamine was enzymatically cyclized by glutamine cyclotransferase (Qcyclase, Qiagen, Venlo, The Netherlands) and the formed pyroglutamyl moiety was subsequently cleaved by the aminopeptidase pGAPase (Qiagen, Venlo, The Netherlands). This protocol was adapted from Staes *et al.* [152], with adjustment of the incubation time to 2 h at 37 °C.

Preparation of PTAG derivates

The free amino groups of the internal peptides were PTAG derivatized in 100 mM KH_2PO_4 (pH 7.5) with DL-glyceraldehyde-3-phosphate (Sigma Aldrich, Zwijndrecht, The Netherlands) at a final concentration of 90 mM and freshly prepared sodium cyanoborohydride in a final concentration of 30 mM at room temperature. Freshly prepared sodium cyanoborohydride was added at 1h and 2h intervals and the reaction mixture was further incubated overnight. Following PTAG derivatization, peptide mixtures were extensively purified by C18 solid phase extraction (SPE) chromatography (column dimensions 5 cm (L) x 200 µm inner diameter (ID), in-house packed with 5 µm Reprosil Pur C18-AQ, (Dr Maisch, Ammerbuch-Entringen, Germany).

Depletion of PTAG-peptides

PTAG-peptides were depleted by TiO_2 affinity chromatography, essentially as previously described [158, 159]. Briefly, SPE-purified samples were evaporated to dryness, reconstituted in 0.1 M acetic acid in water (pH 2.7) and loaded onto a short TiO_2 column at a flow rate of 5 μl/min (100 µl injection loop). The short TiO_2 column comprises of a 1-mm ID PEEK tubing with an Upchurch (Oak Harbor, U.S.A.) 360-mm ID adapter at the front and end for connection to (fritted) micro-capillary tubing and is slurry-packed with a 10-mm (L) bed of 5 μm Titansphere particles (10 mg) (GL Sciences, Tokyo, Japan). Unretained peptides were collected in the void volume. Next, the TiO_2 column was extensively washed with a 100-μl plug (3 column volumes) of acetonitrile/

water/dimethyl sulfoxide in 0.1 M acetic acid (45/45/10/, v/v/v) (Sigma Aldrich, Zwijndrecht, The Netherlands). The TiO_2 flow-through fraction and the wash fraction were pooled, evaporated to dryness by vacuum centrifugation and reconstituted in formic acid/DMSO in water (5/5, v/v) and stored at -20 °C until analysis.

LC-MS/MS analysis

N-terminal peptides-enriched samples (TiO_2 flow-through fraction) were pre-fractionated offline (6-14 fractions) using a mixed bed anion-cation column as described by Motoyama *et al.* [160] or directly analyzed on an LTQ-Orbitrap XL instrument (Thermo Fisher Scientific, Bremen, Germany) and Agilent 1100 HPLC system (Agilent, Amstelveen, The Netherlands) modified for nanoflow LC separations as described previously by Meiring *et al.* [161]. All columns were packed in house. The trap column was a 100-μm ID fritted micro-capillary packed with 20 mm, 5 μm particle size Reprosil Pur C18-AQ particles (Dr. Maisch, Ammerbuch-Entringen, Germany). The analytical column was a 50-μm ID microcapillary packed with 31 cm 3 μm particle size Reprosil Pur C18-AQ, with an integral-pulled tip and operated at a flow rate of 125 nL/min. ESI voltage, typically 1.8 kV, was applied by liquid junction at the top of the column. Solvent A consisted of 0.1 M acetic acid (Sigma Aldrich, Zwijndrecht, The Netherlands) in deionized water (Milli-Q, Millipore, Amsterdam, The Netherlands) and solvent B of 0.1 M acetic acid in acetonitrile (Biosolve, Valkenswaard, The Netherlands). Gradients were as follows: 100% solvent A during sample loading (0-10 min, flow rate 5 μL/min), 7% to 26% solvent B in 160 minutes followed by an increase to 60% solvent B in 20 minutes and reconditioning with solvent A for 10 min (total runtime 200 min). The mass spectrometer was set to acquire full MS spectra (m/z 350 to 1,500) for mass analysis in the Orbitrap at 60,000 resolution (FWHM) followed by data-dependent MS/MS analysis (LTQ) for the top 5 or 7 abundant precursor ions above a threshold value of 10,000 counts. The normalized collision energy was set to 35%, isolation width to 2.0 Da, activation Q to 0.250 and activation time to 30 ms. The maximum ion time (dwell time) for MS scans was set to 200 ms and for MS/MS scans to 2500 s. Charge state screening and preview mode were enabled. Precursor ions with unknown and +1 charge states were excluded for subsequent MS/MS analysis. Dynamic exclusion was enabled (exclusion size list 500) with repeat set to 1 and an exclusion duration of 180 s. The background ion at m/z 391.284280 was used as lock mass for internal mass calibration.

Data analysis

The analysis of mass spectrometric RAW data was carried out using Proteome Discoverer 1.2 software (Thermo Fisher Scientific, Bremen, Germany) applying standard settings unless otherwise noted. MS/MS scans were searched against the *N. meningitidis* strain MC58 database (containing 2,003 entries, 2010, Uniprot) or the *S. cerevisiae* SGD database (http://www.yeastgenome.org, 2010, containing 5,821 entries) using SEQUEST (Proteome Discoverer 1.2, Thermo Fisher Scientific, Bremen, Germany). Precursor ion and MS/MS tolerances were set to 10 ppm and 0.8 Da, respectively. Decoy database searches were performed with False Discovery Rate (FDR) tolerances set to 5% and 1% for modest and high confidence filtering settings, respectively. The data were searched separately with either no enzyme, C-terminal trypsin cleavage specificity, C-terminal chymotrypsin cleavage specificity or C-terminal GluC cleavage specificity allowing five miss-cleavages because lysine cleavage is prevented by dimethyl modification. Cysteine

carbamidomethyl, N-terminal dimethylation and lysine dimethylation were set as fixed modifications while aspargine deamidation and methionine oxidation were set as variable modifications. Similar searches were performed for alternative modifications by substituting N-terminal dimethylation modification with acetylation, ammonia loss, no modification, glyceraldehyde-3-phosphate, and monomethylation (Supplemental Tables 3-5). N-terminal dimethylated, N-terminal acetylated and N-terminal monomethylated proline-starting peptide sequences with high confidence (Xcorr values > 2.2, false discovery rates < 1%), rank no. 1 and linear sequences within the first 70 amino acids were considered for manual data analysis. Peptides possessing charge states of 6+ and higher were excluded. True N-terminal peptides (initiator methionine and methionine cleavage) were kept in the final dataset as well as proteins with signal peptide or transit peptide cleavage sites. Peptidase cleavages sites were verified by prediction software [162] or previous data [163] (Supplemental Table 6-7). Annotated spectra are provided for proteins with only a single confident peptide identification (Supplemental spectra 1-2). The raw data files and protocols associated with this manuscript are available to the reader upon request.

Assessment of binding efficiency of PTAG-peptides

Synthesis of isotopically deuterium-labeled PTAG reagents was started from either D0-tetrahydrofuran or D8-tetrahydrofuran (Sigma Aldrich, Zwijndrecht, The Netherlands). 4-bromobutyl acetate was obtained by ring-opening of tetrahydrofuran and nucleophilic substitution (into the acetate ester) by incubation with 33% hydrobromic acid in acetic acid (Sigma Aldrich, Zwijndrecht, The Netherlands) at room temperature for 1 h. Tetramethylammonium salt of dibenzylphosphate was prepared from the drop wise addition of tetramethylammonium hydroxide into a solution of dibenzylphosphate in methanol/acetone 1/1 (v/v) (Sigma Aldrich, Zwijndrecht, The Netherlands) at -10 °C. Tetramethylammonium salt of dibenzylphosphate was refluxed with 4-bromobutyl acetate for 5 h in dioxane (Sigma Aldrich, Zwijndrecht, The Netherlands). The resulting dibenzyl-4-acetatebutyl phosphate was purified on silica and hydrogenated into dibenzyl-4-hydroxybutyl phosphate with 0.4 M sodium carbonate (Sigma Aldrich, Zwijndrecht, The Netherlands) in 1/1 (v/v) ethanol/water at room temperature for 24 h. The product was extracted from the ethanol/water mixture with dichloromethane and subsequently dried on anhydrous magnesium sulphate (Baker, Deventer, The Netherlands). Dibenzyl-4-hydroxybutyl phosphate was oxidized into dibenzyl-4-oxobutyl phosphate by the incubation with a catalytic amount of pyridinium chlorochromate (PCC, Sigma Aldrich, Zwijndrecht, The Netherlands) in dichloromethane at room temperature for 1 h. Dibenzyl-4-oxobutyl phosphate was purified on silica gel and the dibenzylphosphate functionality was reduced by a catalytic amount of 10% palladium on carbon (Sigma Aldrich, Zwijndrecht, The Netherlands) under a hydrogen atmosphere at room temperature for 1 h. The structure of the final products, D0-4-oxobutyl dihydrogen phosphate and D5-4-oxobutyl dihydrogen phosphate, were verified by NMR (JEOL (400 Mhz), Tokyo, Japan). Partial hydrogen/deuterium exchange was observed as a result of enolization of the deuterated carbonyl functionality. After equilibration of the enolization reaction (storage in water), a $\Delta M = 5.0$ Da between the isotopic variants was obtained. The TiO_2 binding efficiencies of the PTAG-peptides were evaluated using the in-house-synthesized, isotopically-labeled PTAG-reagents. An aliquot corresponding to 100 µg of protein from the OMV fraction of *N. meningitidis* was dimethylated as described above. Proteins were

digested with trypsin and free α-amines of internal peptides were PTAG derivatized with an equimolar mixture of D0-4-oxobutyl dihydrogen phosphate and D5-4-oxobutyl dihydrogen phosphate and the addition of freshly prepared sodium cyanoborohydride (as described above). Peptide mixtures were subjected to TiO_2 affinity chromatography (as described above) and the flow-through fraction was analyzed by LC-MS. Raw data files were converted to the NetCDF file format and imported into MsXelerator software package (v.2.9, MsMetrix, Maarssen, The Netherlands). Co-eluting mass spectral doublets with a ΔM of 5.0306 (PTAG-peptides) were extracted by the search algorithm as previously described by Meiring *et al.* [164].

Results

General description of N-proteome enrichment

A schematic overview of phospho tagging (PTAG) for global N-proteome analysis is depicted in Figure 1. The strategy starts with the denaturation of proteins by reduction and alkylation of cysteines to enhance the accessibility of amino groups for chemical labeling and erratic depletion of cysteine linkages in N-terminal peptides. Reductive dimethylation of primary amines using formaldehyde and sodium cyanoborohydride simultaneously blocks the free α-amines of protein N-termini, except when they are already in vivo blocked by N-acetylation, as well as ε-amines of the lysine side chains [157]. Subsequently, trypsination of the proteome will result in an
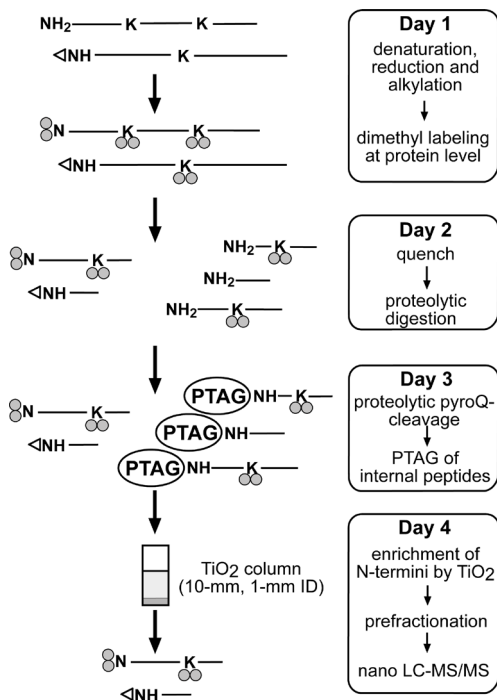
Figure 1. Workflow for recovery of N-terminal peptides with the PTAG strategy.
Protein samples are denaturated, cysteines reduced and alkylated, following by the reductive dimethylation of free α- and ε-amines (double grey dot) (day 1). Proteins are purified from excess reagent by acetone precipitation and remaining residual amounts are quenched by ammonium hydroxide. After proteolytic digestion (day 2), peptides with an N-terminal glutamine are enzymatically converted into pyroglutamate by Qcyclase and subsequently cleaved by pGAPase. Protein internal peptides are Phospho-tagged (PTAG) by the reaction with DL-glyceraldehyde-3-phosphate (GAP3) in the presence of cyanoborohydride (day 3). Peptide mixtures are subsequently desalted and excess reagents were removed by C18 solid phase extraction (SPE) chromatography. PTAG-peptides are depleted by TiO_2 affinity chromatography (day 4) for enrichment of dimethylated (grey double dot) and naturally acetylated (open triangle) in the flow-through fraction.

ArgC like digestion pattern as lysine cleavage is prevented due to the dimethyl modification, as previously shown [144]. The free N-terminal α-amines of the, upon digestion, newly generated internal peptides are susceptible for tagging with the PTAG reagent glyceraldehyde-3-phoshate (GAP3) (Figure 2). PTAG-labeled peptides are subsequently depleted through binding to TiO_2, with the flow-through fraction being highly enriched in N-acetylated and N-dimethylated peptides is analyzed by LC-MS/MS (Supplemental Figure 1). Confident protein assignment may be problematic in N-terminal peptide enrichment strategies because identification is inherently based on a single peptide, referred to as 'one-hit wonders' [165]. For this reason, parallel replicates of each proteome sample were digested with three different proteases (trypsin, endoprotease GluC and chymotrypsin) to generate overlapping N-terminal peptides with different lengths. In addition, N-proteome coverage is increased by the parallel use of proteases, because trypsin alone may generate N-terminal peptides of inappropriate length or poor ionization and fragmentation properties to be identified by LC-MS/MS [134, 154]. Despite the multiple digestion strategy, many proteins are expected to be identified based on a single peptide. To enhance confidence in protein assignment for these single peptide identifications, offline ion exchange pre-fractionation (typically 6 fractions) was performed in combination with high accurate MS analysis using an LTQ-Orbitrap to increase the number of MS/MS identification of a single peptide from technical replicates, different charge states and deamidation or oxidation states [144]. Also, stringent database search criteria were used (false discovery rates < 1%) to obtain high confidence in sequence assignment and annotated spectra for proteins with a single peptide identification are provided (Supplemental spectra 1-2).

Dimethyl labeling on the protein level

High efficiency in reductive dimethylation of N-termini and lysine side chains is critical to minimize erratic depletion of N-terminal peptides [145]. Protective labeling of these amino groups with formaldehyde was investigated for the standard protein Cytochrome C. Progress of the reaction was determined on the 6 available ε-amine groups of the chymotryptic acetylated N-terminal peptide Ac-GDVEKGKKIF. At 3-hour, the reaction yielded an incorporation of 5.9 methyl groups (98%) (Supplemental Figure 2). The reaction was driven to essentially quantitative by the addition of freshly prepared cyanoborohydride after 1-h and 2-h points followed by overnight incubation (data not shown).

Phospho tagging (PTAG) of internal peptides

PTAG-labeling of proteolytically generated internal peptides should reach completion to minimize co-purification of unmodified internal peptides in the final sample mixture. Evaluation of the derivatization reaction for the internal peptides generated from chymotryptic digestion
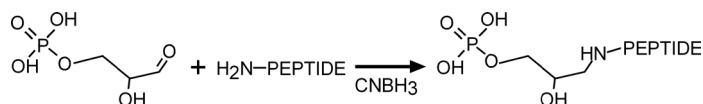

Figure 2. Phospho-tagging reaction scheme.
N-terminal α-amines of proteolytically generated peptides react with glyceraldehyde-3-phosphate (GAP3) into Schiffs bases that are rapidly reduced in the presence of cyanoborohydride. Note, ε-amines of lysine side chains are protected by dimethylation with formaldehyde and cyanoborohydride on the protein level.

of Cytochome C yielded > 99% efficiency without any side reactions. Similar results were found for a more complex (100 μg) trypsinated outer membrane vesicle (OMV) fraction from *N. meningitidis*. OMV are nano-sized spherical protein-lipid vesicles which can be used as a vaccine against serogroup B meningitis [3]. The main antigen present in OMV is the outer membrane porin A protein (PorA), which constitutes approximately 70% of the total protein content. For proteolytically digested OMV proteome, with abundances spanning several orders of magnitude, PTAG derivatization chemistry was nearly quantitative (> 99%). Despite the high labeling yields, unmodified residues could still be detected however at greatly reduced abundances (< 1%) compared to their PTAG-labeled analogues (Supplemental Figure 3). Slow and/or incomplete reactivity of proline-starting internal peptides, as reported by others [136, 152], was not observed for the PTAG reagent.
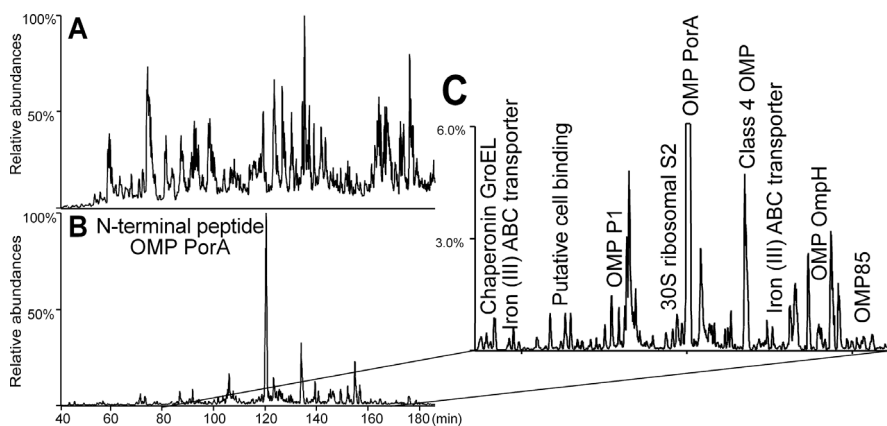
Figure 3.
LC-MS maps of proteolytic peptides (GluC) of *N. meningitidis* outer membrane vesicle (OMV) fraction before (A) and after (B) enrichment of N-terminal peptides. The protein composition of OMV is dominated by the outer membrane PorA protein, accounting for approximately 75% of the total protein content. N-terminal peptides of several proteins, including the high abundant N-terminus of PorA were recovered as predominant ion trace in the enriched sample fraction (B and C), indicating effective depletion of internal peptides.

Depletion efficiency of PTAG-peptides

The most critical step in positional proteomics is the effective depletion of internal peptides while maintaining maximum recovery of N-terminal peptides. The depletion efficiency of internal peptides for the PTAG strategy was evaluated for the chymotryptic digest of Cytochrome C (Supplemental Figure 4). The naturally acetylated N-terminal peptide of Cytochrome C (Ac-GDVEKGKKIF) was detected as the most predominant ion trace in the flow-through fraction. For the N-proteome analysis of complex proteome samples, a high capacity, offline TiO$_2$ affinity chromatography column was prepared in-house (slurry packed). Stringent washing conditions were applied to minimize nonspecific binding [166] (Supplemental Table 2). A 100-μg proteolytic digest of OMV was subjected to TiO$_2$ affinity chromatography (10 mg beads) and effective depletion of PTAG peptides was established in less than 20 minutes at a 1:100 peptide-to-beads ratio (w/w). This is illustrated by the substantial sample simplification of a proteolytic digest
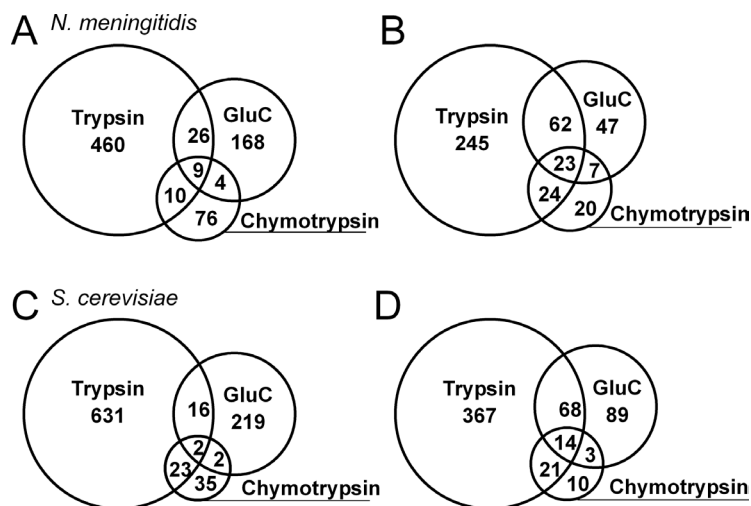
Figure 4.

Venn diagram comparing the number of identified unique N-terminal peptides (A, C) and assigned proteins (B, D) in *N. meningitidis* (combined OMV and whole cells fraction) and *S. cerevisiae*, respectively, by the (parallel) use of different proteases in the PTAG protocol. Both in *N. meningitidis* and *S. cerevisiae* the largest number of confident sequence assignments was obtained for trypsin with little overlap between GluC and chymotrypsin. Parallel digestion with GluC added approximately 25% unique N-terminal peptides and a 15% increase in proteome coverage, while the additional use of chymotrypsin may be superfluous for global N-proteome analysis.

of OMV fraction of *N. meningitidis* (Figure 3). After depletion of internal peptides, N-termini of several low abundant proteins were recovered as the most predominant base peak traces in the chromatogram along with the high abundant N-terminus of PorA. Evaluation of MS/MS-data revealed that PTAG-peptides with poor binding affinity were occasionally identified in the final sample (data not shown). However, identification of these peptides by data-dependent MS/MS analysis may not reflect the total fraction because identification is hampered by substantial neutral loss of phosphate during CID fragmentation [167]. For this purpose, D0- and D5-labeled analogues of the PTAG reagent were synthesized in-house and employed to discriminate PTAG peptides by their unique 5-Da mass difference (doublets) from N-terminal peptides (singlets). In a single LC-MS/MS analysis of a N-terminally enriched OMV sample, approximately 5% of all peptides ions were assigned as poorly retained PTAG peptides (Supplemental Figure 5), thereby again demonstrating the high efficiency in depletion even for complex and high dynamic range proteome samples.
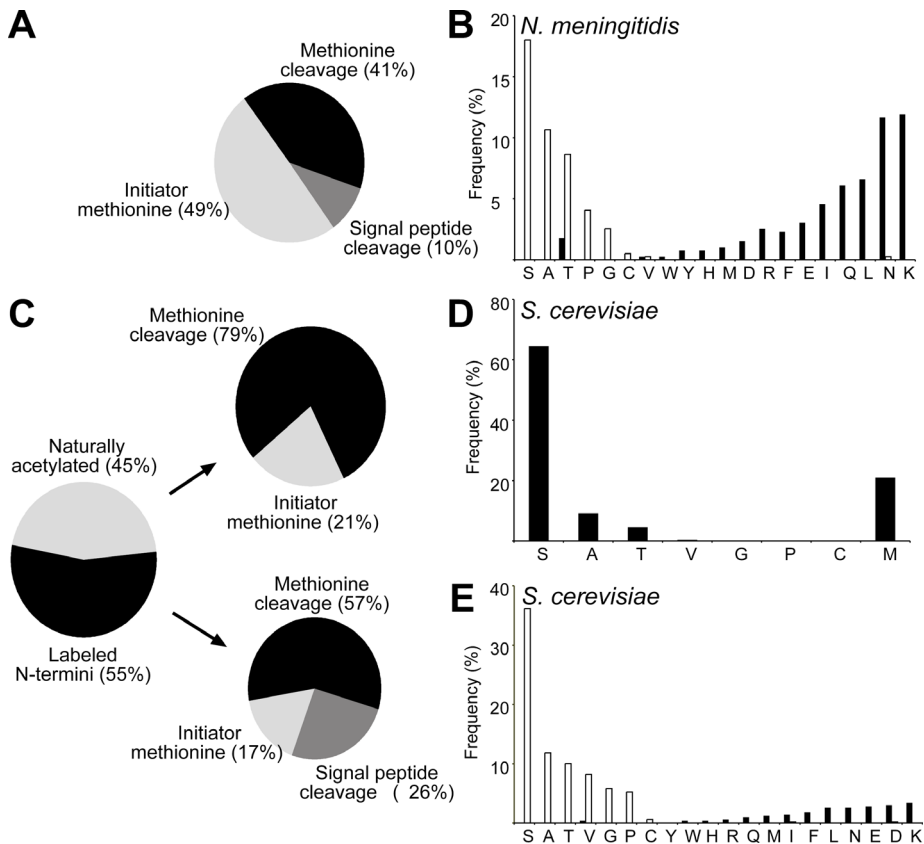
Figure 5. Distribution of N-terminal modifications in mature protein N-termini.
Protein N-termini in *N. meningitidis* are assigned as retained initiator methionine, methionine cleavage and proteins with signal peptide cleavage (A). Frequency distribution of the position 2 (P2) amino acid for removed initiator methionine (open bars) and retained methionine (black bars) (B). Methionine removal is preferred for small and uncharged residues at the P2 position. For *S. cerevisiae*, protein N-termini were identified as naturally acetylated (45%) and free N-termini, which are dimethylated in the PTAG protocol (labeled N-termini, 55%). From the pool of acetylated proteins, 79% showed the methionine cleavage while 21% retained the methionine residue. Frequency distribution of naturally acetylated amino acids at the protein N-termini (D). Labeled N-termini are annotated as retained initiator methionine, methionine cleavage and proteins with signal/transit peptide cleavage (C). Methionine cleavage (open bars) is similar to prokaryotes preferred for small and uncharged residues at the P2 position (E).

Peptide modifications

The results of the PTAG strategy applied to a tryptic whole cell lysate of *N. meningitidis* are summarized in Table 1. In total, 645 unique N-terminal dimethylated peptides were identified by offline ion exchange pre-fractionation (6 fractions) of the TiO$_2$ flow-through fraction and subsequent LC-MS/MS analysis. Of these N-terminal-dimethylated peptides, 423 peptides (312 proteins) were annotated as true protein N-terminal peptides with initiator methionine residues, methionine cleavage sites and proteins with signal peptide cleavage sites. Redundancy was especially observed for high abundant proteins. Multiple unique N-terminal peptides per protein were identified as a result of incomplete initiator methionine or signal peptide processing or

unspecific C-terminal cleavage specificity of trypsin. The remaining 222 N-terminal-dimethylated peptides are so-called neo-N-termini derived from internal cleavage sites throughout the protein. Neo-cleavage sites may originate from unknown proteolytic activity before (in vivo) or during harvesting (cell lysis), or from protein degradation during sample preparation [168]. The high labeling efficiency of the method is underlined by the identification of only 45 unmodified internal peptides (free α-amine). These peptides lack a PTAG affinity label as a result of incomplete derivatization chemistry, but are detected in dramatically reduced abundance compared to their PTAG-labeled analogues (Supplemental Figure 3). Cyclized N-termini are also enriched in the TiO$_2$ flow-through fraction because these peptides lack a free α-amine for PTAG derivatization. Especially N-pyroglutamyl residues were frequently identified during method development (data not shown). Staes *et al.* [152] introduced a method to generate a free α-amine (for subsequent labeling) by enzymatic cyclization of N-terminal glutamine (Qcyclase) and subsequent cleavage (pGAPase) of the formed N-pyroglutamyl moiety. This method was successfully implemented

Table 1. N-proteome analysis of tryptic N. meningitidis and tryptic S. cerevisiae using the PTAG strategy.
The number of unique[a] N-dimethyl- or N-acetyl-modified peptides are listed. Dimethylated N-terminal peptides include (true) protein N-terminal peptides and neo-N-terminal peptides with unknown cleavage specificity from e.g. (in vivo) proteolytic activity. Only N-dimethylated peptides which are assigned to as (true) protein N-termini indicated by retained initiator methionine, methionine cleavage and proteins with signal/transit peptide cleavage are used for further data evaluation. The TiO2 flow-through fraction was co-purified with N-unmodified (internal) peptides (lacking a PTAG due to incomplete derivatization), N-terminally cyclized peptides (N-pyroglutamate, N-pyrocarbamidomethyl cysteine and N-aspargine (P2)) and N-monomethylated peptides.

N-dimethylated or N-acetylated peptide modifications	N. meningitidis whole cells	N. meningitidis OMV fraction	S. cerevisiae whole cells
N-dimethylated peptides, incl. internal cleavages sites	645	897	776
N-dimethylated peptides assigned to protein N-termini	423	215	388
N-acetylated peptides assigned to protein N-termini	–	–	333
Number of proteins identified by N-terminal peptides	312	170	470

Co-purified peptide modifications	N. meningitidis whole cells	N. meningitidis OMV fraction	S. cerevisiae whole cells
N-unmodified (internal) peptides	45	154	187
N-pyroglutamate[b]	14 (12)	6 (5)	18 (17)
N-pyrocarbamidomethyl cysteine[c]	35	23	130
N-aspargine (P2) cyclized[d]	30	17	45
N-monometyl[e]	56	164	95

[a]Peptide deamination and oxidation states are not considered unique.

[b] N-terminal glutamate was enzymatically cyclized by Qcyclase to N-pyroglutamate and subsequently cleaved by pGAPase generating an α-amine for PTAG and depletion. This enzymatic approach is especially inefficient for peptides with a peptidase inhibiting proline (P2) residue next to N-pyroglutamate (depicted between brackets).

[c] Cyclization of N-terminal carbamidomethylated (iodoacetamide) cysteine residues.

[d] N-terminal cyclization of the asparagine side chain is restricted for position 2 (P2) residues.

[e] N-terminal monomethylation of internal peptides as a consequence of residual activity of the reagent formaldehyde during trypsin digestion.

in the PTAG strategy because only 14 N-pyroglutamyl peptides were identified of which 12 peptides had a pGAPase inhibiting proline residue following the pyroglutamyl cleavage site. Furthermore, 35 cyclized peptides with a N-terminal, iodoacetamine-alkylated cysteine residue (pyrocarbamidomethyl cysteine) [152] and 30 peptides where the position 2 aspargine side chain is N-terminally cyclized (X-Asn-X motif) [169] were recovered in the flow-through fraction.

For proline starting proteins [170], the N-terminus (initiator methionine cleavage) is incorporated by a single methyl group by protective labeling with formaldehyde (N-monomethylation). Data evaluation revealed that 56 peptides were N-monomethylated. Several peptides could successfully be assigned as true proline starting protein N-termini, however the vast majority of peptides was identified as internal peptides. It appeared that, due to residual activity of the reagent formaldehyde, proteolytically generated internal peptides were (inefficiently) labeled at the N-terminus by a single methyl group, thereby blocking subsequent PTAG derivatization.

The peptide identification results for tryptic OMV fractions from *N. meningitidis* and tryptic *S. cerevisiae* whole cells are in general similar as discussed above (Table 1). As expected, also quite a few N-acetylated termini (333) were detected in *S. cerevisiae* and none in *N. meningitidis*. Notably, a high number of neo-N-termini from internal cleavage sites were found for OMV in comparison to whole cell lysates. This high number may have been resulted from proteolytic activity upon cell lysis to stimulate OMV release or from protein degradation during OMV purification.

N-proteome characterization

The results of N-proteome enrichment of *N. meningitidis* and *S. cerevisiae* by the parallel use of trypsin, GluC and chymotrypsin are summarized in Figure 4. The results of the OMV fraction and the whole cell fraction of *N. meningitidis* largely overlap in terms of protein and peptide identifications (Supplemental Table 1). These data sets were combined to reduce the number of single peptide identifications ('one hit wonders') and hence reduce the chance of false positive peptide and protein identifications. In total, 753 unique N-terminal peptides were identified for *N. meningitidis* (428 proteins) predominantly by tryptic samples (Figure 4). The majority of the proteins (75%) were assigned by multiple MS/MS spectra of the same peptide at different charge states, deamidation or oxidation states or, more importantly, overlapping peptides with different lengths (Supplemental Table 1).

N-termini were assigned with retained initiator methionine, methionine cleavage sites and proteins with signal peptide cleavage (Figure 5A). Analysis of the native protein N-termini provide a profile for in vivo specificity of methionine removal (Figure 5B). This process depends on the amino acid at position 2 and is preferentially associated with the small and uncharged residues serine, alanine, proline, glycine and cysteine [170]. Furthermore, 123 neo-N-terminal peptides (43 proteins) were identified for proteins of which the signal peptide was removed (Figure 5A). The secretory signal peptide that targets a protein for translocation across membranes is typically 14-30 amino acids long and is removed by a signal peptidase upon translocation. Signal peptide cleavage sites of 43 identified proteins could be accurately verified by prediction software because cleavage is governed by distinct zones (basic N-terminus, a hydrophobic region and a C-terminal region) with high sequence consistency around the cleavage site [162].

N-proteome analysis of *S. cerevisiae* resulted in the identification of 928 unique N-terminal peptides that could be assigned to 572 proteins (Figure 4). Approximately 45% of the proteins were fully or partially N-acetylated, preferentially at alanine, serine, threonine and methionine (Figure 5C-D). Methionine cleavage specificity is conserved in prokaryotes and eukaryotes and preferential for small, uncharged residues at position 2 (Figure 5E) [162]. In addition, 125 neo-N-terminal peptides (71 proteins) were identified for mitochondrial proteins of which the transit peptide was cleaved. Hallmarks for transit peptides cleavages are less well-described and predictable than those for signal peptides in prokaryotes [162]. The sequence consistency around the cleavage site is low, with arginine in position -3 or -2 relative to the cleavage site as the most common motif. For this purpose, accurate verification of peptidase cleavage site specificity was not performed by prediction [162], but instead a comparison was made with a recently published COFRADIC study. Vogtle *et al.* [163] characterized transit peptide cleavage specificity of an enriched mitochondrial protein fraction of *S. cerevisiae*. Identical cleavage sites were found for both positional proteomics strategies for the majority of the PTAG-identified mitochondrial proteins (46 out of 71 proteins).

Recent N-proteome enrichment procedures suffered from under-representation of histidine and arginine containing N-terminal peptides as a result of charge retention on SCX pre-enrichment or side reactivity of histidine residues with NHS-activated sepharose beads [151, 152]. To investigate possible undersampling, the frequency distribution of the amino acids (P2) following the N-terminal methionine was calculated for the experimental data as the theoretical proteome (protein-coding genes). The experimental data correlates reasonably well with the frequency distribution in the complete proteome set for both *N. meningitidis* as *S. cerevisiae*, demonstrating that the obtained data are representative for the global N-proteome (Figure 6).
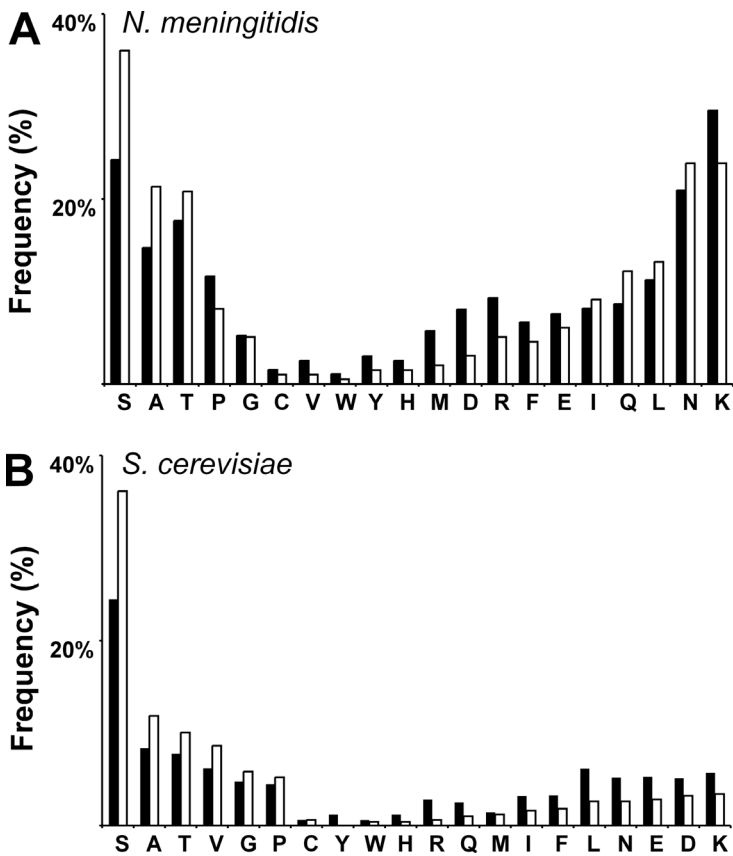
Figure 6.
N-proteome wide frequency distribution of the position 2 (P2) amino acid following the initiator methionine. The frequency distribution calculated for the complete set of proteins (protein-coding genes) is depicted in black bars and the frequency distribution for the experimentally identified protein N-termini is depicted in open bars. For both *N. meningitidis* (A) and *S. cerevisiae* (B), the experimental data correlates with theoretically data, indicating that the outcome the PTAG strategy is representative for the global N-proteome.

Discussion

In MS-based proteomics, complexity in protein samples greatly limits proteome coverage and identification of low abundant proteins [171]. Several advanced enrichment protocols have been introduced over the recent years to address this problem, including N-terminal positional proteomics strategies [140, 172]. Enrichment of N-terminal peptides by complete removal of internal peptides constitutes a major challenge [147]. PTAG was developed for specific labeling of free α-amines of internal peptides after proteolytic digestion. Subsequent, PTAG-labeled peptides were depleted by TiO$_2$ affinity chromatography (Figure 1). High labeling efficiency was established, both at the protein level and at the peptide level, essential for minimizing the loss of N-terminal peptides. Dimethylation by formaldehyde was preferred because it is inexpensive, resistant to hydrolysis and full labeling of protein N-termini and lysine side chains was accomplished (Supplemental Figure 2). In addition, the availability of stable isotopically labeled analogues of formaldehyde and cyanoborohydride enables multiplexed relative quantification in combination with PTAG [144, 157]. Internal peptides were selectively modified by the commercially available PTAG reagent glyceraldehyde-3-phosphate (GAP3). This reagent is similar to formaldehyde, resistant to hydrolysis and showed a high conversion yield (> 99%), thereby reducing possible background contamination of internal peptides (Supplemental Figure 3.). Excellent compatibility to reversed phase C18 ensured easy removal of salts and excess reagents prior to either TiO$_2$ affinity chromatography or direct LC-MS/MS analysis.

For the effective depletion of proteolytically generated internal peptides from a 100-μg proteome sample, a straightforward TiO$_2$-based depletion strategy was developed using in-house slurry-packed columns and including stringent washing conditions to minimize nonspecific adsorption [166] (Supplemental Table 2). The ability to efficiently reduce sample complexity and identify a large number of proteins (207 proteins) in the outer membrane vesicle (OMV) fraction of *N. meningitidis*, with dynamic range spanning several orders of magnitude, underlines the excellent recovery and selectivity of this strategy (Figure 3). It should be noted that the final enriched sample fraction of this complex OMV digest is slightly biased by breakthrough of poorly retained PTAG peptides (5%). These peptides were assigned by employing stable isotopically labeled variants of the PTAG reagent (Supplemental Figure 5 and 6).

N-proteome analysis of *N. meningitidis* and *S. cerevisiae* by the PTAG strategy resulted in the identification of 753 (428 proteins) and 928 (572 proteins) unique N-terminal peptides, respectively. Characterization of native protein N-termini provided a profile for *in vivo* specificity of methionine removal. This process is conserved in prokaryotes and eukaryotes and preferentially associated to small and uncharged residues (Figure 5) [173]. Furthermore, in *S. cerevisiae*, about 45% of the proteins were fully or partially N-terminally acetylated on alanine, serine, threonine or methionine (Figure 5), which is a similar percentage as recently found by others [174]. N-proteome data also include neo-N-termini from subcellular-relocalized membrane (43 proteins, *N. meningitidis*) or mitochondrial proteins (71 proteins, *S. cerevisiae*). Accurate assignment of protease substrate cleavage sites could be problematic because these cleavage sites are typically not annotated in protein sequence databases [175]. Moreover, co-purification of neo-N-termini generated from

background proteolytic activity with unknown specificity could result in the false positive identification of cleavage sites [144]. For this purpose, signal peptide and transit peptide cleavage specificity of the reported proteins were confirmed by either prediction [162] or by experimental data from a recent COFRADIC study [150].

Confidence in protein assignment may be problematic in N-proteome analysis as the majority of proteins are identified by a single peptide. Similar to other positional proteomics strategies [135, 176], pre-fractionation of the N-terminally enriched peptide fraction was performed to increase the number of MS/MS identifications per peptide and combined with strict database search criteria (FDR < 1%) to minimize the number false positive peptide identifications. Also, a number of proteases were used to generate N-terminal peptides with different lengths and hence not only enhance the confidence in protein assignment but also increase proteome coverage (Figure 3). It was estimated by in silico analysis that 50% of trypsin-generated N-terminal peptides could be analyzed by LC-MS/MS and parallel use of trypsin and GluC would increase coverage up to 80% [134, 147]. In practice, the increase in unique protein identifications for the use GluC in addition to trypsin is ~15% (Figure 3). This emphasizes one of the major challenges in N-proteomics: the identification of proteins by single N-terminal peptides with suitable LC-MS/MS characteristics, e.g. peptide length, hydrophobicity, ionization efficiencies and fragmentation properties. Alternative fragmentation techniques complementary to Collision Induced Fragmentation (CID) may be in particular beneficial in N-proteomics. A substantial fraction of the sample consists of long and highly charged N-terminal peptides with poor CID-fragmentation behavior. These long and highly charged peptides are generated by the ArgC digestion pattern of trypsin in combination with the remained ionic state of dimethylated lysine residues. Electron Transfer Dissociation (ETD) and Higher-energy Collisional Dissociation (HCD) have shown to be more effective for these highly charged peptides [177].

Recently, a number of large scale N-proteome studies for prokaryotes and *S. cerevisiae* were published. Timmer *et al.* [148, 149] characterized the N-proteome of *E. coli* by positive selection and identified 393 proteins, while Mc Donald *et al.* [134] identified more than 300 proteins in *E. coli* utilizing NHS-activated sepharose beads for depletion of internal peptides. N-proteome analysis of *S. cerevisiae* by COFRADIC in combination with SCX resulted in the identification of 650 unique N-terminal peptides [178]. Helbig *et al.* [179] characterized protein N-acetylation in *S. cerevisiae* with SCX and detected 756 N-acetylated protein termini, including acetylated neo-N-termini from internal cleavage sites. PTAG enabled the identification and characterization of 753 unique N-terminal peptides (428 proteins) in *N. meningitidis* and 928 unique N-terminal peptides (572 proteins), thereby representing one of the largest N-proteome datasets for these organisms so far. More detailed evaluations of *S. cerevisiae* N-proteome data provided by Helsens *et al.* [178], Helbig *et al.* [179] and N-proteome analysis by PTAG, revealed relative small overlaps between the studies (Supplemental Figure 6). The small overlaps are most likely due to undersampling of the full proteome or differences associated with the used method. For example, the study of Helbig *et al.* [179] was restricted to N-acetylated peptides while Helsens *et al.* [178] used SCX pre-enrichment with known undersampling of histidine containing N-terminal peptides [151, 152]. For N-proteome analysis by PTAG there is no indication of undersampling of certain amino acid sequences (Figure 6). However, a clear disadvantage of the PTAG strategy is the inability

to recover N-termini of proteins of which the N-terminal domain is phosphorylated by nature. N-terminal phosphorylation has for example been demonstrated in the p53 tumor suppression protein [180] and several crucial proteins of the photosystem II (PSII) in *A. thaliana* [181].

In conclusion, the PTAG positional proteomics strategy greatly reduces sample complexity, while maintaining the N-proteome fingerprint of whole cell lysates. The use of commercially available and highly reactive PTAG reagents in combination with high performance TiO_2 affinity chromatography provide a robust platform for global N-proteome analysis and MS-based profiling of proteolytic events. PTAG for unbiased selective isolation of protein N-termini is therefore a welcome alternative to well-established positional proteomics strategies.

Acknowledgments

Chapter 4

Quantitative proteomics reveals distinct differences in the protein content of outer membrane vesicle vaccines

Bas van de Waterbeemd[‡,1]
Geert P.M. Mommen[‡,1,2,3]
Jeroen L.A. Pennings[4]
Michel H. Eppink[5]
René H. Wijffels[5]
Leo A. van der Pol[1]
Ad P.J.M. de Jong[1]

‡ Both authors contributed equally
1 Institute for Translational Vaccinology (Intravacc), Bilthoven, The Netherlands
2 Utrecht Institute for Pharmaceutical Sciences and Bijvoet Center for Biomolecular Research, Utrecht, The Netherlands
3 Netherlands Proteomics Centre, Utrecht, The Netherlands
4 National Institute for Public Health and the Environment, Centre for Health Protection Research, Bilthoven, The Netherlands
5 Wageningen University, Bioprocess Engineering, Wageningen, The Netherlands

Abstract

At present only vaccines containing outer membrane vesicles (OMV) have successfully stopped *Neisseria meningitidis* serogroup B epidemics. These vaccines however require detergent-extraction to remove endotoxin, which changes immunogenicity and causes production difficulties. To investigate this in more detail, the protein content of detergent-extracted OMV is compared with two detergent-free alternatives. A novel proteomics strategy has been developed, which allows quantitative analysis of many biological replicates despite inherent multiplex restrictions of dimethyl labeling. This enables robust statistical analysis of relative protein abundance. The comparison with detergent-extracted OMV reveals that detergent-free OMV are enriched with membrane (lipo)proteins and contain less cytoplasmic proteins due to a milder purification process. These distinct protein profiles are substantiated with serum blot proteomics, confirming enrichment with immunogenic proteins in both detergent-free alternatives. Therefore, the immunogenic protein content of OMV vaccines depends at least partially on the purification process. This study demonstrates that detergent-free OMV have a preferred composition.

Introduction

The use of outer membrane vesicles (OMV) is a promising approach for vaccine development against *Neisseria meningitidis* serogroup B, which causes acute and severe meningitis [18, 50, 51, 53, 182]. OMV consist of a phospholipid bilayer with outer membrane proteins, endotoxin and a lumen with periplasmic proteins [89, 183]. Outer membrane porin A protein (PorA) was identified as the dominant antigen in OMV, but is antigenically variable between circulating strains [57, 58]. To obtain a broadly protective vaccine, recombinant strains with multiple PorA subtypes were developed [5, 7]. Recent studies demonstrated that conserved minor antigens, like factor H binding protein (fHbp, a lipoprotein) or iron-regulated membrane proteins, can complement PorA to further improve cross-protection [63, 64, 71]. In addition to well-described antigens the OMV proteome contains a considerable number of other proteins that may be relevant for immunogenicity [184].

The first OMV vaccines were prepared with detergent-extraction (dOMV) and have successfully stopped *N. meningitidis* serogroup B epidemics in several countries [49-54, 61]. The detergent-extraction was required to remove endotoxin, but removed lipoproteins as well, and caused partially intact and aggregated vesicles [61, 185]. The *lpxL1* mutation successfully attenuated meningococcal endotoxin and allowed a detergent-free process for vaccine development [6, 70]. A detergent-free process either uses extraction with a chelating agent to improve yield (*native* OMV; nOMV) [111, 186-189], or no extraction at all (*spontaneous* OMV; sOMV) [94, 97, 190]. It was found that detergent-free OMV retain lipoproteins like fHbp, which improved cross-protection and functional immunogenicity in mice [63, 104, 185, 191]. These immunological properties of OMV vaccines were measured with SBA (serum bactericidal activity), which is an established correlate of protection in humans but does not provide in-depth information at the protein level [46, 192].

Proteomics has been used to assess the protein content of OMV in more detail. Initial studies on dOMV from *N. meningitidis* serogroup B used gel electrophoresis combined with LC-MS/MS peptide identification [97, 193-195]. One study revealed that dOMV and sOMV vaccines have a different protein content [104]. More recently, quantitative 2D gel analysis with fluorescent labeling identified a limited number of differential proteins in dOMV after growth on two media [196]. Gel-based proteomics however is labor intensive and less compatible with hydrophobic membrane proteins from OMV than a gel-free approach [197]. It also has a strong bias toward highly abundant proteins [198]. To overcome these limitations, several gel-free quantitative proteomics methods have been developed [133, 157, 199]. Compared to other quantitative methods, multiplex dimethyl labeling of amino groups on N-termini and lysine residues is fast, robust and inexpensive [157, 200]. When dimethyl labeling is performed at the protein level, the N-terminal part of the protein (blocked α-amino group) can be selectively purified from the internal peptides after proteolytic cleavage (free α-amino groups). [134-136, 201]. Such a positional proteomics strategy strongly reduces sample complexity and uncovers low-abundant peptides, while preserving the original proteome fingerprint.

Positional proteomics successfully addressed sample complexity issues observed with complex proteomes that are dominated by a few proteins, like human plasma or OMV [202, 203]. Recently the PTAG strategy (phospho-tag) was developed for this purpose, using glyceraldehyde-3-phosphate reagent to derivatize free amino groups of internal peptides after proteolytic cleavage [204]. PTAG-modified internal peptides were depleted with efficient titanium dioxide (TiO_2) affinity chromatography, which purified protein N-terminal peptides for consecutive LC-MS/MS analysis. This PTAG strategy identified 572 unique proteins of *S. cerevisiae* and 428 unique proteins of *N. meningitidis* by their N-terminal peptides, representing one of largest N-proteome data sets available for these organisms. The study included 170 unique proteins from *N. meningitidis* nOMV vaccine, but dimethyl quantification was not implemented.

This work describes the first quantitative proteome comparison of detergent-extracted OMV vaccines with two detergent-free alternatives. A novel quantification method was developed, based on dimethylation with stable isotopes and selective purification of N-terminal peptides. Distinct differences in protein content were observed, including several immunogenic proteins. These findings demonstrate that purification processes can change the protein content of OMV vaccines and support previously observed differences in functional immunogenicity.

Materials and methods

Strain, growth conditions and OMV purification

The *N. meningitidis* vaccine strain that was used is a recombinant variant of isolate H44/76 (serogroup B) [109], combining one wild type and two recombinant PorA antigens (trivalent PorA; subtypes P1.7,16; P1.5-1,2-2 and P1.19,15-1) with a non-functional *porB* gene [7]. The *cps* locus was deleted, resulting in a non-encapsulated phenotype with *galE*-truncated LPS. Additional deletions in *lpxL1* and *rmpM* genes were made to attenuate LPS toxicity and improve OMV yield, respectively [185]. Cultures were grown in chemically defined, iron-rich medium [4]. Erlenmeyer shake flasks with 150 mL medium were inoculated with 10 mL working seedlot (cells at OD_{590} = 1.5 ± 0.1; stored at -135ºC with glycerol). Pre-culture shake flasks were incubated at 35ºC, 200 rpm and 10 mL portions (OD_{590} of 1.5 ± 0.3) were used to inoculate secondary shake flasks. OD_{590} of the secondary flasks was monitored and bacteria were harvested for OMV purification after 5 hours of stationary growth. OMV vaccines were purified as described previously [185]. For OMV quality control, total protein concentration (>1.0 mg/mL; Lowry with Peterson's modification), PorA content (>50% of total protein) and vesicle size distribution (average size 70-110 nm; polydispersity index <0.20) were performed [112, 186]. As reported before, detergent-extraction caused aggregation of dOMV samples which resulted in high polydispersity. nOMV and sOMV vaccines did pass all quality criteria [185].

Dimethyl labeling and N-proteome enrichment

Protein was extracted from OMV vaccines with Trizol reagent (Invitrogen, The Netherlands). An OMV amount corresponding to 500 µg of total protein was used for each extraction. OMV sample volume was first reduced to 20-50 µL with a vacuum dryer before adding 500 µL Trizol. Protein was extracted according to manufacturer's protocol and the resulting pellets were stored at -80°C. Thawed pellets were dissolved in 50 µl buffer (100 mM KH_2PO_4, pH 7.5) containing 4M Guanidine-HCl. Total protein concentration was measured using the Lowry assay with Peterson's modification (sample was diluted at least 100-fold to prevent interference of guanidine with the assay). SDS-PAGE analysis confirmed comparable protein compositions before and after Trizol extraction (data not shown). Protein labeling, digestion and purification protocols (including the PTAG strategy) were described previously[204]. The dimethyl labeling strategy was adapted for relative quantification purposes. The common reference (equal amounts of protein from all experimental protein samples) and the individual experimental samples were incubated with either light formaldehyde label (CH_2O) or heavy label (CD_2O; Sigma Aldrich), respectively, with addition of sodium cyanoborohydride (Sigma Aldrich) for 24 h at room temperature. Each heavy labeled sample was pooled individually with light labeled common reference in a 1:1 (w/w) ratio and digested by trypsin under previously described conditions[204]. A sample aliquot was diluted 100 times in formic acid/DMSO in water (5/5/90, v/v) and stored at -20°C until further analysis. Peptide mixtures after trypsin digestion were PTAG derivatized and the N-terminal peptides were recovered/enriched in flow-through fraction of TiO_2 affinity chromatography. Samples were dried and reconstituted in formic acid/DMSO in water (5/5/90, v/v) and stored at -20°C until analysis.

Peptide search list compilation using data-dependent LC-MS/MS

A search list containing entries with unique combinations of peptide sequence, accurate mass and retention time window was obtained by data-dependent LC-MS/MS analysis [205, 206]. Common reference sample aliquots were collected both before and after PTAG depletion and subsequently fractionated by strong cation exchange (SCX). The common reference samples were loaded onto a biphasic 200μm ID trapping column packed with 20 mm 5 μm C18 resin (Reprosil Pur C18-AQ (Dr. Maisch, Ammerbuch-Entringen, Germany) and 20 mm 5μm SCX resin (Polysulphoethyl A, PolyLC Inc, Colombia, USA) in 0.1M HOAc at 5μL/min. Following RP-to-SCX transfer using 50% acetonitrille in 0.1M HOAc, peptide fractions were recovered by flushing the SCX bed step-wise with 2 μL plugs of potassium chloride in 0.1 mM acetic acid containing acetonitrile. Seven different acetonitrile concentrations were used in the plugs, ranging from 10 to 500 mM. Fractions were dried and reconstituted in formic acid/DMSO in water (5/5/90, v/v) and analyzed by LC-MS/MS. An LTQ-Orbitrap XL instrument (Thermo Fisher Scientific, The Netherlands) and Agilent 1100 HPLC system (Agilent, The Netherlands) was modified for nanoflow LC separations as previously described [207]. The trap column was a 100-μm ID fritted microcapillary packed with 20 mm, 5 μm particle size Reprosil Pur C18-AQ particles (Dr. Maisch, Germany). The analytical column was a 50-μm ID fritted microcapillary packed with 31 cm 3 μm particle size Reprosil Pur C18-AQ. The column effluent was directly electrosprayed into the MS using an in-house prepared, gold and conductive carbon coated fused silica tapered tip of ~2 μm (typically at 2.0 kV) [207]. Solvent A consisted of 0.1 M acetic acid in deionized water and solvent B of 0.1 M acetic acid in acetonitrile. Gradients were as follows: 100% solvent A during sample loading (0-10 min, flow rate 5 μL/min), 7% to 26% solvent B in 160 minutes followed by an increase to 60% solvent B in 20 minutes and reconditioning with solvent A for 10 min (total runtime 200 min). The mass spectrometer was set to acquire full MS spectra (m/z 350 to 1,500) for mass analysis in the Orbitrap at 60,000 resolution (FWHM) followed by data-dependent MS/MS analysis (LTQ) for the top 7 abundant precursor ions above a threshold value of 10^4 counts. The normalized collision energy was set to 35%, isolation width to 2.0 Da, activation Q to 0.250 and activation time to 30 ms. The maximum ion time (dwell time) for MS scans was set to 200 ms and for MS/MS scans to 2500 s. Charge state screening and preview mode were enabled. Precursor ions with unknown and +1 charge states were excluded for subsequent MS/MS analysis. Dynamic exclusion was enabled (exclusion size list with 500 entries) with repeat set to 1 and an exclusion duration of 180 s. The background ion at m/z 391.284280 was used as lock mass for internal mass calibration. Analysis of LC-MS/MS raw data was carried out with Proteome Discoverer 1.2 software (Thermo Fisher Scientific, Bremen, Germany) applying standard settings unless otherwise noted. MS/MS scans were searched against the *N. meningitidis* serogroup B database (Uniprot Knowledgebase, July 18th 2012) using SEQUEST. Precursor ion and MS/MS tolerances were set to 10 ppm and 0.8 Da, respectively. Decoy database searches were performed with False Discovery Rate (FDR) tolerances set to 5% and 1% for modest and high confidence filtering settings, respectively. The data were searched with full trypsin cleavage specificity, allowing 5 miss-cleavages (lysine cleavage is prevented by dimethyl modification). Cysteine carbamidomethyl and lysine dimethylation were set as fixed modifications, while asparagine deamidation and methionine oxidation were set as variable modifications. An additional search was performed using C-terminal trypsin cleavage specificity and implementation a fixed N-terminal dimethyl modification. High confidence peptide sequence identifications (Xcorr values >2.2, false discovery rate <1%, rank No.1) were

exported to an Excel data file (the peptide search list). Raw data files and protocols associated with this manuscript are available for the reader upon request.

High resolution peak quantification using LC-MS

Quantification experiments of light (common reference) and heavy (experimental sample) labeled peptide mixtures were performed on the full MS level, relying on the high mass accuracy of the Orbitrap (data-dependent MS/MS disabled). All analyses were performed with the same nano LC column and identical gradient conditions as described above for maximal chromatographic reproducibility. Light/heavy peptide mixtures prior to PTAG-labeling and TiO_2 purification (15 samples) and N-terminally enriched peptide mixtures after TiO_2 purification (15 samples) were directly analyzed by LC-MS.

Data processing for analysis of relative protein abundance

Relative peptide abundances were determined by using the high resolution LC-MS data in combination with the precompiled peptide search list (accurate mass and retention time approach) [205, 206]. Raw LC-MS data files were deconvoluted to mono-isotopic masses to minimize isobaric interference of contaminants using Xcalibur software (Thermo Scientific; XtractAll plug-in; MH+ mode; S/N threshold = 2) [208]. The output was saved in NetCDF format (Thermo file converter) and imported in MS-Xelerator (MSMetrix, The Netherlands). The MSX-Quant plug-in of this software traced and extracted the peak areas of all peptide entries of the pre-compiled Excel search list using accurate mass (±0.01 Da) and retention time (±10 min) information. Light/heavy peak area ratios were calculated from extracted ion chromatograms. Further data processing was performed in R (http://www.R-project.org). Individual MSX-Quant result files were compiled and stringent quality criteria were applied. A peptide search list entry was positively identified when both light and heavy labeled chromatographic peaks were extracted for at least 3 out of 5 independent biological replicates of at least 1 OMV vaccine type at an intensity threshold of $>10^4$ counts (above background noise). In addition, all chromatographic peaks were required to have an accurate mass deviation of <10 ppm and retention time window ±10 min compared to the search list entry. Starting with entries that were positively identified in any OMV vaccine type, it was determined whether or not these entries were identified in each of the three OMV vaccine types, by using the same quality criteria. The resulting lists of positively identified entries were mapped to corresponding peptides and proteins. The overlap between the respective lists per OMV vaccine type was visualized as Venn diagrams.

Statistical analysis of relative protein abundance

For quantification of relative protein abundance, the light/heavy ratio values of positively identified peptide search list entries were ^{2}log transformed. For entries with a positive identification (found in ≥3 out of 5 replicates) for an OMV type, missing values (due to quality issues) were imputed as the mean of detected values. OMV types with a negative identification for a search list entry (found in ≤2 out 5 replicates) were imputed with background values. Background values were calculated from the mean of the minimal value for that entry across all experimental samples and the minimal value for that experimental sample across all search list entries. This ensured that both sample and entry-dependent background levels were taken into account. Next, log-transformed values of search list entries that belonged to the same peptide were averaged, followed by averaging of values from peptides that belonged to the

same protein. The resulting protein expression data were analyzed across all OMV types with one-way ANOVA. This identified proteins that were differentially expressed between any of the OMV types (maximal Fold ratio >2 and p<0.001). This corresponded to a False Discovery Rate (FDR) of <1%. The expression values of differentially expressed proteins were visualized as a heat map using Genemaths XT (Applied Maths, Belgium). Functional annotations and keywords of identified proteins were adopted from Uniprot Knowledgebase, *N. meningitidis* strain MC58 (http://www.uniprot.org). A few entries were substituted with homologs from strain H44/76 or strain Alpha710, due to an outdated MC58 annotation. Predicted cellular locations were obtained with the PSORTb algorithm (http://www.psort.org/psortb) [209].

Serum blot proteomics

Female BALB/c mice were immunized subcutaneously on day 0 and 28 with either dOMV, nOMV or sOMV vaccine and sera were collected on day 42, as previously described [185]. SDS gel electrophoresis was performed with 4 μg total protein of each OMV vaccine per lane[185]. Gels were either stained with Novex Colloidial Blue (Invitrogen, U.S.A.) or blotted to nitrocellulose membranes and blocked with buffer containing 0.5% Protifar (Nutricia, The Netherlands). Blot membranes were incubated with pooled mice sera after immunization with the corresponding OMV vaccine (200x diluted), with monoclonal antibody against fHbp (NIBSC, United Kingdom) or with PorA P1.19 monoclonal antibody (Intravacc, The Netherlands). Goat-anti-mouse antibody conjugated to alkaline phosphatase was used as a secondary antibody for staining. The protocol for direct surface digestion of blotted proteins was adapted from Luque-Garcia *et al.* [210]. Differential serum bands were excised and incubated in 100 mM KH_2PO_4 (pH 7.5), 10% acetonitrille with trypsin at an enzyme/protein ratio of 1/20 (w/w) at 37°C for 16 h. Peptide mixtures were purified with RP/SCX solid phase extraction as described above (peptide search list compilation paragraph). LC-MS/MS conditions and data analysis were also similar as above, however with 90 min. LC gradients (7%–40% solvent B in 80 min). Cleavage specificity was set to full trypsin allowing 2 miss-cleavages. Aspargine deamidation and methionine oxidation were set as variable modifications. At least 2 unique, high-confidence peptides were required for protein identification and large deviations between theoretical and observed protein molecular weight on the immunoblot were not tolerated. Protein identifications that matched the immunoblot pattern were verified manually, to confirm presence of the corresponding tryptic peptides in the raw chromatographic data.

Results

Development of quantitative proteomics method

A novel quantitative proteomics method was developed based on duplex dimethyl labeling, combined with unbiased selection of N-terminal peptides (PTAG; phospho tagging)[204]. A detailed workflow is shown in Figure 1. Relative quantification was based on comparison of 15 experimental samples (3 different OMV vaccines; 5 biological replicates per vaccine) against a common reference (CR). The CR contained equal amounts of protein from all experimental samples. Samples for high-throughput quantification were collected after proteolytic digestion (all dimethylated peptides) and after PTAG depletion (N-terminal peptides). Quantification was performed with a two-step approach, using stringent quality criteria (Figure 2) [205]. The CR allowed an unrestricted number of biological replicates despite inherent multiplex restrictions of the dimethyl labeling (either duplex or triplex [157, 200]). As a result, each experimental group (OMV vaccine) had 3–5 independent measurements per peptide, allowing robust statistical analysis. Prior to OMV proteome analysis, the quantification method was successfully validated with a standard protein mixture containing known ratios (Appendix 1).

OMV protein identification and evaluation of PTAG procedure

The proteome analysis was performed on OMV vaccines from three different purification processes [185]. A total of 618 unique peptides were positively identified, 400 peptides in dOMV (detergent extraction), 509 peptides in nOMV (detergent-free extraction) and 497 peptides in sOMV (no extraction), with high reproducibility but moderate overlap between the three vaccines (282 peptides; Figure 3A). Merging of peptides with identical accession numbers yielded 185 unique proteins, of which 76 proteins were shared between the three OMV vaccines (Figure 3B). These results were obtained after merging of datasets from internal peptides and N-terminal peptides (S-Table 2B, Supporting Information). Added value of the PTAG strategy was evaluated by comparing the contribution of each dataset to the total number of detected peptides (Figure 3C) and proteins (Figure 3D). At the peptide level, the PTAG strategy resulted in detection of 86 unique N-terminal peptides, of which 62% was not detected before this procedure (53 N-terminal peptides). These 53 additional N-terminal peptides accounted for 7 additional proteins, which indicates that most of the N-termini found with the PTAG strategy belonged to proteins that were already detected by their internal peptides (before PTAG). Cellular location prediction (PSORTb algoritm [209]) did not reveal enrichment in protein groups that were either detected before (143 proteins) or after PTAG (7 proteins; Figure 3D). The 35 proteins that belonged to both groups were enriched with a membrane location (p<0.012). Since this group includes PorA, OpcA, PilQ and other major proteins of OMV, the observed enrichment is most likely related to protein abundance rather than a membrane location. A total of 42 proteins were identified by N-terminal peptides, of which 36 were positively verified. These N-termini were positioned at the first, second or SignalP predicted residue of the full protein sequence, or were cleaved after an AxA motif [297]. To account for unknown signal peptides, N-termini within the first 70 residues of the full protein sequence were also considered valid. The remaining 6 proteins were identified with degradation peptides from abundant proteins (e.g. PorA), which are also dimethylated during the PTAG procedure (neo N-termini). N-terminal peptides of lipoproteins were absent, due to a lipid modification that prevents dimethylation [74]. Details of the verification are provided in S-Table 2E (Supporting Information).
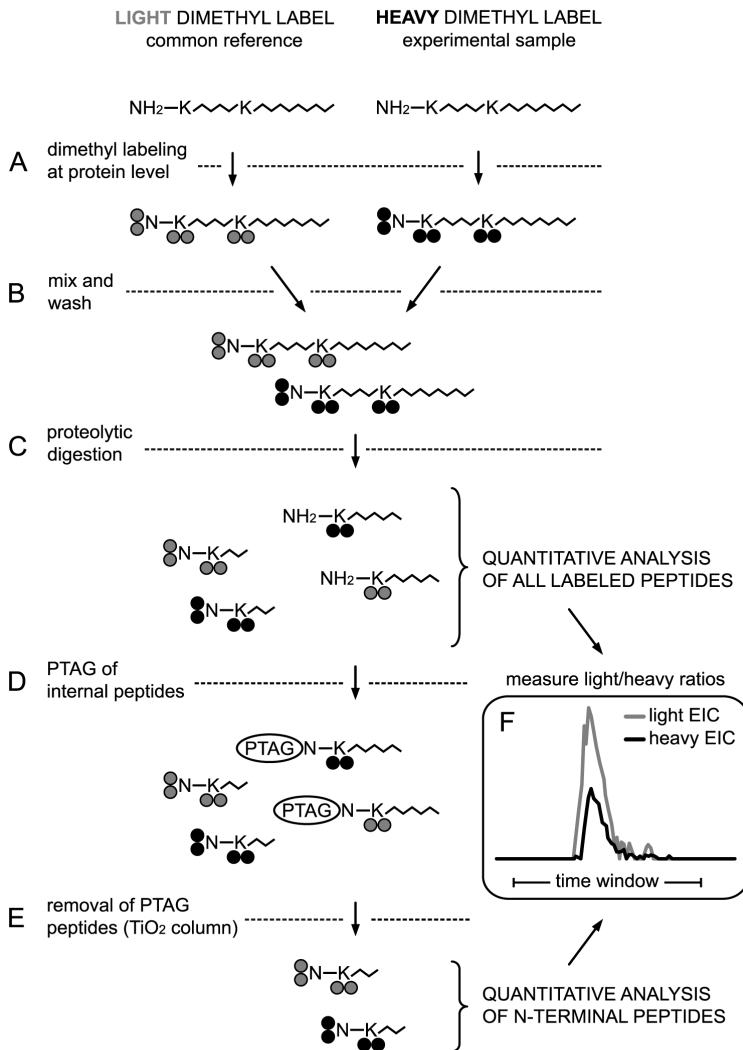
Figure 1. Workflow for purification of dimethylated N-terminal peptides with PTAG.
(A) First, the common reference is mixed from equal amounts of protein from all experimental samples. Free N-terminal and lysine amino groups of the common reference are dimethylated at the protein level with formaldehyde (CH_2O, light label). In parallel, experimental samples are dimethylated with heavy formaldehyde (CD_2O isotope, heavy label). (B) Light and heavy labeled samples are mixed and washed with acetone precipitation. (C) Proteolytic digestion with trypsin generates internal peptides with free N-terminal amino groups. (D) Internal peptides are derivatized on the N-termini with PTAG reagent. (E) PTAG peptides are captured with TiO_2 columns for selective purification of dimethylated N-terminal peptides. (F) Samples are collected after step C (all dimethylated peptides) and after step E (N-terminal peptides) for quantification of light/heavy peak ratios with nano LC-MS (Figure 2).

The dOMV vaccines contain cytoplasmic proteins as a result of lysis

Relative protein abundance of all 185 detected proteins (Figure 3B) was quantified to identify differences between the OMV vaccines. A good overall correlation between biological replicates was observed (R = 0.96, 0.90 and 0.90 for dOMV, nOMV and sOMV, respectively). Proteins were

A PEPTIDE IDENTIFICATION

- compiled search list with all detectable peptides
- stringent quality criteria
- example of detected peptide (PEP0357): HIGLAAKQ
- corresponding protein: factor H binding protein (F0MKC4)

B COMMON REFERENCE-BASED QUANTIFICATION

average of 5 biological replicates for each OMV vaccine

— common reference (CR)
— experimental sample

DOMV = 0.5*CR   NOMV = 1.25*CR   SOMV = 2.0*CR

NOMV/DOMV ratio = 2.5

SOMV/NOMV ratio = 1.6

SOMV/DOMV ratio = 4.0

Figure 2. Common reference-based peptide quantification using stringent quality criteria.
(A) High-throughput peptide identification was done with a two-step approach. First, the common reference (CR) was analyzed to compile a search list with accurate mass, retention time window and sequence ID of all detectable peptides (S-table 2B, Supporting Information) [205, 206]. Second, full LC-MS chromatograms were acquired for all light/heavy mixtures. The light (CR) peptides were traced with the peptide search list. Corresponding heavy (experimental) peptides were matched based on calculated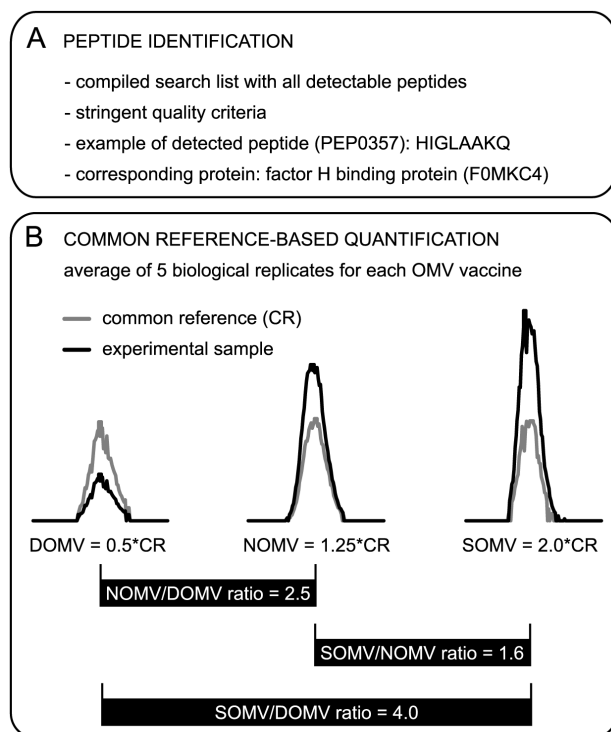 mass and retention time. Stringent criteria were required for a positive identification (see Material and Methods section). Search list entries that complied to these criteria nearly always provided a unique hit. (B) Peak areas were extracted for quantification of light/heavy ratios. The CR was used as an internal standard to calculate ratios between experimental samples, as illustrated for search list entry PEP0357, a peptide from factor H binding protein. After data processing, this protein had a low expression in dOMV compared to nOMV (2.5-fold higher) and sOMV (4.0-fold higher). Each detectable peptide in the search list was quantified with 3–5 independent biological replicates, allowing robust statistical analysis.

clustered in 7 groups based on their expression profile (Figure 4). Group VII contained 39 proteins that were detected without significant differences in relative protein abundance (therefore not shown in Figure 4). This group included several well-known membrane proteins like PorA, OpcA and FetA [43, 48]. Groups I to VI each had a specific expression pattern (e.g. downregulated in dOMV). Functional annotation revealed interesting differences. The 146 differentially expressed proteins in group I to VI together had 33 ribonucleoprotein annotations (from Uniprot keywords) of which 17 were found in group II (upregulated in dOMV; enrichment p-value <0.05). Group II was also significantly enriched in RNA-binding (14/23 annotations), nucleotide binding (9/17), cytoplasm (9/16) and transferase functions (7/12). These proteins originate from the cytoplasm and may be present exclusively in dOMV as a result of lysis, an undesired side-effect of detergent

extraction. Group III (upregulated in dOMV and nOMV) confirmed this hypothesis because it was also significantly enriched in ribonucleoprotein (12/33) and RNA-binding functions (7/23). This group however contained less proteins since nOMV purification (mild, detergent-free extraction) indeed caused less lysis than dOMV, but clearly more than sOMV (no extraction).

Detergent-free OMV vaccines are significantly enriched with membrane (lipo)proteins

The lysis-related results were further substantiated with cellular location predictions (PSORTb algorithm [209]), which confirmed that groups II and III indeed were enriched with cytoplasmic proteins. Group V (upregulated in detergent-free nOMV and sOMV vaccines) however was enriched with proteins that had a membrane location (21/40 annotations) or unknown location (21/34 annotations). Also, this group contained 6 out of 8 proteins with a lipoprotein annotation (all enrichment p-values <0.05). Proteins with such locations or functions are more likely to be relevant for the immunogenicity of OMV vaccines than lysis-derived cytoplasmic proteins. Notably, several oxidoreductases were found specifically in sOMV vaccines (group VI; 7/12 annotations). In addition to these redox-related proteins, sOMV vaccines contained proteins with non-enriched functions that are involved in iron uptake (e.g. heme utilization protein and
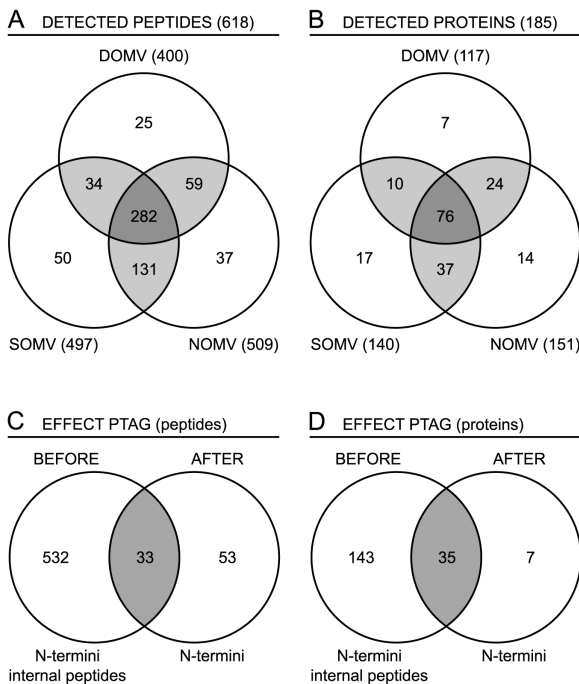
Figure 3. Venn diagrams of identified peptides and proteins.
(A) Peptide overlap between dOMV vaccine (detergent-extraction), nOMV vaccine (detergent-free extraction) and sOMV vaccine (no extraction). A moderate overlap of 282 out of 618 unique peptides was observed. (B) The peptides corresponded to 185 unique proteins, of which 76 were shared. (C) Assessment of the added value of PTAG depletion at the peptide level. A total of 53 N-terminal peptides out of 86 (62%) were uncovered by the PTAG procedure. (D) The additional N-terminal peptides represented only 7 additional proteins, since most proteins were already detected by their internal peptides. This indicates that OMV samples may not have sufficient complexity to challenge the PTAG procedure. S-Table 2 (Supporting Information) links the data in the Venn diagrams to corresponding peptides and proteins.

bacterioferritin BfrA, which is regulated in response to iron availability [211, 212]). Since sOMV are spontaneously released and most similar to natural OMV, these virulence-related proteins may be relevant for the pathogenicity of *N. meningitidis* [213]. Detailed protein information with expression data and functional annotation is available online as Supporting Information. An overview of the PSORTb location distribution per OMV vaccine is shown in Appendix 2.

Serum blot proteomics supports the quantitative proteomics results for several immunogenic proteins

Serum blot proteomics was performed to identify immunogenic proteins in the different OMV vaccines. Figure 5A shows the overall protein composition of the OMV vaccines after 1D gel electrophoresis, visualizing the major contributions of PorA (41 kD), Omp85 (85 kD) and several proteins at 27 kD (e.g. OpcA protein). As discussed above, these proteins were found in all OMV types without significant expression differences. Next, mice sera after two vaccinations were used for immunoblotting against corresponding OMV vaccines. Despite a heavy immuno-dominance of PorA at 41 kD the serum blots revealed clear differences in immunogenicity, especially for dOMV compared to nOMV and sOMV (Figure 5B). This indicated that the different OMV processes retained or removed specific immunogenic proteins. These immunogenic proteins were not visible with 1D gel electrophoresis, therefore they represent a small but potentially important portion of the total protein content.

Immunoblot bands with a differential pattern between OMV sera were excised and separately digested with trypsin, for qualitative LC-MS/MS analysis (serum blot proteomics). The analysis identified several proteins that matched the blot pattern (Figure 5C). At 41 kD, PorA was found abundantly on all blots. Lipoprotein E6MY46 (14 kD) was found on nOMV and sOMV blots, while LptD (LPS assembly protein; 85 kD) was unique for dOMV. In other sections no matching proteins were detected (100 kD, 50-70 kD and 15-20 kD) despite a differential serum blot pattern. Around 27 kD all serum blots had a visible band, but the bands for nOMV and sOMV were clearly more pronounced. Serum blot proteomics of this 27 kD band provided several interesting matches like PilQ, a protein involved in type IV pilus biogenesis and only found in nOMV and sOMV. Proteins Q7DDR0 (putative cell-binding factor) and Q9JYQ6 (uncharacterized protein) were found in nOMV and sOMV, and only in sOMV, respectively, but have not been described in literature. Two important identifications on the 27 kD blot section were fHbp and a C-terminal PorA fragment cleaved-off at the Pro_{268} position. These two immunogenic proteins were verified with monoclonal antibodies (Figure 5D). Detergent-extraction during dOMV purification is known to remove lipoproteins like fHbp[63, 94]. The anti-fHbp immunoblot confirmed that fHbp indeed was absent in dOMV. The blot with anti-PorA monoclonal confirmed an overall strong band at 41 kD and confirmed the C-terminal PorA fragment. This PorA fragment explains the weaker 27 kD band on the dOMV serum blot, while the presence of fHbp explains the stronger 27 kD bands on nOMV and sOMV serum blots. Notably, the serum blot identifications were in full agreement with the quantitative proteomics results. Only LPS assembly protein LptD was somewhat ambiguous. LptD was 5-fold higher in dOMV, which may be induced by the detergent-treatment and matches the serum blot results. The upregulation however was not significant (p-value just above threshold).
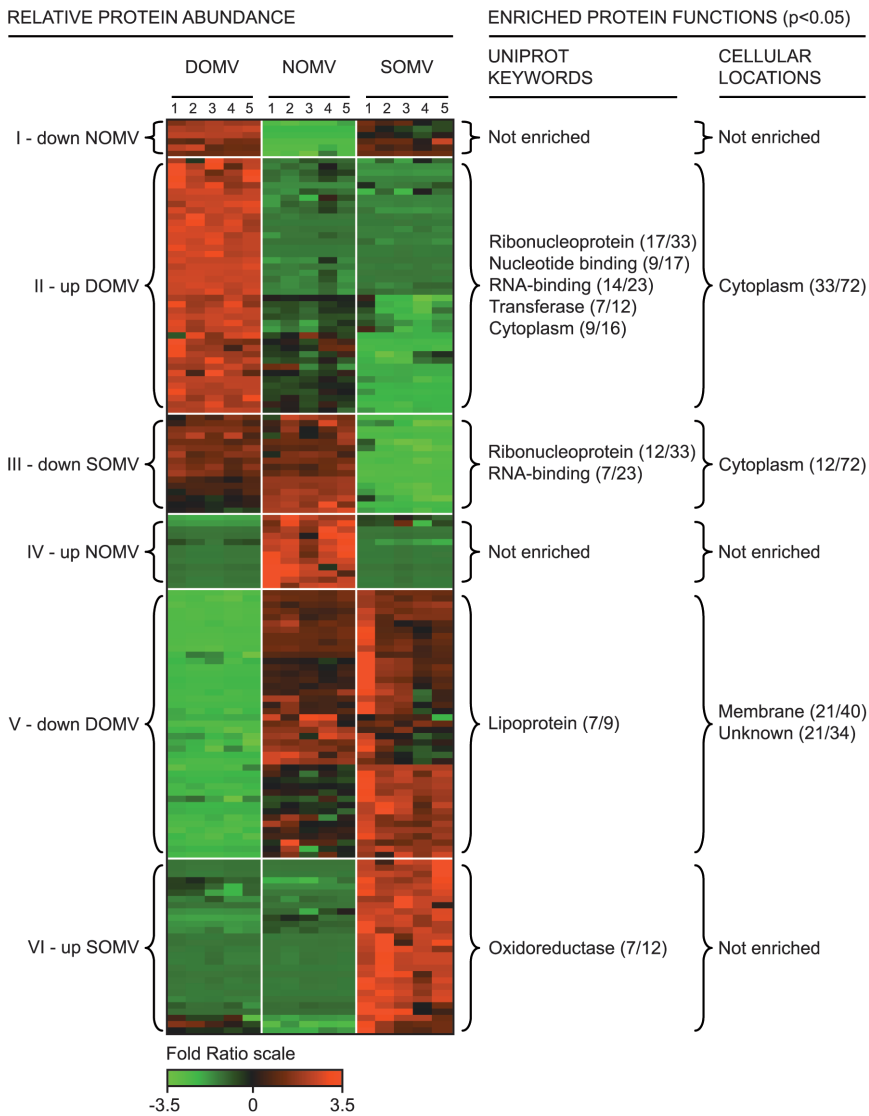
Figure 4. Differentially expressed OMV proteins.

Quantitative proteome analysis was performed on OMV vaccines from 3 different purification processes, using 5 biological replicates per vaccine. Proteins were clustered in expression pattern groups, e.g. group V (downregulated in dOMV). The color scale covers 3.5-fold downregulation (green), via no regulation (black) to 3.5-fold upregulation (red). Functional annotation was based on Uniprot keywords and predicted cellular locations (PSORTb algorithm). Enriched protein functions are depicted for each expression group ($p<0.05$). The results demonstrate that OMV vaccines from biomass extraction processes (especially dOMV and to a lesser extent nOMV) are enriched with lysis-derived cytoplasmic proteins, including proteins with ribonucleoprotein, RNA-binding or nucleotide binding function. nOMV and sOMV vaccines (detergent-free processes) are enriched with membrane proteins and proteins with unknown location, including lipoproteins like fHbp. Therefore detergent-free OMV vaccines, sOMV in particular, have a preferred protein composition.
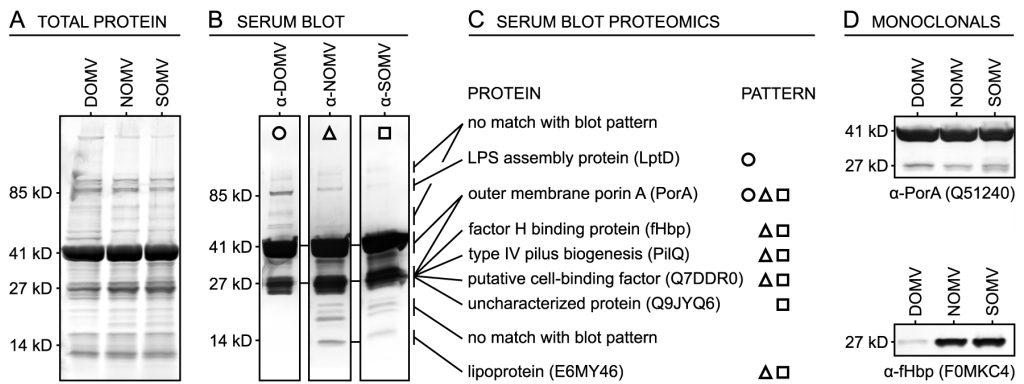
Figure 5. Serum blot proteomics reveals differences in immunogenic protein content.
(A) Protein composition of OMV from three purification processes after SDS gel electrophoresis. (B) Sera of immunized mice were blotted against corresponding OMV vaccines. Despite a comparable SDS page pattern, the serum blots reveal differential immunogenicity (several variable bands at 50–85 kD and 14–27 kD) and confirm immuno-dominance of PorA (41 kD). (C) Serum blot proteomics identified proteins that matched the differential pattern (circle: found in dOMV; triangle: nOMV; square: sOMV). This demonstrates that nOMV and sOMV vaccines (detergent-free process) are enriched with immunogenic proteins. (D) The results were verified with monoclonal antibodies against two protective antigens, PorA and fHbp. This confirms that PorA immunogenicity is not dependent on the purification process, while fHbp lipoprotein is largely removed after detergent-extraction (dOMV process).

Discussion

To investigate previously observed changes in functional immunogenicity, the proteomes of OMV vaccines from different purification processes have been compared and quantified [185]. Dimethyl labeling of free amines at the protein level is followed by selective purification of N-terminal peptides with the PTAG strategy [204]. This novel protocol combines the analysis of internal peptides before PTAG and N-terminal peptides after the PTAG procedure, using a straightforward workflow (Figure 1). Dimethylated peptides are quantified relative to a common reference, which represents an internal standard between all experimental samples (Figure 2). Strong cation exchange (SCX) fractionation followed by LC-MS/MS analysis is only required to compile a peptide search list, linking accurate mass and retention time to peptide and protein identifications [205, 206, 214]. Once the search list is available, a single LC-MS run for each experimental sample is sufficient to identify and quantify all detectable peptides in the OMV proteome. This accurate mass and retention time approach reduces total acquisition time and allows a high number of independent biological replicates, resulting in robust statistical analysis of relative protein abundance. These advantages are not available with other quantitative proteomics methods, which mainly rely on weighed peptide fold-changes in a single biological sample for statistics [199].

The PTAG strategy effectively reduces sample complexity and uncovers the majority of N-terminal peptides in this study. The uncovered N-terminal peptides correspond to only 7 new proteins, since most proteins are already detected by their internal peptides. A limitation of positional proteomics approaches like PTAG is undersampling of the N-proteome, because these methods rely on detection of a single N-terminal peptide [204]. As a result, the N-termini of lipoproteins are absent due to a lipid modification that prevents dimethylation. To our knowledge PTAG does not introduce any other experimental bias. In addition, the strategy is likely to be beneficial for highly complex protein samples like cell lysates, because complexity reduction will improve specificity of the quantification. The present results comprise a dataset of 618 peptides from 185 unique OMV proteins (Figure 3). Other studies identify between 25 and 166 OMV proteins with qualitative methods, like 1D or 2D gel electrophoresis and one gel-free approach [104, 193, 194, 197]. A quantitative 2D electrophoresis study identifies 74 OMV proteins, of which 10 are differentially expressed [196]. Overlap of these studies with the current results is moderate to high (Appendix 3), therefore this study is representative and comprises the largest quantitative OMV dataset available to date.

Quantitative analysis of relative protein abundance reveals distinct differences between OMV vaccines (Figure 4). Several proteins are absent in one or two vaccine types, resulting in large fold ratios (>10). The dataset also contains a variety of subtle changes that remain unnoticed with a qualitative approach. Reproduciblity of biological replicates is sufficient for reliable protein quantification, but the use of less than five independent replicates may reduce the statistical power to detect subtle differences. dOMV vaccines contain substantially more cytoplasmic proteins than nOMV or sOMV vaccines. These proteins may be released during detergent-extraction, which removes endotoxin from dOMV but apparently causes lysis and contamination with cytoplasmic proteins. A much smaller but distinct set of cytoplasmic proteins is shared between dOMV and

nOMV vaccines, while sOMV remains largely free of cytoplasmic contamination. This supports the extraction hypothesis, since nOMV are purified with a milder, detergent-free extraction and sOMV purification does not require any extraction at all. Other studies have also found cytoplasmic proteins in dOMV, including one qualitative comparison of dOMV and sOMV from the New-Zealand vaccine strain [104, 194-197]. The present study adds an intermediate vaccine (nOMV) to the comparison, which demonstrates that cytoplasmic protein contamination of OMV is directly related to the purification process that is used.

In addition to less cytoplasmic contamination, detergent-free OMV vaccines are significantly enriched with membrane proteins and proteins with an unknown cellular location. For sOMV vaccines, the difference is most pronounced (Appendix 2). Such proteins are more likely to be important for the immunogenicity of OMV vaccines than cytoplasmic proteins, which predominantly represent well-characterized aspects of microbial metabolism. The importance of unknown proteins is illustrated by the observation that 6 out of 9 lipoproteins in the dataset have an unknown predicted location rather than a membrane location. The data also shows that lipoproteins are selectively removed after detergent extraction. This includes factor H binding protein (fHbp), which contributes to functional immunogenicity and is currently investigated in clinical trials as a purified protein vaccine [67, 191, 215]. The sOMV vaccines contain an additional set of proteins with virulence-related functions. Therefore detergent-free OMV, in particular sOMV, have a preferred protein composition compared to dOMV.

The detergent-free OMV vaccines in this study previously had improved cross-protection and functional immunogenicity in mice [185], which was confirmed by others [63, 104, 191]. Functional immunogenicity is measured with SBA, which correlates to protection in humans but does not provide in-depth information on the protein content of vaccines. Therefore this study supplements SBA results with quantitative proteomics data. The results are refined with serum blot proteomics to visualize and assess differences in immunogenic protein content. Differential serum blot bands are excised, digested with trypsin and analyzed with qualitative LC-MS/MS. Several antigens match the immunogenicity pattern on the serum blot, including PorA (constant pattern) and proteins that are only found exclusively in detergent-free OMV like fHbp, type IV pilus assembly protein PilQ or putative cell-binding factor (Figure 5). Notably, the pattern of serum blot identifications is in full agreement with the quantitative proteomics results, indicating that both novel methods produced reproducible data. Serum blot proteomics demonstrates that detergent-free OMV are enriched with immunogenic proteins, but this does not necessarily translate to functional immunogenicity [92]. Differential endotoxin content of OMV vaccines should also be taken into account, since attenuated *lpxL1* endotoxin in detergent-free OMV vaccines adjuvates the immune response against proteins in the vaccine [6, 93]. Also the endotoxin itself contributes to functional immunogenicity [187]. Even though these aspects are not covered with proteomics, the current results provide valuable insight in the immunogenic protein content of different OMV vaccines. Such an approach can support functional assays like SBA.

Conclusions

A novel proteomics method has been developed, providing a quantitative fingerprint of complex protein products. Quantification is based on a common reference sample, which enables a high number of independent biological replicates for robust statistics. The method has broad potential applications in the field of biotechnology, like time course analysis of relative protein abundance in whole-cells, or batch-to-batch comparison of product consistency This study compares the proteomes of OMV vaccines from different purification processes and reveals distinct protein profiles. Serum blot proteomics substantiates these results by identifying differential immunogenic proteins. The results indicate that the (immunogenic) protein content of OMV vaccines is at least partially determined by the purification process. This supports previously observed functional differences between OMV vaccines and illustrates that detergent-free OMV have a preferred protein composition.

Acknowledgments

Appendix 1

Validation of quantitative proteomics method.
The quantitative proteomics method was validated with a protein mixture containing known ratios. The mixture included carbonic anhydrase (1:1 ratio), lysozyme (1:1 ratio), insulin (1:2 ratio), alpha casein (1:5 ratio) and serum albumin (1:10 ratio) and was analyzed with 5 independent replicates. Internal peptides before PTAG-labeling and TiO2 depletion allowed quantification of all proteins except carbonic anhydrase, because this protein has no lysine residues in its internal peptides (required for labeling). N-termini after depletion could be quantified for 3 out of 5 proteins. The N-terminus of lysozyme is too short for detection because trypsin cleaves off the N-terminus at the Asn2 residue. The serum albumin N-terminus was only detected for the light peptide, but not for the 10-fold less abundant heavy labeled peptide. The abundance was most likely below noise threshold, since several internal peptides of serum albumin had the same problem (data not shown). The noise threshold is determined by the detection sensitivity, but also by the accuracy of mono-isotopic mass deconvolution. Deconvolution errors are most likely to occur for isotope pairs with a greatly downregulated heavy labeled peptide (like serum albumin), due to overlapping isotope envelopes from the light labeled peptide. Other serum albumin peptides that were correctly detected had a variable ratio (25 ± 18). The large standard deviation indicates that the 1:10 ratio of serum albumin represents the outer limit of the dynamic range. Therefore, larger ratios are scored as >10 in the remainder of this study. Proteins with ratios between 1:1 and 1:5 were quantified with good to high accuracy, indicating that the method can be used to measure unknown ratios.

Protein	Uniprot ID	Internal peptides	N-terminus	Fold ratio	
				Expected	Observed
Carbonic anhydrase	P00921	not quantified*	quantified	1.0	1.0 ± 0.0
Lysozyme	P00698	quantified	not detectable**	1.0	1.3 ± 0.4
Insulin	P013017	quantified	quantified	2.0	2.1 ± 0.2
Alpha casein	P02662	quantified	quantified	5.0	5.1 ± 1.1
Serum albumin	P02769	quantified	not quantified***	10.0	25 ± 18

*Labeling not possible (no lysine residues).
**N-terminal peptide too short for detection.
***Heavy labeled peptide below noise threshold.

Appendix 2

PREDICTED PROTEIN LOCATION (PSORTb algorithm)
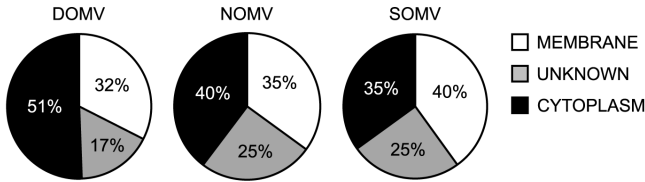
Distribution of predicted protein locations.
The different OMV vaccines in this study had a process-dependent protein location distribution. Detergent-extraction of dOMV vaccines resulted in enrichment with cytoplasmic proteins (51% of all proteins) due to bacterial lysis, while sOMV (no extraction) contained 35% cytoplasmic proteins. The mild, detergent-free extraction of nOMV resulted in an intermediate amount (40% cytoplasmic proteins). Due to the low amount of cytoplasmic proteins, detergent-free OMV vaccines (nOMV and sOMV) were enriched with membrane and unknown proteins, which are more likely to be relevant for immunogenicity. Cellular locations were predicted using the PSORTb algorithm (http://www.psort.org/psortb).

Appendix 3

Overlap of this study with available literature.
Available studies on OMV vaccines identified 25–166 proteins with several different proteomics methods (gel-free processing versus 1D or 2D gel electrophoresis, combined with qualitative or quantitative LC-MS/MS). Overlap of these studies with the current results was moderate to high, 43–61% of all detected proteins. Therefore the results of this study are likely to be representative and comprise the largest OMV dataset available to date.

OMV study	Proteomics method	# OMV proteins	overlap
(A) Vipond *et al.*	Qualitative 2D electrophoresis; LC-MS/MS	25	60%
(B) Vipond *et al.*	Qualitative 1D electrophoresis; LC-MS/MS	41	61%
(C) Tsolakos *et al.*	Quantitative 2D electrophoresis; LC-MS/MS	74	58%
(D) Gil *et al.*	Qualitative gel-free LC-MS/MS	101	50%
(E) Ferrari *et al.*	Qualitative 1D/2D electrophoresis; LC-MS/MS	166	43%
this study	Quantitative gel-free LC-MS/MS	185	100%

References
(A) Proteomics. 2006, 6(11): p3400-13.
(B) Human Vaccines. 2005, 1(2): p80-4.
(C) Vaccine. 2010, 28(18): p3211-8.
(D) Human Vaccines. 2009, 5(5): p347-56.
(E) Proteomics. 2006, 6(6): p1856-66.

Chapter 5

●●

Identification and optimization of critical process parameters for the production of nOMV vaccine against *Neisseria meningitidis*

Bas van de Waterbeemd[1]
Mathieu Streefland[2]
Lonneke van Keulen[1]
Jan van den IJssel[1]
Alex de Haan[1]
Michel H. Eppink[2]
Leo A. van der Pol[1]

[1] Institute for Translational Vaccinology (Intravacc), Bilthoven, The Netherlands
[2] Wageningen University, Department of Bioprocess Engineering, Wageningen, The Netherlands

Abstract

Outer membrane vesicles (OMV) are used as a vaccine against *Neisseria meningitidis* serogroup B and traditionally produced with detergent-extraction to remove toxic lipoploysaccharide. Engineered strains with attenuated lipopolysaccharide allow the use of native vesicles (nOMV) with improved stability and immunogenicity. In the nOMV production process detergents are omitted and vesicle release is stimulated with EDTA extraction (a chelating agent) to enable a higher yield. Many process parameters may affect the EDTA extraction efficiency, but it is unknown what the optimal ranges for these parameters are in terms of quality. The present study systematically optimizes EDTA extraction and is representative for production at large-scale. Two critical process parameters have been identified, harvest point of the cultivation (*harvest*) and pH of the extraction buffer (*pH*), which significantly affects yield (7-fold) and bacterial lysis (35-fold). The other quality attributes remain unchanged. Optimization of *harvest* and *pH* reveals that the desired low bacterial lysis coincides with intermediate but sufficient yield. High functional immunogenicity and low toxicity of the optimized vaccine are also confirmed. The EDTA extraction is therefore a robust process step which produces high quality OMV if *harvest* and *pH* are controlled accurately.

Introduction

The use of outer membrane vesicles (OMV) is an established strategy for development of a vaccine against *N. meningitidis* serogroup B, which causes acute and severe meningitis [3, 18, 182, 216]. OMV are released from growing *N. meningitidis* bacteria and consist of a phospholipid bilayer with outer membrane protein, lipopolysaccharide (LPS) and a lumen with periplasmic constituents [89]. PorA outer membrane protein was identified as the major protective antigen [57, 90]. OMV vaccines that have successfully stopped outbreaks in Norway, Cuba and New Zealand were made with a process that used detergent extraction (dOMV, *detergent* OMV) to decrease the amount of toxic LPS in the vesicles [49, 51, 53, 88]. It was established that deletion of specific lipid A biosynthesis genes, like *lpxL1*, resulted in attenuated LPS toxicity [6]. OMV from strains with attenuated LPS did not require detergent-extraction, which enabled further development of detergent-free approaches. Detergent-free OMV with attenuated LPS were intrinsically better than dOMV, because they had equally low toxicity and improved stability [72, 94, 185, 187]. In addition, detergent-free OMV contained lipoproteins that contributed to a protective immune response [73, 74, 94].

There are two types of detergent-free OMV. The first type, sOMV (*spontaneous* OMV), is produced by the bacterium itself. The sOMV are purified from the cultivation supernatant without any treatment to enhance OMV release [97, 99]. Even though up to 11% of total biomass can be present as sOMV further yield improvement is required for economically feasible vaccine production [98]. This may be established by deletion of the *rmpM* gene, which anchors the outer membrane to the peptidoglycan layer [108, 121, 185], or through the deletion of *gna33*, which has been associated with increased sOMV release through an unknown mechanism [104]. The second detergent-free OMV type uses extraction with a chelating agent (EDTA; ethylenediaminetetraacetic acid) to further increase yield [185]. EDTA destabilizes the outer membrane by chelating calcium and magnesium ions, which stimulates the release of nOMV (*native* OMV) [111, 189, 217]. Despite the use of an extraction step, nOMV have a native composition with biochemical and immunological properties that are more similar to sOMV than to dOMV [40, 185]. Vaccines based on nOMV were successfully tested in preclinical and clinical phase I/II studies, but clinical phase III studies have not been reported [94, 100, 101, 103, 187, 218, 219]. For such studies, a robust and fully scalable production process is an important requirement. The central step in such a process for the production of nOMV is the EDTA extraction, which actively releases nOMV from the bacteria before purification.

Many process parameters may influence the outcome of detergent-free extraction during nOMV production. These include physiological parameters like the pH of the extraction buffer, the amount of EDTA in the extraction buffer and duration or temperature of the extraction step. Process parameters that affect the concentrated biomass, which is the input material for the extraction, may also have an effect. These are the condition of the cells at harvest point or the method for concentrating the biomass that was chosen [220]. Setpoint estimates for these process parameters can be obtained from literature [2, 40], but it is currently unknown whether they are optimal or how they interact to affect nOMV quality. Quality is herein defined as a set of quality attributes whose values must be within predefined targets to obtain an effective vaccine.

High quality nOMV must be biochemically stable, non-toxic and able to induce functional immunogenicity. Furthermore the production process should provide sufficient yield and low bacterial lysis (low DNA release). Lysis is an issue because genomic DNA is an undesirable component of the final nOMV vaccine, especially when the bacteria have recombinant genes in their genome [69]. The viscosity of DNA also complicates nOMV purification when (ultra)filtration or gelfiltration equipment is used.

The present study describes the optimization of EDTA extraction during large-scale production of nOMV from *N. meningitidis*. Five potentially critical process parameters have been assessed with an approach that was aiming at Quality by Design (QbD) [221-223]. First, the quality attributes of the vaccine were defined, then the process parameters that affect these attributes were explored and finally the process was optimized.

Materials and methods

Experimental design and data analysis

Modde 9.0 Design of Experiments software (Umetrics, Umea, Sweden) was used to create a fractional factorial resolution V experimental design containing 5 factors (process parameters), with the goal to identify critical process parameters. This resulted in 19 extraction experiments, including 3 centre points (Appendix 1). A partial least squares (PLS) model was fitted for each nOMV quality attribute, describing the mathematical relation between process parameters and quality attribute for the entire preliminary design space. Quality attribute models were individually refined by excluding process parameters with non-significant effects. Model validity was verified by performing ANOVA and lack of fit statistical analyses and by calculating R^2 and Q^2 values. Quality attribute models were considered valid, if ANOVA p-value was <0.05, lack of fit p-value was >0.05, R^2 (correlation) was >0.7 and Q^2 (explained variation) was >0.7 (Appendix 2). Since a valid model not necessarily represents large variation, biological significance of observed quality attribute variation was also assessed. Aggregation percentages above 10% and a >2.0 fold change in nOMV size, yield or ratio of biochemical components were considered biologically significant (Table 2). Quality attribute predictions (Figures 2 and 3) were calculated with Modde, using the model coefficients (Appendix 2) for a range of process parameter setpoints.

Quality attributes of nOMV

Previous work indicated that PorA content in OMV may be dependent on growth rate, while phospholipid content did not show significant changes [112]. Therefore phospholipid yield was used to estimate nOMV yield, thus allowing detection of relative changes in PorA, total protein and LPS content. This approach required stable nOMV with invariable size (confirmed, see results section) and invariable fatty acid composition of the phospholipid (confirmed; data not shown). Yield of nOMV (phospholipid yield), total protein yield, PorA yield and LPS yield were measured in the final nOMV sample. DNA release was measured in the supernatant of the first ultracentrifugation cycle. Yield was expressed as the amount of biochemical component (μg) obtained after purification of 60 mL (maximum volume of the ultracentrifugation tubes) crude nOMV extract, which originated from 0.62 gram of dry cells. Ratios were calculated by dividing the yield of one biochemical component (e.g. PorA yield) with the yield of another biochemical component (e.g. nOMV yield), followed by ^{2}log transformation to obtain a linear scale. For optimization purposes, the amount of LPS per OMV (LPS/OMV ratio) was used to assess potential toxicity effects. Potential immunogenicity effects were assessed with the amount of PorA and total protein per OMV (PorA/OMV and total protein/OMV ratios). After the optimization, toxicity and functional immunogenicity were verified with established correlates (IL-6 monocyte activation [125] and serum bactericidal activity (SBA) [46, 192], respectively).

Bacterial strain and growth conditions

The *N. meningitidis* strain that was used is a recombinant variant of serogroup B isolate H44/76 [109], combining one wild type and two recombinant PorA subtypes (trivalent PorA; subtypes P1.7,16; P1.5-1,2-2 and P1.19,15-1) with a non-functional *porB* gene [7]. The *cps* locus containing *siaA*, *siaD* and *galE* genes was deleted, resulting in a non-encapsulated phenotype with *galE*-truncated LPS. Additional deletions in *lpxL1* and *rmpM* genes were made to attenuate LPS

toxicity and improve yield (2-4 fold higher) [185]. All cultures were grown in chemically defined growth medium, containing glucose, amino acids, salts, iron and trace elements [4]. A primary, 150 mL pre-culture was inoculated with 10 mL working seedlot (cells at $OD_{590} = 1.5 \pm 0.1$; stored at -135°C with glycerol) and incubated in disposable 500 mL erlenmeyer shake flasks with vented closure (Nalgene, Rochester NY, U.S.A.) at 35°C, 200 rpm. The pre-culture was used to inoculate a secondary pre-culture, grown in a 5 L bioreactor with 3 L working volume (Applikon, Schiedam, The Netherlands). At OD_{590} values between 1.5 and 4.5, a fixed amount of bacteria was transferred to the 60L production bioreactor with 40 L working volume (Applikon, Schiedam, The Netherlands). Bioreactors were operated as described previously [4]. Harvest point samples were taken for OMV extraction and subsequent purification at 1, 5 and 9 hours after onset of the stationary growth phase (10 L, 5 L and 10 L of cultivation, respectively).

nOMV purification process

At each harvest point, biomass was concentrated approximately 5-fold using hollow fiber microfiltration units with 0.22 μm pore size and 0.37 m^2 surface area (Spectrum Laboratories, Rancho Dominguez CA, U.S.A). Circulation was constant at 0.9 L/min and feed pressure was monitored at-line. The concentrated biomass sample was diafiltrated with the microfiltration unit using 2 volumes of buffer (100 mM Tris-HCl, pH 8.6). Final volume of the diafiltrated biomass was normalized between harvest points based on the OD_{590} before microfiltration, to assure equal amounts of bacteria per mL. For OMV extraction, subportions of 280 mL diafiltrated biomass were used to allow parallel handling of multiple experiments. The pH was adjusted and 10x concentrated EDTA solution was added to a final concentration of 5-15 mM according to the experimental design (Appendix 1). Subsequent OMV extractions were performed accordingly. After extraction, bacteria were removed from the crude OMV extract by subsequent centrifugation (75 min., 12500x g, 4°C) and filtration (SuporMach V system with 0.22 μm PES membrane; Nalgene, Rochester NY, U.S.A.). The nOMV were purified with ultracentrifugation (65 min., 125000x g, 4°C) and resuspension in storage buffer (10 mM Tris-HCl pH7.4, 3% (w/v) sucrose). PorA concentration was measured and nOMV samples were diluted with storage buffer to a final concentration of 1 mg/mL PorA and stored at 4°C. Thiomersal (0.01% (w/v)) was added as a preservative.

Analytical procedures

Fatty acid composition was analyzed to characterize phospholipid composition (OMV) and quantify LPS concentration, using a modified gas chromatography method as described previously [185]. Total protein concentration of nOMV was measured using the Lowry protein assay with Peterson's modification, according to manufacturer's protocol (Sigma-Aldrich, Zwijndrecht, The Netherlands) [112]. PorA concentration was measured with quantitative SDS gel electrophoresis under denaturing conditions [112, 113]. Per lane, 4 μg total protein from nOMV was loaded. Gels were stained with Novex Colloidal Blue (Invitrogen, Breda, The Netherlands) and PorA was quantified as a percentage of total protein using TL100 1D gel analysis software (Totallab, Newcastle upon Tyne, U.K.). DNA in the ultracentrifugation supernatant was quantified with fluorescence spectroscopy using Quant-it Picogreen dsDNA reagent (Invitrogen, Breda, The Netherlands), according to manufacturer's protocol. The nOMV size and aggregation were measured after 3 months storage at 4°C as described previously [185], by using dynamic

light scattering (nOMV size) and by measuring total protein content of nOMV before and after centrifugation at low speed (aggregation percentage). Serum bactericidal activity and IL-6 monocyte activation were measured as described previously [185].

Table 1. Potentially critical process parameters for OMV extraction.
Parameters were selected by a project team. *Reduc* and *stir* were excluded based on risk assessment and historical data. The remaining process parameters were used in an experimental design (Appendix 1) which systematically explored the preliminary design space, defined by the combined setpoint limits.

potentially critical process parameter			setpoints experimental design		
abbreviation	description	units	lower limit	centre point	upper limit
pH	pH extraction buffer	–	7.4	8.6	9.0
EDTA	EDTA concentration extraction buffer	mmol	5	10	15
harvest	harvest point of cultivation	hours stat. growth	1	5	9
temp	extraction temperature	°C	4	20	35
time	extraction length	minutes	5	30	55
reduc	volume reduction method for biomass	–	not included (microfiltration)		
stir	extraction stirrer speed	rpm	not included (100 rpm)		

Results

Experimental strategy

Potentially critical process parameters were selected in a project team, resulting in 7 candidates (Table 1). Risk assessment and historical data review allowed exclusion of 'volume reduction method for biomass' (*reduc*) and 'extraction stirrer speed' (*stir*). Fixed setpoints were chosen for these process parameters based on historical data (microfiltration (qualitative) and 100 rpm, respectively). Broad setpoint ranges were assigned to the remaining process parameters, based on historical data and further refined with preliminary experiments. The *pH* upper limit value was initially set at 9.8 but lowered to 9.0 because the preliminary experiments revealed major processing difficulties above pH 9.0, caused by fast lysis of the bacterial suspension (data not shown). The pH centre point value was chosen asymmetrically (at pH 8.6) based on historical data. The setpoint ranges together defined a preliminary design space that was explored with fractional factorial experimental design. Triplicate centre point experiments were added to measure reproducibility, giving a total of 19 extraction experiments (Appendix 1). For each extraction experiment, the quality attributes listed in Table 2 were measured and their values were used as input for modeling and optimization of a preliminary design space.

Process parameter effects

The nOMV extractions were performed on samples from a 40 L cultivation. Growth characteristics of the experimental batch (batch 1) were compared with 5 replicate batches (Figure 1). Regression analysis confirmed that growth curves were reproducible (R^2 = 0.993) and that batch 1 was representative, since the OD_{590} measurements of this batch fall within the 95% prediction limits shown in Figure 1. Controller and sensor output profiles of the cultivations (e.g. gas flows, temperature and oxygen uptake rate) were equally comparable (data not shown). The results showed that process parameters *time*, *EDTA* and *temp* did not affect any of the quality attributes, indicating that they are not critical within the tested ranges (Table 2). *Harvest* and *pH* did have significant effects on many quality attributes, confirming that they are critical process parameters for OMV extraction. Previous work indicated that PorA content in OMV may be dependent on growth rate, while phospholipid content remained constant [112]. Therefore phospholipid yield was used to estimate nOMV yield, which allowed detection of potential changes in relative PorA, total protein and LPS content. The yields of nOMV (phospholipid), PorA, total protein and LPS increased at higher *harvest* setpoints, as did the DNA release (bacterial lysis). The *pH* setpoint also affected quality attributes, however to a smaller extent than *harvest*. For some quality attributes, *harvest*harvest* effects were observed, indicating an exponential change of a quality attribute value towards specific *harvest* setpoints. In addition, a *harvest*pH* effect was observed which results in either amplification or levelling of a quality attribute value, caused by interactions between both process parameters. A comprehensive overview of process parameter effects is given in Table 2.
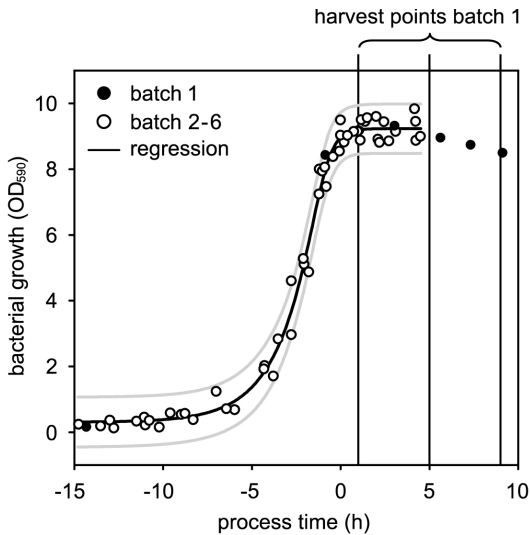
Figure 1. Bacterial growth of replicate cultivations at 40 L scale.
OMV extraction experiments were performed on cultivation samples from batch 1, at the depicted harvest points (vertical lines at T=1, 5 and 9 hours of stationary growth), which correspond to the values used for harvest in the experimental design. T=0 indicates onset of stationary growth. A sigmoid growth curve was fitted through the data using regression (black line; R2 = 0.993) with 95% prediction limits (grey lines), showing that batch 1 had a representative cultivation profile.
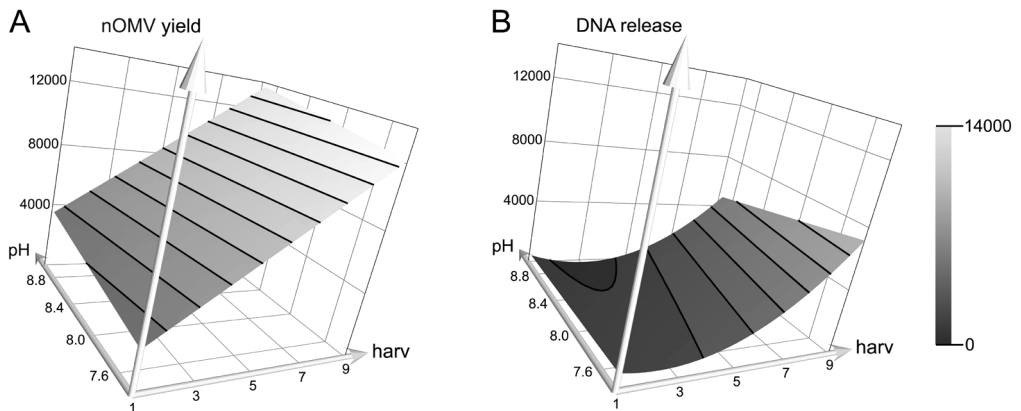
Figure 2. Relation between critical process parameters and quality attributes of the nOMV vaccine.
Critical process parameters harvest and pH are depicted on the x- and y-axes, nOMV quality attributes on the z-axis. The nOMV yield increased 7-fold towards late harvest and high pH (panel A). Bacterial lysis (DNA release) increased even more, 35-fold, which had implications for the manufacturing process (panel B). Quality attribute surfaces are scaled identically from low (black) to high (white) values. Z-axes represent yield units (in $\mu g/60$ mL crude extract; obtained from 0.62 gram of dry cells).

Quality attribute variation

PLS models were fitted which mathematically described the entire preliminary design space for each quality attribute and validity was assessed. Since a valid PLS model not necessarily represents large quality attribute variation, biological significance of the variation was also estimated. The results are summarized in Table 2 and complemented with a list of all PLS model coefficients (Appendix 2). Constant quality attribute values and invalid PLS models were obtained for aggregation (2.8 ± 2.2%), nOMV size (78 ± 5 nm) and PorA/total protein ratio (79 ± 3%), indicating that the entire preliminary design space provided stable nOMV with high PorA purity. Valid quality attribute models were obtained for ratios of LPS/OMV, PorA/OMV and total protein/OMV, but the observed variation was small and biologically insignificant (<2-fold change). Constant ratios are favorable, because these quality attributes were used to screen for potential effects on toxicity (LPS/OMV ratio) and immunogenicity (ratios of PorA/OMV and total protein/OMV) of the vaccine. The yields did change significantly for all measured biochemical components. The observed variation was between 5.0-fold (PorA yield) and 34.7-fold (DNA release).

Setpoint optimization of *harvest* and *pH*

For optimization of *harvest* and *pH* setpoints, relevant quality attributes were first selected. Figure 2A shows the nOMV yield response surface defined by both critical process parameters, revealing a 7-fold change within the preliminary design space. Response patterns of PorA, total protein and LPS yield resembled nOMV yield closely (data not shown) and had therefore no added value for the optimization. The DNA release surface (Figure 2B) had a different pattern, revealing that bacterial lysis increased exponentially compared to nOMV yield when setpoints were adjusted towards late *harvest* and high *pH*. This suggested that both nOMV yield and DNA release may be relevant for the optimization. Variation in the ratios of LPS, PorA, and total protein per OMV was biologically insignificant. Observed variation was <2-fold, indicating that there was no need to include these quality attributes in the optimization. After selection of relevant quality attributes, *harvest* and *pH* setpoints were optimized for nOMV yield and DNA release. When nOMV yield was maximized without DNA release restriction, 13646 ± 1029 μg nOMV and 4820 ± 531 μg DNA was obtained (*harvest* = 9.0 and *pH* = 9.0). This corresponds to 27.8 ± 2.1 mg PorA per gram of dry cells and represented the highest possible yield, however requires a large-scale purification process with high DNA removal capacity (>4820 μg/60 mL crude extract) to compensate bacterial lysis. Not removing the DNA would result in major processing difficulties caused by viscosity. For regulatory approval, genomic (recombinant) DNA is considered an undesirable component of the final vaccine. Therefore, yield was maximized while maintaining minimized DNA release (Figure 3; DNA target = 0 μg). An nOMV yield of 5965 ± 641 μg (corresponding to 13.9 ± 1.3 mg PorA per gram of dry cells) and DNA release of 0 ± 617 μg was obtained for *harvest* = 3.3 and *pH* = 8.4 setpoints. These values represent the true optimum, in which sub-maximal but feasible nOMV yield was allowed to ensure the benefits of a crude nOMV extract with low DNA content. This optimum was visualized in Figure 3 and was situated in the centre of the preliminary design space. It also revealed that the margins which guarantee an optimal result are narrower towards lower *pH* values.
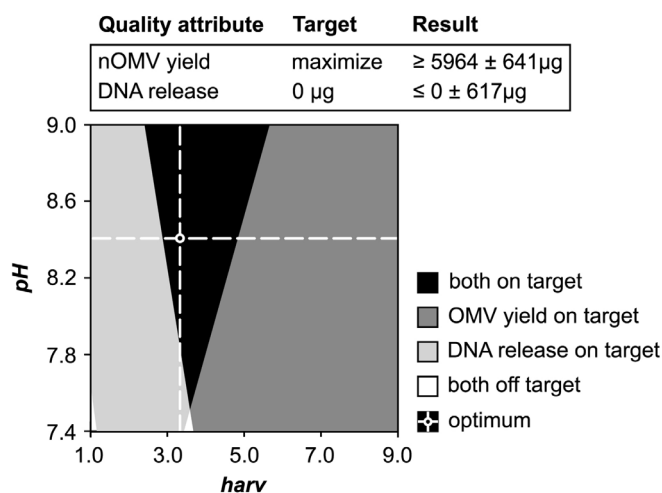
Figure 3. Optimization of critical process parameters harvest and pH.
Relevant quality attributes for optimization (nOMV yield and DNA release) were selected as described in the results section. The targets were chosen to combine high nOMV yield with low DNA release. Grey areas indicate which quality attributes meet the target (see legend). The optimum (white circle) is depicted at the intersection of *harvest* = 3.3 and *pH* = 8.4 and the black area corresponds to the model error around this optimum. Within the black, optimal area the nOMV yield was feasible but below maximum, however the benefits of a crude extract with low viscosity (low DNA) were ensured. Towards lower *pH* values, a more accurate control of *harvest* is required to guarantee an optimal result.

Verification of functional immunogenicity and toxicity

For optimization purposes, potential toxicity and immunogenicity effects were monitored with fast biochemical assays for all 19 nOMV samples from batch 1 (Figure 1). The optimal *harvest* and *pH* setpoints were then applied during the production of a new vaccine batch (batch 2, Figure 1) and functional immunogenicity and toxicity were verified with established correlates (SBA and IL-6 monocyte activation, respectively [46, 125, 192]). Table 3 shows that the optimized vaccine induced high bactericidal titers against all 3 PorA subtypes in mice sera after 2 immunizations. Mean ^{2}log titers of responders were 11.8 ± 1.1 (PorA P1.7,16), 12.1 ± 1.1 (PorA P1.5-1,2-2) and 9.1 ± 1.6 (PorA P1.19,15-1). For PorA subtypes P1.7,16 and P1.5-1,2-2 all 10 mice responded to vaccination. P1.19,15-1 had only 5 responders but this PorA was expected to be less immunogenic in mice [5, 126]. Next, IL-6 monocyte activation of the optimized vaccine was compared to a reference vaccine with low toxicity. The reference vaccine consisted of detergent-extracted OMV with reduced amounts of toxic *galE*-LPS and was well tolerated by toddlers and children [60]. An experimental reference vaccine with high toxicity was also included to provide a context for the results (spontaneously released OMV with high amounts of toxic *galE*-LPS (ΔR-sOMV) [185]). The results showed that the optimized vaccine and the low toxicity reference induced comparable amounts of IL-6 in monocytes (0.44 and 2.36 ng IL-6 per μg PorA, respectively). As expected, the high toxicity reference induced substantially more pro-inflammatory cytokine (2.3x10^4 ng IL-6 per μg PorA). These results indicate that the optimized vaccine was non-toxic and induced high functional immunogenicity.

Table 2. Overview of process parameters effects on quality attributes.
Quality attributes were significantly affected by *harvest* and *pH* (critical process parameters). The effect of a higher process parameter setpoint was listed as either positive (+), negative (–), or absent (0) for each quality attribute. Statistical significance of effects was indicated with * ($p<0.05$), ** ($p<0.01$), or *** ($p<0.001$). Exponential effects (i.e. *harvest*harvest*) and interaction effects (i.e. *harvest*pH*) were also assessed and included in the table if significant effects were found. Validity of quality attribute models and biological significance of the observed variation was indicated in the last two columns. Appendix 2 contains all model coefficients.

nOMV quality attribute				effect process parameter on quality attribute							quality attribute model	
name	quality aspect	target	observed variation	harvest	pH	harvest* harvest	harvest* pH	time	EDTA	temp	validity	biological significance
aggregation	stability	<10%	2.8 ± 2.2%	0	0	0	0	0	0	0	not valid	not significant
nOMV size	stability	20-200 nm	78 ± 5 nm	0	0	0	0	0	0	0	not valid	not significant
PorA/total protein ratio	PorA purity	50-100%	79 ± 3%	0	0	0	0	0	0	0	not valid	not significant
DNA release	bacterial lysis	minimize	34.7 fold	+ ***	– ***	+ ***	– ***	0	0	0	valid	significant
nOMV yield	yield	maximize	7.6 fold	+ ***	+ *	0	0	0	0	0	valid	significant
total protein yield	yield	maximize	5.1 fold	+ ***	+ **	0	0	0	0	0	valid	significant
PorA yield	yield	maximize	5.0 fold	+ ***	+ *	0	0	0	0	0	valid	significant
LPS yield	yield	maximize	6.0 fold	+ ***	– *	– *	0	0	0	0	valid	significant
total protein/OMV ratio	immunogenicity (initial screening)	constant	1.6-fold	– ***	– *	0	0	0	0	0	valid	not significant
PorA/OMV ratio	immunogenicity (initial screening)	constant	1.7 fold	– ***	– *	0	0	0	0	0	valid	not significant
LPS/OMV ratio	toxicity (initial screening)	constant	1.3 fold	– **	– ***	0	+ ***	0	0	0	valid	not significant

Discussion

Production of nOMV vaccine against *N. meningitidis* serogroup B requires extraction with a chelating agent (EDTA) to destabilize the bacterial outer membrane [63, 73, 94, 100-103]. This study systematically explores the impact of changing extraction conditions on nOMV quality, with the goal to identify and optimize critical process parameters (Table 1; Appendix 1). Experiments have been performed on samples from a 40 L cultivation which is representative for vaccine production at large-scale (Figure 1) and the experimental strategy is aiming at Quality by Design (QbD) guidelines [4, 221-223]. The combined process parameter ranges define a preliminary design space in which the effect on nOMV quality attributes has been measured (Table 2). The results have been used to build PLS models that accurately predict quality attribute values for any given setpoint combination in the preliminary design space (Figure 2; Appendix 2).

The temperature, duration and EDTA concentration of the extraction have been assessed as potentially critical process parameters (Table 1), but have no effect on nOMV quality within broad setpoint ranges (Table 2). This indicates that the extraction step is robust for these important physiological parameters. Harvest point of the cultivation (*harvest*) and pH of the extraction buffer (*pH*) are critical and able to cause significant change in quality attributes nOMV yield and bacterial lysis (Figure 2). The 7-fold nOMV yield increase towards late *harvest* suggests an increased sensitivity for the EDTA extraction, higher spontaneous OMV release by the bacteria, or both. The setpoints for *harvest* are all within the stationary phase, in which the bacteria encounter nutrient limitations that result in growth arrest. Exposure to nutrient limitation, high temperature or toxic agents is known to increase OMV release in other gram-negative bacteria [79-81, 224, 225], but these observations have not been described for *N. meningitidis*. The present results indicate that *N. meningitidis* has a similar response to stress as these other gram-negative bacteria. Nutrient limitation is the most likely cause, but the current study is not designed to substantiate such a hypothesis.

The preliminary design space provides unaggregated nOMV with a highly homogeneous vesicle size and high PorA purity for any combination of process parameter setpoints. These important findings reconfirm that detergent-free nOMV are an improvement compared to detergent-extracted dOMV, which are more heterogeneous and tend to aggregate [61, 185, 226] even though this does not affect immunogenicity [107]. Towards late *harvest*, DNA release increases exponentially compared to nOMV yield (Figure 2). This is caused by bacterial lysis, as reflected in the growth curve (Figure 1). The late harvest point has a lower OD_{590}, indicating that the stationary phase is approaching death phase. This confirms that the latest possible harvest point has been included in this study. Setpoint optimization of *harvest* and *pH* for minimized bacterial lysis resulted in an nOMV yield that is economically feasible but below maximum (Figure 3). For regulatory approval genomic DNA is an undesirable component of the final vaccine [69]. Therefore, large-scale processing of crude nOMV extract should include sufficient DNA removal capacity to allow further nOMV yield improvement. Combined nuclease treatment and gel filtration chromatography may be a suitable approach because they are fully scalable, remove DNA effectively and decrease viscosity for simplified and faster processing [227, 228].

Table 3. Functional immunogenicity and toxicity of the optimized vaccine.
Optimal setpoints for *harvest* and *pH* were used to produce a representative batch of nOMV vaccine (Figure 1; batch 2). The optimized vaccine induced high bactericidal titres in mice against all three PorA subtypes, including P1.19,15-1 which is known to be less immunogenic in mice (less reponders) [5, 126]. In addition, monocyte activation was comparable to a reference vaccine with low toxicity [60]. An experimental reference vaccine with high toxicity [185] induced substantially more IL-6. Therefore the setpoint optimization did not affect functional properties of the vaccine.

serum bactericidal activity		
strain	mean ^{2}log titre responders	number of responders
H44/76 P1.7,16	11.8 ± 1.1	10/10
H44/76 P1.5-1,2-2	12.1 ± 1.1	10/10
H44/76 P1.19.15-1	9.1 ± 1.6	5/10

monocyte activation	
vaccine	IL-6 induction (ng/µg PorA)
optimized vaccine	0.44
low toxicity reference	2.36
high toxicity reference	2.3×10^4

The optimization is based on biochemical properties like nOMV size, aggregation and yield or ratios of vesicle components. The assays that are used do not require animal experiments or cell culture and have been performed in parallel for many samples with high technical reproducibility, which is a prerequisite for optimization experiments. Functional properties like serum bactericidal activity (functional immunogenicity) [46, 192], or IL-6 monocyte activation (toxicity) [125] have been verified after the optimization, on a representative nOMV vaccine that has been produced with the optimal setpoints for *harvest* and *pH* (Figure 1; batch 2). The optimized vaccine induces high bactericidal titers in mice against all three PorA subtypes, as shown in Table 3. One PorA antigen (P1.19,15-1) has 5 responders out of 10 mice, but this has been observed before and is not caused by the optimization [5, 126]. IL-6 induction in monocytes is comparable to a reference dOMV vaccine with low toxicity [60]. Therefore the optimization of *harvest* and *pH* is unlikely to change functional properties of the vaccine. The optimal setpoints have been obtained for a process that is representative for production at large-scale, which is an important requirement for clinical studies. The previously optimized growth medium [4] and previously selected production strain with specific genetic modifications [185] have not been included as variables. Therefore the optimum may not be valid for all *N. meningitidis* serogroup B strains or for other growth media. Especially strains that do not have the *rmpM* deletion to increase yield may behave differently. Despite these limitations, the current results illustrate that process parameters *harvest* and *pH* can be of major importance for the production of nOMV vaccine against *N. meningitidis*.

This study shows that large-scale EDTA extraction yields high quality nOMV within broad process parameter ranges. Only two process parameters, *pH* and *harvest*, are critical and have a significant effect on yield and bacterial lysis. The impact of *harvest* is related to biological processes that occur during the stationary growth phase, but detailed understanding of its effect on yield is

currently not available. Setpoint optimization has revealed that low bacterial lysis coincides with intermediate but sufficient yield and it has been confirmed that these optimal setpoints do not change functional properties of the vaccine. The EDTA extraction is therefore a robust process step which produces high quality nOMV if *harvest* and *pH* are controlled accurately.

Acknowledgements

Experimental design with nOMV quality attribute results.
The 19 OMV extractions were randomized and performed according to the experimental design (center points in grey were used to measure reproducibility). A fractional factorial resolution V design was generated to screen for critical process parameters. Quality attributes are grouped in catergories (yield, composition and other) and obtained experimental values are listed.

OMV extraction experiment	process parameter setpoint					quality attribute results											
	harvest	pH	time	EDTA	temp	yield				composition					other		
						OMV	total protein	PorA	LPS	total protein/OMV	PorA/OMV	LPS/OMV	PorA/total protein	DNA/OMV	DNA release	aggregation	nOMV size
	(h)	-	min.	mM	°C	µg	µg	µg	µg	2log ratio	2log ratio	2log ratio	2log ratio	2log ratio	µg	%	nm
1	1	7.4	5	5	35	2065	4633	3706	1488	1.17	0.84	-0.47	-0.32	-1.94	537	0.00	72.00
2	1	7.4	5	15	4	2530	6126	4901	1800	1.28	0.95	-0.49	-0.32	-1.51	888	2.30	71.02
3	1	7.4	55	5	4	2989	7274	6037	2007	1.28	1.01	-0.57	-0.27	-2.94	389	2.46	74.17
4	1	7.4	55	15	35	2331	5688	4323	1661	1.29	0.89	-0.49	-0.40	-1.37	899	5.60	68.71
5	1	9.0	5	5	4	3335	7450	5587	1868	1.16	0.74	-0.84	-0.42	-2.80	481	0.76	84.10
6	1	9.0	5	15	35	3346	7099	5608	1952	1.09	0.75	-0.78	-0.34	-3.21	361	3.44	75.52
7	1	9.0	55	5	35	3895	9233	7202	2224	1.25	0.89	-0.81	-0.36	-3.60	321	7.80	83.51
8	1	9.0	55	15	4	3912	8287	5967	2225	1.08	0.61	-0.81	-0.47	-4.07	233	2.89	77.00
9	5	8.6	30	10	20	6076	11237	8765	3748	0.89	0.53	-0.70	-0.36	-3.14	691	0.70	75.34
10	5	8.6	30	10	20	7101	12548	9537	4468	0.82	0.43	-0.67	-0.40	-3.49	631	3.20	75.59
11	5	8.6	30	10	20	6873	11934	9189	4478	0.80	0.42	-0.62	-0.38	NA	NA	1.63	75.77
12	9	7.4	5	5	4	11534	18051	14441	7127	0.65	0.32	-0.69	-0.32	-0.57	7780	0.00	82.57
13	9	7.4	5	15	35	11745	18137	14872	7246	0.63	0.34	-0.70	-0.29	-0.85	6511	4.60	76.70
14	9	7.4	55	5	35	10284	16011	13129	6205	0.64	0.35	-0.73	-0.29	-0.51	7201	4.71	79.11
15	9	7.4	55	15	4	13954	22264	18034	8445	0.67	0.37	-0.72	-0.30	-0.79	8074	6.60	81.77
16	9	9.0	5	5	35	13581	21135	17330	8096	0.64	0.35	-0.75	-0.29	-1.41	5116	3.20	84.20
17	9	9.0	5	15	4	14897	22107	18570	8838	0.57	0.32	-0.75	-0.25	-1.87	4071	0.00	83.01
18	9	9.0	55	5	4	13020	21125	17534	7848	0.70	0.43	-0.73	-0.27	-1.24	5494	2.70	82.85
19	9	9.0	55	15	35	15650	23612	18654	8860	0.59	0.25	-0.82	-0.34	-1.73	4730	0.36	83.10

Appendix 2

Full list of quality attribute model coefficients with descriptive statistics.

Modelled quality attribute values can be calculated for any combination of process parameter setpoints with the following equation: *quality attribute value = k + c1*(harvest) + … + c10*(temp*temp)*. Model validity was determined from the combined results of ANOVA p-value, lack of fit p-value, R²(correlation) and Q²(explained variation). Statistics that did not meet criteria for model validity are depicted in grey.

quality attribute	model coefficients											model statistics				
	constant	harvest	pH	time	EDTA	temp	harvest* harvest	harvest* pH	harvest* EDTA	pH*temp	temp*temp	ANOVA	lack of fit	R²	Q²	validity
	k	c1	c2	c3	c4	c5	c6	c7	c8	c9	c10	p <0.05	p >0.05	>0.70	>0.70	
aggregation	1.38	0	0	0.05	0	0	0	0	0	0	0	0.036	0.286	0.23	0.09	not valid
nOMV size	44.98	7.03	4.87	0	-0.67	-1.25	0	-0.82	0.11	0.06	0.02	0.000	0.030	0.96	0.76	not valid
PorA/total protein ratio	0.77	0.01	0.00	0	0	0	0	0.00	0	0	0	0.012	0.117	0.32	0.22	not valid
DNA release	-320	959	277	0	0	0	565	-363	0	0	0	0.000	0.074	0.98	0.96	valid
nOMV yield	-7670	2514	983	0	0	0	0	0	0	0	0	0.000	0.457	0.95	0.94	valid
total protein yield	-9112	3342	1534	0	0	0	0	0	0	0	0	0.000	0.406	0.95	0.93	valid
PorA yield	-7149	2795	1170	0	0	0	0	0	0	0	0	0.000	0.289	0.94	0.93	valid
LPS yield	-2175	79	463	0	0	0	234	0	0	0	0	0.000	0.621	0.97	0.95	valid
total protein/OMV ratio	1.61	-0.07	-0.04	0	0	0	0	0	0	0	0	0.000	0.576	0.96	0.90	valid
PorA/OMV ratio	1.37	-0.06	-0.06	0	0	0	0	0	0	0	0	0.000	0.553	0.89	0.82	valid
LPS/OMV ratio	1.01	-0.17	-0.20	0	0	0	0	0	0	0	0	0.000	0.416	0.92	0.87	valid

Chapter 6

●●

Cysteine depletion causes oxidative stress and triggers outer membrane vesicle release by *Neisseria meningitidis*; implications for vaccine development

Bas van de Waterbeemd[1]
Gijsbert Zomer[1]
Jan van den IJssel[1]
Lonneke van Keulen[1]
Michel H. Eppink[2]
Peter van der Ley[1]
Leo A. van der Pol[1]

[1] Institute for Translational Vaccinology (Intravacc), Bilthoven, The Netherlands
[2] Wageningen University, Department of Bioprocess Engineering, Wageningen, The Netherlands

Abstract

Outer membrane vesicles (OMV) contain immunogenic proteins and contribute to *in vivo* survival and virulence of bacterial pathogens. The first OMV vaccines successfully stopped *Neisseria meningitidis* serogroup B outbreaks but required detergent-extraction for endotoxin removal. Current vaccines use attenuated endotoxin, to preserve immunological properties and allow a detergent-free process. The preferred process is based on spontaneously released OMV (sOMV), which are most similar to *in vivo* vesicles and easier to purify. The release mechanism however is poorly understood resulting in low yield. This study with *N. meningitidis* demonstrates that an external stimulus, cysteine depletion, can trigger growth arrest and sOMV release in sufficient quantities for vaccine production (±1500 human doses per liter cultivation). Transcriptome analysis suggests that cysteine depletion impairs iron-sulfur protein assembly and causes oxidative stress. Involvement of oxidative stress has been confirmed by showing that addition of reactive oxygen species during cysteine-rich growth also triggers vesiculation. The sOMV in this study are similar to vesicles from natural infection, therefore cysteine-dependent vesiculation is likely to be relevant for the *in vivo* pathogenesis of *N. meningitidis*.

Introduction

The release of outer membrane vesicles (OMV) is observed among many bacterial species including gram-negative pathogens like *Escherichia coli*, *Vibrio cholerae*, *Salmonella typhimurium* or *Neisseria meningitidis* [183]. Pathogens produce OMV for *in vivo* survival, virulence or interactions with the host immune system [76, 229, 230]. The vesicles are spherical particles with a diameter of 50-200 nm, containing a phospholipid bilayer with outer membrane proteins, lipopolysaccharide (LPS or endotoxin) and a lumen with periplasmic constituents [76, 213]. *N. meningitidis* serogroup B epidemics in Norway, Cuba and New-Zealand were successfully controlled with outer membrane vesicle vaccines, which was a milestone for the application of OMV in vaccinology [3, 50, 51, 53]. These vaccines however required extraction with a detergent (deoxycholate), to decrease the amount of toxic LPS. The detergent-extraction was effective but resulted in partially intact and aggregated vesicles with an altered composition [61, 104, 185]. Discovery of the *lpxL1* mutation successfully attenuated the LPS of *N. meningitidis* and allowed the use of detergent-free OMV [6]. This provided vaccine concepts with equally low toxicity but improved immunological and biochemical properties [94, 104, 185, 187]. Detergent-free OMV are more similar to *in vivo* produced vesicles [213] and are now used for the development of several next-generation vaccines against serogroup B meningococcal disease [63, 70, 71, 73, 231].

There are two types of detergent-free OMV. The first type, sOMV (spontaneously released OMV), is as similar to *in vivo* vesicles as possible with a production system for human vaccines [213]. The sOMV are released by the bacterium during *in vitro* growth, without any treatments to enhance vesiculation [97, 99]. The second type, nOMV (native OMV) [63, 186, 187]), uses detergent-free extraction with ethylenediaminetetraacetic acid (EDTA) to chelate calcium and magnesium ions. This destabilizes the outer membrane which enhances nOMV release and preserves the desired biochemical and immunological properties, even though nOMV are not fully identical to sOMV [40, 111, 185, 189, 217]. The properties do change significantly when detergents are added to the extraction buffer. The purification of nOMV is less straightforward than sOMV purification due to more complicated handling (i.e. the extraction step; Appendix 1). New approaches that release sOMV in sufficient quantities to compensate the EDTA extraction step are therefore relevant for vaccine development.

Even though the existence of sOMV is known for decades, the mechanism that triggers their release is not fully understood [42, 232]. A model was proposed for *S. typhimurium* in which the density of associations between inner membrane, outer membrane and peptidoglycan layer regulates vesicle release [76]. This model was in agreement with observations that disruption of transmembrane anchor genes increased vesiculation (i.e. *tol*, *pal* and *ompA* in *E. coli* or *rmpM* in *N. meningitidis*) [185, 233]. Not only physical changes to the outer membrane but also external stimuli can trigger sOMV release. For *E. coli* these stimuli include heat shock, activitation of the envelope stress response pathway or lysine depletion [41, 79-81]. Such external triggers have not been identified for *N. meningitidis* but recent work indicated that vesicle yield increased significantly during stationary growth [186].

This study demonstrates that a novel external stimulus, depletion of cysteine, can trigger the onset of stationary growth and sOMV release by *N. meningitidis*. It is substantiated that cysteine depletion causes oxidative stress as the intracellular signal for increased vesiculation. The results also demonstrate that this approach is applicable for vaccine production.

Materials and methods

Bacterial strain and shake flask cultivations

The *N. meningitidis* vaccine strain that was used is a recombinant variant of serogroup B isolate H44/76 [109], combining one wild-type and two recombinant PorA antigens (trivalent PorA; subtypes P1.7,16; P1.5-1,2-2 and P1.19,15-1) with a non-functional *porB* gene [7]. The *cps* locus was deleted, resulting in a non-encapsulated phenotype with *galE*-truncated LPS. Additional deletions in *lpxL1* and *rmpM* genes attenuate LPS toxicity and improve yield [185]. All cultures were grown in chemically defined growth medium [4]. For shake flask cultivations, 150 mL pre-culture was inoculated with 10 mL working seedlot (cells at OD_{590} = 1.5 ± 0.1; stored at -135°C with glycerol) and incubated in 500 mL erlenmeyer shake flasks (Nalgene, Rochester NY, U.S.A.) at 35°C, 200 rpm. At an OD_{590} of 1.5 ± 0.3, 10 mL portions from the pre-culture shake flask were used to inoculate several secondary shake flasks, containing media with different arginine and cysteine concentrations (for Figure 1). Alternatively, secondary shake flasks with normal medium were grown to an OD_{590} of 2.5 ± 0.3 for repletion experiments (for Figure 3). Shake flasks for Figure 3 were pooled and centrifuged in 150 mL portions (20 min.; 3000x g; 4°C). Pellets were resuspended, washed in 75 mL medium (with/without cysteine) and re-centrifuged. The depletion/repletion experiments started after resuspending the pellets in 150 mL medium with/without cysteine. To induce oxidative stress, 150 μM peroxide was added to each shake flask (triplicates) directly after depletion/repletion (t=0). Growth was then monitored with hourly OD_{590} measurements. If the average optical density increased >10% between 2 measurements, 50 μM peroxide was added to repress growth. This was necessary at t=2.5 and 5.5 hours after depletion/repletion (arrows in Figure 3).

Bioreactor cultivations

Transcriptome analysis (Figure 2) and OMV production (Figure 4) was performed on samples from a fully instrumented, 5 L bench top bioreactor (Applikon, Schiedam, The Netherlands) with 6-blade Rushton impeller for mixing and gas dispersion and initial working volume of 3.5 L. Controller set points were 35.0 ± 0.5 °C (temperature), 30 ± 5% (dissolved oxygen concentration), 7.2 ± 0.1 (pH), 300-750 rpm (stirrer speed). The bioreactor was inoculated with 150 mL pre-culture at OD_{590} = 1.5 ± 0.3. The bioreactor was connected to an ADI-1040 control system (Applikon), operated with BCSV software (Compex, Gent, Belgium). After inoculation, dissolved oxygen concentration was first controlled by gradually increasing stirrer speed to 750 rpm. Then the fraction of oxygen in the headspace increased gradually while maintaining a constant total gas flow of 1.0 L/min. Samples for nutrient analysis were sterile filtered (0.22 μm) and stored at 4°C.

Transcriptome analysis

Microarray analysis was performed as described previously [234, 235]. RNA samples were analyzed with a full-genome *N. meningitidis* MC58 microarray [236], which covered 93% of predicted ORFs (Operon, Köln, Germany). Oligonucleotides were spotted in triplicate on UltraGAPS II coated slides (Corning, Corning NY, USA). The transcriptome profile was preserved by mixing 1 volume of bacterial culture (corresponding to 2.5 mL at OD_{590} = 1) with 2 volumes of RNA-later solution (Ambion, Paisley, United Kingdom), then concentrated with centrifugation (20 min.; 3000x g; 4°C) and stored at -80°C until RNA extraction. Bacterial pellets

were thawed and pre-treated in Tris-EDTA buffer with 0.5 mg/mL lysozyme (Sigma–Aldrich, Zwijndrecht, The Netherlands) prior to RNA extraction according to manufacturer's protocol (SV Total RNA isolation kit; Promega, Fitchburg WI, USA). Nucleic acid concentration was adjusted with ethanol precipitation and spectral analysis was used to determine purity and concentration. RNA integrity was measured with the Bioanalyzer RNA6000 Nano assay (Agilent Technologies, Santa Clara CA, USA), according to the manufacturers' protocol. RNA integrity number (RIN) scores were used to assess RNA integrity (score >8.0 required for inclusion) [237]. Total RNA from triplicate samples at each time point were reverse transcribed to cDNA and labeled with Cy3 dye using the Chipshot Indirect Labeling and Clean-Up kit (Promega), according to the manufacturer's protocol. Common reference samples, containing equal amounts of total RNA from all experimental samples, were labeled with Cy5. The labeled and purified cDNA samples were pooled in Cy3/Cy5 pairs. Hybridization buffer was added to a final concentration of 25% formamide, 56 SSC and 0.1% SDS. Samples were applied to the microarray slides and incubated in a hybridization chamber (16-20 h; 42°C; dark). Differential gene expression was calculated through comparison with the common reference. Microarrays were scanned with a ScanArray Express microarray scanner (Perkin Elmer, Waltham MA, USA) and median fluorescence intensities were quantified for each spot using ArrayVision software (Imaging Research). The data were natural-log transformed, quantile normalized and values of replicate spots were averaged. These data processing steps were done with the statistical software R, using an in-house developed script. P-values were calculated with one-way ANOVA statistical analysis. Significantly regulated genes were selected with a False Discovery Rate (FDR) of <10% to adjust p-values for multiple testing. Fold ratio (FR) values were expressed as the natural log of the normalized signal difference between the two groups. To further select for biologically relevant effects, a FR threshold of >2.0 (untransformed value) was applied to obtain the final results. Gene annotations were obtained from Uniprot Knowledge Base (www.uniprot.org; *N. meningitidis* MC58; version July 2011). Principal component analysis (PCA) and clustering of differentially expressed genes in expression groups was performed with Genemaths XT software (Applied Maths, Sint-Martens-Latem, Belgium). Overall gene expression differences between samples were assessed by calculating the Euclidian distance between gene expression values over the entire set of genes (this corresponds to the distance in a PCA plot). Functional annotations of cysteine regulated genes were retrieved from the Gene Ontology database, using corresponding Uniprot protein IDs (www.geneontology.org; version February 2012). Enrichment for a specific Gene Ontology was assessed by comparing the number of hits in the cysteine dataset with the number of hits in the MC58 genome. Enrichment p-values were obtained by calculating the binomial distribution probability. The binomial distribution probability was also used to calculate a p-value for the overlap between gene lists, allowing comparison of the cysteine dataset with relevant literature.

OMV purification and characterization

This study used small-scale, detergent-free OMV purifications as described previously [185]. Cultivation samples (250-400 mL) were taken from the bioreactor and purified. The samples were split in supernatant (for sOMV) and pellet (for nOMV) with centrifugation (20 min.; 3000x g; 4°C). To purify sOMV, supernatant was sterile filtered (0.22 μm) and concentrated with ultrafiltration (UF), using centrifugal units with 100 kD cutoff (Centricon 70-plus Ultracell, Millipore, Billerica

MA, USA). UF units were washed with saline, filled with 70 mL supernatant and concentrated to 10-15 mL by centrifugation. The retentate was re-diluted to 70 mL with fresh supernatant and the cycle was repeated until the full sample was processed (centrifugation at 1500x g; 4°C). Final retentate was diluted to 70 mL with storage buffer and concentrated to 10 mL (first wash step). The sOMV in the retentate were then pelleted with ultracentrifugation (120 min.; 125000x g; 4°C) and resuspended in a suitable volume of storage buffer (second wash step). To purify nOMV, the bacterial pellet was resuspended in 7.5 volumes (mL/g wet weight) of EDTA buffer (100 mM Tris-HCl pH8.6 with 10 mM EDTA) and incubated (30 min. ambient temperature). Cells were discarded by semi high-speed centrifugation (75 min.; 20000x g; 4°C). Ultracentrifugation was used to pellet nOMV in the supernatant (120 min.; 125000x g; 4 °C) and the pellet was resuspended in a suitable volume of storage buffer. Final total protein concentration was 1.0 ± 0.5 mg/mL for all OMV samples. Total protein concentration, PorA quantity and vesicle size distribution of OMV samples were performed as described previously [112, 185]. Briefly, total protein concentration was measured with the Lowry protein assay. Peterson's modification was used to reduce the effect of interfering substances. PorA antigen content was determined by SDS gel electrophoresis, followed by total protein staining and quantification of the 40-44 kD bands (PorA). Gels were stained with Novex Colloidal Blue (Invitrogen, Breda, The Netherlands) and PorA was quantified as a percentage of total protein using TL100 1D gel analysis software (Totallab, Newcastle upon Tyne, U.K.). Vesicle size distribution was measured with dynamic light scattering (DLS) at 25°C with a Malvern 4700 system. Homogeneity of the vesicle size distribution was reflected in the polydispersity index (PdI), which ranges between 0.0 (fully homogeneous size distribution) and 1.0 (random size distribution).

Quantification of nutrients and sOMV release

Cysteine (after reaction with bromoacetic acid and reduction using tris(2-ethylcarboxy)phosphine (TCEP)) and arginine were quantified by HPLC after derivatization with orthophtalic anhydride (OPA). Release of sOMV in the culture supernatant was monitored by using the fluorescent signal of a phospholipid-specific probe (SynaptoRed C2, Biotium, Hayward, CA, USA; ex500, em650). An aqueous solution of SynaptoRed C2 (0.05 mM, 50 μL) was mixed with 50 μL of sterile filtered culture supernatant or OMV standard with a known concentration. Fluorescence of the resulting mixture was recorded in black microtiter plates using a fluorometer (Synergy MX microplate reader; Biotek, Bad Friedrichshall, Germany). A calibration curve was constructed from the responses of the standards (dilutions of purified nOMV standard corresponding to 0-10 mg/L PorA antigen). Concentration of sOMV in culture supernatant samples was calculated from this calibration curve.

Results

Cysteine is the growth-limiting medium component

Previous work showed that vesicle release by *N. meningitidis* increased during the stationary growth phase [186]. To identify the growth-limiting medium component of these experimental conditions, nutrient consumption was monitored. Arginine and cysteine were depleted upon onset of stationary growth, while the growth medium still contained sufficient amounts of all other components (data not shown). Therefore, concentrations of arginine and cysteine were lowered systematically to identify the growth-limiting component (Figure 1). Control medium with normal amounts of cysteine and arginine produced regular growth curves in shake flasks (exponential growth; dry biomass yield 3.9 ± 0.1 gdw/L). Medium with normal cysteine but half the normal amount of arginine gave identical growth (exponential; 4.2 ± 0.3 gdw/L), indicating that less arginine did not have an effect on growth. Media with half the amount of cysteine however produced half the amount of biomass, regardless the amount of arginine (1.9 ± 0.1 gdw/L and 2.1 ± 0.1 gdw/L for normal and low arginine, respectively). Nutrient analysis confirmed that cysteine was indeed depleted upon onset of stationary growth for all 4 media, while arginine depletion occurred at a different time point (Appendix 2). These results indicate that cysteine, not arginine, is the growth-limiting component of the medium.
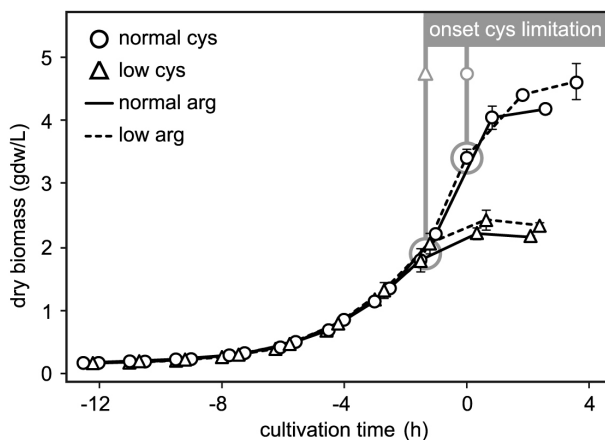

Figure 1. Cysteine is the growth-limiting medium component.
Previous work demonstrated that vesicle release by *N. meningitidis* increased during the stationary growth phase [186]. Nutrient analysis of the chemically defined medium indicated that only arginine and cysteine were depleted during early stationary growth. Therefore, concentrations of both components were systematically lowered to identify the growth-limiting nutrient. Black lines and black intersected lines represent growth curves on media with normal and low arginine concentration, respectively. Normal and low cysteine concentrations are marked with circles and triangles. Cultivation time t=0 represents the expected onset of stationary growth on reference medium with normal amounts of cysteine and arginine. The results indicate that cysteine, not arginine is the growth-limiting component. See Appendix 2 for corresponding nutrient data.

Transcriptome analysis identifies 149 cysteine regulated genes

Transcriptome analysis was performed with DNA microarrays to identify genes that are regulated after cysteine depletion. Growth and cysteine availability of triplicate cultivations on normal growth medium were monitored. Transcriptome analysis was performed on samples at -2.5, -1.4 and -0.4 hours (before cysteine depletion) and at +1.4 and +3.5 hours (after cysteine depletion). Principal component analysis on the full transcriptome confirmed high reproducibility of replicates (Appendix 3A). The experimental treatment (cysteine depletion) accounted for 70% of total gene expression variation and resulted in 2 distinct groups on the first principal component axis (PC1; corresponding to 'before' and 'after' cysteine depletion). PC2 explained 7% of all variation and the other principal components <5%, indicating that additional effects had only a minor impact on overall gene expression. Subsequent statistical analysis selected 149 significantly regulated genes (Fold Ratio >2.0 and False Discovery Rate <0.10). Upon cysteine depletion, 90 genes were upregulated and 48 were downregulated. A variable expression pattern was observed for 11 genes (Appendix 3B).

The gene expression profile of cysteine depletion resembles (oxidative) stress and virulence

Cysteine regulated genes were compared with available literature. Genes from a heat shock study [238] had significant overlap with peroxide stress [239] (p<0.0001; binomial distribution probability). Since both studies investigated stress stimuli they were compiled into a single group ('stress') for the comparison with cysteine depletion. In addition, studies on iron depletion [212] and two host interaction studies [240, 241] were compiled to 'virulence' based on significant overlap (p<0.0001). Studies on restrictive oxygen conditions [242] and putative pathogenicity genes [236] were not used due to insufficient overlap with cysteine regulated genes and/or available literature. The compiled gene sets 'stress' and 'virulence' were then compared with the cysteine depletion genes, revealing a significant overlap between the 3 groups (p<0.0001). The overlap indicates that similar mechanisms may be involved in these biological events (Figure 2A). Functional annotation of 149 cysteine regulated genes revealed 36 enriched Gene Ontologies (p<0.05), related to 11 functional groups (Figure 2B). Functional groups with distinct expression patterns were sulfur metabolism (9/9 genes upregulated), iron-sulfur cluster (6/6 upregulated), translation (13/16 downregulated), metal ion uptake (11/16 upregulated), cell wall (3/3 downregulated) and stress (2/2 upregulated). Non-distinct patterns were observed for redox (27 genes), membrane transport (23 genes), amino acid biosynthesis (10 genes), energy metabolism (4 genes) and other functions (19 genes). Some functional groups were directly related to the experimental context, like sulfur metabolism and amino acid biosynthesis (cysteine depletion), downregulated translation machinery (stationary growth) or membrane transport (upregulated sulfate uptake genes). The remaining functional groups were primarily related to oxidative stress (redox, iron-sulfur cluster, metal ion uptake and stress). Details are available online as Supplemental Information.

Cysteine depletion triggers increased sOMV release

Based on the transcriptome results it was hypothesized that in addition to growth arrest, cysteine depletion causes oxidative stress as an intracellular signal for sOMV release. The hypothesis was verified with a medium repletion experiment in shake flasks (Figure 3). Precultures on control
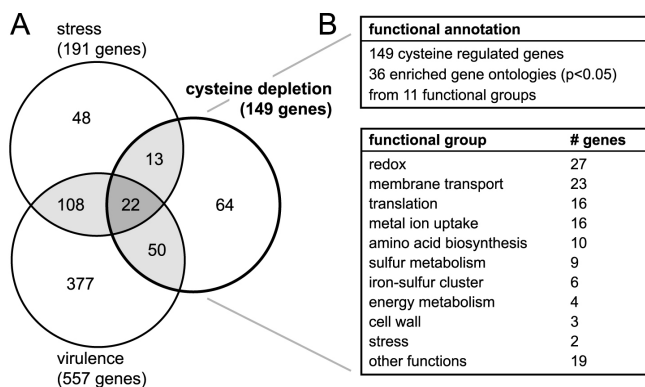
Figure 2. The gene expression profile of cysteine depletion resembles (oxidative) stress and virulence. Intracellular effects of cysteine depletion were explored with transcriptome analysis, resulting in 149 significantly regulated genes. (A) Significant overlap is found (p<0.0001) between cysteine regulated genes and relevant literature (compiled gene sets 'stress' [238, 239] and 'virulence' [212, 240, 241]), indicating that similar mechanisms are involved in these different stimuli. (B) Functional annotation of cysteine regulated genes identified 36 enriched Gene Ontologies (p<0.05) from 11 functional groups. In addition to expected groups like sulfur metabolism or translation, several functional groups are related to oxidative stress (e.g. redox or iron-sulfur cluster). Therefore it is hypothesized that cysteine depletion impairs the sulfur supply for iron-sulfur protein biogenesis, ultimately resulting in oxidative stress. Details of the transcriptome analysis are provided in Appendix 3 (principal component analysis and gene clustering) and Appendix 4 (expression data with functional annotation).

medium with the normal amount of cysteine were pooled and repleted with control medium or medium without cysteine (two groups). A third group was repleted with control medium but growth was repressed with peroxide to induce oxidative stress. Repleted cultures were monitored for growth and sOMV release. The sOMV were measured in small culture supernatant samples (sterile filtered; <3 mL) with a fluorescent probe that specifically binds phospholipid bilayer structures. Biomass concentration of the pooled preculture (0.78 gdw/L) was comparable to the biomass density directly after repletion (0.76 ± 0.05 gdw/L), indicating that no biomass losses occurred during the repletion procedure. Shake flasks that were repleted with control medium continued growth to a final dry biomass concentration of 3.75 ± 0.02 gdw/L. Cysteine depleted and oxidative stress shake flasks did not grow, resulting in final biomass concentrations of 0.64 ± 0.01 and 1.28 ± 0.20 gdw/L, respectively (Figure 3A). The sOMV results however revealed opposite effects. Control shake flasks grew normally but had a low specific sOMV yield of 1.1 ± 0.2 mg PorA antigen/gdw, while the cysteine depleted shake flasks yielded 13.7 ± 1.3 mg PorA/gdw (with a constant sOMV release rate). Oxidative stress shake flasks temporarily released sOMV after each peroxide addition (variable sOMV release rate) resulting in an intermediate yield (7.7 ± 0.8 mg PorA/gdw; Figure 3B). Shake flasks were harvested before cysteine in the control medium was exhausted, to prevent unintended sOMV release. Integrity of sOMV in the culture supernatant was confirmed with dynamic light scattering (DLS), which measured a distinct peak around 100 nm indicating that the bacteria were not disintegrating while releasing the OMV (data not shown). The above results demonstrate that cysteine depletion triggers increased sOMV release. Other stress stimuli like growth repression with peroxide can mimic this effect.
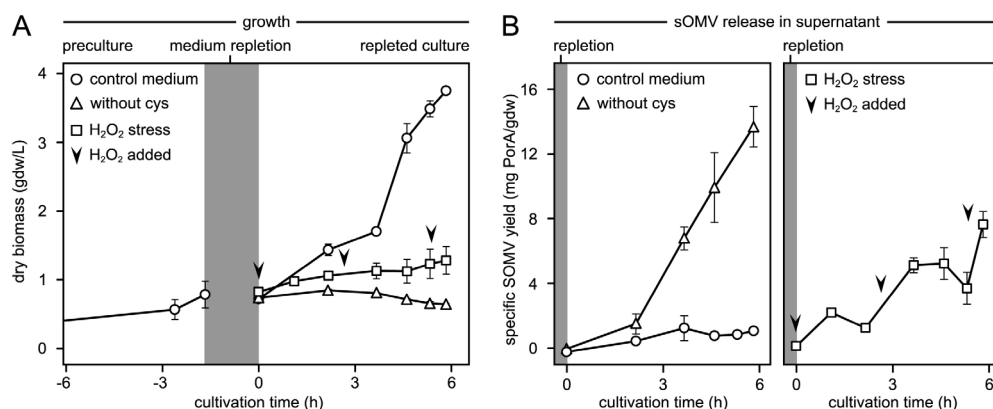
Figure 3. Cysteine depletion triggers sOMV release.
The effect of cysteine depletion on sOMV release is demonstrated with a repletion experiment in shake flasks. (A) Pre-cultures are grown on control medium with cysteine (circles). Harvested cells are repleted with control medium (circles) or medium without cysteine (triangles). Shake flasks without cysteine enter the stationary phase, while cysteine repleted flasks continue growth normally. A third group (squares) is repleted with control medium, but growth is repressed with peroxide to mimic oxidative stress and verify the transcriptome data (arrows indicate peroxide additions). Y-axis represents dry biomass concentration (g dry weight per L). (B) Vesicle release in the cultivation supernatant is monitored with a fluorescent probe up to 6 hours after repletion. Shake flasks with control medium grow normally but do not release sOMV, while cysteine depletion triggers a sustained release of vesicles. Oxidative stress has a similar but transient effect, since sOMV are released temporarily after each peroxide addition. Cysteine depletion is therefore an external stimulus for sOMV release, which induces oxidative stress as the intracellular signal. Y-axis represents specific sOMV yield (mg PorA antigen per g dry weight).

Cysteine depletion approach is feasible for sOMV vaccine production

The shake flask repletion experiment measured sOMV yield directly in the supernatant without taking purification losses or vaccine quality into account. To assess whether the cysteine depletion approach was feasible for vaccine production, larger samples (250-400 mL) were taken from a bioreactor system to purify nOMV (reference vaccine) and sOMV (experimental vaccine) in parallel, according to the protocol in Appendix 1. Purifications were done at several time points before and after cysteine depletion. The cultivations were monitored to measure biomass concentration and cysteine (time points A to N). As observed in shake flasks, biomass growth during the exponential phase was reproducible for all 6 replicate bioreactor cultivations (R^2 = 0.975) and growth arrest occurred upon cysteine depletion (time point G; Figure 4A).

Purification of nOMV and sOMV vaccines was performed at time points D, F (before) and I, K, M (after cysteine depletion). Yield of purified nOMV (reference) correlated to the amount of biomass that was used, resulting in a constant amount of 6.3 ± 0.3 mg PorA antigen/gdw regardless nutrient availability (Figure 4B). Yield of purified sOMV however depended on cysteine availability. Before depletion the yield was just above detection limit (0.2 ± 0.1 and 0.3 ± 0.1 mg PorA/gdw, respectively). Cysteine depletion then triggered sOMV release resulting in a cumulative increase during time point I (0.9 ± 0.4 mg PorA/gdw), time point K (2.0 ± 0.4 mg/gdw) and time point M (4.3 ± 1.4 mg/gdw). The reference yield (nOMV) was significantly higher
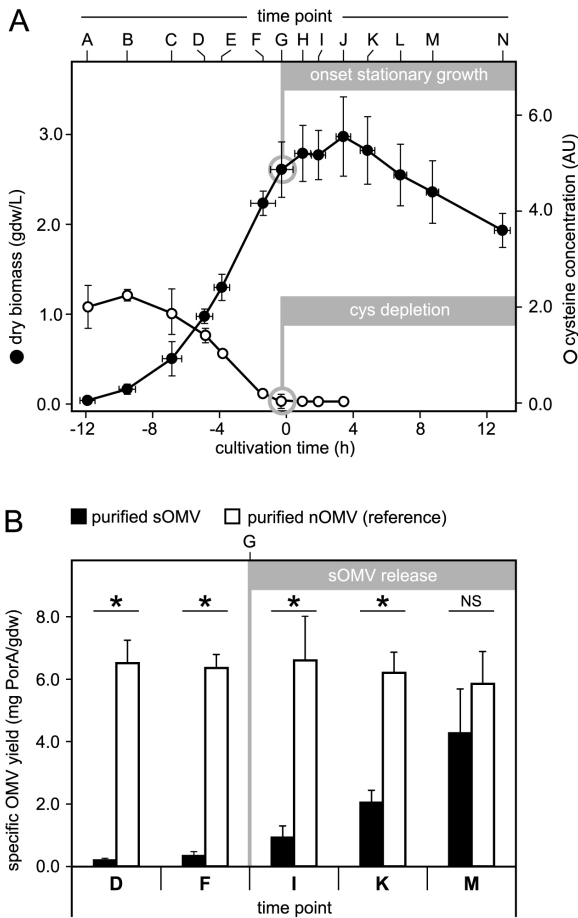
Figure 4. Implications for vaccine development.
A novel approach for the production of sOMV vaccine against N. meningitidis serogroup B is explored by utilizing the effect of cysteine depletion. (A) Biomass concentration (closed circles) is monitored in bioreactor cultivations (time points A to N). Time point G marks onset of stationary growth, caused by depletion of cysteine (open circles). (B) Yield of purified sOMV vaccine (black bars) is compared with nOMV reference vaccine, which uses detergent-free biomass extraction to improve yield (white bars). Several time points before (D, F) and after (I, K, M) cysteine depletion are included. After cysteine depletion, sOMV yield increases steadily to quantities that are comparable to the nOMV reference (no significant difference at time point M). Significant yield differences are indicated with asterikses (p<0.05). 'NS' indicates a non-significant difference.

than sOMV at most time points (D, F, I and K; p<0.001) but no significant difference was found at time point M, indicating that the cysteine depletion approach can generate sufficient sOMV for feasible vaccine production. Protein composition and vesicle size distribution were measured to assess vaccine quality. Purified nOMV had a comparable overall protein composition at all time points, with a high PorA antigen content (64 ± 3% of total protein; Figure 5A). Purified sOMV were comparable to nOMV at time points F, I, K and M (PorA content 61 ± 5%), but time point D had a low and variable purity (43 ± 23%) caused by a yield that was below the threshold for reliable

analysis. Vesicle size averages of nOMV (reference) and sOMV samples were comparable (83 ± 5 and 97 ± 9 nm respectively). The sOMV samples however had a slightly broader size distribution and contained minor particle peaks at ~5 μm, indicating that the purification procedure may require improvements (Figure 5B).
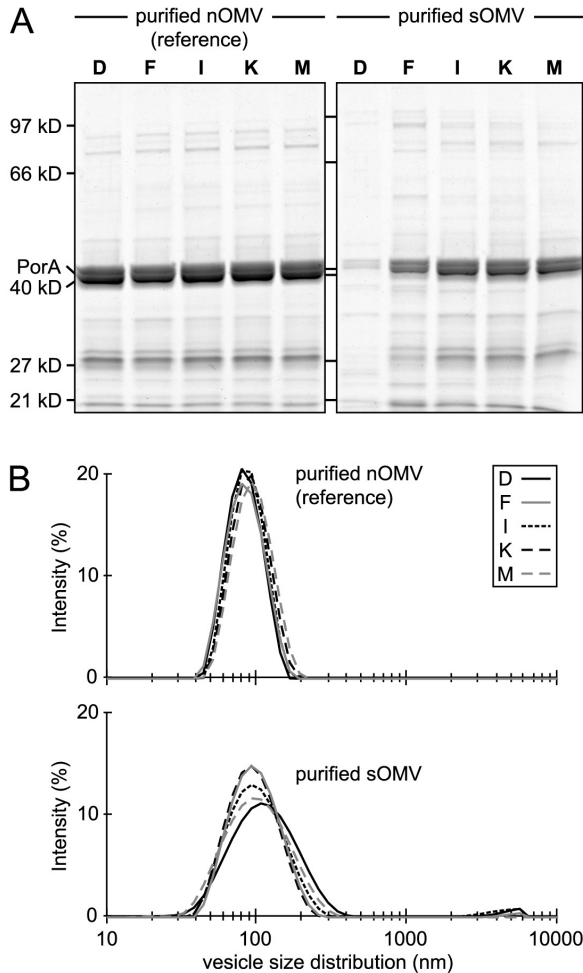
Figure 5. Quality of sOMV and nOMV vaccines.
In addition to yield, quality of the sOMV and nOMV vaccines is compared. It was previously demonstrated that both vaccine types provide low toxicity and high functional immunogenicity in mice [185]. (A) Protein composition of nOMV reference vaccines is comparable to sOMV vaccines after cysteine depletion (time points I, K, M). Each lane contains 4 μg total protein, except sOMV at time points D and F (low protein concentration due to a low yield; maximal sample volume is loaded). PorA antigen (~41 kD) has a major contribution to total protein content (>60%) in all vaccines. (B) Dynamic light scattering analysis reveals that sOMV vaccines have a slightly broader size distribution and minor aggregation compared to the nOMV references, indicating that the purification procedure is not yet fully consistent. X-axis represents vesicle size distribution (nm).

Discussion

This study with *Neisseria meningitidis* demonstrates that cysteine depletion can trigger growth arrest and the release of outer membrane vesicles (OMV) in sufficient quantities for vaccine production. The vesicles are released spontaneously (sOMV) and are as similar to *in vivo* vesicles as possible with a production system for human vaccines [213]. Therefore the obtained results may be relevant for the *in vivo* vesiculation and pathogenesis of *N. meningitidis*. To our knowledge, external stimuli that trigger sOMV release were not previously described for *N. meningitidis* or for cysteine as the limiting nutrient. Cysteine was found to be the growth-limiting component of human serum when supplemented to a chemically defined medium [243]. In serum-free media, some strains had an absolute cysteine requirement but others were able to grow on a variety of sulfur sources after adaptation [244, 245]. The vaccine production strain in this study is unable to adapt its sulfur metabolism after cysteine depletion, resulting in stationary growth despite a genetic ability to use alternate sulfur sources from the medium (Figure 1). The strain has specific mutations to express multiple protective PorA antigens, attenuate LPS toxicity and improve OMV yield, which are required for detergent-free vaccine production [185]. These mutations however may cause an inability to adapt to cysteine depleted conditions, since previous work with a strain that resembled the H44/76 parent strain more closely did not reveal an absolute cysteine requirement for growth [246].

Nutrient depletion was not previously associated with increased sOMV release by *N. meningitidis*, but specific genetic modifications are known to have a comparable outcome. The strain in this study has a disrupted *rmpM* gene to prevent anchoring of the outer membrane to the peptidoglycan layer with an OmpA-like domain [108, 121, 185]. The *gna33* mutation increases vesiculation through an unknown mechanism [104]. External stimuli for vesiculation have been identified in *E. coli*, including heat shock, lysine depletion or conditions that activate the σ^E envelope stress response pathway [41, 79-81]. In agreement with these observations, this study identified an external stress stimulus for *N. meningitidis* vesiculation. It remains unknown to what extent the current results are restricted to cysteine as the depleted nutrient or to this specific *N. meningitidis* strain.

Transcriptome analysis was performed to elucidate the intracellular effects of cysteine depletion in more detail. The transcriptome profile resembles studies with *N. meningitidis* that investigated stress [238, 239] and virulence stimuli [212, 240, 241] (Figure 2). Functional annotation revealed several pathways that are directly related to cysteine depletion or a decreased growth rate. The remaining pathways are related to oxidative stress, with a central role for iron-sulfur protein biogenesis. Iron-sulfur proteins are highly conserved in prokaryotes and eukaryotes. Mutants with an impaired biogenesis accumulate free intracellular iron and produce reactive oxygen species (ROS), which causes oxidative stress [247, 248]. In addition, iron-sulfur protein biogenesis requires sulfur acquisition and storage protein for free iron [249, 250]. These aspects are all represented by genes that are upregulated after cysteine depletion, including iron-sulfur cluster assembly (*erpA*, *nifU*), cysteine synthase/desulfurase (*cysK*, *iscS*), storage of Fe^{2+} ions (*bfrA*), ROS scavenging (*sodB*, *sodC*) and several reductases. Therefore it is hypothesized that impaired iron-

sulfur protein biogenesis also occurs in *N. meningitidis* after cysteine depletion, causing increased intracellular iron levels and oxidative stress.

Recent work by our group showed that sOMV release by *N. meningitidis* increased significantly during the stationary growth phase, but the mechanism was not fully understood [186]. By comparing cysteine repleted with depleted conditions, this study demonstrates that cysteine depletion is the trigger for onset of stationary growth and increased sOMV release (Figure 3). It also shows that growth repression with oxidative stress, the hypothesized outcome of cysteine depletion, mimics this effect temporarily. Release of sOMV increases directly after each peroxide addition but then stabilizes, while cysteine depletion results in sustained vesicle release. Also, the peroxide dose range is narrow and critical for bacterial viability (data not shown). Despite these limitations, the results confirm involvement of oxidative stress as an intracellular signal for sOMV release and support the transcriptome data. *N. meningitidis* encounters oxidative stress *in vivo*, when phagocytes use 'oxidative burst' to eliminate the invading pathogen [251, 252]. In such conditions vesiculation may provide decoys for phagocytosis and enhance bacterial survival.
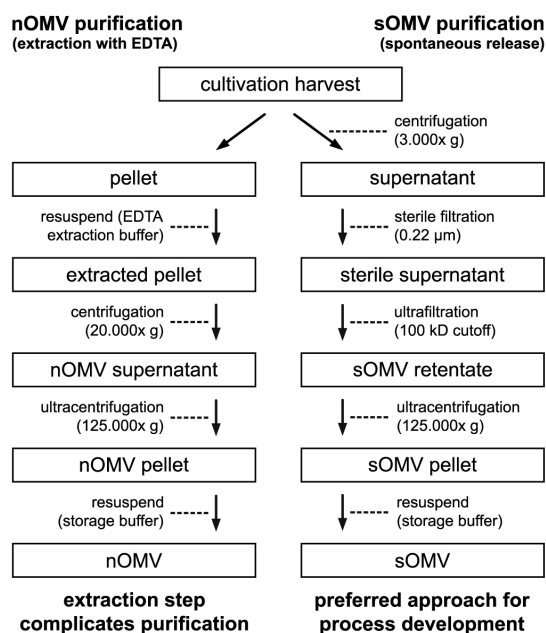
This study provides a novel approach for the production of sOMV vaccine against *N. meningitidis* serogroup B, in which onset of stationary growth and vesiculation is determined by the cysteine concentration of the growth medium. The use of a synthetic medium with a single growth-limiting component greatly improves process control. Other media for *N. meningitidis* have unidentified limiting nutrients and contain undefined components like casamino acids, resulting in less predictable growth [49, 61, 63, 253]. Purification of sOMV does not require concentration, resuspension or extraction of the bacterial biomass (Appendix 1). These steps are labor intensive and complicate processing, especially when translated to large-scale processes. Therefore sOMV purification is the preferred approach for process development. To assess feasibility, yield and quality of sOMV vaccines were compared with nOMV references at several time points before and after cysteine depletion. In agreement with the initial observations (Figure 3), sOMV release is triggered after cysteine depletion and then increases over time. Final yield is comparable to the nOMV reference, indicating that cysteine depletion can also provide a feasible yield (Figure 4; ±1500 human doses sOMV vaccine per L cultivation). The sOMV have a slightly broader size distribution, indicating that the purification procedure is not yet fully consistent. This procedure may improve by replacing the centrifugal ultrafiltration units with more robust and scalable equipment like tangential flow ultrafiltration [254].

In conclusion, this study shows that cysteine depletion can trigger growth arrest and outer membrane vesicle release by *N. meningitidis*. Transcriptome data suggests a relation between cysteine depletion and impaired iron-sulfur protein assembly, resulting in oxidative stress. This hypothesis is substantiated by showing that induced oxidative stress during cysteine-rich growth also triggers vesiculation. Cysteine depletion improves the production of a vaccine against serogroup B meningococcal disease, resulting in substantial amounts of sOMV. Since the sOMV are more similar to vesicles from natural infection, cysteine-dependent vesiculation is likely to be relevant for the *in vivo* pathogenesis of *N. meningitidis*.

Acknowledgments

Appendix 1

nOMV purification
(extraction with EDTA)

sOMV purification
(spontaneous release)

cultivation harvest

centrifugation
(3.000x g)

| pellet | supernatant |

resuspend (EDTA extraction buffer)

sterile filtration
(0.22 µm)

| extracted pellet | sterile supernatant |

centrifugation
(20.000x g)

ultrafiltration
(100 kD cutoff)

| nOMV supernatant | sOMV retentate |

ultracentrifugation
(125.000x g)

ultracentrifugation
(125.000x g)

| nOMV pellet | sOMV pellet |

resuspend
(storage buffer)

resuspend
(storage buffer)

| nOMV | sOMV |

**extraction step
complicates purification**

**preferred approach for
process development**

Detergent-free OMV purification.
There are two different detergent-free OMV purification types; sOMV (spontaneously released OMV) are purified from the culture supernatant without additional treatments to enhance vesicle release, while nOMV (native OMV) are obtained after detergent-free extraction of the bacterial biomass with a chelating agent (EDTA). Therefore both OMV types can be purified in parallel from a single cultivation. This study uses nOMV as a reference for high yield and quality [186]. Cultivation harvest was split in supernatant and bacterial pellet with low speed centrifugation. The supernatant was sterilized with filtration, then sOMV were concentrated with ultrafiltration and pelleted with ultracentrifugation. Purified sOMV were resuspended in a suitable volume of storage buffer. The bacterial pellet was resuspended in EDTA extraction buffer to release nOMV. Cells were incubated and discarded with semi high-speed centrifugation. Ultracentrifugation was used to concentrate nOMV and the pellet was resuspended in a suitable volume of storage buffer. Purification of nOMV requires several complicated steps in terms of handling (concentration, resuspension and extraction of the bacterial biomass). Therefore sOMV purification is the preferred approach for process development.

Appendix 2
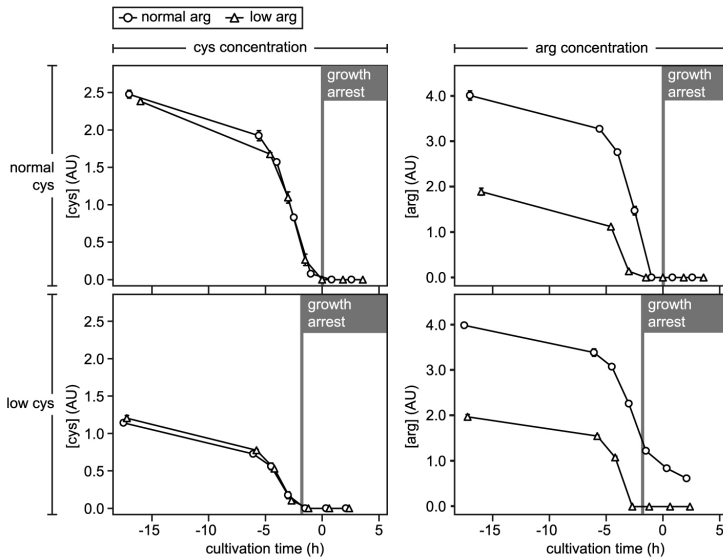
Nutrient monitoring identifies the growth-limiting medium component.
Media with different combinations of cysteine (cys) and arginine (arg) are tested to determine the growth-limiting component. Upper plots represent nutrient concentrations in media with normal cys, while the lower plots represent media with low cys. Media with normal or low arg are indicated with circles or triangles, respectively. Y-axes represent cys concentration (plots on the left) or arg concentration (plots on the right), The X-axis represents cultivation time, with t=0 as the expected time point of growth arrest (confirmed for control medium with normal amounts of cys and arg; upper left plot, circles). Grey vertical lines indicate the observed growth arrest time point (obtained from Figure 1). The results demonstrate that growth arrest depends on cys availability and is independent of arg.

Appendix 3

Details of the transcriptome analysis are available online as Supporting Information (Figure S3):
http://dx.plos.org/10.1371/journal.pone.0054314

Appendix 4

Details of the functional annotation are available online as Supporting Information (Table S1):
http://dx.plos.org/10.1371/journal.pone.0054314

Chapter 7

Improved production process for native outer membrane vesicle vaccine against *Neisseria meningitidis*

Bas van de Waterbeemd[1]
Gijsbert Zomer[1]
Patricia Kaaijk[1]
Nicole Ruiterkamp[2]
René Wijffels[3]
Germie P.J.M. van den Dobbelsteen [1‡]
Leo A. van der Pol[1]

[1] Institute for Translational Vaccinology (Intravacc), Bilthoven, The Netherlands
[2] Bilthoven Biologicals, Quality Control Bacterial Vaccines, Bilthoven, The Netherlands
[3] Wageningen University, Bioprocesses Engineering, Wageningen, The Netherlands
[‡] Present address: Crucell, Leiden, The Netherlands

Abstract

An improved detergent-free process has been developed to produce vaccine based on native outer membrane vesicles (nOMV) against *Neisseria meningitidis* serogroup B. Performance was evaluated with the NonaMen vaccine concept, which provides broad coverage based on nine distinct PorA antigens. Scalable aseptic equipment was implemented, replacing undesirable steps like ultracentrifugation, inactivation with phenol, and the use of preservatives. The resulting process is more consistent and gives a higher yield than published reference processes, enabling nOMV production at commercial scale. Product quality met preliminary specifications for 9 consecutive batches, and an ongoing study confirmed real-time stability up to 12 months after production. As the nOMV had low endotoxic activity and induced high bactericidal titers in mice, they are expected to be safe and effective in humans. The production process is not limited to NonaMen and may be applicable for other *N. meningitidis* serogroups and other gram-negative pathogens. The current results therefore facilitate the late-stage development and clinical evaluation of nOMV vaccines.

Introduction

Neisseria meningitidis is a human pathogen that causes acute meningitis and septicemia with high fatality rates [18]. Outbreaks of serogroup B meningococcal disease in Norway, New Zealand, and Cuba were successfully controlled with outer membrane vesicle (OMV) vaccines, which was a milestone for the application of OMV in vaccinology [3, 50, 51, 53]. The outer membrane porin A protein (PorA) is the dominant protective antigen but varies among strains [57, 90]. Recombinant strains with multiple PorA subtypes were developed to increase vaccine coverage, resulting in a nonavalent OMV vaccine (NonaMen concept) with potential coverage of 80% [5, 7, 62, 255]. Coverage has also been increased by complementing multiple Pores with conserved antigens, like fHbp or FetA [63, 64]. In addition OMV improved the immunogenicity of a vaccine with purified fHbp, NadA and NHBA protein, which has been submitted for regulatory review in Europe [66-68]. The use of OMV-based vaccines therefore remains a promising approach for the control of serogroup B meningococcal disease [71].

The vaccine strains used in Norway, New Zealand, and Cuba contained lipopolysaccharide (LPS) with strong endotoxic activity. To remove most of the LPS, the production process required extraction by deoxycholate, a detergent of animal origin [2, 49, 61]. The resulting detergent-extracted OMV (dOMV) tended to aggregate, and the deoxycholate was not fully removed during purification [49, 61, 185]. These issues, together with a high strain specificity of the immune response, have delayed the late-phase development of broadly protective dOMV vaccines. Van der Ley *et al.* attenuated LPS by introducing the *lpxL1* mutation rather than physically removing it with detergent [6]. As *lpxL1*-LPS has low endotoxic activity, it enables the development vaccines based on native OMV (nOMV) for use in humans [70]. nOMV are very similar to the natural vesicles released during infection [213]. Vaccines based on nOMV therefore have several advantages over those based on dOMV, including absence of aggregation and a broader immunogenicity provided by protective lipoproteins like fHbp [72-74, 185].

nOMV vaccines against *N. meningitidis* gave promising results in preclinical and clinical studies, but were either produced at small-scale or required process steps that are undesirable at commercial scale [82, 185, 187, 188, 190, 253]. These steps include the use of growth medium with undefined components of animal origin (casamino acids), inactivation of bacteria with hazardous chemicals like phenol, or the use of excessive mechanical force to release or homogenize nOMV (e.g., blender, micro fluidizer). Other problems involve use of preservatives with toxic components (like thiomersal) and use of ultracentrifugation, which limits production scale and complicates handling. nOMV production for phase III clinical trials and commercial use demands an efficient and reliable process that fully meets present-day regulatory requirements. As such a process was unavailable for nOMV vaccines, a novel process was developed. Performance was assessed with the NonaMen concept, a vaccine with broad coverage based on nonavalent PorA. Our results show that this new process provides a robust production platform for the late-stage development and clinical evaluation of nOMV vaccines.

Materials and methods

Trivalent strains and seedlots

The nOMV vaccines in this study were produced with RL strains 1, 2 and 3 (Appendix 1). Deletion of *rmpM* (R) and *lpxL1* (L) genes improved yield and attenuated LPS toxicity [185]. The RL strains are non-encapsulated variants of the *N. meningitidis* serogroup B isolate H44/76 [109] derived by deletion of the *cps*-locus (*siaA*, *siaD* and *galE* genes). Each RL production strain has 3 cloning sites for recombinant antigens, which were used to express unique PorA subtype variants (NonaMen concept; nonavalent PorA). For each strain, the research seedlot was adapted to the production medium in Erlenmeyer shake flasks to obtain frozen master seedlots (Figure 1, phase A). One master seedlot was used to generate approximately 50 frozen working seedlots through two additional expansions in shake flasks (two-tiered seedlot system). Master and working seedlots (cells at $OD_{590} = 1.5 \pm 0.3$; stored at -135°C with 17% (v/v) glycerol) were produced according to GMP guidelines.

Production of nOMV

Bulk nOMV were produced according to standard operating procedures in a non-GMP pilot facility, but future use of the process in a GMP facility was anticipated. Evaluation of deviations, batch review, and batch release were performed by QA/QP officers according to GMP standards. All cultures were grown in chemically defined production medium free of animal components and containing glucose, amino acids, salts, iron, and trace elements [4]. A primary 150 mL pre-culture was inoculated with 10 mL working seedlot and incubated in disposable 500 mL shake flasks with vented closure (Nalgene, Rochester NY, U.S.A.) at 35°C, 200 rpm. The pre-culture was used to inoculate a secondary pre-culture, grown in a 5 L bioreactor with 3 L working volume (Applikon, Schiedam, The Netherlands). At OD_{590} values between 1.5 and 4.5, a fixed amount of bacteria (corresponding to 1 L at $OD_{590} = 3$) was transferred to the 60L production bioreactor with 40 L working volume (Applikon, Schiedam, The Netherlands). Bioreactors were operated as described previously [4]. Antifoam was omitted, and a mechanical foam breaker was used to control foaming at 40 L scale (the 5 L reactor did not require a foam breaker) [4]. The production culture was harvested 3 hours after onset of the stationary phase (Figure 1, phase B), as observed with online monitoring of the oxygen consumption. Biomass was concentrated 5-fold using hollow-fiber microfiltration units with 0.2 μm pore size and 1.8 m² surface area (Spectrum Laboratories, Rancho Dominguez CA, U.S.A). Circulation was constant at 6.5 L/min, and feed pressure was monitored (phase C). Concentrated biomass was then diafiltrated with the microfiltration unit, using 2 volumes of buffer (100 mM Tris-HCl, pH 8.6). Concentrated EDTA solution was added to a final concentration of 10 mM to stimulate nOMV release (30 min at ambient temperature with continuous stirring). Bacteria were separated from the crude OMV by centrifugation (6 buckets with a content of max. 1 L; 75 min., 12500x g, 4°C), and the supernatant was depth-filtered (0.5-0.2 μm) to remove any residual pathogens (phase D). In phase E, the crude OMV extract was concentrated 12-fold and washed with ultra(dia)filtration (100 kD cut-off; 100 mM Tris-HCl pH 8.6). In phase F, any DNA that might be present was digested with 1000 U/L Benzonase (Merck; Schiphol-Rijk; The Netherlands). To remove impurities (bacterial host proteins, salts, small DNA), the nOMV were loaded onto a gel filtration chromatography column packed with Sepharose 6 Fast Flow size exclusion matrix (GE Healthcare, Hoevelaken,

The Netherlands). During gel filtration (phase G), the buffer was changed to storage buffer containing 10 mM Tris-HCl pH 7.4 with 3% (w/v) sucrose [107]. Bulk nOMV were sterilized with filtration (0.22 μm; Pall, Mijdrecht, The Netherlands), diluted to storage concentration (1 mg PorA/mL), and safely stored in the dark at 2-8 °C until further use (phase H). Stability of the bulk NOMV under these conditions is at least one year (ongoing real-time stability study). To prepare nonavalent vaccines for preclinical evaluation purposes (phase I), aseptic fill and finish were performed according to GMP guidelines. First, bulk nOMV from three trivalent RL strains were mixed to achieve nonavalent vaccine, then diluted to dose concentration with storage buffer, based on PorA concentration. Vials with 0.6 mL extractable volume were filled with vaccine and labeled. Each vaccine dose (0.5 mL) contained 15 μg of each PorA with a total of nine different PorA subtypes (Appendix 1).

Quality Control

QC tests were performed according to GMP and European Pharmacopoeia guidelines. **PorA identity** was verified with qualitative ELISA, using specific antibodies for each PorA subtype [61]. OMV from monovalent PorA strains and a Δ*porA* strain were used as controls. **Total protein concentration** (Ph. Eur. 2.5.33) was measured with the Lowry protein assay. Peterson's modification was used to reduce the effect of interfering substances [112]. The assay was performed according to manufacturer's protocol (Sigma-Aldrich, Zwijndrecht, the Netherlands). PorA content was determined by SDS gel electrophoresis (Ph. Eur. 2.2.31) followed by total protein staining and quantification of the 40-44 kD PorA bands. Gels were stained with Novex Colloidal Blue (Invitrogen, Breda, The Netherlands), and PorA was quantified as a percentage of total protein using TL100 1D gel analysis software (Totallab, Newcastle upon Tyne, U.K.) [112, 113]. Total nucleic acid concentration was used to estimate **residual genomic DNA**. Samples were incubated with ethidium bromide solution (MP Biochemicals, Illkirch, France), and fluorescence intensity was measured to quantify DNA concentration based on a salmon sperm DNA standard (Invitrogen, Breda, The Netherlands) [4, 114]. For bulk nOMV and nonavalent vaccines, there was no need to discriminate between RNA and DNA with an RNAse pre-treatment, because total nucleic acid concentration was low (<0.06 mg/mL). RNAse pre-treatment was used for in-process controls on intermediate products (before phase F). Fatty acid composition was analyzed to quantify **LPS concentration** with a modified gas chromatography method [115, 116] (Ph. Eur. 2.2.28). LPS was isolated with hot phenol-water extraction [117] and quantified using the peak height of C14:0-3OH, with C12:0-2OH as the internal standard (two C14:0-3OH residues per LPS). The molecular weight of *galE-lpxL1*-LPS in the RL strains was previously estimated at 2848 g/mol [185], but recent mass spectrometry work provided a more reliable estimation of 3191 g/mol, which was used for this study (Pupo Escalona *et al.*, manuscript in preparation). **Identity of *galE-lpxL1*-LPS** was verified with mass spectrometry [119]. An aliquot of 200 μL isolated LPS (see above; 50 nmol/ml) was freeze-dried and taken up in 0.1 ml of 2% acetic acid (pH 2.8). The mixture was heated to hydrolyze the LPS and release the lipid A moiety. Chloroform-methanol (2:1 v/v) was used to extract the lipid A and, after phase separation, the upper phase was used for analysis with mass spectroscopy (nano electrospray tandem MS on a Finnigan LCQ instrument in the negative-ion mode) [256]. **Vesicle size distribution** was measured with dynamic light scattering (DLS) at 25°C with a Malvern 4700 system [185] (Ph. Eur. 2.9.31). The vesicle size distribution was reflected in the polydispersity index (PdI), which ranges between

0.0 (fully homogeneous size distribution) and 1.0 (random size distribution). **Aggregation** was quantified by comparing the protein content of the nOMV starting material with the protein content of the supernatant after centrifugation at low speed (10 min. at 5000 xg) [185], using the total protein assay described above. Aggregation was calculated by expressing the difference between the total protein content of supernatant and starting material as a percentage of the starting material. **Sterility** was determined by filtration (Ph. Eur. 2.6.1). Aliquots of 30 mL were filtered through a membrane (<0.45 μm pore size) to retain any contaminating organisms and remove constituents that might inhibit growth. The membrane was incubated in shake flasks with 180 mL tryptic soy broth (TSB) for 14 days at 30-35ºC, with continuous aeration. The shake flask was inspected for visible growth and, if negative or sterile, it was inoculated with 10-100 cfu of *Bacillus subtilis* and re-incubated as a positive control for medium quality. **Endotoxic activity** of bulk nOMV was measured as described previously by stimulating IL-6 production in human macrophage cell line MM6 [120] (Ph. Eur. 2.6.30) [185]. Macrophages were seeded in 96-well plates ($3.75x10^4$ cells/well) in 125 μL IMDM medium supplemented with penicillin, streptomycin, L-glutamine, and fetal calf serum (Invitrogen, Breda, The Netherlands). Two-fold dilution series were made for all bulk nOMV samples in the supplemented IMDM medium, and cells were stimulated by adding 125 μL to each well. DOMV vaccine with known low toxicity (containing reduced amounts of non-attenuated *galE*-LPS) [257] and DTP-IPV vaccine (RIVM Bilthoven, The Netherlands) were included as references. A human dose of DTP-IPV vaccine contained 4 IU whole-cell pertussis, 30 IU diphtheria toxoid, 60 IU tetanus toxoid, and 40, 4 and 7.5 D-antigen units of inactivated poliovirus (type 1, 2 and 3, respectively). A human dose of OMV vaccine corresponded to 15 μg of each PorA subtype. Cells were stimulated for 16-18 hours at 37ºC with 5% CO_2 and IL-6 was quantified in the supernatant using ELISA, according to manufacturer's protocol (PeliKine Compact, Amsterdam, The Netherlands). Endotoxic activity was expressed in ng/mL IL-6 per human dose. **Serum bactericidal activity** of trivalent bulk nOMV was measured in sera of NIH mice (19-25 grams; <8 weeks old) after two subcutaneous immunizations on day 0 and 14 with 22.5 μg PorA (7.5 μg of each PorA subtype), with 10 mice per group. Sera were collected at day 28 and stored at -20ºC. Bactericidal titers were measured as described before [118]. **PorA epitope concentrations** were quantified in bulk nOMV using biosensor analysis on a Biacore T100 (GE Healthcare Benelux, Diegem, Belgium). One representative PorA subtype was chosen for each RL production strain: P1.7,16 for strain 1; P1.22,14 for strain 2, and P1.12,13 for strain 3. Quantification was based on titration of free antibody after incubation with bulk nOMV. Recombinant PorA protein of a specific subtype was diluted in the presence of 0.05% (w/v) Zwittergent 3.14 and subsequently coupled to a CM5 sensor chip using an amine coupling kit according to manufacturer's protocol (GE Healthcare), with immobilization levels between 10.000 and 12.000 response units (RU). Dilution series of bulk nOMV in HBS-P buffer (GE Healthcare) were made, and samples were incubated overnight with PorA-specific monoclonal antibody in a suitable dilution. An OMV reference with known epitope concentration was also included. After incubation, the mixtures were centrifuged (5 min. at 3000x g) to remove any aggregates. The antibody excess was quantified by injecting samples on the sensor chip (10 μl/min for two minutes). Assay data were analyzed by fitting a four-parameter logistic curve with Biacore T100 evaluation software. PorA epitope concentrations of bulk nOMV were calculated relative to the reference OMV.

Strain stability

Genetic stability of the RL production strains was assessed by continuing bacterial growth several generations beyond the normal harvest point of the production culture, using shake flasks. The age of the master seedlot was set at N=0 generations, and experimental seedlots were stored at N=30 generations of growth (regular production harvest), N=45 generations (post-production A), and N=60 generations (post-production B). The total number of generations at each time-point was calculated by taking the cumulative result of all previous passages in shake flasks and bioreactors. The number of generations from an individual passage was calculated with the formula: $\ln(\Delta OD_{590}) / \ln(2)$, in which ΔOD_{590} was the difference between the initial and final OD_{590} of a passage. At each time-point, relevant genetic modifications of the RL production strains (Appendix 1) were verified: PorA identity, identity of *galE-lpxL1*-LPS, *rmpM* and *porB* gene disruptions. Resistance against erythromycin, kanamycin, and chloramphenicol was tested by plating on GC agar with these antibiotics.

nOMV stability

Stability of bulk nOMV was monitored in an ongoing three-year stability study. The results up to 12 months after production are currently available. Bulk nOMV (n=3; one bulk product from each RL strain) were stored at a total PorA concentration of 1 mg/mL, at 4°C in the dark. At t=0, 3, 6 and 12 months, PorA epitope concentration (one representative epitope for each bulk product), PorA content, OMV size, aggregation, and pH were tested as described above. Sterility was tested at t = 0 and 12 months after production. Results were assessed with trend analysis. Data from replicates and time-points were merged for each stability parameter and analyzed for normality and sufficient sample size (D'Agostino's K^2 test; prerequisite for further analysis). A trend line was fitted with linear regression, and trends were tested for significant deviations from a non-zero slope (F test).

Results

Process outline and specifications

The improved NOMV production process is outlined in Figure 1. Product phases A to H describe the production of trivalent bulk nOMV. The upstream process starts with thawing of a working seedlot (phase A). After multiple passages of growth, the 40 L production culture is harvested (phase B), and biomass is concentrated with microfiltration (phase C). After a detergent-free treatment using the chelating agent EDTA (ethylenediaminetetraacetic acid), biomass is removed with consecutive centrifugation and filtration steps to obtain the pathogen-free, crude nOMV (phase D), which are the input material for downstream processing. Crude nOMV are concentrated and washed with ultra(dia)filtration (phase E), and DNA is digested with nuclease (phase F). The resulting nOMV are purified with gel filtration to remove salts and digested DNA fragments and also to enable a buffer change to storage buffer (phase G). After sterile filtration (phase H), the bulk nOMV from strains with trivalent PorA can be stored until they are combined as a nonavalent vaccine and diluted to the appropriate dose concentration
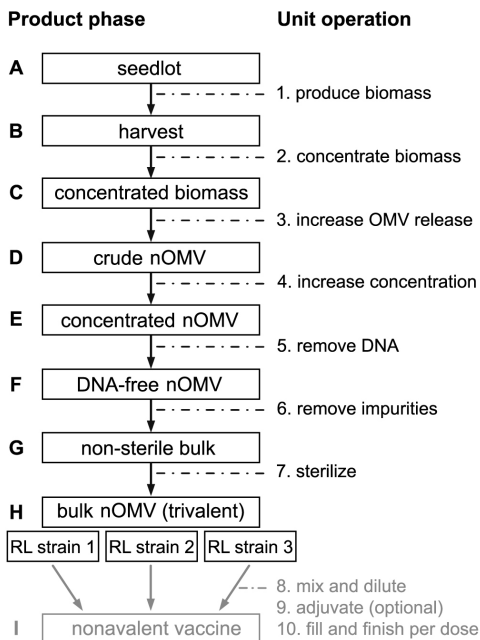

Figure 1. Flow-chart for improved nOMV production.
Process performance was evaluated with the NonaMen concept, a nonavalent PorA vaccine comprised of three trivalent RL production strains (ΔrmpM-ΔlpxL1 mutant strains; Appendix 1). Production of trivalent bulk nOMV is depicted in phases A to H. The transition from one phase to the next requires a specific unit operation (1 to 10). The seedlot (A) is first expanded in shake flask and bioreactor pre-cultures, then used to inoculate the production bioreactor. Harvested cells (B) are concentrated with microfiltration (C), and vesicle release is stimulated with a detergent-free buffer containing the chelating agent EDTA (D). Cells are discarded, and the crude nOMV are concentrated with ultrafiltration (E). Any residual DNA is digested with nuclease (F), and the extract is purified with gel filtration chromatography. The non-sterile bulk (G) is then sterilized by filtration to obtain the bulk nOMV (H). The trivalent product can be stored for at least one year before mixing as nonavalent vaccine and diluting to dose concentration (I).

Table 1. Specifications for improved nOMV production.
An outline with 7 consecutive unit operations (corresponding to Figure 1) was used as a starting point for process development and optimization. One large-scale nOMV process [253] and two large-scale dOMV processes [49, 61] were used as references to define desired specifications for each unit operation (Appendix 2). Solutions that are expected to provide these specifications are summarized, together with their implementation status in the current production process.

unit operation	specification	solution/result	current status
1. produce biomass	reproducible growth	chemically defined growth medium	optimized
	scalable >500 L	40 L bioreactor, scalable to 800 L	optimized [4]
	no antifoam	Low-shear foam breaker	optimized [4]
	on-line harvest point decision	oxygen consumption monitoring	optimized
2. concentrate biomass	replace centrifugation	hollow fiber microfiltration	functional [186]
3. increase OMV release	mild, low-shear	blender omitted	functional
	high extraction efficiency	critical process parameters identified	optimized [186]
	aseptic biomass removal	continuous centrifugation	not functional
	inactivation without phenol	depth filtration 0.5-0.2 µm	optimized
4. increase concentration	replace ultracentrifugation	ultrafiltration 100 kD cutoff	functional
5. remove DNA	replace ultracentrifugation	nuclease treatment	functional
6. remove impurities	replace ultracentrifugation	gel filtration chromatography	optimized
7. sterilize	replace thiomersal	sterile filtration 0.2 µm	optimized
	high efficiency	detergent-free (prevents aggregation)	optimized [186]

(phase I). The bulk nOMV vaccines in this study were produced for use in preclinical evaluation. As a starting point for process development, specifications were defined for processing aspects based on analysis of three reference processes: one large-scale nOMV process [253] and two large-scale dOMV processes [49, 61]. Appendix 2 compares these references with the current process. Table 1 summarizes the solutions designed to meet the specifications and their current status of implementation.

Bacterial strains

The three RL production strains ($\Delta rmpM$-$\Delta lpxL1$ mutant strains; Appendix 1) with different combinations of PorA antigens were adapted to the production medium and stored as frozen master and working seedlots. Quality Control testing confirmed microbiological identity (*N. meningitidis*), bacterial monoculture (no contaminating organisms), cell viability (>10^5 cfu/mL), and PorA identity (trivalent). Seedlots were produced, released, and stored according to GMP guidelines and may therefore be used to produce vaccines for clinical evaluation. Genetic stability of the RL production strains was constant at all four time-points that were assessed: master seedlot (N=0 generations of growth), production harvest (N=29 ± 1 generations), and two post-production time-points (N=43 ± 2 and N=61 ± 1 generations of growth, respectively). PorA identity results matched the subtypes in Appendix 1, as did the LPS identity (*galE-lpxL1*-LPS). Gene disruptions of *rmpM* and *porB* were confirmed with PCR (data not shown). Disruption of the *cps* locus (*siaA*, *siaD* and *galE* genes) was confirmed at all time-points by testing functionality of the erythromycin resistance gene (*ery^R*) used for disruption. Comparable tests confirmed kanamycin

and chloramphenicol resistance at all time-points, providing supplementary confirmation of *lpxL1* and *rmpM* disruption. These results indicate that the RL production strains are genetically stable for at least 30 generations of growth beyond the usual production harvest, in the absence of selective antibiotics.

Upstream production process

The primary pre-culture was inoculated with a thawed working seedlot, grown in a shake-flask to an OD_{590} of 1.4 ± 0.2 and used to inoculate the secondary pre-culture, which was grown in bioreactors to an OD_{590} of 2.9 ± 0.9. Inoculants were transferred during the exponential growth phase. All cultures were grown on chemically defined growth medium, without antifoam, and a mechanical foam breaker was implemented for the production bioreactor [4]. Production cultures started at an OD_{590} of 0.12 ± 0.02, at 40 L cultivation volume. Biomass growth was monitored by measuring OD_{590} and expressed as dry biomass concentration (1 OD_{590} unit corresponds to 0.32 g/L dry biomass or 2.47 g/L wet biomass). In addition, oxygen consumption was monitored on-line to determine the harvest point. The resulting characteristics are shown in Figure 2. Biomass
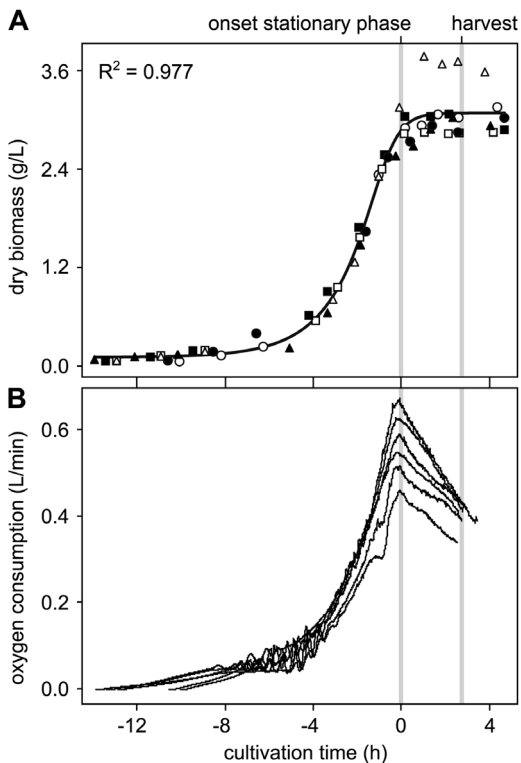

Figure 2. Upstream process characteristics.
(A) The upstream process was performed at 40 L scale, which was representative for large-scale (800 L [4]). Biomass growth (black line) on chemically defined production medium was highly reproducible (regression $R^2 = 0.977$). Cultivations from RL production strain 1, 2, and 3 were are indicated by squares, circles, and triangles (respectively). Duplicates for each strain are indicated with open and closed symbols, giving a total of 6 cultivations. (B) Oxygen consumption was monitored continuously. Cultivations were aligned at the time-point of maximal oxygen consumption (t=0), which represented onset of the stationary phase. Harvest point of the cultivations was previously optimized at t=3 hours [186].

growth was highly reproducible for all cultivations (n=6; duplicates for each strain; $R^2 = 0.977$). Cultivation profiles were aligned at the time-point of maximal oxygen consumption, which represented the onset of the stationary phase (t=0). The production cultures were harvested for further processing at 3.1 ± 0.3 hours after onset of the stationary phase, with a wet biomass yield of 23.8 ± 2.2 g/L. Harvest was concentrated 5-8 fold with microfiltration (scalable, aseptic) and washed with 2.1 ± 0.2 volumes Tris-HCl pH 8.6 buffer to adjust pH. This ensured a pH of 8.3–8.6. The EDTA treatment was performed with optimal setpoints for 'harvest' and 'pH', which were previously identified as critical process parameters [186].

Downstream production process

In the NonaMen vaccine concept, PorA is the primary protective antigen, and therefore a high PorA content is desired. When nOMV from the trivalent RL strains are properly purified, PorA content comprises more than 55% of total protein present in the vesicles [185, 186]. Figure 3A shows how PorA content evolves through the phases of the downstream process. During phases D, E and F, it was relatively low at an average of $26 \pm 5\%$ of total protein. Gel filtration chromatography removed impurities effectively and reproducibly, resulting in a final PorA content of $71 \pm 7\%$ at phases G and H. This was significantly higher than at the previous phases (p<0.0001). Figure 3A also shows the PorA recovery at various production phases. Initial PorA yield after EDTA treatment of cells (phase D) was set at 100%, and recovery at downstream phases (E to H) was
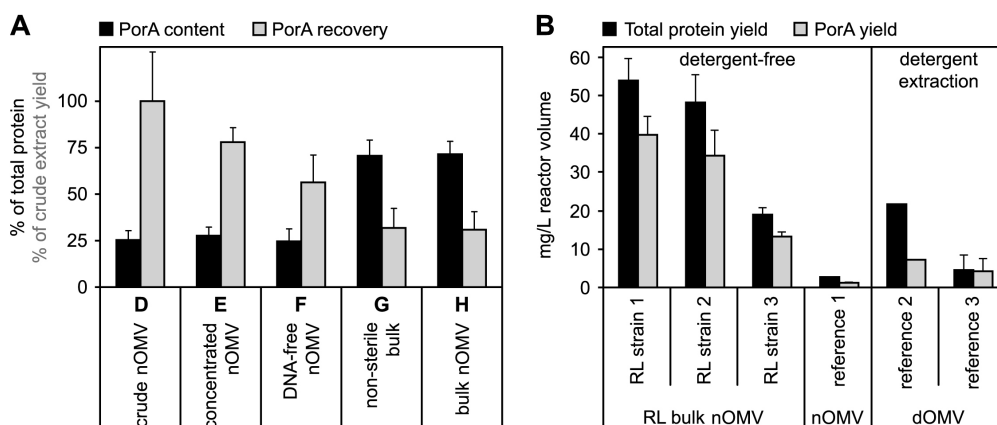

Figure 3. Downstream process characteristics.
(A) PorA content and recovery are shown for the consecutive product phases of the downstream process, from crude nOMV to bulk nOMV (Figure 1, phase D to H). PorA content (black bars) reaches final values from phase G onwards, indicating that the gel filtration chromatography effectively removed impurities. PorA recovery relative to phase D (grey bars) showed that losses were spread equally across the process, but notably not during sterile filtration (phase G to H), resulting in a reproducible and good overall recovery. Error bars indicate standard deviation of combined data from the three RL production strains (n=9). (B) Total protein and PorA yield of RL bulk nOMV (phase H) and large-scale reference processes. Reference 1 [253] is most comparable the current process since both are detergent-free (nOMV product). References 2 [49] and 3 [61] use detergent-extraction (dOMV product). All RL strains have a higher PorA yield than the references. RL strain 3 has a lower yield than the other two RL strains, resulting in a total protein yield that is comparable to reference 2 but still higher than the other references. The results of individual RL strains are reproducible, therefore this yield difference is not caused by the process. Error bars indicate standard deviation of replicate batches (n=3).

expressed as percentages of the initial yield. Losses were distributed evenly across phases E, F and G (22 ± 8%, 22 ± 7%, and 25 ± 7% yield loss, respectively), resulting in a good overall PorA recovery of 31 ± 10%. PorA recovery for RL strain 3 was lower than for the other strains, resulting in slightly elevated standard deviations. Notably, sterile filtration (phase G to H) was performed with a recovery of 96 ± 6%, indicating that the OMV passed the 0.2 μm filter without detectable losses.

Process yield

Mean yield of the novel process was substantially higher than the yield of large-scale reference processes, as illustrated in Figure 3B. Reference 1 [253] is most comparable to the current process, since they are both detergent-free, whereas references 2 [49] and 3 [61] use detergent-extraction (Appendix 2). The mean yield of three RL production strains was 40 ± 17 mg total protein per L reactor volume, which was 15-fold higher than reference 1 (2.7 mg/L), 2-fold higher than reference 2 (21.7 mg/L), and 9-fold higher than reference 3 (1.9–7.4 mg/L). However, the individual RL strains varied: RL strain 3 had a yield of 19 ± 2 mg/L, which was considerably less than RL strains 1 and 2 (54 ± 6 and 48 ± 7 mg/L, respectively). Figure 3B therefore shows the individual RL yields rather than their average. In addition, Figure 3B confirms a substantially higher PorA yield for all RL strains (2–30 fold). According to the literature, yield of reference 1 was based on 270 L reactor volume, 450 mL product with 0.8 mg/mL total protein and PorA content of 50% (our estimation); yield was multiplied by 2.03, because 49.3% (not 100%) of total biomass was processed. Reference 2 yield was based on 15 L reactor volume; 13000 doses (25 μg total protein with 33% PorA). Reference 3 yield was based on 135 L reactor volume; 250 to 1000 mg total protein with 89% PorA.

Quality Control

The most important aspect of process performance is the resulting product quality, in this case the quality of bulk nOMV with trivalent PorA. Therefore, batches of bulk nOMV (n=9; three for each RL production strain) were characterized with Quality Control tests according to GMP and European Pharmacopoeia (EP) guidelines. The analyses confirmed that quality was within preliminary specifications for all batches (Table 2A). The nOMV were sterile, had the expected PorA identity (trivalent), high total protein content (1.4 ± 0.2 mg/mL), high total PorA content (0.98 ± 0.09 mg/mL), and low residual DNA (0.007 ± 0.002 mg/mL). They also had native amounts of *galE-lpxL1*-LPS (0.23 ± 0.06 mg/mL), homogeneous OMV size (81 ± 7 nm), and absence of aggregation (3 ± 3%). Three batches of bulk nOMV (one for each trivalent RL strain) were assessed for endotoxic activity, functional immunogenicity, stability, and appearance (see paragraphs below). In addition, bulk nOMV were mixed to produce nonavalent vaccine, for evaluation in mice and rabbits. This separate study confirmed that the nonavalent vaccine induces broad immunogenicity and is well-tolerated [258].

The endotoxic activity of bulk nOMV (n=3) was measured with IL-6 monocyte activation (Table 2B). Used as references were a dOMV vaccine with low toxicity, as proven in a phase I clinical study [257], and a DTP-IPV vaccine (containing diphtheria and tetanus toxoid, whole-cell pertussis, and inactivated polio virus). The bulk nOMV induced 27 ± 2 ng/mL of IL-6 per human dose (26, 27 and 29 ng/mL for RL strains 1, 2 and 3, respectively; one human dose corresponded to 15 μg PorA of each PorA subtype). This was approximately 25-fold lower than both reference vaccines. The dOMV vaccine induced 700 ng/mL of IL-6 per human dose, and the DTP-IPV

vaccine induced 778 ng/mL of IL-6 per human dose. Therefore the nOMV are expected to be safe for parenteral use in humans.

Functional immunogenicity was assessed by measuring serum bactericidal activity in mice sera after two immunizations with trivalent bulk nOMV, one for each RL strain (Table 2C). High bactericidal titers (>4 fold increase in mean ^{2}log titer of responders) were observed for 8 of 9 tested PorA subtypes. PorA subtype P1.18-1,3,6 had a low titer, with only 1 mouse of 10 responding to vaccination. Of the 8 PorA subtypes with high titers, P1.19,15-1 was just above threshold, and P1.7-1,1 had a lower number of responders (5 out of 10 mice). These results indicate that the bulk nOMV induced high functional immunogenicity in mice for most PorA antigens. In addition to the Quality Control tests, we assessed protein composition and appearance of the nOMV. Total protein composition (determined by SDS gel electrophoresis) is shown in Figure 4A, illustrating the major contribution of PorA protein (42 kD; 71 ± 7% of total protein). Overall protein composition of bulk nOMV was comparable among the three trivalent RL production strains, resulting in nonavalent vaccine with an equally comparable composition. Dynamic light scattering (DLS) was used to visualize nOMV appearance (Figure 4B) and found non-aggregation; homogeneous size distribution with averages of 86.2 nm (RL strain 1), 86.7 nm (RL strain 2), and 73.8 nm (RL strain 3); and low polydispersity indices of 0.12, 0.08, and 0.11, respectively. A representative electron micrograph of non-adjuvated nonavalent vaccine after dilution to dose concentration (Figure 4C) showed fully intact, non-aggregated vesicles with a size between 40 and 100 nm.
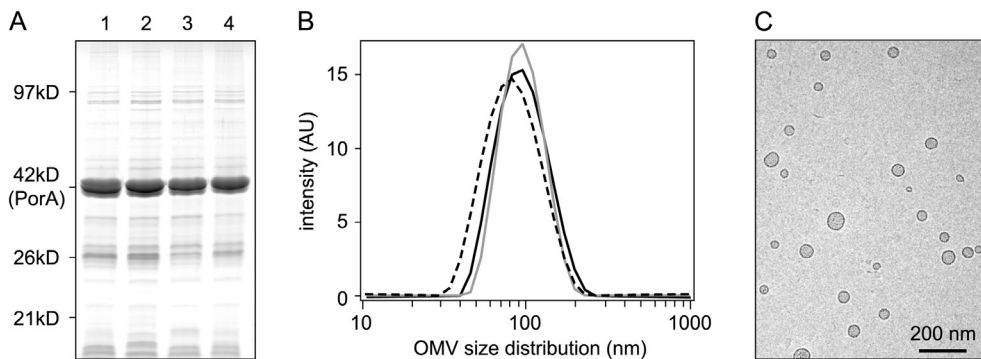

Figure 4. Protein composition and appearance of nOMV.
(A) Protein composition of trivalent bulk nOMV is shown in lanes 1 to 3 for RL strains 1, 2 and 3, respectively (phase H), and composition of the nonavalent vaccine (phase I) in lane 4. Bulk nOMV from the three RL production strains were comparable, therefore the nonavalent vaccine had an equally comparable protein composition. (B) Vesicle size of trivalent bulk nOMV was similar for RL strain 1 (black line), RL strain 2 (grey line), and RL strain 3 (dashed line). All bulk nOMV were non-aggregated and had comparable, homogeneous size distributions, with averages between 74 and 87 nm. (C) Electron micrograph of nonavalent vaccine (non-adjuvated) after dilution to dose concentration shows that vaccine contained fully intact, non-aggregated OMV, an important benefit of the detergent-free production process.

Table 2. Quality Control testing of bulk nOMV.
(A) General characteristics include biochemical composition, PorA identity, and sterility for which preliminary specifications were set. (B) Endotoxic activity of the bulk nOMV was approximately 25-fold lower than in dOMV and DTP-IPV reference vaccines. (C) In addition, high bactericidal titers were induced in mice (^{2}log titers >4 for 8 out of 9 PorA subtypes), with few non-responders. These results indicate that the bulk nOMV have a consistent product quality and are likely to be safe and immunogenic in humans.

2A – general characteristics		
QC parameter	preliminary specification	result (n=9)
sterility	no growth	no growth
PorA identity	trivalent	trivalent
total protein	>1.0 mg/mL*	1.4 ± 0.2 mg/mL
total PorA	1.00 ± 0.25 mg/mL*	0.98 ± 0.09 mg/mL
PorA content	>55% of total protein	71 ± 7%
galE-lpxL1-LPS	0.25 ± 0.15 mg/mL	0.23 ± 0.06 mg/mL
OMV size	<220 nm	81 ± 7 nm
aggregation	no specification	3 ± 3%
DNA	<0.050 mg/mL	0.007 ± 0.002 mg/mL

2B – endotoxic activity		
vaccine	preliminary specification	result (ng/mL IL-6 per human dose)
bulk nOMV (n=3)	<DTP-IPV reference	27 ± 2
dOMV low toxicity	–	700
DTP-IPV reference	–	778

2C – serum bactericidal activity			
vaccine	PorA subtype	^{2}log titer**	responders
bulk nOMV strain 1 (n=1)	P1.7,16	10.3 (>4)	9/10
	P1.5-1,2-2	12.0 (>4)	10/10
	P1.19,15-1	4.6 (>4)	9/10
bulk nOMV strain 2 (n=1)	P1.22,14	8.7 (>4)	10/10
	P1.7-1,1	6.2 (>4)	5/10
	P1.18-1,3,6	3.0 (<4)	1/10
bulk nOMV strain 3 (n=1)	P1.5-2,10	10.2 (>4)	10/10
	P1.12-1,13	7.7 (>4)	10/10
	P1.7-2,4	6.4 (>4)	7/10

*During processing PorA concentration of bulk nOMV is set at 1 mg/mL for storage purposes.
**Mean titers of responders.

nOMV stability

The production dates of three batches of bulk nOMV (one for each RL strain) were used as starting points for an ongoing real-time stability study. The nOMV were stored at a total PorA concentration of 1 mg/mL, at 4°C in the dark. Quality Control tests focused on biochemical aspects (PorA content, OMV size, aggregation, and pH), sterility, and epitope concentration (determined by quantitative Biacore assay with specific antibodies against a PorA subtype, using

one representative PorA selected for each RL strain). Stability data at 0, 3, 6 and 12 months after production are presented in Appendix 3. The data did not contain trends with significant non-zero slopes, indicating that the nOMV were sterile and had a stable PorA content, vesicle size, and pH. Aggregation was low at all time points (<5%), but trend analysis could not be performed due to skewed distribution. Epitope concentrations seemed constant, but sample size at t=12 was still too small for reliable trend analysis. The table shows results for all time-points up to t=12, indicating that the bulk nOMV were stable for at least one year after production. Trivalent bulk nOMV were also mixed to produce nonavalent vaccine [258]. Functional immunogenicity of this vaccine in mice will be monitored up to 36 months after production in a second, real-time stability study (data not yet available).

Discussion

An efficient and consistent process for the detergent-free production of nOMV vaccine against *N. meningitidis* has been developed (Figure 1). Compared to previously described processes, this process offers important improvements that are likely to enable production at commercial scale (Table 1; Appendix 2) [49, 61, 253]. Process performance was evaluated with the NonaMen vaccine concept, which provides broad protection against serogroup B meningococcal disease based on nine different PorA antigens [5, 60, 62].

The upstream process uses production strains with multiple recombinant antigens that are genetically stable in the absence of selective antibiotics. The strains also have mutations in *lpxL1* and *rmpM* genes to attenuate LPS toxicity and improve yield [6, 185] (Appendix 1). Without these genetic modifications, the detergent-free approach would not be feasible. To prevent hydrophobic interactions with the outer membrane, antifoam is omitted from the growth medium. Instead, a mechanical foam breaker was implemented that does not impose significant shear force or lysis [4]. The resulting growth curves are highly reproducible (Figure 2A) and with a higher biomass yield than large-scale references [49, 253]. Biomass yield can be further improved by implementing a feed strategy, since onset of the stationary phase is triggered by nutrient depletion rather than limitations in the oxygen supply (data not shown). The production culture is harvested after three hours of the stationary phase, and the harvest point is detected online with oxygen consumption monitoring (Figure 2B). Biomass density is constant during this period, but the oxygen consumption does not stabilize. It is therefore uncertain whether the stationary phase is a temporary transition from exponential growth to death phase, or a truly stationary phase in which growth remains at maintenance levels for a prolonged period.

Harvested biomass is concentrated with scalable, aseptic equipment, and nOMV release is stimulated with a detergent-free EDTA buffer under optimized conditions [186]. The EDTA treatment does not require a blender, which is likely to increase lysis. Spent biomass is then separated from the crude nOMV with consecutive centrifugation and depth-filtration. These steps remove all pathogenic activity from the crude nOMV without the need for hazardous chemicals like phenol. However, the centrifugation still requires handling in a biohazard cabinet, with risk of contamination, and limits the process scale to approximately 100 L cultivation volume. Therefore future improvements will include the implementation of alternatives, like continuous flow centrifugation for initial biomass removal, as demonstrated for *Bordetella pertussis* and fragile mammalian cells [259, 260].

During downstream processing (Figure 3A), the crude nOMV are concentrated with ultrafiltration, and nuclease is added for digestion of any DNA. Subsequent gel filtration chromatography removes impurities and ensures a high final PorA content. These steps replace ultracentrifugation, which is commonly used and effective but limits the production scale. Ultracentrifugation also requires manual homogenization of multiple nOMV pellets. This is performed in a flow cabinet, with risk of contamination, and followed by a micro fluidizer treatment that imposes excessive shear force. The current process uses scalable, aseptic equipment and allows the nOMV to remain a stable colloid suspension during all production stages. Overall PorA recovery is good,

approximately one third of the initial crude nOMV yield. The ultrafiltration and nuclease steps give reproducible results but are not yet optimized, resulting in higher losses and offering room for future improvement. Importantly, sterile filtration of bulk nOMV is performed without detectable losses and obviates the need for preservatives like thiomersal. This is an notable benefit of the detergent-free approach, ensuring that the nOMV are non-aggregated and smaller than the filter cut-off (<220 nm). Detergent-extracted OMV are prone to aggregation and more heterogeneous in size, resulting in significant losses during sterile filtration [61, 185, 226]. Even though these issues do not affect immunogenicity, it is clearly beneficial to prevent them by omitting the detergent-extraction [107].

Overall PorA yield of the new production process is substantially higher than the yield of published reference processes with or without detergent-extraction (Figure 3B) [49, 61, 253]. This is a cumulative benefit of production strains with *rmpM* mutation [185], a higher biomass yield, and a generally more efficient process. RL strain 3 had a lower yield than the other strains but not as a result of the process, which gave reproducible results for all three strains. The lower yield may originate from a less effective assembly of recombinant PorA antigens in strain 3, but this remains speculative. One of the reference processes [49] was commercialized to control a meningitis epidemic in New Zealand. Compared to that reference, the current process shows a higher PorA yield for all RL strains, avoids components of animal origin (deoxycholate), and is scalable to at least 800 L cultivation volume [4]. Therefore it is likely to be feasible at commercial scale.

Quality Control testing showed that product quality is within preset criteria for all 9 bulk nOMV batches, an important indicator for process performance (Table 2A). The product quality has been constant for at least the first year of an ongoing real-time stability study (Appendix 3*).* This study seeks to show stability for up to three years. Endotoxic activity of the bulk nOMV is approximately 25-fold lower than a low-toxicity vaccine based on detergent-extracted OMV [257] or the DTP-IPV vaccine with whole-cell pertussis component. Long used in the Dutch national vaccination program, that DTP-IPV vaccine had a relatively high rate of adverse events and was replaced in 2005 with one containing acellular pertussis [261, 262]. It thus represents the upper range of low endotoxic activity, providing a useful context for our results. Functional immunogenicity of the trivalent bulk nOMV in mice is high, and comparable to detergent-extracted HexaMen and NonaMen vaccine [5, 61]. The improved production process therefore generates high quality nOMV that are likely to be well-tolerated and induce a functional immune response in humans (Table 2B-C). The contribution of individual PorA antigens needs to be assessed in more detail, since subtypes P1.7-1,1 and P1.18-1,3,6 gave low titers or few responders. Other studies with multivalent PorA vaccine confirm this observation [5, 258]. Priming with monovalent OMV from less immunogenic PorA subtypes before immunization with the multivalent vaccine may solve this issue [126]. A recent study with mice and rabbits confirmed that NonaMen vaccine from the improved process induced broad immunogenicity without related toxicity or pathology. These results encourage clinical evaluation [258].

The scope of the novel production process is not restricted to the NonaMen concept and may be applicable for the late-stage development of other nOMV vaccines. These include promising serogroup B concepts with a different antigen composition or vaccines against other *N. meningitidis*

serogroups [63, 64, 82, 187, 188, 190, 231]. The outer membrane vesicles from gram-negative pathogens in general, like *Escherichia coli*, *Vibrio cholera*, or *Bordetella pertussis*, are also within the scope if the upstream process is adjusted to meet the nutritional requirements of these pathogens [83, 84, 263-267]. Even recombinant antigens derived from other pathogens may benefit from an OMV presentation form [70, 268-270]. This work thus provides a robust production platform to facilitate the late-stage development and clinical evaluation of nOMV vaccines.

Acknowledgments

Appendix 1

Genetic modifications of the trivalent RL production strains.

The RL strains are non-encapsulated variants of strain H44/76, in which *rmpM* (R) and *lpxL1* (L) genes have been disrupted to improve yield and attenuate LPS toxicity (*galE* truncated *lpxL1*-LPS). Each RL strain has 3 cloning sites for recombinant antigens. The NonaMen vaccine concept (nonavalent PorA) was used to evaluate performance of the new production process. Therefore all cloning sites of the trivalent RL strains contained PorA subtype variants. The RL strains are genetically stable for at least 30 generations of growth beyond the regular production harvest, in the absence of selective antibiotics.

Strain	Cloning site 1	Cloning site 2	Cloning site 3	LPS type	Other mutations	Genetic stability
RL strain 1	*porA* P1.7,16	*porA* P1.5-1,2-2	*porA* P1.19,15-1	*ΔgalE* *ΔlpxL1*	Δ*cps* Δ*rmpM* Δ*porB* ery-R kan-R cam-R	confirmed
RL strain 2	*porA* P1.22,14	*porA* P1.7-1,1	*porA* P1.18-1,3,6			confirmed
RL strain 3	*porA* P1.5-2,10	*porA* P12-1,13	*porA* P1.7-2,4			confirmed

Appendix 2

Comparison of large-scale OMV production processes.

The table shows how important OMV processing aspects are addressed in the current production process and in large-scale reference processes. Reference 1 [253] is most comparable to the current process, since both are detergent-free. References 2 [49] and 3 [61] use detergent-extraction.

process aspect	current process	reference process 1	reference process 2	reference process 3
reduce LPS toxicity	Δ*lpxL1*	Δ*lpxL1*	deoxycholate extraction	deoxycholate extraction
components of animal origin	none	casamino acids	casamino acids, deoxycholate	deoxycholate
working volume bioreactor	40 L*	270 L	15 L	135 L
undefined medium components	none	casamino acids	casamino acids, yeast extract	yeast extract
reduce foam	foam breaker	antifoam	not described	not described
concentrate biomass	microfiltration	continuous centrifugation	centrifugation	cont. centrifugation, centrifugation
increase OMV release	Δ*rmpM*, detergent-free extraction	blender, detergent-free extraction	deoxycholate extraction	deoxycholate extraction
inactivate biomass	depth filtration	phenol, heat	deoxycholate	deoxycholate
remove biomass	centrifugation**	centrifugation	centrifugation	centrifugation
increase OMV concentration	ultrafiltration	ultrafiltration	ultracentrifugation	ultracentrifugation
remove impurities	nuclease, gel filtration	nuclease, ultracentrifugation	ultracentrifugation	ultracentrifugation
sterilize	filtration	micro fluidizer, filtration	thiomersal	thiomersal

*The 40 L bioreactor has been successfully scaled to 800 L [4]. **Will be replaced with continuous centrifugation if scale-up to >100 L cultivation volume is required.

Appendix 3

Real-time stability of bulk nOMV.

Results of an ongoing stability study are shown at 0, 3, 6 and 12 months after production. They are presented as (A) Quality Control tests for general stability aspects and (B) Stability of selected PorA epitopes. Results were highly reproducible throughout the study, as confirmed by trend analysis, indicating that the bulk nOMV were stable for at least one year after production.

3A – general characteristics (n=3)						
QC parameter	unit	t = 0	t = 3	t = 6	t = 12	trend p-value*
sterility	–	sterile	not available	not available	sterile	not applicable
PorA content	% total protein	72 ± 8	77 ± 3	72 ± 4	73 ± 5	>0.05 (0.91)
OMV size	nm	82 ± 7	82 ± 7	82 ± 7	81 ± 7	>0.05 (0.86)
aggregation	%	3 ± 4	1 ± 2	2 ± 2	0 ± 1	not available**
pH	–	7.4 ± 0.1	7.3 ± 0.2	7.4 ± 0.1	7.3 ± 0.2	>0.05 (0.61)

3B – epitope concentration (n=1)						
bulk NOMV	unit	t = 0	t = 3	t = 6	t = 12	trend p-value*
RL strain 1 (P1.7,16)	mg/mL	0.39	0.41	0.53	0.55	not available**
RL strain 2 (P1.22,14)	mg/mL	0.50	0.47	NA***	0.47	not available**
RL strain 3 (P1.12,13)	mg/mL	0.63	0.54	0.57	0.50	not available**

*P-value >0.05 indicates that the time trend does not deviate significantly from a non-zero slope (confirms stability). **Skewed distribution and/or sample size too small. ***Missing data point.

Chapter 8

Preclinical safety and immunogenicity evaluation of a nonavalent PorA native outer membrane vesicle vaccine against serogroup B meningococcal disease

Patricia Kaaijk[1]
Ineke van Straaten[2]
Bas van de Waterbeemd[1]
Elmieke P.J Boot[2]
Lonneke M.A.R. Levels[2]
Harry H. van Dijken[3]
Germie P.J.M. van den Dobbelsteen[1*]

[1] Institute for Translational Vaccinology (Intravacc), Bilthoven, The Netherlands
[2] Bilthoven Biologicals, Quality Control Bacterial Vaccines, Bilthoven, The Netherlands
[3] National Institute for Public Health and the Environment, Centre for Immunology of Infectious Diseases and Vaccines, Bilthoven, The Netherlands
[*] Present address: Crucell, Leiden, The Netherlands

Abstract

Background. An improved nonavalent PorA native outer membrane vesicle vaccine was developed with intrinsic adjuvating activity due to presence of less-toxic (lpxL1) LPS. In the present study, the safety and immunogenicity of this next-generation NonaMen vaccine were evaluated following repeated vaccination in rabbits and mice.

Methods. A repeated–dose toxicology study was performed in rabbits. Immunogenicity of next-generation NonaMen was evaluated by determining the serum bactericidal antibody (SBA) titers against meningococcal serogroup B strains containing several PorA subtypes. Release of the pro-inflammatory cytokine, interleukin-6 (IL-6), by the human monocyte cell line (MM6) was measured to estimate pyrogenic activity.

Results. No toxicologically relevant findings were noted in vaccinated rabbits receiving plain next-generation NonaMen. In agreement, next-generation NonaMen induced reduced amounts of the pro-inflammatory cytokine, IL-6, released by human monocyte cell line. In both rabbits and mice, next-generation NonaMen induced high SBA titers against all tested MenB strains regardless of whether or not aluminum phosphate adjuvant is used.

Conclusions. The data suggests that next-generation NonaMen is a safe vaccine with the potential to develop a broadly protective immune response and encourage the start of the first clinical studies.

Introduction

At present, no broadly protective vaccine against MenB strain infections is available. So far, only MenB vaccines based on OMV have been proven successful in controlling prevailing MenB epidemics [3, 50-54]. OMV vaccines have been traditionally prepared with detergent extraction to remove reactogenic lipopolysaccharides (LPS) and to increase vesicle release. The LPS of *N. meningitidis* is highly toxic, but residual amounts are needed to maintain the outer membrane vesicle structure and to potentiate the immune response by its adjuvating activity [93]. The use of a detergent has major disadvantages. Along with LPS, detergents remove phospholipids and membrane lipoproteins that may contribute to immunogenicity [72, 94]. In addition, the vesicle integrity can be affected by treatment with detergent resulting in aggregation of the OMV vaccine product [61, 185]. A detergent-free OMV purification process retains all LPS, which results not only in a preserved native vesicle structure, but also in an OMV vaccine product that is too toxic for parenteral immunization [3]. Discovery of *lpxL1* mutant strains, at the Institute for Translational Vaccinology (Intravacc) in the Netherlands, provides a solution for the undesired toxic effect of LPS [6, 70]. Inactivation of the *lpxL1* gene attenuates LPS toxicity, while preserving the adjuvant activity needed to potentiate the immune response [6, 94]. Human monocytes, macrophages or peripheral blood mononuclear cells exposed to *lpxL1*-LPS induced less pro-inflammatory cytokines compared to exposure to wild-type LPS, indicating that the reactogenicity of *lpxL1*-LPS in human is expected to be far less than that of wild-type LPS [72, 94, 185, 271, 272]. Furthermore, it was found that the poor immunogenicity of OMV from LPS-deficient strains could be restored by adding external *lpxL1*-LPS [105, 106].

PorA protein (class 1 protein) has been identified as major protective antigen of *N. meningitidis*. However, many PorA protein variants exist among circulating strains which complicates development of a broadly protective vaccine. To circumvent this, three meningococcal serogroup B vaccine strains obtained from the H44/76 parental strain were genetically engineered to express three different PorA subtypes [5, 273]. OMV from these three recombinant strains were pooled to obtain the nonavalent PorA vaccine (NonaMen). NonaMen has the potential to prevent the majority of serogroup B infections in Europe, i.e. 80% of cases [5, 7, 62]. Based on the most recent national surveillance data available, our NonaMen vaccine formulation is expected to protect in 2007, 2008, 2009, 2010 and 2011 against respectively 89.0%, 89.3%, 94.0%, 91.7% and 85.5% of the occurring MenB sero-subtypes in the Netherlands. Previously, detergent-extracted NonaMen was shown to be safe and immunogenic in rabbits and mice and well-tolerated in healthy adults [5, 273]. Unfortunately, the need of a detergent for removal of toxic LPS in the production process of this NonaMen resulted in an OMV product with lower quality, i.e. partially disintegrated and aggregated vesicles [61]. Inactivation of the *lpxL1* gene has solved this problem and facilitated a stable OMV vaccine product without the need for detergent extraction to remove toxic LPS. To address the safety and immunogenicity of this next-generation NonaMen vaccine, a repeated dose study was conducted in both rabbits and mice.

Material and methods

Vaccine preparations

Three trivalent PorA vaccine strains, which were genetically modified by inactivation of the *lpxL1* gene, were developed from a *rmpM* deletion mutant of the H44/76 MenB parental strain (Figure 1). [6, 185]. The subsequent three trivalent bulk OMV products were pooled to generate the next-generation nonavalent vaccine (NonaMen). Vaccine doses were based on total PorA concentration. Plain NonaMen 7.5 or 15 (contained respectively 7.5 μg or 15 μg PorA per subtype per dose of 0.5 mL) were formulated in Tris-sucrose buffer. Adjuvated NonaMen 15 (15 μg PorA per subtype per dose of 0.5 mL) was formulated in Tris-sucrose buffer containing aluminum phosphate (3 mg/mL). A dose of 15 μg/PorA type in 0.5 mL represents the highest intended human dose. Placebo consisted of Tris-sucrose buffer containing aluminum phosphate (3 mg/mL) without MenB component.
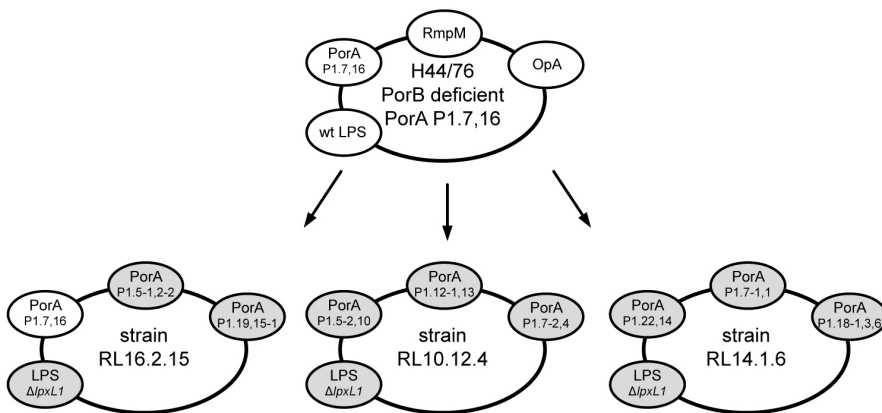

Figure 1.
Schematic design of the three trivalent vaccine strains derived from the H44/76 parental (PorB deficient) strain that were used for preparing next-generation NonaMen.

GLP toxicology study in rabbits

A fully GLP compliant repeated-dose toxicology study (including local tolerance) was performed by an external contract research laboratory. Four groups of New Zealand White rabbits (2-3 kg), each consisting of 5 main animals per sex, and 3 recovery animals per sex, were immunized by 5 intramuscular injections, on days 1, 15, 29, 43 and 57, in alternating hind limbs. At day 60, main animals were bled under anesthesia. Recovery of initial pathological effects was investigated in the remaining recovery animals that were sacrificed and bled at day 71. The four groups received respectively, placebo, plain NonaMen 7.5, plain NonaMen 15 or adjuvated NonaMen 15. Rectal body temperature was measured 4 hours after vaccination based on results of a previous study in which body temperature was measured continuously by using implanted temperature data showing a peak temperature 4 hours after vaccination with NonaMen [274]. At the end of the study, macroscopic examination of organs, including organ weights, and histopathology on selected tissues were performed by a veterinary pathologist. Blood samples were taken at days 4, 57, 60, and 71 to determine relevant hematology and biochemical safety parameters.

Monocyte activation test

The pyrogenicity of the next-generation NonaMen was assessed by an *in vitro* monocyte activation test (MAT) as previously described [185]. Apart from the adjuvated and plain next-generation NonaMen 15, a Diphtheria toxoid (30 IU), Tetanus toxoid (60 IU), whole cell Pertussis (4 IU), Inactivated Poliomyelitis Virus (type 1 (40 D-antigen units (DU)); type 2 (4 DU); type 3 (7.5 IU)) (DTwcP-IPV) vaccine (supplied by Netherlands Vaccine Institute) and a previously clinically tested deoxycholate-extracted OMV (dOMV) NonaMen (lot005; containing *galE*-LPS; 15 μg PorA per subtype per human dose of 0.5 mL) [273], were included in MAT. Briefly, human monocytic MM6 cells [120] were incubated for 20 hours at 37 °C in a humid atmosphere with 5% CO_2 with various dilutions of the vaccine samples. Release of human interleukin-6 (IL-6) by MM6 cells was determined with a commercially available enzyme immunoassay (ELISA) according to the manufacturers' instructions (Sanquin, Amsterdam, The Netherlands). Dilution series of supernatants and IL-6 standard were tested in quadruplicates.

Biochemical analysis of vaccine

Total protein concentration, total PorA concentration and LPS concentration of the vaccine samples were determined for plotting IL-6 release from MAT against these parameters (Figure 2) Total protein concentration was measured as described previously [112]. Total PorA concentration was determined with quantitative SDS gel electrophoresis PorA under denaturing conditions [275]. LPS concentration was determined with a modified gas chromatography method as described previously [185]. Amount of LPS per vaccine sample was calculated based on the mass of the corresponding LPS molecules. The molecular weight of the *galE-lpxL1*-LPS present in next-generation NonaMen vaccine and the *galE*-LPS present in dOMV NonaMen were estimated at respectively 3191 g/mol and 3374 g/mol based on mass spectrometry data. The molecular mass of LPS present in DTwcP-IPV was estimated at 3728 g/mol, which was calculated based on the published LPS structure of Bordetella pertussis [276].

Immunogenicity in rabbits and mice by serum bactericidal activity assay

NIH female mice aged between 6-8 weeks were obtained from own breeding facilities. A total of 10 mice were immunized four times subcutaneously in the groin area at days 1, 22, 43 and 64 with either plain NonaMen 1.5 (1.5 μg per PorA), plain NonaMen 0.75 (0.75 μg per PorA) or adjuvated NonaMen 1.5 (1.5 μg per PorA). Blood samples from mice were taken two weeks after the fourth immunization, since a 4-dose vaccination schedule is intended for humans. Animals were bled under anesthesia. In addition, blood samples from rabbits of the GLP toxicology study were used that were taken two weeks after the fourth immunization. Collected sera were stored until analysis at -20 °C. The serum bactericidal antibody (SBA) assay was performed as previously described [5, 118]. In this assay, the lytic activity of sera from the immunized animals was determined against nine monovalent isogenic MenB test strains derived from H44/76 parental strain, each representing PorA present in the NonaMen vaccine strains, i.e. P1.5-1,2-2; P1.7,16; P1.19,15-1; P1.5-2,10; P1.12-1,13; P1.7-2,4; P1.22,14; P1.7-1,1; P1.18-1,3,6. Briefly, sera were thawed and heat-inactivated for 30 minutes at 56°C. Two-fold serial dilutions of serum with 105 bacteria CFU/mL were allowed to incubate for 15 minutes at room temperature in 96-well plates. Baby rabbit complement was added at a final concentration of 20% (Invitrogen), zero-time samples were taken, and the 96-well plates were incubated at 37°C for 60 minutes. The serum bactericidal

titer was reported as the reciprocal of the lowest serum dilution yielding ≥ 90% bacterial killing. A SBA titer of < 8, the lowest serum dilution determined in the assay, was considered negative, i.e. non-responder. All animal experiments were performed according to the current animal welfare regulations in the Netherlands. According to Dutch legislation, the institutional Animal Ethical Review Committee evaluated and approved all experiments.

Statistical analysis

Dunnett-test based on pooled variance significance was performed to compare body temperature of NonaMen-treated animals with placebo treated animals in the GLP toxicology study (Table 1). SBA titers were statistically analyzed with the non-parametric Mann-Whitney test to compare differences between the various treatment groups. P-values below 0.05 were considered to be significant.
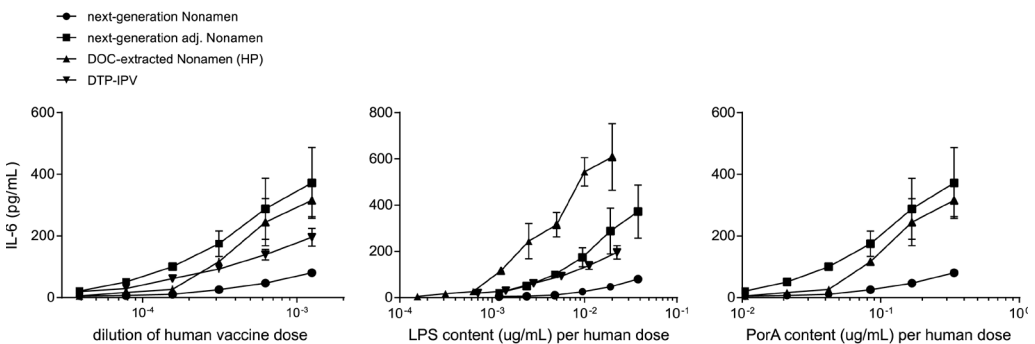

Figure 2.

IL-6 release by MM6 cells after incubation of various dilutions of human dose of plain next-generation NonaMen (15 μg per PorA/human dose; > 60% PorA of protein content, with 10-20% (*lpxL1*-)LPS of protein content) (circles), aluminum phosphate adjuvated next-generation NonaMen (15 μg per PorA/human dose; squares), deoxycholate-extracted OMV NonaMen (15 μg per PorA/human dose; > 60% PorA of protein content, with 2-8 % LPS of protein content; upright triangle) and a human dose of diphtheria, tetanus, whole cell pertussis, inactivated poliomyelitis combination vaccine (DTwcP-IPV) vaccine (standing down triangle). IL-6 release was plotted against dilution factor, LPS concentration and PorA protein concentration of the vaccine samples.

Results

GLP toxicology study in rabbits

No relevant findings regarding local and systemic toxicology were macroscopically noted in the vaccinated rabbits. A slight increase in rectal temperature (0.1°C–0.9°C) was found in NonaMen-treated animals compared to placebo at 4 hours after each dosing. However, 24 hours after vaccination, no difference in body temperature was observed in any animal (Table 1). Treatment-related changes in hematology and clinical biochemistry parameters were generally minor and transient. An independent expert rated the observed changes as expected effects of vaccination in general rather than vaccine-specific signs of toxicity. Histopathological findings were limited to injection sites, regional iliac lymph nodes and bone marrow. In both plain NonaMen treatment groups, an inflammatory reaction at the injection site was characterized by infiltration of lymphocytes, which is inherent to the generation of an immune response to vaccination, whereas in the placebo treatment groups more often macrophages were present. In animals receiving adjuvated NonaMen 15 occasionally granulomatous inflammation areas were observed at the injection site. In conclusion, next-generation NonaMen was well-tolerated in rabbits receiving five injections.

Monocyte activation test

IL-6 release by MM6 cells was considerably lower after incubation with next-generation NonaMen compared to the reference vaccine samples, DTwcP-IPV vaccine and dOMV NonaMen, with established safety profile in humans [273, 277] (Figure 2). Adjuvated next-generation NonaMen, however, induced release of IL-6 levels that was comparable to DTwcP-IPV vaccine and dOMV NonaMen. MM6 cells incubated with aluminum phosphate alone, in similar concentrations as present in adjuvated vaccine samples, did not release any IL-6 above background levels.

Immunogenicity in rabbits and mice

In rabbits, NonaMen induced high SBA titers against all nine monovalent MenB strains that expressed the different PorA's present in NonaMen, i.e., P1.7,16; P1.5-1,2-2; P1.19,15-1; P1.5-2,10; P1.12-1,13; P1.7-2,4; P1.22,14; P1.7-1,1 and P1.18-1,3,6 (Figure 3A). High SBA titers were also found in mice, but were more variable between the different PorA subtypes (Figure 3B). Considering both geometric mean SBA titers and number of responders of the mice, high SBA responses were measured against P1.7,16, P1.5-1,2-2, P1.5-2,10 and P1.12-1,13, intermediate responses were observed to P1.7-2,4 and P1.22,14 and lower responses to P1.19,15-1, P1.18-1,3,6, and P1.7-1,1. Rabbits receiving 4 doses of plain NonaMen 15 (15 μg per PorA) had a SBA titer that was slightly, but statistically significant, higher compared to rabbits receiving the lower vaccine dose (7.5 μg per PorA) against 5 out of the 9 PorA subtypes, i.e. P1.7,16; P1.19,15-1; P1.7-2,4; P1.22,14 and P1.7-1,1 (Figure 3A). In mice, only for the P1.5-1,2-2 PorA subtype a slightly, but statistically significant, higher SBA titer was found in the highest vaccine dose of 1.5 μg per PorA compared to the lower dose (0.75 μg/PorA). Strikingly, no potentiating immunogenic effect of aluminum phosphate adjuvant was observed for the 9 PorA antigens, except for a small, but statistically significant, increase in SBA titer against the P1.5-1,2-2 subtype in rabbits (Figure 3B).

Table 1.

Average body temperature in °C (± standard deviation) of rabbits measured after vaccination. */** Dunnett-test based on pooled variance significance at 5% (*) or 1% (**) level. Body temperature of animals vaccinated with next-generation NonaMen (next-Nona) was compared with aluminum-phosphate adjuvated placebo (adj. placebo) treated animals. Body temperature 24 hours after vaccination was only measured if one of the animals had a body temperature ≥ 40.0 °C.

| time after vacc.	Female treatment groups				Male treatment groups			
	adj. placebo	next-Nona (7.5)	next-Nona (15)	adj. next-Nona (15)	adj. placebo	next-Nona (7.5)	next-Nona (15)	adj. next-Nona (15)
Day 1 (1st vaccination)								
4 hrs	39.3 ± 0.1	39.8** ± 0.2	40.0** ± 0.3	39.7** ± 0.2	39.1 ± 0.2	39.9** ± 0.2	40.0** ± 0.4	39.9** ± 0.3
24 hrs	39.1 ± 0.2	39.2 ± 0.1	39.1 ± 0.2	39.1 ± 0.1	39.0 ± 0.1	39.0 ± 0.2	39.1 ± 0.1	39.2 ± 0.3
Day 15 (2nd vaccination)								
4 hrs	39.2 ± 0.2	39.6* ± 0.2	39.7** ± 0.4	39.5* ± 0.1	39.0 ± 0.2	39.5** ± 0.2	39.7** ± 0.2	39.6* ± 0.2
24 hrs	39.1 ± 0.2	39.2 ± 0.1	39.1 ± 0.3	39.1 ± 0.1	-	-	-	-
Day 29 (3rd vaccination)								
4 hrs	39.1 ± 0.1	39.4* ± 0.1	39.4* ± 0.2	39.3 ± 0.2	39.0 ± 0.1	39.4* ± 0.3	39.5** ± 0.2	39.6** ± 0.4
24 hrs	-	-	-	-	39.0 ± 0.2	39.0 ± 0.2	39.1 ± 0.2	39.1 ± 0.2
Day 43 (4th vaccination)								
4 hrs	39.3 ± 0.1	39.4 ± 0.2	39.5 ± 0.3	39.5 ± 0.2	39.1 ± 0.1	39.5** ± 0.2	39.6** ± 0.2	39.7** ± 0.3
24 hrs	-	-	-	-	39.0 ± 0.2	39.0 ± 0.2	39.1 ± 0.2	39.1 ± 0.1
Day 57 (5th vaccination)								
4 hrs	39.3 ± 0.1	39.6** ± 0.1	39.5* ± 0.2	39.4 ± 0.1	39.0 ± 0.2	39.6** ± 0.3	39.7** ± 0.2	39.6** ± 0.2
24 hrs	-	-	-	-	-	-	-	-
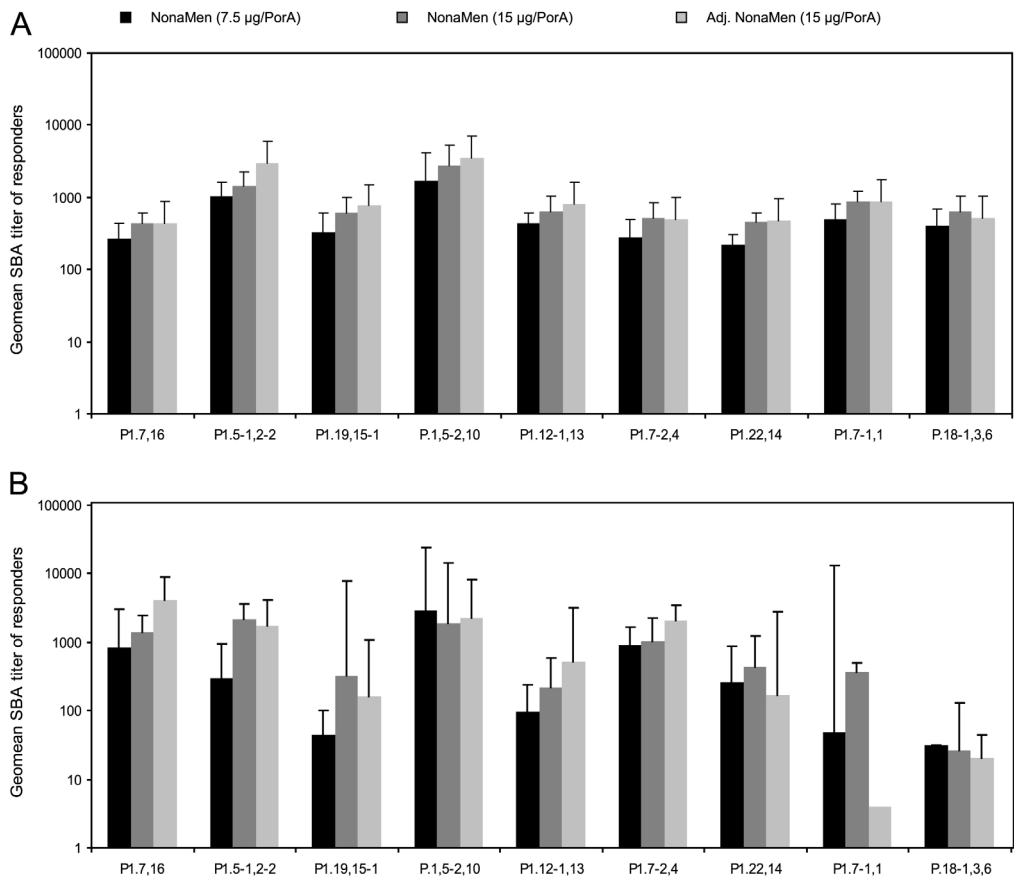
Figure 3.

Serum bactericidal antibody responses to monovalent isogenic MenB test strains each expressing a single PorA subtype present in the vaccine strains, i.e. P1.5-1,2-2; P1.7,16; P1.19,15-1; P1.5-2,10; P1.12-1,13; P1.7-2,4; P1.22,14; P1.7-1,1; P1.18-1,3,6 are presented for immunized in rabbits (A) and mice (B). Animals were four times immunized with low dose next-generation NonaMen (7.5 µg and 0.75 µg per PorA resp. for rabbits and mice; black bars), high dose next-generation NonaMen (15 µg and 1.5 µg per PorA resp. for rabbits and mice; dark gray bars), and next-generation aluminum phosphate adjuvated NonaMen (15 µg and 1.5 µg per PorA resp. for rabbits and mice; light gray bars). Geometric mean SBA titers and standard deviation are presented for each PorA sero-subtype per treatment group.

Discussion

The present study evaluated the safety and immunogenicity of next-generation NonaMen vaccine in rabbits and mice. Next-generation NonaMen contains nine different PorA subtypes to provide broad coverage against MenB disease [5, 7, 62]. Previously, deoxycholate-extracted OMV (dOMV) NonaMen vaccine was shown to be well-tolerated in healthy adults [273]. dOMV NonaMen (15 μg per PorA/per dose; > 60% PorA of protein content) had low LPS content (2-8% of protein content). However, the use of detergents to remove toxic LPS resulted in a vaccine with lower quality caused by partially disintegrated and aggregated vesicles. For this reason, next-generation NonaMen, containing attenuated *lpxL1* LPS, was developed with an optimized detergent-free and animal-free production process [275]. Next-generation NonaMen (15 μg per PorA/per dose; > 60% PorA of protein content), with no need to remove LPS with detergent extraction, had consequently higher (*lpxL1*-)LPS content (10-20% of protein content). The (*lpxL1*-)LPS content of next-generation NonaMen may be relatively low compared to other native OMV vaccine concepts containing (*lpxL1*-)LPS, which can be explained by the fact that the EDTA extraction step in our vaccine production process have shown to remove a (minor) portion of (*lpxL1*-)LPS [185].

In order to evaluate the safety of next-generation NonaMen, a GLP toxicology study in rabbits was performed. No relevant findings regarding clinical signs or biochemical/hematology safety parameters were noted after five immunizations. Some animals receiving adjuvated NonaMen but not plain NonaMen had localized inflammations at the injection site that were sometimes accompanied with granulomatous areas with central necrosis. With respect to body temperature, only a minimal and transient increase (≤ 0.9 °C) was observed after vaccination with NonaMen compared to placebo. These results are in agreement with a pilot study performed prior to the GLP toxicology study using implanted data loggers for continuous body temperature monitoring in rabbits after vaccination with next-generation NonaMen [274].

Pharmaceutical products intended for parenteral administration, including vaccines, have to be tested for its pyrogenic risk. Until recently, the rabbit pyrogen test and the Limulus Amebocyte Lysate (LAL) test were the standard methods accepted by regulatory authorities for the detection of pyrogens [278, 279]. Since both tests are intended to detect minimal pyrogen contamination, they are less suitable for bacterial vaccines that contain considerable amount of LPS. The monocyte activation test (MAT) represents a more suitable alternative method for estimating pyrogenicity of pharmaceuticals [278-280] and has recently been accepted by regulatory authorities and included within the European Pharmacopoeia (Chapter 2.6.30 Monocyte Activation Test). The MAT, measuring the release of pro-inflammatory cytokines by monocytic cells, is expected to reflect the reactions of the human innate immune system better than the other two conventional methods. In the present study, monocytic cells released less IL-6 following incubation with next-generation NonaMen than DTwcP-IPV vaccine or aluminum-phosphate adjuvated dOMV NonaMen vaccine. Previously, adjuvated dOMV NonaMen was well-tolerated in healthy adults without any cases of fever in the treatment groups receiving only the NonaMen vaccine [273]. MAT results therefore indicate that the pyrogenic activity of next-generation NonaMen is likely to be low, which is in line with the limited effect observed on body temperature of the rabbits in

the toxicology study. In agreement, studies with other OMV products from *lpxL* mutant strains have shown reduced toxicity based on MAT data [6, 63, 94, 185]. Adjuvated next-generation NonaMen induced considerably more IL-6 release than plain NonaMen, which was comparable to adjuvated dOMV NonaMen and DTwcP-IPV vaccine. Apparently, OMV product together with aluminum phosphate adjuvant resulted in an increased release of IL-6. This difference between plain and adjuvated NonaMen was not reflected in the effects on body temperature in the rabbits of the toxicology study, however, the rabbits that received adjuvated NonaMen did show more local reactions compared to plain NonaMen.

Currently, the SBA assay is the primary serological assay for the evaluation of the immunogenicity of vaccines against *N. meningitidis* and has generally been accepted as surrogate endpoint of group B meningococcal vaccine efficacy [46, 281, 282]. The present study showed that next-generation NonaMen, even without adjuvant, was immunogenic in both rabbits and mice (Figure 3). SBA titers in rabbits were generally high, while the SBA titers in mice varied more between the different PorA subtypes. It should be taken into account that mice received only one-tenth of the vaccine dose (1.5 µg per PorA subtype) that was given to the rabbits in the toxicology study, i.e. the highest intended human dose (15 µg per PorA subtype). Nevertheless, differences in immunogenicity between PorA subtypes have been observed in other preclinical and clinical studies as well. In agreement with our findings in mice, in clinical studies with MenB OMV vaccines the immunogenicity of PorA subtype P1.19,15 was lower than the P1.7,16 subtype [55, 283, 284]. Our results were also in accordance with previous studies in mice with our nonavalent or hexavalent PorA dOMV vaccines showing variable SBA titers among the different PorA subtypes [5, 118]. Previously, it has been shown that PorA dOMV vaccines from Intravacc induced SBA responses against wild-type isolate strains with PorA vaccine subtypes at the same magnitude as the isogenic vaccine strains in vaccinated toddlers and school children [285]. In addition, cross-reactivity against several patient isolates from non-vaccine PorA sero-subtypes was observed in this clinical study [285].

In the present preclinical study, aluminum-phosphate adjuvant did not further potentiate the immunogenicity of the PorA subtypes significantly, indicating that there is probably no need for an adjuvant for next-generation NonaMen containing *lpxL1*-LPS. The majority of lipoproteins that have shown to be removed by detergent-extraction in dOMV NonaMen are preserved in next-generation NonaMen (nOMV) as determined by proteomic technologies (manuscript submitted for publication). Additionally, we showed that a trivalent PorA native OMV (nOMV) vaccine product, prepared with a detergent-free production process, elicited cross-protection against meningococcal serogroup B strains of non-vaccine PorA sero-subtypes [185]. This suggests that other minor conserved antigens with the potential to induce bactericidal activity, such as NadA or factor H binding protein (fHbp), are retained in next-generation NonaMen, but also (*lpxL1*)LPS may induce bactericidal activity [63, 286-288]. This is in accordance with preclinical and clinical study results from another group with nOMV vaccine made from a meningococcal serogroup B strain with deleted *lpxL1* gene [63, 286-288]. This vaccine was also prepared with a detergent-free process, but with several undesirable process steps, such as phenol inactivation. The vaccine induced higher SBA titers against a PorA heterologous strain than against the parental vaccine strain [63, 286]. Furthermore, this experimental nOMV vaccine induced bactericidal

antibodies against clinical isolates of other *N. meningitidis* serogroups C, Y, W, X, and NadA-expressing serogroup A strains [287, 288]. This underlines that the nOMV vaccine has a broad cross-protective potential with a good safety profile [286-288]. Another group has developed an experimental nOMV vaccine based on detoxified LPS with L3 immunotype without expression of PorA proteins and iron-binding FrpB proteins. This vaccine was produced with detergent treatment. Even though the vaccine appeared to be safe and well-tolerated in healthy adults, the immunogenicity was disappointing [289].

Summarizing, NonaMen has the potential to prevent the majority of serogroup B infection in Europe [5, 62, 70]. The present study showed that next-generation NonaMen has a good safety profile in rabbits. In agreement with this, the MAT data indicated an acceptable pyrogenicity of next-generation NonaMen. The vaccine induced a good functional immune response in both rabbits and mice against different PorA proteins. Strikingly, adding aluminum phosphate to next-generation NonaMen resulted in increased toxicity with respect to local reactions in rabbits and *in vitro* IL-6 release, while the immunogenicity was not further enhanced. Therefore, the balance of risks and benefits favors the use of plain next-generation NonaMen instead of the adjuvated vaccine. At present, a fully scalable, animal-free, optimized production process has been developed, which allows production of GMP clinical batches of next-generation NonaMen (manuscript submitted for publication). The presented preclinical results support the start of the first clinical studies with this next-generation NonaMen containing *lpxL1*-LPS, in which, safety in humans and the broad potential coverage against wild-type strains can be further explored.

Acknowledgments

Chapter 9

General discussion

Abstract

OMV vaccines successfully stopped *N. meningitidis* serogroup B outbreaks but have limited coverage and are difficult to produce, due to a detergent-extraction step with deoxycholate [3, 61]. The detergent-extraction removes toxic lipopolysaccharide (LPS), but compromises OMV integrity [185, 290]. Meningococcal LPS can be attenuated with the *lpxL1* mutation, which may allow a detergent-free approach [6, 94]. This thesis explores the impact of such an alternative approach with the goal to develop an improved, next-generation OMV vaccine. The designation 'next-generation' refers to the combination of OMV with attenuated *lpxL1*-LPS and a detergent-free process [70]. Mutations that improve OMV yield (i.e. Δ*rmpM*) may also be beneficial [75]. This thesis covers the full preclinical development phase through evaluation of five hypotheses (Figure 1). After strain selection and optimization of specific process steps, a robust pilot-scale production process has been developed. The quality of OMV from this optimized process is stable and within pre-set specifications for nine consecutive batches. Studies in mice and rabbits suggest that next-generation OMV are immunogenic and safe for parenteral use in humans. Therefore these vaccines are now ready for clinical evaluation. In addition to *N. meningitidis* serogroup B, other meningococcal serogroups and several gram-negative pathogens were found to release immunogenic OMV [229]. It should require only minor adjustments to produce these other OMV with the pilot-scale production process described in this thesis. Therefore the current results are likely to be relevant for the broader field of vaccinology.
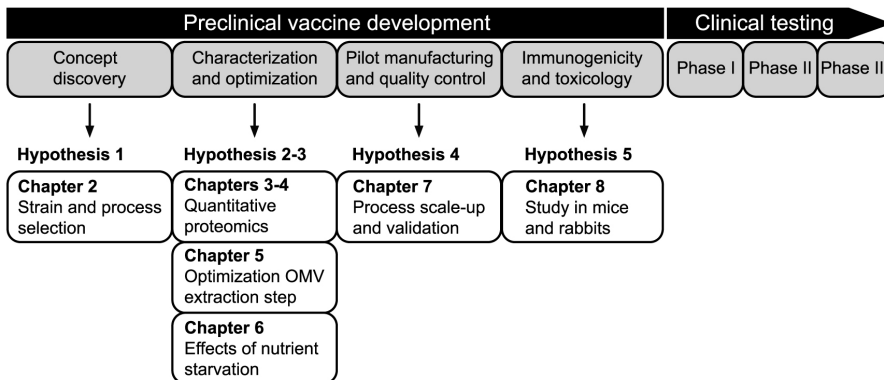
Figure 1. Preclinical vaccine development stages.
This thesis covers all stages of preclinical vaccine development for next-generation OMV vaccine. Concept discovery is described in chapter 2, while chapters 3–6 evaluate important characterization and optimization aspects. Chapter 7 describes the development of a robust pilot-scale production process, which has been used to produce next-generation NonaMen vaccine with broad potential coverage against serogroup B meningococcal disease. Safety and immunogenicity of this product has been confirmed in mice and rabbits (chapter 8). The results of these different chapters have generated a scientific basis for the hypotheses and central research question of this thesis, confirming that next-generation OMV vaccines provide improved quality and process robustness.

Hypothesis 1: Next-generation OMV vaccines provide improved quality compared to detergent-extracted OMV

Previous studies have identified important but separate aspects of next-generation OMV, like a detergent-free process [100], attenuated LPS toxicity [6] or a hypothesized positive effect of *rmpM* deletion on OMV yield [75]. Chapter 2 systematically combines these aspects to assess feasibility for further development. Three OMV purification processes have been compared, referred to as dOMV, nOMV and sOMV (Figure 2). The dOMV process uses bacterial extraction with deoxycholate buffer (detergent) to release vesicles and remove most of the LPS [2, 49], while nOMV uses a buffer which retains LPS (detergent-free extraction) [100, 101]. The sOMV process purifies spontaneously released vesicles without additional treatments (detergent-free, no extraction) [97]. These processes have been tested on vaccine strains with mutations to attenuate LPS toxicity (Δ*lpxL1*) or improve OMV yield (Δ*rmpM*).
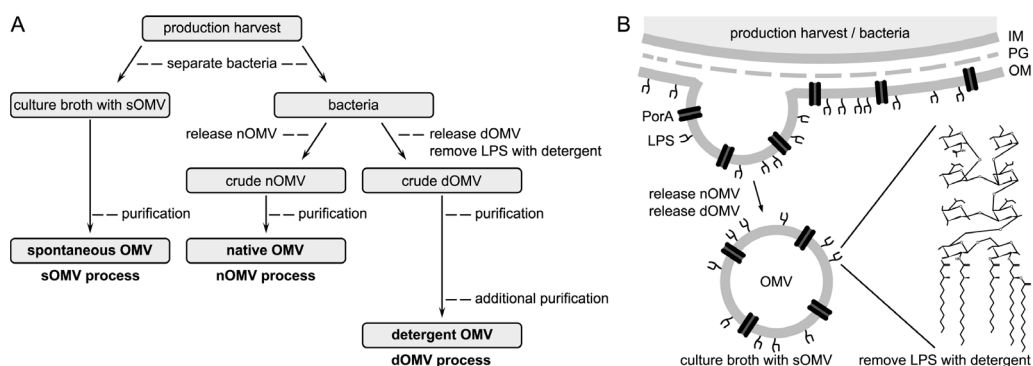

Figure 2. Differences between OMV production processes.
(A) Production harvest can be purified to OMV with three different processes, referred to as dOMV, nOMV or sOMV. First, the bacteria are separated from the culture broth. Bacteria can be extracted with a deoxycholate buffer (detergent). This dOMV process releases detergent OMV and removes most of the lipopolysaccharide (LPS), but requires extensive downstream purification for deoxycholate removal. The nOMV process uses a detergent-free buffer with EDTA to stimulate native OMV release. This approach retains LPS and allows simplified purification. The sOMV process purifies spontaneous OMV directly from the culture broth, without any treatments to increase vesicle release. This alternative detergent-free approach also retains LPS. The sOMV process is the most straightforward, but the vesicle yield is typically lower than for dOMV or nOMV. (B) Effects of the different OMV purification processes at the bacterium, OMV and LPS level. Most of the descriptions refer to section A. The bacterial cell envelope consists of IM (inner membrane), PG (peptidoglycan layer) and OM (outer membrane). The LPS and PorA antigen (outer membrane porin A protein) are located in the OM.

Despite a beneficial effect of Δ*rmpM*, the sOMV yield is much lower than other processes. During clinical trials this difference may not be problematic, but for commercial production sOMV will be the more expensive option. Therefore adjustments that further increase sOMV release yield will improve feasibility. A promising example of such an adjustment is cysteine starvation during the stationary growth phase, which is explored in chapter 6 of this thesis. Chapter 2 also demonstrates that detergent-free processes, sOMV in particular, produce vaccines with improved immunological properties compared to dOMV (Table 1). The improved immunogenicity has been confirmed by Zollinger *et al.* and substantiates hypothesis 1 [63]. In addition, next-generation nOMV and sOMV vaccines have superior biochemical properties and are likely to be safe for

parenteral use in humans [185]. These results provide justification for further development of a pilot-scale production process for clinical trials (chapters 5-8).

Hypothesis 2: Biomass extraction during processing changes the immunogenic protein content of OMV vaccines

The effect of different purification processes on protein composition of OMV has been investigated with a novel proteomics method. The method uses selective purification of N-terminal peptides with phospho-tagging (PTAG). Chapter 3 demonstrates that the PTAG strategy is effective and broadly applicable [204]. Chapter 4 adds a robust quantification protocol and the protein content of sOMV, nOMV and dOMV vaccines has been analyzed. Due to a milder purification process, both detergent-free OMV vaccines (nOMV and sOMV) contain less lysis proteins and are enriched with potentially immunogenic membrane (lipo)proteins. Serum blot proteomics confirms that biomass extraction with detergent (dOMV) indeed removes immunogenic proteins, including factor H binding protein [298]. The results of chapter 3–4 therefore confirm hypothesis 2, but there are other aspects likely to be relevant for immunogenicity. This includes a differential LPS content, which may change the adjuvanting capacity of the vaccine [63, 93]. In dOMV vaccine almost all LPS is removed, but this thesis also reveals a difference in LPS content between both detergent-free alternatives. Apparently the EDTA treatment removes a small portion of the LPS as well. Together with the observed differences in immunogenic protein content, this may explain the increasing cross-protection from dOMV, through nOMV to sOMV vaccine observed in chapter 2. The proteome analyses in chapter 4 have provided detailed insight in the effects of biomass extraction on OMV protein content. It is demonstrated that next-generation OMV, sOMV in particular, have a preferred composition.

Table 1. Quality characteristics of reference and next-generation OMV vaccines.
Reference dOMV vaccine is prepared with detergent-extraction to remove toxic LPS [61]. Next-generation OMV vaccines use strains with attenuated *lpxL1*-LPS (ΔL mutation) and a detergent-free process (either sOMV or nOMV). The *rmpM* mutation (ΔR) improves OMV yield [3]. The vaccines have a different quality with respect to yield, toxicity, morphology, immunogenicity and cross-protection. Undesired characteristics are depicted in grey. Table 1 indicates that next-generation nOMV vaccine has the best quality, closely followed by next-generation sOMV due to a low yield. The dOMV reference has limited cross-protection and is partly aggregated, which complicates processing.

OMV vaccine	properties		OMV quality				
	strain	process	yield	toxicity	morphology	immunogenicity	cross-protection
reference	ΔR	dOMV	+ + +	low	partly aggregated	+	–
next-generation 1	ΔR ΔL	sOMV	+ –	low	defined Ø80 nm	+ + +	+ + +
next-generation 2	ΔR ΔL	nOMV	+ +	low	defined Ø80 nm	+ +	+

Hypothesis 3: Biological stimuli can trigger OMV release by N. meningitidis and can be applied to improve vaccine production

Based on the result of chapters 2–4, next-generation nOMV vaccine was selected as the primary candidate for further development towards clinical trials. The sOMV vaccine had slightly better immunogenicity and a more straightforward large-scale process, but these advantages were outweighed by a low yield for which no obvious solution was available. During optimization of the nOMV process, it became clear that spontaneous OMV release increased significantly during the stationary growth phase, most likely caused by nutrient limitation [186]. This effect was also suggested in another recent study by Santos et al. and may improve the sOMV yield [291]. In agreement with these observations, chapter 6 has identified cysteine depletion as the first known vesiculation stimulus for *N. meningitidis*. Cysteine depletion causes stationary growth and sufficient sOMV release for feasible vaccine production [292]. These results confirm hypothesis 3. However, minor quality concerns remain, most likely due to a non-optimized sOMV process. Measures to prevent cell lysis during the stationary phase would be beneficial. It would also be interesting to assess potential differences in immunogenicity and proteomes of sOMV vaccines before and after cysteine depletion. The effect of cysteine on a panel wild-type strains would demonstrate whether the observed vesiculation is unique for Δ*rmpM*–Δ*lpxL1* strains. In addition, there may be other effective vesiculation triggers for *N. meningitidis* like heat shock [41, 80, 81]. Despite these unknown aspects, chapter 6 demonstrated that cysteine depletion can be successfully applied to solve the yield issues associated with sOMV production.

Hypothesis 4: Next-generation OMV vaccines allow a more consistent and efficient large-scale production process

Chapter 5 has optimized the central processing step of next-generation nOMV vaccine: detergent-free biomass extraction with EDTA. Out of five process parameters, only harvest point of the cultivation and extraction pH are critical and have subsequently been optimized. With the optimized EDTA extraction in place, a pilot-scale nOMV production process with 40 L cultivation volume has been developed in chapter 7. Scalable aseptic equipment is implemented throughout the process, replacing undesirable steps like ultracentrifugation, inactivation with phenol and the use of preservatives. The improved process is robust, scalable to at least 800 L cultivation volume [4] and with 9–21 fold higher average PorA yield than reference processes [49, 61, 253]. In addition, quality of the nOMV vaccines is stable and within preset specifications for nine consecutive batches [299]. Chapter 7 therefore supports hypothesis 4. The current improvements are expected to enable next-generation nOMV production at commercial scale.

Hypothesis 5: Despite a high LPS content, next-generation OMV vaccines are safe for parenteral use in humans.

Next-generation NonaMen vaccine consists of nOMV from three Δ*rmpM*–Δ*lpxL1* strains, each expressing three different PorA's [5, 7]. The vaccine has been produced with the pilot-scale production process from chapter 7, which retains potentially toxic LPS. In vitro analyses already suggested that *lpxL1*-LPS is safe for human use [6, 63, 94], but animal testing is an obligatory prerequisite for safety evaluation in humans. Therefore chapter 8 assessed repeated-dose toxicity and immunogenicity of next-generation NonaMen in mice and rabbits. The vaccine induced high bactericidal titers without signs of toxicology or histopathology. Bactericidal activity may however be sligthly overestimated, due to the use of rabbit complement. Notably there is no need for an adjuvant, confirming the intrinsic adjuvanting capacity of *lpxL1*-LPS [93]. The TLR4-mediated adjuvanting capacity observed in mice may not be fully representative for humans [300], but OMV with *lpxL1*-LPS were found to elicit broad functional immunogenicity in non-human primates as well [190]. The results of this thesis therefore encourage clinical safety evaluation, as successfully performed for a related next-generation OMV vaccine [187], and provide strong additional evidence for hypothesis 5.

Perspectives

At present, next-generation nOMV vaccine is the best option for clinical testing. The choice for nOMV vaccine is arguable and mainly based on the low yield of sOMV vaccine. Both options are a significant improvement, but sOMV vaccine has the better immunogenicity and cross-protection (Table 1) [185]. However, implementation of an effective vesiculation trigger would greatly improve feasibility [292]. Future sOMV process optimization should focus on the upstream process, especially the stationary phase in which vesiculation occurs. A robust upstream process requires a stable stationary phase with cysteine as the sole depleted nutrient. To prevent additional nutrient depletions, a cysteine-free feed that supports maintenance metabolism may be required. This minimizes bacterial lysis and allows a clean harvest for downstream processing. Vesiculation monitoring would be another beneficial improvement. The fluorescent, phospholipid-specific probe described in chapter 6 is well-suited for this purpose. This fast phospholipid assay can be automated for monitoring of sOMV release, to pinpoint the optimal harvest point. With these improvements a highly reproducible upstream process is obtained, which facilitates a straightforward downstream process.

Several groups are now developing innovative next-generation OMV concepts. The main focus remains *N. meningitidis* serogroup B, but OMV concepts with broad potential coverage against other serogroups and concepts against other gram-negative pathogens are emerging [64, 82, 188, 190, 231]. These include *E. coli* vesicles with insertion sites for heterologous proteins [269, 270]. Recent work also suggests that OMV can enhance the immunogenicity of purified recombinant proteins and stimulate Th1-oriented cellular immunity [264, 293]. These findings demonstrate that OMV have the potential to become a versatile technology platform for prophylactic and therapeutic vaccines. Such a platform requires a reliable production process to generate substantial quantities of high quality product. The next-generation nOMV process described in chapter 7 is well-suited for this purpose. OMV concepts that are potentially compatible with this process are listed in Table 2.

Most OMV concepts in Table 2 are still in the early preclinical development phase, with the primary goal to obtain immunogenic vesicles. Assessment of LPS toxicity, cross-protection or yield is often incomplete, even though these aspects are essential for final feasibility. Like meningococcal LPS, the LPS of other gram-negative pathogens can cause adverse events. This is illustrated by the whole cell pertussis vaccine, which has been used for decades but was recently replaced with a less reactogenic, purified protein vaccine [261, 262]. Toxicity of *B. pertussis* LPS can be attenuated with the Δ*pagL* mutation [119]. For *E. coli* a comparable mutation is available (Δ*lpxM*) [270, 295]. Like the Δ*lpxL1* mutation in *N. meningitidis*, these mutations target acyl chain biosynthesis. Since the next-generation nOMV process retains LPS, the other gram-negative pathogens in Table 2 will likely require a comparable modification.

Potential LPS toxicity, cross-protection or yield issues must be properly addressed for new OMV concepts. Once this is done, it should require only minor adjustments to adopt these concepts to the next-generation nOMV process. The organisms in Table 2 are all gram-negative pathogens with comparable nutritional requirements. The growth medium used in this thesis is developed

for *N. meningitidis* and is chemically defined without components of animal origin [4, 246]. It supports high biomass densities for other vesiculating pathogens as well, which has recently been confirmed for *Shigella dysenteriae*, *Vibrio cholerae*, *Klebsiella pneumoniae* and *Acinetobacter baumannii* (unpublished data). Demanding pathogens like *B. pertussis* will likely require fed-batch cultivation to obtain sufficient biomass for feasible OMV processing [296]. This may be beneficial for *N. meningitidis* as well, since nOMV yield correlates directly to biomass yield in this thesis [292]. The downstream process can be uniform regardless the pathogen that is used. All studies in Table 2 have obtained vesicle sizes between 20–200 nm with comparable biochemical characteristics. The vesicle size distribution is well within the pore size range of the various filters that are used for pilot-scale processing. This allows easy pore size adjustment and the use of identical gel filtration matrices. Therefore compatibility issues with the next-generation nOMV downstream process are not expected.

Table 2. OMV vaccine concepts that are potentially compatible with the next-generation nOMV process.
The table provides a concept description, the target organism and required modifications. Most concepts are still in early preclinical development, where assessment of yield, cross-protection and toxicity is often incomplete. These aspects need to be addressed before further development.

OMV concept	Target organism	Required modifications
nOMV nonavalent PorA [258]	*N. meningitidis* serogroup B	none (this thesis)
sOMV over-expressed fHbp [190]*	*N. meningitidis* serogroup B	Δ*rmpM*; biomass extraction
dOMV enriched with *lpxL1*-LPS [231]	*N. meningitidis* serogroup B	Δ*rmpM*; omit detergent
strains with PorA/FetA variants [64]	*N. meningitidis* serogroup B	Δ*rmpM*; Δ*lpxL1*; omit detergent
nOMV multiple PorA, fHbp, LPS antigens [188]	*N. meningitidis* serogroup B, C, W, X, Y	Δ*rmpM*
sOMV cross-protective fHbp [82]*	*N. meningitidis* serogroup A, B, W, X	Δ*rmpM*; biomass extraction
dOMV from different serogroups [294]	*N. meningitidis* serogroup A, W	Δ*rmpM*; Δ*lpxL1*; omit detergent
sOMV from high-density cell culture [254][‡]	*Shigella sonnei*	growth medium; biomass extraction
cross-protective sOMV [83]*[Δ]	*Vibrio cholerae*	growth medium; biomass extraction
sOMV protein expression platform [270]*[‡]	heterologous expression (*E. coli*)	growth medium; biomass extraction
sOMV protein expression platform [269]*[Δ‡]	heterologous expression (*E. coli*)	growth medium; biomass extraction
sOMV [263]*[Δ‡]	*Acinetobacter baumannii*	growth medium; biomass extraction
dOMV [84]*[Δ‡]	*Bordetella pertussis*	growth medium; omit detergent
sOMV [265]*[Δ‡]	*Escherichia coli* (enterotoxigenic)	growth medium; biomass extraction
sOMV [266]*[Δ‡]	*Francisella novicida*	growth medium; biomass extraction
sOMV [264]*[Δ‡]	*Burkholderia pseudomallei*	growth medium; biomass extraction

*OMV yield assessment not performed.
[Δ]LPS toxicity assessment not performed.
[‡]Cross-protection assessment not performed.

Conclusions

This thesis describes the full preclinical development and characterization of next-generation OMV vaccine, based on strains with attenuated LPS and a detergent-free process [70]. The new production process is fully scalable and in agreement with current regulatory requirements. This is expected to resolve the production difficulties associated with dOMV technology. In addition, next-generation OMV vaccines provide good preclinical safety and immunogenicity [258]. Clinical evaluation of broadly protective OMV against *N. meningitidis* serogroup B is a logical next step, due to the extensive experience with this organism [187]. In the meanwhile, the results of this thesis can be applied for other meningococcal serogroups and for other pathogens. OMV with heterologous antigens may also be within reach. These developments are likely to be compatible with the robust OMV production platform described in this thesis. Due to a substantial public health interest, this work was funded by the Dutch Ministry of Health, Welfare and Sport [1]. The results encourage technology transfer to a commercial partner, with the goal to translate next-generation OMV technology into actual vaccines and improve global public health.

Summary
Samenvatting
Dankwoord
Curriculum Vitae
Publications
Training activities
References

Summary

The development of a vaccine against *Neisseria meningitidis* serogroup B is of major importance for public health. At present only vaccines containing outer membrane vesicles (OMV) have proven efficacy. OMV vaccines, however, have limited coverage and are difficult to produce, due to a detergent-extraction step with deoxycholate. The detergent-extraction removes toxic lipopolysaccharide (LPS), but also compromises OMV integrity. The *lpxL1* mutation attenuates meningococcal LPS and may allow detergent-free OMV production process. The impact of such an alternative approach is explored in this thesis, with the goal to develop an improved, next-generation OMV vaccine. The designation 'next-generation' refers to the combination of OMV with attenuated LPS and a detergent-free process.

Chapter 2 systematically compares three different OMV purification processes (dOMV, nOMV and sOMV) in combination with genetic modifications that are expected to attenuate LPS toxicity (Δ*lpxL1*) or improve OMV yield (Δ*rmpM*). The sOMV purification has yielded significantly less OMV than the other processes due to the absence of biomass extraction. Approximately 50% of this yield loss can be compensated with the *rmpM* mutation. Chapter 2 also gives strong evidence that next-generation nOMV and sOMV vaccines from Δ*rmpM*-Δ*lpxL1* mutant strains provide superior vaccine quality, in terms of vesicle morphology and functional immunogenicity. These results justify further development towards clinical trials (chapters 5–8).

Chapter 3–4 describes the development of a novel quantitative proteomics method, which has been used to assess the effect of different purification processes on protein content of OMV. The method uses the phospho-tag strategy (PTAG) to selectively purify N-terminal peptides after proteolytic cleavage. Chapter 3 demonstrates that the PTAG strategy is effective and broadly applicable. Chapter 4 adds a quantification protocol and the proteomes of sOMV, nOMV and dOMV vaccines have been analyzed. Due to a milder purification process, both detergent-free OMV vaccines (nOMV and sOMV) contain less lysis proteins and are enriched with potentially immunogenic membrane (lipo)proteins. Serum blot proteomics confirmed that biomass extraction with detergent (dOMV) indeed removes immunogenic proteins. Therefore, next-generation OMV vaccines, sOMV in particular, have a preferred protein composition.

Based on the result of chapters 2–4, next-generation nOMV vaccine has been selected as the primary candidate for further development towards clinical trials, mainly due to the low yield of the sOMV process. Later on, it became clear that vesiculation increases significantly during the stationary phase. Chapter 6 demonstrates that the vesiculation is caused by cysteine depletion and that this stimulus is applicable for sOMV vaccine production. The sOMV yield became comparable to nOMV reference yield after approximately 8 hours of cysteine-limited stationary phase, therefore this approach may solve the yield issues associated with next-generation sOMV vaccine.

Chapter 5 optimizes the central processing step of next-generation nOMV vaccine: detergent-free biomass extraction with EDTA. Out of five process parameters, only harvest point of the cultivation and extraction pH are critical and have subsequently been optimized. Next, a pilot-

scale nOMV production process with 40 L cultivation volume has been developed in chapter 7. The new process is robust, scalable and with 9–21 fold higher PorA yield than reference processes. In addition, quality of the nOMV vaccines is stable and within preset specifications for 9 consecutive batches. These improvements are expected to enable next-generation nOMV production at commercial scale. Chapter 8 assesses repeated-dose toxicity and immunogenicity of next-generation NonaMen, consisting of nOMV from three vaccine strains, each expressing three different PorA antigens. The vaccine induces high bactericidal titers in mice and rabbits and none of the rabbits developed signs of toxicity or pathology. These results suggest that next-generation NonaMen is broadly immunogenic and safe for parenteral use in humans.

This thesis shows that next-generation OMV have significantly improved quality characteristics and are now ready for clinical evaluation. The new, pilot-scale production process is expected to resolve the difficulties associated with dOMV technology. Clinical evaluation of broadly protective OMV against *N. meningitidis* serogroup B is a logical next step, but promising OMV concepts for other meningococcal serogroups and for other pathogens are also emerging. These concepts are likely to be compatible with the nOMV production platform described in this thesis.

Samenvatting

De ontwikkeling van een vaccin tegen *Neisseria meningitidis* serogroep B (meningokokken) is belangrijk voor de volksgezondheid. Op dit moment geven alleen vaccins die gebaseerd zijn op 'outer membrane vesicles' (OMV's, ofwel buitenmembraan deeltjes) bescherming tegen deze ziekte. De breedte van de bescherming is bij OMV vaccins echter beperkt en ze zijn moeilijk te produceren, door een extractie stap met het detergens deoxycholaat. Deze detergens-extractie verwijdert toxisch lipopolysaccharide (LPS), maar beschadigt daarbij de OMV's. De *lpxL1* mutatie zorgt ervoor dat het LPS niet langer toxisch is en maakt daarmee wellicht een detergens-vrij productieproces mogelijk. Dit proefschrift verkent de implicaties van zo'n alternatief productieproces, met als doel een 2^e generatie OMV vaccin te ontwikkelen. De benaming '2^e generatie' verwijst naar de combinatie van niet-toxisch LPS met een detergens-vrij productieproces.

Hoofdstuk 2 is een systematische vergelijking van drie verschillende OMV productieprocessen (dOMV, nOMV en sOMV), die zijn toegepast op genetisch gemodificeerde meningokokken met niet-toxisch LPS (Δ*lpxL1*) en/of een verbeterde OMV opbrengst (Δ*rmpM*). Het sOMV purificatieproces blijkt een significant lagere OMV opbrengst te hebben dan de andere twee processen, doordat er geen biomassa-extractie stap wordt gebruikt. Ongeveer 50% van het opbrengst verlies kan gecompenseerd worden door de *rmpM* mutatie te introduceren. Hoofdstuk 2 bewijst bovendien dat 2^e generatie nOMV en sOMV vaccins, geproduceerd met genetisch gemodificeerde Δ*rmpM*-Δ*lpxL1* stammen, een sterk verbeterde vaccinkwaliteit bieden. Dit geldt zowel voor de morfologie van de OMV's, als voor de functionele immunogeniciteit van het vaccin. Deze resultaten verantwoorden verdere ontwikkeling richting klinische studies (hoofdstukken 5 t/m 8).

Hoofdstuk 3 en 4 beschrijven de ontwikkeling van een nieuwe kwantitatieve proteomics methode, die is gebruikt om het effect van verschillende productieprocessen op de eiwitsamenstelling van het vaccin te onderzoeken. De methode is gebaseerd op de 'phospho-tag strategie' (PTAG), die N-terminale peptiden na proteolyse selectief kan zuiveren. Hoofdstuk 3 laat zien dat PTAG effectief is en bovendien breed inzetbaar. In hoofdstuk 4 wordt een kwantificeringsprotocol ontwikkeld, waarna de eiwitsamenstelling van sOMV, nOMV en dOMV vaccins is geanalyseerd. Dankzij een milder zuiveringsproces, bevatten beide detergens-vrije vaccins (nOMV en sOMV) minder celdood eiwitten. Daarnaast zijn deze vaccins verrijkt met potentieel immunogene membraan- en lipoproteïnen. Serumblot analyse bevestigt deze bevindingen door aan te tonen dat biomassa extractie met detergens (dOMV proces) inderdaad immunogene eiwitten verwijdert. Om deze redenen hebben 2^e generatie OMV vaccins, sOMV vaccin in het bijzonder, de meest geschikte eiwitsamenstelling.

Gebaseerd op de resultaten van hoofdstuk 2–4, is 2^e generatie nOMV vaccin geselecteerd voor verdere ontwikkeling richting klinische studies, vooral vanwege de lage opbrengst van het 2^e generatie sOMV vaccin. Later werd duidelijk, dat spontane OMV vorming sterk toeneemt tijdens de stationaire kweekfase. Hoofdstuk 6 laat zien dat de spontane OMV vorming wordt veroorzaakt door cysteine limitatie en dat een dergelijke stimulus kan worden gebruikt om de

opbrengst van sOMV vaccin productie te verbeteren. Na ongeveer 8 uur cysteine-gelimiteerde stationaire fase werd de sOMV opbrengst namelijk vergelijkbaar met die van het nOMV proces. Deze cysteine limitatie aanpak kan mogelijk de lage OMV opbrengst van het 2^e generatie sOMV vaccin verhelpen.

Hoofdstuk 5 optimaliseert de meest centrale processtap van het 2^e generatie nOMV vaccin: detergens-vrije biomassa extractie met behulp van EDTA. Van de vijf geteste procesparameters, bleken alleen het oogstmoment van de kweekstap en de pH kritisch te zijn voor het eindresultaat. Deze kritieke procesparameters zijn daarna succesvol geoptimaliseerd. In hoofdstuk 7 is een pilot-schaal nOMV productieproces met 40 L kweekvolume ontwikkeld. Dit nieuwe productieproces bleek robuust en opschaalbaar, met een 9–21 keer hogere OMV opbrengst dan gepubliceerde referentie processen. Bovendien bleek de kwaliteit van de nOMV vaccins stabiel te zijn en voor 9 achtereenvolgende producties te voldoen aan vooraf gestelde specificaties. Dankzij deze verbeteringen is een nOMV productie proces op commerciële schaal binnen handbereik. Hoofdstuk 8 meet de toxiciteit en immunogeniciteit van 2^e generatie NonaMen vaccin, wat is samengesteld uit OMV's van 3 vergelijkbare serogroep B meningokokken, die elk 3 unieke PorA antigenen tot expressie brengen. Het vaccin induceerde hoge bactericide titers in het serum van muizen en konijnen. Bovendien konden er geen relevante tekenen van toxiciteit of pathologie worden ontdekt in konijnen die werden geïmmuniseerd met vijf humane doses vaccin. Deze resultaten suggereren, dat 2^e generatie NonaMen vaccin breed beschermend is en veilig voor humane toepassingen.

Dit proefschrift toont aan dat 2^e generatie OMV vaccins een sterk verbeterde kwaliteit hebben en geschikt lijken voor gebruik in klinische studies. Het nieuwe, pilot-schaal productie proces ondervangt naar verwachting alle belangrijke nadelen van dOMV technologie. Klinische evaluatie van breed beschermende OMV vaccins tegen serogroep B meningokokken is een logische volgende stap. Veelbelovende OMV concepten voor vaccins tegen andere serogroepen en andere pathogenen zijn echter ook in opkomst. Het nOMV productieplatform beschreven in dit proefschrift is naar verwachting inzetbaar om ook deze nieuwe vaccins te produceren.

Curriculum vitae

Bas van de Waterbeemd
Born on April 23rd 1979, Helmond, The Netherlands
Phone: +31 6 46 391 321
Email (work): bas.van.de.waterbeemd@intravacc.nl
Email (home): basvandewaterbeemd@hotmail.com
www.linkedin.com/in/basvandewaterbeemd

1991–1997
VWO, Strabrecht College, Geldrop

1997–1998
Music technology, Utrecht School of Arts, Faculty of Art, Media and Technology, Hilversum
Qualification: propedeuse piano

1998–2005
Biology, specialization Cell Biology, Wageningen University, Wageningen
Thesis: development of a transmission blocking vaccine against *Plasmodium falciparum*
(Radboud University, Nijmegen)
Qualification: Master of Science in Biology

2005–2007
Research technician, Institute for Translational Vaccinology (Intravacc), Process Development
department, Bilthoven

2007–present
Scientist bacterial vaccines, Institute for Translational Vaccinology (Intravacc), Process
Development department, Bilthoven

2009–2012
PhD project, Wageningen University, Bioprocess Engineering group
Thesis: Next-generation Outer Membrane Vesicles Vaccines; from Concept to Clinical Trials
PhD defense on May 8th 2013

Publications

van de Waterbeemd B, van der Pol LA. A process for detergent-free production of outer membrane vesicles. Patent number WO2013006055.

van de Waterbeemd B, Mommen GPM, Pennings JLA, Eppink MH, Wijffels RH, van der Pol LA, de Jong APJM. Quantitative proteomics reveals distinct differences in the protein content of outer membrane vesicle vaccines. Journal of Proteome Research 2013 Feb: http://pubs.acs.org/doi/abs/10.1021/pr301208g (accepted for publication).

van de Waterbeemd B, Zomer G, van den IJssel J, van Keulen L, Eppink MH, van der Ley P, et al. Cysteine depletion causes oxidative stress and triggers outer membrane vesicle release by *Neisseria meningitidis*; implications for vaccine development. PloS One 2013;8(1):e54314.

Kaaijk P, van Straaten I, van de Waterbeemd B, Boot EPJ, Levels LMAR, van Dijken HH, et al. Preclinical safety and immunogenicity evaluation of a nonavalent PorA native outer membrane vesicle vaccine against serogroup B meningococcal disease. Vaccine 2013 Feb 4;31(7):1065-71.

Mommen GP, van de Waterbeemd B, Meiring HD, Kersten G, Heck AJ, de Jong AP. Unbiased selective isolation of orotein N-terminal peptides from complex proteome samples using Phospho Tagging (PTAG) and TiO2-based depletion. Molecular and Cellular Proteomics 2012 Sep;11(9):832-42.

van de Waterbeemd B, Streefland M, van Keulen L, van den IJssel J, de Haan A, Eppink MH, et al. Identification and optimization of critical process parameters for the production of nOMV vaccine against *Neisseria meningitidis*. Vaccine 2012 May 21;30(24):3683-90.

van de Waterbeemd B, Streefland M, van der Ley P, Zomer B, van Dijken H, Martens D, et al. Improved OMV vaccine against *Neisseria meningitidis* using genetically engineered strains and a detergent-free purification process. Vaccine 2010 Jul 5;28(30):4810-6.

Baart GJ, Langenhof M, van de Waterbeemd B, Hamstra HJ, Zomer B, van der Pol LA, et al. Expression of phosphofructokinase in *Neisseria meningitidis*. Microbiology 2010 Feb;156(Pt 2):530-42.

van de Waterbeemd B, Streefland M, Pennings J, van der Pol L, Beuvery C, Tramper J, et al. Gene-expression-based quality scores indicate optimal harvest point in *Bordetella pertussis* cultivation for vaccine production. Biotechnology and Bioengineering 2009 Mar 25;103(5):900-8.

Streefland M, Van Herpen PF, Van de Waterbeemd B, Van der Pol LA, Beuvery EC, Tramper J, et al. A practical approach for exploration and modeling of the design space of a bacterial vaccine cultivation process. Biotechnology and Bioengineering 2009 Jun 1;104(3):492-504.

Streefland M, van de Waterbeemd B, Kint J, van der Pol LA, Beuvery EC, Tramper J, et al. Evaluation of a critical process parameter: Oxygen limitation during cultivation has a fully reversible effect on gene expression of *Bordetella pertussis*. Biotechnology and Bioengineering 2008 Jun 18;102(1):161-7.

Streefland M, van de Waterbeemd B, Happe H, van der Pol LA, Beuvery EC, Tramper J, et al. PAT for vaccines: The first stage of PAT implementation for development of a well-defined whole-cell vaccine against whooping cough disease. Vaccine 2007 Jan 22;25(16):2994-3000.

Training activities

Discipline specific activities

Advances in microarray technology (conference, London, United Kingdom)[1]

8th international symposium saga of the genus *Bordetella* (conference, Paris, France)[1]

Applied genomics of industrial fermentation (course, Kluyver Centre, Delft)[2]

An introduction to Design of Experiments (course, The Productivity Factory, Bilthoven)[2]

Design of Experiments; pharma applications (course, Umetrics, Bilthoven)[2]

Troubleshooting of industrial processes using chemometrics (course, TIPb, Bilthoven)[2]

13th European congress on biotechnology (conference, Barcelona, Spain)[1]

5th Vaccine conference (conference, Amsterdam, The Netherlands)[2]

12[e] Nederlands biotechnologie congres (conference, Ede, The Netherlands)[2]

13[e] Nederlands biotechnologie congres (conference, Ede, The Netherlands)[1]

Werkgroependag Nederlandse Biotechnologische Vereniging (symposium, Ede, The Netherlands)[3]

7th Immunology conference (conference, Varadero, Cuba)[3]

NWO vaccine workgroup (symposium, Utrecht, The Netherlands)[3]

Vaccine Technology IV (conference, Albufeira, Portugal)[3]

General courses

Veilige microbiologische technieken (course, Hogeschool van Utrecht, Utrecht)[2]

GMP productie van vaccins (course, RIVM, Bilthoven)[2]

Visie op op Arbo en veiligheid (course, RIVM, Bilthoven)[2]

Effectief projectmanagement (course, GITP trainingen, Bilthoven)[2]

Optional activities

PhD excursion to United States (Wageningen University, Bioprocess Engineering group)[1]

PhD excursion to Spain (Wageningen University, Bioprocess Engineering group)[1,3]

[1]Poster presentation
[2]Attended
[3]Oral presentation

References

[1]   Health Council of the Netherlands. Universal vaccination against meningococcal serogroup C and pneumococcal disease. The Hague, 2001; publication no. 2001/27E. ISBN 90-5549-414-3.

[2]   Frasch CE, Van Alphen L, Holst J, Poolman J, Rosenqvist E. Meningococcal Vaccines, Methods and Protocols. Totowa, NJ: Humana Press Inc 2001:81-107.

[3]   Holst J, Martin D, Arnold R, Huergo CC, Oster P, O'Hallahan J, et al. Properties and clinical performance of vaccines containing outer membrane vesicles from Neisseria meningitidis. Vaccine 2009 Jun 24;27 Suppl 2:B3-12.

[4]   Baart GJ, de Jong G, Philippi M, van't Riet K, van der Pol LA, Beuvery EC, et al. Scale-up for bulk production of vaccine against meningococcal disease. Vaccine 2007 Aug 21;25(34):6399-408.

[5]   van den Dobbelsteen GP, van Dijken HH, Pillai S, van Alphen L. Immunogenicity of a combination vaccine containing pneumococcal conjugates and meningococcal PorA OMVs. Vaccine 2007 Mar 22;25(13):2491-6.

[6]   van der Ley P, Steeghs L, Hamstra HJ, ten Hove J, Zomer B, van Alphen L. Modification of lipid A biosynthesis in Neisseria meningitidis lpxL mutants: influence on lipopolysaccharide structure, toxicity, and adjuvant activity. Infect Immun 2001 Oct;69(10):5981-90.

[7]   van der Ley P, van der Biezen J, Poolman JT. Construction of Neisseria meningitidis strains carrying multiple chromosomal copies of the porA gene for use in the production of a multivalent outer membrane vesicle vaccine. Vaccine 1995 Mar;13(4):401-7.

[8]   Janda WM, Knapp JS. Manual of clinical microbiology, vol 1. Neisseria and Moraxella catarrhalis. Amer Soc Microbiol 2003:585-608.

[9]   Weichselbaum A. Ueber die Aetoliogie der akuten meningitis cerebrospinalis. Fortschr Med 1887;5:573-83.

[10]   Caugant DA, Hoiby EA, Magnus P, Scheel O, Hoel T, Bjune G, et al. Asymptomatic carriage of Neisseria meningitidis in a randomly sampled population. Journal of clinical microbiology 1994 Feb;32(2):323-30.

[11]   Stephens DS. Uncloaking the meningococcus: dynamics of carriage and disease. Lancet 1999 Mar 20;353(9157):941-2.

[12]   van Deuren M, Brandtzaeg P, van der Meer JW. Update on meningococcal disease with emphasis on pathogenesis and clinical management. Clinical microbiology reviews 2000 Jan;13(1):144-66, table of contents.

[13]   Nassif X, So M. Interaction of pathogenic neisseriae with nonphagocytic cells. Clinical microbiology reviews 1995 Jul;8(3):376-88.

[14]   Rosenstein NE, Perkins BA, Stephens DS, Popovic T, Hughes JM. Meningococcal disease. The New England journal of medicine 2001 May 3;344(18):1378-88.

[15]   Swartley JS, Marfin AA, Edupuganti S, Liu LJ, Cieslak P, Perkins B, et al. Capsule switching of Neisseria meningitidis. Proc Natl Acad Sci U S A 1997 Jan 7;94(1):271-6.

[16]   Cookson ST, Corrales JL, Lotero JO, Regueira M, Binsztein N, Reeves MW, et al. Disco fever: epidemic meningococcal disease in northeastern Argentina associated with disco patronage. The Journal of infectious diseases 1998 Jul;178(1):266-9.

[17]   Stuart JM, Cartwright KA, Robinson PM, Noah ND. Effect of smoking on meningococcal carriage. Lancet 1989 Sep 23;2(8665):723-5.

[18]   Girard MP, Preziosi MP, Aguado MT, Kieny MP. A review of vaccine research and development: meningococcal disease. Vaccine 2006 May 29;24(22):4692-700.

[19]   Greenwood B. Manson Lecture. Meningococcal meningitis in Africa. Transactions of the Royal Society of Tropical Medicine and Hygiene 1999 Jul-Aug;93(4):341-53.

[20] Wang JF, Caugant DA, Li X, Hu X, Poolman JT, Crowe BA, et al. Clonal and antigenic analysis of serogroup A Neisseria meningitidis with particular reference to epidemiological features of epidemic meningitis in the People's Republic of China. Infect Immun 1992 Dec;60(12):5267-82.

[21] Sharip A, Sorvillo F, Redelings MD, Mascola L, Wise M, Nguyen DM. Population-based analysis of meningococcal disease mortality in the United States: 1990-2002. The Pediatric infectious disease journal 2006 Mar;25(3):191-4.

[22] Gray SJ, Trotter CL, Ramsay ME, Guiver M, Fox AJ, Borrow R, et al. Epidemiology of meningococcal disease in England and Wales 1993/94 to 2003/04: contribution and experiences of the Meningococcal Reference Unit. Journal of medical microbiology 2006 Jul;55(Pt 7):887-96.

[23] Tzeng YL, Stephens DS. Epidemiology and pathogenesis of Neisseria meningitidis. Microbes and infection / Institut Pasteur 2000 May;2(6):687-700.

[24] Stephens DS, Greenwood B, Brandtzaeg P. Epidemic meningitis, meningococcaemia, and Neisseria meningitidis. Lancet 2007 Jun 30;369(9580):2196-210.

[25] Stephens DS. Conquering the meningococcus. FEMS microbiology reviews 2007 Jan;31(1):3-14.

[26] Gold R, Lepow ML, Goldschneider I, Draper TL, Gotschlich EC. Clinical evaluation of group A and group C meningococcal polysaccharide vaccines in infants. The Journal of clinical investigation 1975 Dec;56(6):1536-47.

[27] Mayer LW, Reeves MW, Al-Hamdan N, Sacchi CT, Taha MK, Ajello GW, et al. Outbreak of W135 meningococcal disease in 2000: not emergence of a new W135 strain but clonal expansion within the electophoretic type-37 complex. The Journal of infectious diseases 2002 Jun 1;185(11):1596-605.

[28] Al-Mazrou Y, Khalil M, Borrow R, Balmer P, Bramwell J, Lal G, et al. Serologic responses to ACYW135 polysaccharide meningococcal vaccine in Saudi children under 5 years of age. Infect Immun 2005 May;73(5):2932-9.

[29] Trotter CL, Andrews NJ, Kaczmarski EB, Miller E, Ramsay ME. Effectiveness of meningococcal serogroup C conjugate vaccine 4 years after introduction. Lancet 2004 Jul 24-30;364(9431):365-7.

[30] Wuorimaa T, Dagan R, Vakevainen M, Bailleux F, Haikala R, Yaich M, et al. Avidity and subclasses of IgG after immunization of infants with an 11-valent pneumococcal conjugate vaccine with or without aluminum adjuvant. The Journal of infectious diseases 2001 Nov 1;184(9):1211-5.

[31] Snape MD, Perrett KP, Ford KJ, John TM, Pace D, Yu LM, et al. Immunogenicity of a tetravalent meningococcal glycoconjugate vaccine in infants: a randomized controlled trial. Jama 2008 Jan 9;299(2):173-84.

[32] Miller E, Salisbury D, Ramsay M. Planning, registration, and implementation of an immunisation campaign against meningococcal serogroup C disease in the UK: a success story. Vaccine 2001 Oct 15;20 Suppl 1:S58-67.

[33] Balmer P, Borrow R, Miller E. Impact of meningococcal C conjugate vaccine in the UK. Journal of medical microbiology 2002 Sep;51(9):717-22.

[34] de Greeff SC, de Melker HE, Spanjaard L, Schouls LM, van Derende A. Protection from routine vaccination at the age of 14 months with meningococcal serogroup C conjugate vaccine in the Netherlands. The Pediatric infectious disease journal 2006 Jan;25(1):79-80.

[35] Ramsay ME, Andrews NJ, Trotter CL, Kaczmarski EB, Miller E. Herd immunity from meningococcal serogroup C conjugate vaccination in England: database analysis. BMJ (Clinical research ed 2003 Feb 15;326(7385):365-6.

[36] Wyle FA, Artenstein MS, Brandt BL, Tramont EC, Kasper DL, Altieri PL, et al. Immunologic response of man to group B meningococcal polysaccharide vaccines. The Journal of infectious diseases 1972 Nov;126(5):514-21.

[37] Finne J, Leinonen M, Makela PH. Antigenic similarities between brain components and bacteria causing meningitis. Implications for vaccine development and pathogenesis. Lancet 1983 Aug 13;2(8346):355-7.

[38]   Griffiss JM, Yamasaki R, Estabrook M, Kim JJ. Meningococcal molecular mimicry and the search for an ideal vaccine. Transactions of the Royal Society of Tropical Medicine and Hygiene 1991;85 Suppl 1:32-6.

[39]   Bruge J, Bouveret-Le Cam N, Danve B, Rougon G, Schulz D. Clinical evaluation of a group B meningococcal N-propionylated polysaccharide conjugate vaccine in adult, male volunteers. Vaccine 2004 Mar 12;22(9-10):1087-96.

[40]   Zollinger WD, Kasper DL, Veltri BJ, Artenstein MS. Isolation and characterization of a native cell wall complex from Neisseria meningitidis. Infect Immun 1972 Nov;6(5):835-51.

[41]   Knox KW, Vesk M, Work E. Relation between excreted lipopolysaccharide complexes and surface structures of a lysine-limited culture of Escherichia coli. Journal of bacteriology 1966 Oct;92(4):1206-17.

[42]   Chatterjee SN, Das J. Electron microscopic observations on the excretion of cell-wall material by Vibrio cholerae. Journal of general microbiology 1967 Oct;49(1):1-11.

[43]   Tsai CM, Frasch CE, Mocca LF. Five structural classes of major outer membrane proteins in Neisseria meningitidis. Journal of bacteriology 1981 Apr;146(1):69-78.

[44]   Zollinger WD, Mandrell RE, Griffiss JM, Altieri P, Berman S. Complex of meningococcal group B polysaccharide and type 2 outer membrane protein immunogenic in man. The Journal of clinical investigation 1979 May;63(5):836-48.

[45]   Mayrand D, Grenier D. Biological activities of outer membrane vesicles. Canadian journal of microbiology 1989 Jun;35(6):607-13.

[46]   Holst J, Feiring B, Fuglesang JE, Hoiby EA, Nokleby H, Aaberge IS, et al. Serum bactericidal activity correlates with the vaccine efficacy of outer membrane vesicle vaccines against Neisseria meningitidis serogroup B disease. Vaccine 2003 Jan 30;21(7-8):734-7.

[47]   Zollinger WD, Mandrell RE, Altieri P, Berman S, Lowenthal J, Artenstein MS. Safety and immunogenicity of a Neisseria meningitidis type 2 protein vaccine in animals and humans. The Journal of infectious diseases 1978 Jun;137(6):728-39.

[48]   Frasch CE. Vaccines for prevention of meningococcal disease. Clinical microbiology reviews 1989 Apr;2 Suppl:S134-8.

[49]   Fredriksen JH, Rosenqvist E, Wedege E, Bryn K, Bjune G, Froholm LO, et al. Production, characterization and control of MenB-vaccine "Folkehelsa": an outer membrane vesicle vaccine against group B meningococcal disease. NIPH Ann 1991 Dec;14(2):67-79; discussion -80.

[50]   Bjune G, Hoiby EA, Gronnesby JK, Arnesen O, Fredriksen JH, Halstensen A, et al. Effect of outer membrane vesicle vaccine against group B meningococcal disease in Norway. Lancet 1991 Nov 2;338(8775):1093-6.

[51]   Sierra GV, Campa HC, Varcacel NM, Garcia IL, Izquierdo PL, Sotolongo PF, et al. Vaccine against group B Neisseria meningitidis: protection trial and mass vaccination results in Cuba. NIPH Ann 1991 Dec;14(2):195-207; discussion 8-10.

[52]   de Moraes JC, Perkins BA, Camargo MC, Hidalgo NT, Barbosa HA, Sacchi CT, et al. Protective efficacy of a serogroup B meningococcal vaccine in Sao Paulo, Brazil. Lancet 1992 Oct 31;340(8827):1074-8.

[53]   Thornton V, Lennon D, Rasanathan K, O'Hallahan J, Oster P, Stewart J, et al. Safety and immunogenicity of New Zealand strain meningococcal serogroup B OMV vaccine in healthy adults: beginning of epidemic control. Vaccine 2006 Feb 27;24(9):1395-400.

[54]   Boslego J, Garcia J, Cruz C, Zollinger W, Brandt B, Ruiz S, et al. Efficacy, safety, and immunogenicity of a meningococcal group B (15:P1.3) outer membrane protein vaccine in Iquique, Chile. Chilean National Committee for Meningococcal Disease. Vaccine 1995 Jun;13(9):821-9.

[55]   Tappero JW, Lagos R, Ballesteros AM, Plikaytis B, Williams D, Dykes J, et al. Immunogenicity of 2 serogroup B outer-membrane protein meningococcal vaccines: a randomized controlled trial in Chile. Jama 1999 Apr 28;281(16):1520-7.

[56] Holst J, Feiring B, Naess LM, Norheim G, Kristiansen P, Hoiby EA, et al. The concept of "tailor-made", protein-based, outer membrane vesicle vaccines against meningococcal disease. Vaccine 2005 Mar 18;23(17-18):2202-5.

[57] Martin DR, Ruijne N, McCallum L, O'Hallahan J, Oster P. The VR2 epitope on the PorA P1.7-2,4 protein is the major target for the immune response elicited by the strain-specific group B meningococcal vaccine MeNZB. Clin Vaccine Immunol 2006 Apr;13(4):486-91.

[58] van der Ley P, Heckels JE, Virji M, Hoogerhout P, Poolman JT. Topology of outer membrane porins in pathogenic Neisseria spp. Infect Immun 1991 Sep;59(9):2963-71.

[59] Frosch M, Schultz E, Glenn-Calvo E, Meyer TF. Generation of capsule-deficient Neisseria meningitidis strains by homologous recombination. Mol Microbiol 1990 Jul;4(7):1215-8.

[60] de Kleijn E, van Eijndhoven L, Vermont C, Kuipers B, van Dijken H, Rumke H, et al. Serum bactericidal activity and isotype distribution of antibodies in toddlers and schoolchildren after vaccination with RIVM hexavalent PorA vesicle vaccine. Vaccine 2001 Nov 12;20(3-4):352-8.

[61] Claassen I, Meylis J, van der Ley P, Peeters C, Brons H, Robert J, et al. Production, characterization and control of a Neisseria meningitidis hexavalent class 1 outer membrane protein containing vesicle vaccine. Vaccine 1996 Jul;14(10):1001-8.

[62] Trotter CL, Ramsay ME. Vaccination against meningococcal disease in Europe: review and recommendations for the use of conjugate vaccines. FEMS microbiology reviews 2007 Jan;31(1):101-7.

[63] Zollinger WD, Donets MA, Schmiel DH, Pinto VB, Labrie J, Moran EE, et al. Design and evaluation in mice of a broadly protective meningococcal group B native outer membrane vesicle vaccine. Vaccine 2010 May 24.

[64] Urwin R, Russell JE, Thompson EA, Holmes EC, Feavers IM, Maiden MC. Distribution of surface protein variants among hyperinvasive meningococci: implications for vaccine design. Infect Immun 2004 Oct;72(10):5955-62.

[65] Rappuoli R. Reverse vaccinology. Curr Opin Microbiol 2000 Oct;3(5):445-50.

[66] Findlow J, Borrow R, Snape MD, Dawson T, Holland A, John TM, et al. Multicenter, open-label, randomized phase II controlled trial of an investigational recombinant Meningococcal serogroup B vaccine with and without outer membrane vesicles, administered in infancy. Clin Infect Dis 2010 Nov 15;51(10):1127-37.

[67] Snape MD, Dawson T, Oster P, Evans A, John TM, Ohene-Kena B, et al. Immunogenicity of 2 Investigational Serogroup B Meningococcal Vaccines in the First Year of Life: A Randomized Comparative Trial. The Pediatric infectious disease journal 2010 Sep 14.

[68] Bai X, Findlow J, Borrow R. Recombinant protein meningococcal serogroup B vaccine combined with outer membrane vesicles. Expert opinion on biological therapy 2011 Jul;11(7):969-85.

[69] ICH. International Conference on Harmonisation; guidance on specifications: test procedures and acceptance criteria for biotechnological/biological products. Notice. Food and Drug Administration, HHS. Federal register 1999 Aug 18;64(159):44928-35.

[70] van der Ley P, van den Dobbelsteen G. Next-generation outer membrane vesicle vaccines against Neisseria meningitidis based on nontoxic LPS mutants. Hum Vaccin 2011 Aug;7(8):886-90.

[71] Zollinger WD, Poolman JT, Maiden MC. Meningococcal serogroup B vaccines: will they live up to expectations? Expert review of vaccines 2011 May;10(5):559-61.

[72] Fisseha M, Chen P, Brandt B, Kijek T, Moran E, Zollinger W. Characterization of native outer membrane vesicles from lpxL mutant strains of Neisseria meningitidis for use in parenteral vaccination. Infect Immun 2005 Jul;73(7):4070-80.

[73] Duplicate of reference [271]. Koeberling O, Giuntini S, Seubert A, Granoff DM. Meningococcal OMV Vaccines from Mutant Strains Engineered to Express Factor H Binding Proteins from Antigenic Variant Groups 1 and 2. Clin Vaccine Immunol 2008 Dec 24.

[74] Kovacs-Simon A, Titball RW, Michell SL. Lipoproteins of bacterial pathogens. Infect Immun 2010 Oct 25.

[75] Steeghs L, Berns M, ten Hove J, de Jong A, Roholl P, van Alphen L, et al. Expression of foreign LpxA acyltransferases in Neisseria meningitidis results in modified lipid A with reduced toxicity and retained adjuvant activity. Cell Microbiol 2002 Sep;4(9):599-611.

[76] Deatherage BL, Lara JC, Bergsbaken T, Rassoulian Barrett SL, Lara S, Cookson BT. Biogenesis of bacterial membrane vesicles. Mol Microbiol 2009 Jun;72(6):1395-407.

[77] Harms J, Wang X, Kim T, Yang X, Rathore AS. Defining Process Design Space for Biotech Products: Case Study of Pichia pastoris Fermentation. Biotechnology progress 2008 Apr 16.

[78] Mandenius CF, Brundin A. Bioprocess optimization using design-of-experiments methodology. Biotechnology progress 2008 Nov-Dec;24(6):1191-203.

[79] Bishop DG, Work E. An extracellular glycolipid produced by Escherichia coli grown under lysine-limiting conditions. The Biochemical journal 1965 Aug;96(2):567-76.

[80] Katsui N, Tsuchido T, Hiramatsu R, Fujikawa S, Takano M, Shibasaki I. Heat-induced blebbing and vesiculation of the outer membrane of Escherichia coli. Journal of bacteriology 1982 Sep;151(3):1523-31.

[81] McBroom AJ, Kuehn MJ. Release of outer membrane vesicles by Gram-negative bacteria is a novel envelope stress response. Mol Microbiol 2007 Jan;63(2):545-58.

[82] Pajon R, Fergus AM, Koeberling O, Caugant DA, Granoff DM. Meningococcal factor H binding proteins in epidemic strains from Africa: implications for vaccine development. PLoS neglected tropical diseases 2011 Sep;5(9):e1302.

[83] Roy N, Barman S, Ghosh A, Pal A, Chakraborty K, Das SS, et al. Immunogenicity and protective efficacy of Vibrio cholerae outer membrane vesicles in rabbit model. FEMS immunology and medical microbiology 2010 Oct;60(1):18-27.

[84] Roberts R, Moreno G, Bottero D, Gaillard ME, Fingermann M, Graieb A, et al. Outer membrane vesicles as acellular vaccine against pertussis. Vaccine 2008 Aug 26;26(36):4639-46.

[85] Kaplan SL, Schutze GE, Leake JA, Barson WJ, Halasa NB, Byington CL, et al. Multicenter surveillance of invasive meningococcal infections in children. Pediatrics 2006 Oct;118(4):e979-84.

[86] Trotter CL, Chandra M, Cano R, Larrauri A, Ramsay ME, Brehony C, et al. A surveillance network for meningococcal disease in Europe. FEMS microbiology reviews 2007 Jan;31(1):27-36.

[87] Morley SL, Pollard AJ. Vaccine prevention of meningococcal disease, coming soon? Vaccine 2001 Dec 12;20(5-6):666-87.

[88] Martin DR, Walker SJ, Baker MG, Lennon DR. New Zealand epidemic of meningococcal disease identified by a strain with phenotype B:4:P1.4. The Journal of infectious diseases 1998 Feb;177(2):497-500.

[89] Duplicate of reference [76]. Deatherage BL, Lara JC, Bergsbaken T, Barrett SL, Lara S, Cookson BT. Biogenesis of Bacterial Membrane Vesicles. Mol Microbiol 2009 May 8.

[90] Saukkonen K, Leinonen M, Abdillahi H, Poolman JT. Comparative evaluation of potential components for group B meningococcal vaccine by passive protection in the infant rat and in vitro bactericidal assay. Vaccine 1989 Aug;7(4):325-8.

[91] Arigita C, Luijkx T, Jiskoot W, Poelen M, Hennink WE, Crommelin DJ, et al. Well-defined and potent liposomal meningococcal B vaccines adjuvated with LPS derivatives. Vaccine 2005 Oct 17;23(43):5091-8.

[92] Arigita C, Kersten GF, Hazendonk T, Hennink WE, Crommelin DJ, Jiskoot W. Restored functional immunogenicity of purified meningococcal PorA by incorporation into liposomes. Vaccine 2003 Feb 14;21(9-10):950-60.

[93] Steeghs L, Tommassen J, Leusen JH, van de Winkel JG, van der Ley P. Teasing apart structural determinants of 'toxicity' and 'adjuvanticity': implications for meningococcal vaccine development. J Endotoxin Res 2004;10(2):113-9.

[94] Koeberling O, Seubert A, Granoff DM. Bactericidal antibody responses elicited by a meningococcal outer membrane vesicle vaccine with overexpressed factor H-binding protein and genetically attenuated endotoxin. J Infect Dis 2008 Jul 15;198(2):262-70.

[95] van der Voort ER, van der Ley P, van der Biezen J, George S, Tunnela O, van Dijken H, et al. Specificity of human bactericidal antibodies against PorA P1.7,16 induced with a hexavalent meningococcal outer membrane vesicle vaccine. Infect Immun 1996 Jul;64(7):2745-51.

[96] Cametti C. Polyion-induced aggregation of oppositely charged liposomes and charged colloidal particles: the many facets of complex formation in low-density colloidal systems. Chem Phys Lipids 2008 Oct;155(2):63-73.

[97] Post DM, Zhang D, Eastvold JS, Teghanemt A, Gibson BW, Weiss JP. Biochemical and functional characterization of membrane blebs purified from Neisseria meningitidis serogroup B. The Journal of biological chemistry 2005 Nov 18;280(46):38383-94.

[98] Devoe IW, Gilchrist JE. Release of endotoxin in the form of cell wall blebs during in vitro growth of Neisseria meningitidis. J Exp Med 1973 Nov 1;138(5):1156-67.

[99] Hoekstra D, van der Laan JW, de Leij L, Witholt B. Release of outer membrane fragments from normally growing Escherichia coli. Biochim Biophys Acta 1976 Dec 14;455(3):889-99.

[100] Guthrie T, Wong SY, Liang B, Hyland L, Hou S, Hoiby EA, et al. Local and systemic antibody responses in mice immunized intranasally with native and detergent-extracted outer membrane vesicles from Neisseria meningitidis. Infect Immun 2004 May;72(5):2528-37.

[101] Katial RK, Brandt BL, Moran EE, Marks S, Agnello V, Zollinger WD. Immunogenicity and safety testing of a group B intranasal meningococcal native outer membrane vesicle vaccine. Infect Immun 2002 Feb;70(2):702-7.

[102] Saunders NB, Shoemaker DR, Brandt BL, Moran EE, Larsen T, Zollinger WD. Immunogenicity of intranasally administered meningococcal native outer membrane vesicles in mice. Infect Immun 1999 Jan;67(1):113-9.

[103] Drabick JJ, Brandt BL, Moran EE, Saunders NB, Shoemaker DR, Zollinger WD. Safety and immunogenicity testing of an intranasal group B meningococcal native outer membrane vesicle vaccine in healthy volunteers. Vaccine 1999 Aug 20;18(1-2):160-72.

[104] Ferrari G, Garaguso I, Adu-Bobie J, Doro F, Taddei AR, Biolchi A, et al. Outer membrane vesicles from group B Neisseria meningitidis delta gna33 mutant: proteomic and immunological comparison with detergent-derived outer membrane vesicles. Proteomics 2006 Mar;6(6):1856-66.

[105] Steeghs L, Kuipers B, Hamstra HJ, Kersten G, van Alphen L, van der Ley P. Immunogenicity of outer membrane proteins in a lipopolysaccharide-deficient mutant of Neisseria meningitidis: influence of adjuvants on the immune response. Infect Immun 1999 Oct;67(10):4988-93.

[106] Fransen F, Boog CJ, van Putten JP, van der Ley P. Agonists of Toll-like receptors 3, 4, 7, and 9 are candidates for use as adjuvants in an outer membrane vaccine against Neisseria meningitidis serogroup B. Infect Immun 2007 Dec;75(12):5939-46.

[107] Arigita C, Jiskoot W, Westdijk J, van Ingen C, Hennink WE, Crommelin DJ, et al. Stability of mono- and trivalent meningococcal outer membrane vesicle vaccines. Vaccine 2004 Jan 26;22(5-6):629-42.

[108] Klugman KP, Gotschlich EC, Blake MS. Sequence of the structural gene (rmpM) for the class 4 outer membrane protein of Neisseria meningitidis, homology of the protein to gonococcal protein III and Escherichia coli OmpA, and construction of meningococcal strains that lack class 4 protein. Infect Immun 1989 Jul;57(7):2066-71.

[109] Holten E. Serotypes of Neisseria meningitidis isolated from patients in Norway during the first six months of 1978. Journal of clinical microbiology 1979 Feb;9(2):186-8.

[110] Jennings MP, van der Ley P, Wilks KE, Maskell DJ, Poolman JT, Moxon ER. Cloning and molecular analysis of the galE gene of Neisseria meningitidis and its role in lipopolysaccharide biosynthesis. Molecular microbiology 1993 Oct;10(2):361-9.

[111] Prachayasittikul V, Isarankura-Na-Ayudhya C, Tantimongcolwat T, Nantasenamat C, Galla HJ. EDTA-induced membrane fluidization and destabilization: biophysical studies on artificial lipid membranes. Acta Biochim Biophys Sin (Shanghai) 2007 Nov;39(11):901-13.

[112] Baart GJ, Willemsen M, Khatami E, de Haan A, Zomer B, Beuvery EC, et al. Modeling Neisseria meningitidis B metabolism at different specific growth rates. Biotechnology and bioengineering 2008 Dec 1;101(5):1022-35.

180

[113]   Lugtenberg B, Meijers J, Peters R, van der Hoek P, van Alphen L. Electrophoretic resolution of the "major outer membrane protein" of Escherichia coli K12 into four bands. FEBS Lett 1975 Oct 15;58(1):254-8.

[114]   Gerhardt P, Murray RGE, Wood WA, Krieg NR. Methods for general and molecular bacteriology. Washington DC: American Society for Microbiology 1994.

[115]   Welch DF. Applications of cellular fatty acid analysis. Clinical microbiology reviews 1991 Oct;4(4):422-38.

[116]   Jantzen E, Bryn K, Bergan T, Bovre K. Gas chromatography of bacterial whole cell methanolysates; V. Fatty acid composition of Neisseriae and Moraxellae. Acta Pathol Microbiol Scand B Microbiol Immunol 1974 Dec;82(6):767-79.

[117]   Westphal O, Jann JK. Bacterial lipopolysaccharide extraction with phenol-water and further application of the procedure. Methods Carbohydr Chem 1965;5:83-91.

[118]   Luijkx TA, van Dijken H, Hamstra HJ, Kuipers B, van der Ley P, van Alphen L, et al. Relative immunogenicity of PorA subtypes in a multivalent Neisseria meningitidis vaccine is not dependent on presentation form. Infect Immun 2003 Nov;71(11):6367-71.

[119]   Geurtsen J, Steeghs L, Hamstra HJ, Ten Hove J, de Haan A, Kuipers B, et al. Expression of the lipopolysaccharide-modifying enzymes PagP and PagL modulates the endotoxic activity of Bordetella pertussis. Infect Immun 2006 Oct;74(10):5574-85.

[120]   Ziegler-Heitbrock HW, Thiel E, Futterer A, Herzog V, Wirtz A, Riethmuller G. Establishment of a human cell line (Mono Mac 6) with characteristics of mature monocytes. Int J Cancer 1988 Mar 15;41(3):456-61.

[121]   Grizot S, Buchanan SK. Structure of the OmpA-like domain of RmpM from Neisseria meningitidis. Mol Microbiol 2004 Feb;51(4):1027-37.

[122]   Koebnik R. Proposal for a peptidoglycan-associating alpha-helical motif in the C-terminal regions of some bacterial cell-surface proteins. Mol Microbiol 1995 Jun;16(6):1269-70.

[123]   Prinz T, Tommassen J. Association of iron-regulated outer membrane proteins of Neisseria meningitidis with the RmpM (class 4) protein. FEMS Microbiol Lett 2000 Feb 1;183(1):49-53.

[124]   Pridmore AC, Wyllie DH, Abdillahi F, Steeghs L, van der Ley P, Dower SK, et al. A lipopolysaccharide-deficient mutant of Neisseria meningitidis elicits attenuated cytokine release by human macrophages and signals via toll-like receptor (TLR) 2 but not via TLR4/MD2. The Journal of infectious diseases 2001 Jan 1;183(1):89-96.

[125]   Gaines Das RE, Brugger P, Patel M, Mistry Y, Poole S. Monocyte activation test for pro-inflammatory and pyrogenic contaminants of parenteral drugs: test design and data analysis. J Immunol Methods 2004 May;288(1-2):165-77.

[126]   Luijkx T, van Dijken H, van Els C, van den Dobbelsteen G. Heterologous prime-boost strategy to overcome weak immunogenicity of two serosubtypes in hexavalent Neisseria meningitidis outer membrane vesicle vaccine. Vaccine 2006 Mar 6;24(10):1569-77.

[127]   Welsch JA, Moe GR, Rossi R, Adu-Bobie J, Rappuoli R, Granoff DM. Antibody to genome-derived neisserial antigen 2132, a Neisseria meningitidis candidate vaccine, confers protection against bacteremia in the absence of complement-mediated bactericidal activity. The Journal of infectious diseases 2003 Dec 1;188(11):1730-40.

[128]   Serruto D, Spadafina T, Ciucchi L, Lewis LA, Ram S, Tontini M, et al. Neisseria meningitidis GNA2132, a heparin-binding protein that induces protective immunity in humans. Proc Natl Acad Sci U S A Feb 3.

[129]   Leive L. Release of lipopolysaccharide by EDTA treatment of E. coli. Biochem Biophys Res Commun 1965 Nov 22;21(4):290-6.

[130]   Duplicate of reference [69]. ICH. Specifications (Q6B): Test Procedures and Acceptance Criteria for Biotechnological/Biological Products. wwwichorg 1999.

[131]   Sybachin AV, Efimova AA, Litmanovich EA, Menger FM, Yaroslavov AA. Complexation of polycations to anionic liposomes: composition and structure of the interfacial complexes. Langmuir 2007 Sep 25;23(20):10034-9.

[132] Yaroslavov AA, Efimova AA, Lobyshev VI, Kabanov VA. Reversibility of structural rearrangements in the negative vesicular membrane upon electrostatic adsorption/desorption of the polycation. Biochim Biophys Acta 2002 Feb 18;1560(1-2):14-24.

[133] Cox J, Mann M. Quantitative, high-resolution proteomics for data-driven systems biology. Annual review of biochemistry 2011 Jun 7;80:273-99.

[134] McDonald L, Robertson DH, Hurst JL, Beynon RJ. Positional proteomics: selective recovery and analysis of N-terminal proteolytic peptides. Nat Methods 2005 Dec;2(12):955-7.

[135] McDonald L, Beynon RJ. Positional proteomics: preparation of amino-terminal peptides as a strategy for proteome simplification and characterization. Nat Protoc 2006;1(4):1790-8.

[136] Gevaert K, Goethals M, Martens L, Van Damme J, Staes A, Thomas GR, et al. Exploring proteomes and analyzing protein processing by mass spectrometric identification of sorted N-terminal peptides. Nature biotechnology 2003 May;21(5):566-9.

[137] Doucet A, Butler GS, Rodriguez D, Prudova A, Overall CM. Metadegradomics: toward in vivo quantitative degradomics of proteolytic post-translational modifications of the cancer proteome. Mol Cell Proteomics 2008 Oct;7(10):1925-51.

[138] Van Damme P, Arnesen T, Gevaert K. Protein alpha-N-acetylation studied by N-terminomics. FEBS J 2011 Oct;278(20):3822-34.

[139] Nakazawa T, Yamaguchi M, Okamura TA, Ando E, Nishimura O, Tsunasawa S. Terminal proteomics: N- and C-terminal analyses for high-fidelity identification of proteins using MS. Proteomics 2008 Feb;8(4):673-85.

[140] Huesgen PF, Overall CM. N- and C-terminal degradomics: new approaches to reveal biological roles for plant proteases from substrate identification. Physiol Plant 2011 Oct 24.

[141] Schilling O, Barre O, Huesgen PF, Overall CM. Proteome-wide analysis of protein carboxy termini: C terminomics. Nat Methods 2010 Jul;7(7):508-11.

[142] Van Damme P, Staes A, Bronsoms S, Helsens K, Colaert N, Timmerman E, et al. Complementary positional proteomics for screening substrates of endo- and exoproteases. Nat Methods 2010 Jul;7(7):512-5.

[143] Staes A, Impens F, Van Damme P, Ruttens B, Goethals M, Demol H, et al. Selecting protein N-terminal peptides by combined fractional diagonal chromatography. Nat Protoc 2011 Aug;6(8):1130-41.

[144] Kleifeld O, Doucet A, auf dem Keller U, Prudova A, Schilling O, Kainthan RK, et al. Isotopic labeling of terminal amines in complex samples identifies protein N-termini and protease cleavage products. Nat Biotechnol Mar;28(3):281-8.

[145] Kleifeld O, Doucet A, Prudova A, auf dem Keller U, Gioia M, Kizhakkedathu JN, et al. Identifying and quantifying proteolytic events and the natural N terminome by terminal amine isotopic labeling of substrates. Nat Protoc 2011 Oct;6(10):1578-611.

[146] Beaudette P, Rossi NA, Huesgen PF, Yu X, Shenoi RA, Doucet A, et al. Development of soluble ester-linked aldehyde polymers for proteomics. Anal Chem 2011 Sep 1;83(17):6500-10.

[147] Agard NJ, Wells JA. Methods for the proteomic identification of protease substrates. Curr Opin Chem Biol 2009 Dec;13(5-6):503-9.

[148] Timmer JC, Enoksson M, Wildfang E, Zhu W, Igarashi Y, Denault JB, et al. Profiling constitutive proteolytic events in vivo. Biochem J 2007 Oct 1;407(1):41-8.

[149] Timmer JC, Zhu W, Pop C, Regan T, Snipas SJ, Eroshkin AM, et al. Structural and kinetic determinants of protease substrates. Nat Struct Mol Biol 2009 Oct;16(10):1101-8.

[150] Mahrus S, Trinidad JC, Barkan DT, Sali A, Burlingame AL, Wells JA. Global sequencing of proteolytic cleavage sites in apoptosis by specific labeling of protein N termini. Cell 2008 Sep 5;134(5):866-76.

[151] Zhang X, Ye J, Engholm-Keller K, Hojrup P. A proteome-scale study on in vivo protein Nalpha-acetylation using an optimized method. Proteomics Jan;11(1):81-93.

[152]   Staes A, Van Damme P, Helsens K, Demol H, Vandekerckhove J, Gevaert K. Improved recovery of proteome-informative, protein N-terminal peptides by combined fractional diagonal chromatography (COFRADIC). Proteomics 2008 Apr;8(7):1362-70.

[153]   Dormeyer W, Mohammed S, Breukelen B, Krijgsveld J, Heck AJ. Targeted analysis of protein termini. J Proteome Res 2007 Dec;6(12):4634-45.

[154]   Helbig AO, Gauci S, Raijmakers R, van Breukelen B, Slijper M, Mohammed S, et al. Profiling of N-acetylated protein termini provides in-depth insights into the N-terminal nature of the proteome. Mol Cell Proteomics 2010 May;9(5):928-39.

[155]   Mohammed S, Heck A, Jr. Strong cation exchange (SCX) based analytical methods for the targeted analysis of protein post-translational modifications. Curr Opin Biotechnol 2011 Feb;22(1):9-16.

[156]   Duplicate of reference [185]. van de Waterbeemd B, Streefland M, van der Ley P, Zomer B, van Dijken H, Martens D, et al. Improved OMV vaccine against Neisseria meningitidis using genetically engineered strains and a detergent-free purification process. Vaccine Jul 5;28(30):4810-6.

[157]   Boersema PJ, Raijmakers R, Lemeer S, Mohammed S, Heck AJ. Multiplex peptide stable isotope dimethyl labeling for quantitative proteomics. Nat Protoc 2009;4(4):484-94.

[158]   Lemeer S, Pinkse MW, Mohammed S, van Breukelen B, den Hertog J, Slijper M, et al. Online automated in vivo zebrafish phosphoproteomics: from large-scale analysis down to a single embryo. J Proteome Res 2008 Apr;7(4):1555-64.

[159]   Pinkse MW, Mohammed S, Gouw JW, van Breukelen B, Vos HR, Heck AJ. Highly robust, automated, and sensitive online TiO2-based phosphoproteomics applied to study endogenous phosphorylation in Drosophila melanogaster. J Proteome Res 2008 Feb;7(2):687-97.

[160]   Motoyama A, Xu T, Ruse CI, Wohlschlegel JA, Yates JR, 3rd. Anion and cation mixed-bed ion exchange for enhanced multidimensional separations of peptides and phosphopeptides. Anal Chem 2007 May 15;79(10):3623-34.

[161]   Meiring HD, van der Heeft E, ten Hove GJ, de Jong APJM. Nanoscale LC–MS(n): technical design and applications to peptide and protein analysis. Sep Sci 2002;25(9):557-68.

[162]   Emanuelsson O, Brunak S, von Heijne G, Nielsen H. Locating proteins in the cell using TargetP, SignalP and related tools. Nat Protoc 2007;2(4):953-71.

[163]   Vogtle FN, Wortelkamp S, Zahedi RP, Becker D, Leidhold C, Gevaert K, et al. Global analysis of the mitochondrial N-proteome identifies a processing peptidase critical for protein stability. Cell 2009 Oct 16;139(2):428-39.

[164]   Meiring HD, Soethout EC, de Jong AP, van Els CA. Targeted identification of infection-related HLA class I-presented epitopes by stable isotope tagging of epitopes (SITE). Curr Protoc Immunol 2007 May;Chapter 16:Unit 16 3.

[165]   Veenstra TD, Conrads TP, Issaq HJ. What to do with "one-hit wonders"? Electrophoresis 2004 May;25(9):1278-9.

[166]   Raijmakers R, Kraiczek K, de Jong AP, Mohammed S, Heck AJ. Exploring the human leukocyte phosphoproteome using a microfluidic reversed-phase-TiO2-reversed-phase high-performance liquid chromatography phosphochip coupled to a quadrupole time-of-flight mass spectrometer. Anal Chem Feb 1;82(3):824-32.

[167]   Boersema PJ, Mohammed S, Heck AJ. Phosphopeptide fragmentation and analysis by mass spectrometry. J Mass Spectrom 2009 Jun;44(6):861-78.

[168]   Plasman K, Van Damme P, Kaiserman D, Impens F, Demeyer K, Helsens K, et al. Probing the efficiency of proteolytic events by positional proteomics. Mol Cell Proteomics Feb;10(2):M110 003301.

[169]   Zhang X, Hojrup P. Cyclization of the N-Terminal X-Asn-Gly Motif during Sample Preparation for Bottom-Up Proteomics. Anal Chem Oct 15;82(20):8680-5.

[170]   Frottin F, Martinez A, Peynot P, Mitra S, Holz RC, Giglione C, et al. The proteomics of N-terminal methionine cleavage. Mol Cell Proteomics 2006 Dec;5(12):2336-49.

[171]   Michalski A, Cox J, Mann M. More than 100,000 detectable peptide species elute in single shotgun proteomics runs but the majority is inaccessible to data-dependent LC-MS/MS. J Proteome Res Apr 1;10(4):1785-93.

[172]   Mischerikow N, Heck AJ. Targeted large-scale analysis of protein acetylation. Proteomics 2011 Feb;11(4):571-89.

[173]   Mogk A, Schmidt R, Bukau B. The N-end rule pathway for regulated proteolysis: prokaryotic and eukaryotic strategies. Trends Cell Biol 2007 Apr;17(4):165-72.

[174]   Arnesen T, Van Damme P, Polevoda B, Helsens K, Evjenth R, Colaert N, et al. Proteomics analyses reveal the evolutionary conservation and divergence of N-terminal acetyltransferases from yeast and humans. Proc Natl Acad Sci U S A 2009 May 19;106(20):8157-62.

[175]   Lange PF, Overall CM. TopFIND, a knowledgebase linking protein termini with function. Nat Methods 2011 Sep;8(9):703-4.

[176]   auf dem Keller U, Prudova A, Gioia M, Butler GS, Overall CM. A statistics-based platform for quantitative N-terminome analysis and identification of protease cleavage products. Mol Cell Proteomics May;9(5):912-27.

[177]   Frese CK, Altelaar AF, Hennrich ML, Nolting D, Zeller M, Griep-Raming J, et al. Improved peptide identification by targeted fragmentation using CID, HCD and ETD on an LTQ-Orbitrap Velos. J Proteome Res 2011 May 6;10(5):2377-88.

[178]   Helsens K, Van Damme P, Degroeve S, Martens L, Arnesen T, Vandekerckhove J, et al. Bioinformatics analysis of a Saccharomyces cerevisiae N-terminal proteome provides evidence of alternative translation initiation and post-translational N-terminal acetylation. J Proteome Res 2011 Aug 5;10(8):3578-89.

[179]   Helbig AO, Rosati S, Pijnappel PW, van Breukelen B, Timmers MH, Mohammed S, et al. Perturbation of the yeast N-acetyltransferase NatB induces elevation of protein phosphorylation levels. BMC Genomics 2010;11:685.

[180]   Miller Jenkins LM, Durell SR, Mazur SJ, Appella E. p53 N-Terminal Phosphorylation: A Defining Layer of Complex Regulation. Carcinogenesis 2012 Apr 12.

[181]   Vener AV, Harms A, Sussman MR, Vierstra RD. Mass spectrometric resolution of reversible protein phosphorylation in photosynthetic membranes of Arabidopsis thaliana. J Biol Chem 2001 Mar 9;276(10):6959-66.

[182]   Jodar L, Feavers IM, Salisbury D, Granoff DM. Development of vaccines against meningococcal disease. Lancet 2002 Apr 27;359(9316):1499-508.

[183]   Ellis TN, Kuehn MJ. Virulence and immunomodulatory roles of bacterial outer membrane vesicles. Microbiol Mol Biol Rev 2010 Mar;74(1):81-94.

[184]   Wheeler JX, Vipond C, Feavers IM. Exploring the proteome of meningococcal outer membrane vesicle vaccines. Proteomics Clin Appl 2007 Sep;1(9):1198-210.

[185]   van de Waterbeemd B, Streefland M, van der Ley P, Zomer B, van Dijken H, Martens D, et al. Improved OMV vaccine against Neisseria meningitidis using genetically engineered strains and a detergent-free purification process. Vaccine 2010 Jul 5;28(30):4810-6.

[186]   van de Waterbeemd B, Streefland M, van Keulen L, van den IJssel J, de Haan A, Eppink MH, et al. Identification and optimization of critical process parameters for the production of NOMV vaccine against Neisseria meningitidis. Vaccine 2012 May 21;30(24):3683-90.

[187]   Duplicate of reference [286]. Keiser PB, Biggs-Cicatelli S, Moran EE, Schmiel DH, Pinto VB, Burden RE, et al. A phase 1 study of a meningococcal native outer membrane vesicle vaccine made from a group B strain with deleted lpxL1 and synX, over-expressed factor H binding protein, two PorAs and stabilized OpcA expression. Vaccine 2010 Dec 31.

[188]   Duplicate of reference [287]. Pinto VB, Moran EE, Cruz F, Wang XM, Fridman A, Zollinger WD, et al. An experimental outer membrane vesicle vaccine from N. meningitidis serogroup B strains that induces serum bactericidal activity to multiple serogroups. Vaccine 2011 Aug 7.

184

[189] Haque H, Russell AD. Effect of chelating agents on the susceptibility of some strains of gram-negative bacteria to some antibacterial agents. Antimicrobial agents and chemotherapy 1974 Aug;6(2):200-6.

[190] Koeberling O, Seubert A, Santos G, Colaprico A, Ugozzoli M, Donnelly J, et al. Immunogenicity of a meningococcal native outer membrane vesicle vaccine with attenuated endotoxin and over-expressed factor H binding protein in infant rhesus monkeys. Vaccine 2011 Jun 24;29(29-30):4728-34.

[191] Koeberling O, Delany I, Granoff DM. A critical threshold of meningococcal factor h binding protein expression is required for increased breadth of protective antibodies elicited by native outer membrane vesicle vaccines. Clin Vaccine Immunol 2011 May;18(5):736-42.

[192] Borrow R, Balmer P, Miller E. Meningococcal surrogates of protection--serum bactericidal antibody activity. Vaccine 2005 Mar 18;23(17-18):2222-7.

[193] Vipond C, Suker J, Jones C, Tang C, Feavers IM, Wheeler JX. Proteomic analysis of a meningococcal outer membrane vesicle vaccine prepared from the group B strain NZ98/254. Proteomics 2006 Jun;6(11):3400-13.

[194] Vipond C, Wheeler JX, Jones C, Feavers IM, Suker J. Characterization of the protein content of a meningococcal outer membrane vesicle vaccine by polyacrylamide gel electrophoresis and mass spectrometry. Human vaccines 2005 Mar-Apr;1(2):80-4.

[195] Williams JN, Skipp PJ, Humphries HE, Christodoulides M, O'Connor CD, Heckels JE. Proteomic analysis of outer membranes and vesicles from wild-type serogroup B Neisseria meningitidis and a lipopolysaccharide-deficient mutant. Infect Immun 2007 Mar;75(3):1364-72.

[196] Tsolakos N, Lie K, Bolstad K, Maslen S, Kristiansen PA, Hoiby EA, et al. Characterization of meningococcal serogroup B outer membrane vesicle vaccines from strain 44/76 after growth in different media. Vaccine 2010 Apr 19;28(18):3211-8.

[197] Gil J, Betancourt LH, Sardinas G, Yero D, Niebla O, Delgado M, et al. Proteomic study via a non-gel based approach of meningococcal outer membrane vesicle vaccine obtained from strain CU385: A road map for discovery new antigens. Human vaccines 2009 May 8;5(5):347-56.

[198] Gevaert K, Van Damme P, Ghesquiere B, Impens F, Martens L, Helsens K, et al. A la carte proteomics with an emphasis on gel-free techniques. Proteomics 2007 Aug;7(16):2698-718.

[199] Bantscheff M, Schirle M, Sweetman G, Rick J, Kuster B. Quantitative mass spectrometry in proteomics: a critical review. Analytical and bioanalytical chemistry 2007 Oct;389(4):1017-31.

[200] Boersema PJ, Aye TT, van Veen TA, Heck AJ, Mohammed S. Triplex protein quantification based on stable isotope labeling by peptide dimethylation applied to cell and tissue lysates. Proteomics 2008 Nov;8(22):4624-32.

[201] Duplicate of reference [144]. Kleifeld O, Doucet A, auf dem Keller U, Prudova A, Schilling O, Kainthan RK, et al. Isotopic labeling of terminal amines in complex samples identifies protein N-termini and protease cleavage products. Nature biotechnology 2010 Mar;28(3):281-8.

[202] Guryca V, Lamerz J, Ducret A, Cutler P. Qualitative improvement and quantitative assessment of N-terminomics. Proteomics 2012 Apr;12(8):1207-16.

[203] Wildes D, Wells JA. Sampling the N-terminal proteome of human blood. Proc Natl Acad Sci U S A 2010 Mar 9;107(10):4561-6.

[204] Mommen GP, van de Waterbeemd B, Meiring HD, Kersten G, Heck AJ, de Jong AP. Unbiased Selective Isolation of Protein N-terminal Peptides from Complex Proteome Samples Using Phospho Tagging (PTAG) and TiO2-based Depletion. Mol Cell Proteomics 2012 Sep;11(9):832-42.

[205] Smith RD, Anderson GA, Lipton MS, Pasa-Tolic L, Shen Y, Conrads TP, et al. An accurate mass tag strategy for quantitative and high-throughput proteome measurements. Proteomics 2002 May;2(5):513-23.

[206] Conrads TP, Anderson GA, Veenstra TD, Pasa-Tolic L, Smith RD. Utility of accurate mass tags for proteome-wide protein identification. Analytical chemistry 2000 Jul 15;72(14):3349-54.

[207] Duplicate of reference [161]. Meiring HD, van der Heeft E, ten Hove GJ, de Jong APJM. Nanoscale LC–MS(n): technical design and applications to peptide and protein analysis. Journal of Separation Science 2002;25(9):557-68.

[208] Cappadona S, Baker PR, Cutillas PR, Heck AJ, van Breukelen B. Current challenges in software solutions for mass spectrometry-based quantitative proteomics. Amino acids 2012 Sep;43(3):1087-108.

[209] Yu NY, Wagner JR, Laird MR, Melli G, Rey S, Lo R, et al. PSORTb 3.0: improved protein subcellular localization prediction with refined localization subcategories and predictive capabilities for all prokaryotes. Bioinformatics (Oxford, England) 2010 Jul 1;26(13):1608-15.

[210] Luque-Garcia JL, Zhou G, Spellman DS, Sun TT, Neubert TA. Analysis of electroblotted proteins by mass spectrometry: protein identification after Western blotting. Mol Cell Proteomics 2008 Feb;7(2):308-14.

[211] van Ulsen P, Kuhn K, Prinz T, Legner H, Schmid P, Baumann C, et al. Identification of proteins of Neisseria meningitidis induced under iron-limiting conditions using the isobaric tandem mass tag (TMT) labeling approach. Proteomics 2009 Apr;9(7):1771-81.

[212] Grifantini R, Sebastian S, Frigimelica E, Draghi M, Bartolini E, Muzzi A, et al. Identification of iron-activated and -repressed Fur-dependent genes by transcriptome analysis of Neisseria meningitidis group B. Proc Natl Acad Sci U S A 2003 Aug 5;100(16):9542-7.

[213] Kulp A, Kuehn MJ. Biological functions and biogenesis of secreted bacterial Outer Membrane Vesicles. Annual Review of Microbiology 2010;64:163-84.

[214] Andreev VP, Petyuk VA, Brewer HM, Karpievitch YV, Xie F, Clarke J, et al. Label-Free Quantitative LC-MS Proteomics of Alzheimer's Disease and Normally Aged Human Brains. Journal of proteome research 2012 May 17.

[215] Jiang HQ, Hoiseth SK, Harris SL, McNeil LK, Zhu D, Tan C, et al. Broad vaccine coverage predicted for a bivalent recombinant factor H binding protein based vaccine to prevent serogroup B meningococcal disease. Vaccine 2010 Aug 23;28(37):6086-93.

[216] Lewis S, Sadarangani M, Hoe JC, Pollard AJ. Challenges and progress in the development of a serogroup B meningococcal vaccine. Expert review of vaccines 2009 Jun;8(6):729-45.

[217] Haque H, Russell AD. Effect of ethylenediaminetetraacetic acid and related chelating agents on whole cells of gram-negative bacteria. Antimicrobial agents and chemotherapy 1974 May;5(5):447-52.

[218] Keiser PB, Gibbs BT, Coster TS, Moran EE, Stoddard MB, Labrie JE, 3rd, et al. A phase 1 study of a group B meningococcal native outer membrane vesicle vaccine made from a strain with deleted lpxL2 and synX and stable expression of opcA. Vaccine 2010 Aug 20.

[219] Duplicate of reference [70]. van der Ley P, van den Dobbelsteen G. Next-generation outer membrane vesicle vaccines against Neisseria meningitidis based on nontoxic LPS mutants. Human vaccines 2011 Aug 1;7(8).

[220] Perez-Pardo MA, Ali S, Balasundaram B, Mannall GJ, Baganz F, Bracewell DG. Assessment of the manufacturability of Escherichia coli high cell density fermentations. Biotechnology progress May 2.

[221] Rathore AS, Winkle H. Quality by design for biopharmaceuticals. Nature biotechnology 2009 Jan;27(1):26-34.

[222] ICH. International Conference on Harmonisation; guidance on Q8(R1) Pharmaceutical Development; addition of annex; availability. Notice. Federal register 2009 Jun 9;74(109):27325-6.

[223] Rathore AS. Roadmap for implementation of quality by design (QbD) for biotechnology products. Trends in biotechnology 2009 Sep;27(9):546-53.

[224] Vasilyeva NV, Tsfasman IM, Suzina NE, Stepnaya OA, Kulaev IS. Outer membrane vesicles of Lysobacter sp. Doklady 2009 May-Jun;426:139-42.

[225] Rothfield L, Pearlman-Kothencz M. Synthesis and assembly of bacterial membrane components. A lipopolysaccharide-phospholipid-protein complex excreted by living bacteria. Journal of molecular biology 1969 Sep 28;44(3):477-92.

[226] Gorringe A, Vincent P, Halliwell D, Reddin K. Patent WO2006/008504 A1: Stable compositions containing outer membrane vesicles, methods of manufacturing. 2006.

[227] Eglon MN, Duffy AM, O'Brien T, Strappe PM. Purification of adenoviral vectors by combined anion exchange and gel filtration chromatography. The journal of gene medicine 2009 Nov;11(11):978-89.

[228] Tin Lee C, Morreale G, Middelberg AP. Combined in-fermenter extraction and cross-flow microfiltration for improved inclusion body processing. Biotechnology and bioengineering 2004 Jan 5;85(1):103-13.

[229] Unal CM, Schaar V, Riesbeck K. Bacterial outer membrane vesicles in disease and preventive medicine. Seminars in immunopathology 2011 Sep;33(5):395-408.

[230] Namork E, Brandtzaeg P. Fatal meningococcal septicaemia with "blebbing" meningococcus. Lancet 2002 Nov 30;360(9347):1741.

[231] Weynants V, Denoel P, Devos N, Janssens D, Feron C, Goraj K, et al. Genetically modified L3,7 and L2 lipooligosaccharides from Neisseria meningitidis serogroup B confer a broad cross-bactericidal response. Infect Immun 2009 May;77(5):2084-93.

[232] Work E, Knox KW, Vesk M. The chemistry and electron microscopy of an extracellular lipopolysaccharide from Escherichia coli. Annals of the New York Academy of Sciences 1966 Jun 30;133(2):438-49.

[233] Henry T, Pommier S, Journet L, Bernadac A, Gorvel JP, Lloubes R. Improved methods for producing outer membrane vesicles in Gram-negative bacteria. Research in microbiology 2004 Jul-Aug;155(6):437-46.

[234] Baart GJ, Langenhof M, van de Waterbeemd B, Hamstra HJ, Zomer B, van der Pol LA, et al. Expression of phosphofructokinase in Neisseria meningitidis. Microbiology (Reading, England) 2010 Feb;156(Pt 2):530-42.

[235] van de Waterbeemd B, Streefland M, Pennings J, van der Pol L, Beuvery C, Tramper J, et al. Gene-expression-based quality scores indicate optimal harvest point in Bordetella pertussis cultivation for vaccine production. Biotechnology and bioengineering 2009 Mar 25;103(5):900-8.

[236] Tettelin H, Saunders NJ, Heidelberg J, Jeffries AC, Nelson KE, Eisen JA, et al. Complete genome sequence of Neisseria meningitidis serogroup B strain MC58. Science (New York, NY 2000 Mar 10;287(5459):1809-15.

[237] Schroeder A, Mueller O, Stocker S, Salowsky R, Leiber M, Gassmann M, et al. The RIN: an RNA integrity number for assigning integrity values to RNA measurements. BMC Mol Biol 2006;7:3.

[238] Guckenberger M, Kurz S, Aepinus C, Theiss S, Haller S, Leimbach T, et al. Analysis of the heat shock response of Neisseria meningitidis with cDNA- and oligonucleotide-based DNA microarrays. Journal of bacteriology 2002 May;184(9):2546-51.

[239] Grifantini R, Frigimelica E, Delany I, Bartolini E, Giovinazzi S, Balloni S, et al. Characterization of a novel Neisseria meningitidis Fur and iron-regulated operon required for protection from oxidative stress: utility of DNA microarray in the assignment of the biological role of hypothetical genes. Mol Microbiol 2004 Nov;54(4):962-79.

[240] Grifantini R, Bartolini E, Muzzi A, Draghi M, Frigimelica E, Berger J, et al. Previously unrecognized vaccine candidates against group B meningococcus identified by DNA microarrays. Nature biotechnology 2002 Sep;20(9):914-21.

[241] Dietrich G, Kurz S, Hubner C, Aepinus C, Theiss S, Guckenberger M, et al. Transcriptome analysis of Neisseria meningitidis during infection. Journal of bacteriology 2003 Jan;185(1):155-64.

[242] Bartolini E, Frigimelica E, Giovinazzi S, Galli G, Shaik Y, Genco C, et al. Role of FNR and FNR-regulated, sugar fermentation genes in Neisseria meningitidis infection. Mol Microbiol 2006 May;60(4):963-72.

[243] Holbein BE. Growth and surface binding of proteins by Neisseria meningitidis in normal human serum. Current Microbiology 1981;6(4):213-6.

[244] Catlin BW. Nutritional profiles of Neisseria gonorrhoeae, Neisseria meningitidis, and Neisseria lactamica in chemically defined media and the use of growth requirements for gonococcal typing. The Journal of infectious diseases 1973 Aug;128(2):178-94.

[245] Port JL, DeVoe IW, Archibald FS. Sulphur acquisition by Neisseria meningitidis. Canadian journal of microbiology 1984 Dec;30(12):1453-7.

[246] Baart GJ, Zomer B, de Haan A, van der Pol LA, Beuvery EC, Tramper J, et al. Modeling Neisseria meningitidis metabolism: from genome to metabolic fluxes. Genome Biol 2007 Jul 6;8(7):R136.

[247] Jang S, Imlay JA. Micromolar intracellular hydrogen peroxide disrupts metabolism by damaging iron-sulfur enzymes. The Journal of biological chemistry 2007 Jan 12;282(2):929-37.

[248] Rouault TA, Tong WH. Iron-sulphur cluster biogenesis and mitochondrial iron homeostasis. Nature reviews 2005 Apr;6(4):345-51.

[249] Bitoun JP, Wu G, Ding H. Escherichia coli FtnA acts as an iron buffer for re-assembly of iron-sulfur clusters in response to hydrogen peroxide stress. Biometals 2008 Dec;21(6):693-703.

[250] Johnson DC, Dean DR, Smith AD, Johnson MK. Structure, function, and formation of biological iron-sulfur clusters. Annual review of biochemistry 2005;74:247-81.

[251] Moslen MT. Reactive oxygen species in normal physiology, cell injury and phagocytosis. Advances in experimental medicine and biology 1994;366:17-27.

[252] Ng VH, Cox JS, Sousa AO, MacMicking JD, McKinney JD. Role of KatG catalase-peroxidase in mycobacterial pathogenesis: countering the phagocyte oxidative burst. Mol Microbiol 2004 Jun;52(5):1291-302.

[253] Zollinger WD. Vaccine against gram negative bacteria - US patent: US6,558,677 B2. 2003.

[254] Berlanda Scorza F, Colucci AM, Maggiore L, Sanzone S, Rossi O, Ferlenghi I, et al. High yield production process for Shigella outer membrane particles. PloS one 2012;7(6):e35616.

[255] Cartwright K, Morris R, Rumke H, Fox A, Borrow R, Begg N, et al. Immunogenicity and reactogenicity in UK infants of a novel meningococcal vesicle vaccine containing multiple class 1 (PorA) outer membrane proteins. Vaccine 1999 Jun 4;17(20-21):2612-9.

[256] Wilm M, Mann M. Analytical properties of the nanoelectrospray ion source. Analytical chemistry 1996 Jan 1;68(1):1-8.

[257] Rots NY, Kleijne DE. Safety of a nonavalent meningococcal serogroup B vaccine in healthy adult volunteers in a randomised, controlled, single blind study. 16th International Pathogenic Neisseria Conference, Rotterdam, 7-12 September 2008.

[258] Kaaijk P, van Straaten I, van de Waterbeemd B, Boot EPJ, Levels LMAR, van Dijken HH, et al. Preclinical safety and immunogenicity evaluation of a nonavalent PorA native outer membrane vesicle vaccine against serogroup B meningococcal disease. Vaccine 2013 Feb 4;31(7):1065-71.

[259] Van Hemert P. Strictly aseptic techniques for continuous centrifugation. Antonie van Leeuwenhoek, International Journal of General and Molecular Microbiology 1980;46(5):501.

[260] Kempken R, Preissmann A, Berthold W. Clarification of animal cell cultures on a large scale by continuous centrifugation. Journal of industrial microbiology 1995 Jan;14(1):52-7.

[261] Howson CP, Fineberg HV. Adverse events following pertussis and rubella vaccines. Summary of a report of the Institute of Medicine. Jama 1992 Jan 15;267(3):392-6.

[262] van der Maas NA, David S, Kemmeren JM, Vermeer-de Bondt PE. Safety surveillance in the National Vaccination Programme; fewer adverse events with the DTP-IPV-Hib vaccine after the transition to an acellular pertussis component in 2005. Nederlands tijdschrift voor geneeskunde 2007 Dec 8;151(49):2732-7.

[263] McConnell MJ, Rumbo C, Bou G, Pachon J. Outer membrane vesicles as an acellular vaccine against Acinetobacter baumannii. Vaccine 2011 Aug 5;29(34):5705-10.

[264] Nieves W, Asakrah S, Qazi O, Brown KA, Kurtz J, Aucoin DP, et al. A naturally derived outer-membrane vesicle vaccine protects against lethal pulmonary Burkholderia pseudomallei infection. Vaccine 2011 Oct 26;29(46):8381-9.

[265] Roy K, Hamilton DJ, Munson GP, Fleckenstein JM. Outer membrane vesicles induce immune responses to virulence proteins and protect against colonization by enterotoxigenic Escherichia coli. Clin Vaccine Immunol 2011 Nov;18(11):1803-8.

[266] Pierson T, Matrakas D, Taylor YU, Manyam G, Morozov VN, Zhou W, et al. Proteomic characterization and functional analysis of outer membrane vesicles of Francisella novicida suggests possible role in virulence and use as a vaccine. Journal of proteome research 2011 Mar 4;10(3):954-67.

[267] Collins BS. Gram-negative outer membrane vesicles in vaccine development. Discovery medicine 2011 Jul;12(62):7-15.

[268] Kesty NC, Kuehn MJ. Incorporation of heterologous outer membrane and periplasmic proteins into Escherichia coli outer membrane vesicles. The Journal of biological chemistry 2004 Jan 16;279(3):2069-76.

[269] Chen DJ, Osterrieder N, Metzger SM, Buckles E, Doody AM, DeLisa MP, et al. Delivery of foreign antigens by engineered outer membrane vesicle vaccines. Proc Natl Acad Sci U S A 2010 Feb 16;107(7):3099-104.

[270] Kim SH, Kim KS, Lee SR, Kim E, Kim MS, Lee EY, et al. Structural modifications of outer membrane vesicles to refine them as vaccine delivery vehicles. Biochim Biophys Acta 2009 Aug 18.

[271] Koeberling O, Giuntini S, Seubert A, Granoff DM. Meningococcal outer membrane vesicle vaccines derived from mutant strains engineered to express factor H binding proteins from antigenic variant groups 1 and 2. Clin Vaccine Immunol 2009 Feb;16(2):156-62.

[272] Stoddard MB, Pinto V, Keiser PB, Zollinger W. Evaluation of a whole-blood cytokine release assay for use in measuring endotoxin activity of group B Neisseria meningitidis vaccines made from lipid A acylation mutants. Clin Vaccine Immunol 2010 Jan;17(1):98-107.

[273] Duplicate of reference [257]. Rots NY, Kleijne DE. Safety of a nonavalent meningococcal serogroup B vaccine in healthy adult volunteers in a randomised, controlled, single blind study. In: Program and abstracts of the 16th International Pathogenic Neisseria Conference (Rotterdam, The Netherlands) 2008:Abstract P207.

[274] Kaaijk P, van der Ark AAJ, van Amerongen G, van den Dobbelsteen GPJM. Nonclinical vaccine safety evaluation: Advantages of continuous temperature monitoring using abdominally implanted data loggers Journal of Applied Toxicology 2012 (in press).

[275] Duplicate of reference [186]. van de Waterbeemd B, Streefland M, van Keulen L, van den IJssel J, de Haan A, Eppink MH, et al. Identification and optimization of critical process parameters for the production of NOMV vaccine against Neisseria meningitidis. Vaccine 2012 Mar 30.

[276] Caroff M, Brisson J, Martin A, Karibian D. Structure of the Bordetella pertussis 1414 endotoxin. FEBS Lett 2000 Jul 14;477(1-2):8-14.

[277] David S, Vermeer-de Bondt PE, van der Maas NA. Reactogenicity of infant whole cell pertussis combination vaccine compared with acellular pertussis vaccines with or without simultaneous pneumococcal vaccine in the Netherlands. Vaccine 2008 Oct 29;26(46):5883-7.

[278] Hoffmann S, Peterbauer A, Schindler S, Fennrich S, Poole S, Mistry Y, et al. International validation of novel pyrogen tests based on human monocytoid cells. J Immunol Methods 2005 Mar;298(1-2):161-73.

[279] Poole S, Mistry Y, Ball C, Gaines Das RE, Opie LP, Tucker G, et al. A rapid 'one-plate' in vitro test for pyrogens. J Immunol Methods 2003 Mar 1;274(1-2):209-20.

[280] Duff GW, Atkins E. The detection of endotoxin by in vitro production of endogenous pyrogen: comparison with limulus amebocyte lysate gelation. J Immunol Methods 1982 Aug 13;52(3):323-31.

[281] Borrow R, Carlone GM, Rosenstein N, Blake M, Feavers I, Martin D, et al. Neisseria meningitidis group B correlates of protection and assay standardization--international meeting report Emory University, Atlanta, Georgia, United States, 16-17 March 2005. Vaccine 2006 Jun 12;24(24):5093-107.

[282] Goldschneider I, Gotschlich EC, Artenstein MS. Human immunity to the meningococcus. I. The role of humoral antibodies. J Exp Med 1969 Jun 1;129(6):1307-26.

[283] de Kleijn ED, de Groot R, Labadie J, Lafeber AB, van den Dobbelsteen G, van Alphen L, et al. Immunogenicity and safety of a hexavalent meningococcal outer-membrane-vesicle vaccine in children of 2-3 and 7-8 years of age. Vaccine 2000 Feb 14;18(15):1456-66.

[284] Perkins BA, Jonsdottir K, Briem H, Griffiths E, Plikaytis BD, Hoiby EA, et al. Immunogenicity of two efficacious outer membrane protein-based serogroup B meningococcal vaccines among young adults in Iceland. J Infect Dis 1998 Mar;177(3):683-91.

[285]   Vermont CL, van Dijken HH, Kuipers AJ, van Limpt CJ, Keijzers WC, van der Ende A, et al. Cross-reactivity of antibodies against PorA after vaccination with a meningococcal B outer membrane vesicle vaccine. Infect Immun 2003 Apr;71(4):1650-5.

[286]   Keiser PB, Biggs-Cicatelli S, Moran EE, Schmiel DH, Pinto VB, Burden RE, et al. A phase 1 study of a meningococcal native outer membrane vesicle vaccine made from a group B strain with deleted lpxL1 and synX, over-expressed factor H binding protein, two PorAs and stabilized OpcA expression. Vaccine 2011 Feb 4;29(7):1413-20.

[287]   Pinto VB, Moran EE, Cruz F, Wang XM, Fridman A, Zollinger WD, et al. An experimental outer membrane vesicle vaccine from N. meningitidis serogroup B strains that induces serum bactericidal activity to multiple serogroups. Vaccine 2011 Oct 13;29(44):7752-8.

[288]   Moran EE, Burden R, Labrie JE, 3rd, Wen Z, Wang XM, Zollinger WD, et al. Analysis of the Bactericidal Response to an Experimental Neisseria meningitidis Vesicle Vaccine. Clin Vaccine Immunol 2012 May;19(5):659-65.

[289]   Bonvehi P, Boutriau D, Casellas J, Weynants V, Feron C, Poolman J. Three doses of an experimental detoxified L3-derived lipooligosaccharide meningococcal vaccine offer good safety but low immunogenicity in healthy young adults. Clin Vaccine Immunol 2010 Sep;17(9):1460-6.

[290]   Tsai CM, Frasch CE, Rivera E, Hochstein HD. Measurements of lipopolysaccharide (endotoxin) in meningococcal protein and polysaccharide preparations for vaccine usage. Journal of biological standardization 1989 Jul;17(3):249-58.

[291]   Santos S, Arauz LJ, Baruque-Ramos J, Lebrun I, Carneiro SM, Barreto SA, et al. Outer membrane vesicles (OMV) production of Neisseria meningitidis serogroup B in batch process. Vaccine 2012 Aug 4.

[292]   van de Waterbeemd B, Zomer G, van den IJssel J, van Keulen L, Eppink MH, van der Ley P, et al. Cysteine Depletion Causes Oxidative Stress and Triggers Outer Membrane Vesicle Release by Neisseria meningitidis; Implications for Vaccine Development. PloS ONE 2013;8(1):e54314.

[293]   Aghasadeghi MR, Salmani AS, Sadat SM, Javadi F, Memarnejadian A, Vahabpour R, et al. Application of outer membrane vesicle of Neisseria meningitidis serogroup B as a new adjuvant to induce strongly Th1-oriented responses against HIV-1. Current HIV research 2011 Dec 1;9(8):630-5.

[294]   Norheim G, Tunheim G, Naess LM, Kristiansen PA, Caugant DA, Rosenqvist E. An outer membrane vesicle vaccine for prevention of serogroup A and W-135 meningococcal disease in the African meningitis belt. Scandinavian journal of immunology 2012 Aug;76(2):99-107.

[295]   Clementz T, Zhou Z, Raetz CR. Function of the Escherichia coli msbB gene, a multicopy suppressor of htrB knockouts, in the acylation of lipid A. Acylation by MsbB follows laurate incorporation by HtrB. The Journal of biological chemistry 1997 Apr 18;272(16):10353-60.

[296]   Thalen M, Venema M, Dekker A, Berwald L, van den IJssel, Zomer B, et al. Fed-batch cultivation of Bordetella pertussis: metabolism and Pertussis Toxin production. Biologicals 2006 Dec;34(4):289-97.

[297]   Petersen, T. N.; Brunak, S.; von Heijne, G.; Nielsen, H., SignalP 4.0: discriminating signal peptides from transmembrane regions. Nat Methods 2011, 8, (10), 785-6.

[298]   van de Waterbeemd B, Mommen GPM, Pennings JLA, Eppink MH, Wijffels RH, van der Pol LA, de Jong APJM. Quantitative proteomics reveals distinct differences in the protein content of outer membrane vesicle vaccines. Journal of Proteome Research; accepted for publication 2013 Feb: http://pubs.acs.org/doi/abs/10.1021/pr301208g.

[299]   van de Waterbeemd B, Zomer G, Kaaijk P, Ruiterkamp N, Wijffels RH, van den Dobbelsteen GPJM, van der Pol LA. Improved Production Process for Native Outer Membrane Vesicle Vaccine against Neisseria meningitidis. Submitted for publication.

[300]   Steeghs L, Keestra AM, van Mourik A, Uronen-Hansson H, van der Ley P, Callard R, Klein N, van Putten JP. Differential activation of human and mouse Toll-like receptor 4 by the adjuvant candidate LpxL1 of Neisseria meningitidis. Infect Immun 2008;76(8):3801-7.